

NWS FLDWAV MODEL:

THEORETICAL DESCRIPTION by D.L. Fread

USER DOCUMENTATION by J.M. Lewis

November 28, 1998

Hydrologic Research Laboratory
Office of Hydrology
National Weather Service (NWS), NOAA
Silver Spring, Maryland 20910

TABLE OF CONTENTS

	<u>Page</u>
Abstract	v
1. INTRODUCTION	1.1
1.1 Model Development	1.2
1.2 Scope	1.3
1.3 Summary Preview of FLDWAV	1.4
1.4 Comparison of FLDWAV to DAMBRK and DWOPER Models	1.4
1.4.1 Obsolete DAMBRK Capabilities	1.5
1.4.2 Obsolete DWOPER/NETWORK Capabilities	1.5
1.4.3 Current FLDWAV Capabilities Common to DAMBRK/DWOPER	1.5
1.4.4 New Enhancements to FLDWAV	1.8
1.4.5 Future Enhancements to FLDWAV	1.9
2. SOLUTION OF THE BASIC EQUATIONS	2.1
2.1 Expanded Saint-Venant Equations	2.3
2.2 Solution Technique for Saint-Venant Equations	2.9
3. BOUNDARY CONDITIONS	3.1
3.1 Upstream Boundary	3.1
3.2 Downstream Boundary	3.2
3.3 Internal Boundaries	3.6
3.3.1 Dams	3.7
3.3.2 Bridges	3.12
3.3.3 Waterfalls or Rapids	3.14
3.3.4 Lock and Dams	3.14
4. INITIAL CONDITIONS	4.1
5. MIXED (SUBCRITICAL/SUPERCritical) FLOW	5.1
5.1 Local Partial Inertia (LPI) Technique	5.2
5.2 Mixed-Flow Algorithm	5.6
5.3 Characteristics-Based Upwind Explicit Routing	5.10
6. DAM-BREACH MODELING	6.1
6.1 Breach Outflow	6.1
6.2 Breach Parameter Selection	6.2
6.2.1 Concrete Dams	6.4
6.2.2 Earthen Dams	6.5
6.3 Breach Parameter Sensitivity	6.9

7. RIVER SYSTEMS	7.1
7.1 Single River	7.1
7.2 Dendritic River Systems	7.3
7.2.1 Relaxation Solution Algorithm	7.3
7.2.2 Initial Conditions for Dendritic River System	7.5
8. CROSS SECTIONS	8.1
8.1 Active Sections	8.1
8.2 Inactive (Dead) Off-Channel Storage Sections.	8.3
8.3 Cross-Section Interpolation	8.7
9. SELECTION OF MANNING n	9.1
10. FLOODPLAINS	10.1
10.1 Composite Option or Conveyance Option	10.1
10.2 Sinuosity Factors Associated with Floodplains	10.2
11. COMPUTATIONAL PARAMETER SELECTION	11.1
11.1 Selection of Computational Distance Steps	11.1
11.2 Selection of Computational Time Steps	11.6
12. OTHER MODELING CAPABILITIES	11.1
12.1 Lateral Flows	12.1
12.2 Levee Overtopping/Crevasse Flows and Floodplain Interactions	12.2
12.3 Routing Losses Due to Floodplain Infiltration or Depression Storage	12.5
12.4 Pressurized Flow	12.6
12.5 Kalman Filter	12.8
13. ROBUST COMPUTATIONAL FEATURES	13.1
13.1 Low-Flow Filter	13.1
13.2 Automatic Time Step Reduction	13.2
14. MODEL CALIBRATION	14.1
14.1 Manning n by Trial-Error	14.1
14.2 Manning n by Automatic Calibration Option	14.1
14.2.1 Basic Formulation.	14.1
14.2.3 Decomposition of River System	14.7
14.3 Cross Sections by Automatic Option	14.10
15. OTHER ROUTING TECHNIQUES	15.1
15.1 Diffusion Routing	15.1
15.2 Level-Pool Routing	15.2

16. LIMITATIONS OF FLDWAV	16.1
16.1 Governing Equations	16.1
16.2 Fixed-Bed Assumption	16.2
16.3 Manning n Uncertainty	16.2
16.4 Dam-Break Floods	16.4
16.5 Volume Losses	16.4
17. MODEL TESTING	17.1
17.1 Teton Dam Flood	17.1
17.2 Buffalo Creek Flood	17.7
17.3 Lower Mississippi River System	17.12
17.4 Mississippi-Ohio-Cumberland-Tennessee (MOCT) River System	17.16
18. DAM-BREAK FLOOD FORECASTING USING FLDWAV	18.1
18.1 Dam and Reservoir Considerations	18.1
18.2 Dam-Break Simulation Numerical Difficulties	18.2
19. REAL-TIME FORECASTING USING FLDWAV	19.1
19.1 The River System and Required Data	19.1
19.2 Calibration Procedure	19.3
19.3 Operational Forecast Using FLDWAV Operation in NWSRFS	19.4
19.4 Real-Time Forecasting Numerical Difficulties	19.6
20. FLDWAV MODEL INPUT	20.1
20.1 Input Data Structure and Data Variable Definition for FLDWAV Model	20.1
20.2 Alphabetical Listing of Data Variables for FLDWAV	20.29
21. FLDWAV MODEL OUTPUT	21.1
21.1 Line Printer Output	21.1
21.2 Graphical Output Utility - FLDGRF	21.29
21. 21.2.1 Computer Requirements for FLDGRF	21.41
22. ILLUSTRATIVE EXAMPLES OF DATA INPUT	22.1
22.1 FLDWAV Example 1.0 – Single Dam with Dynamic Routing	22.1
22.2 FLDWAV Example 2.0 – Single Dam with Level-Pool Routing	22.9
22.3 FLDWAV Example 3.0	22.16
22.4 FLDWAV Example 4.0 -- Level-Pool Routing, Average Movable Gate, Conveyance	22.23
22.5 FLDWAV Example 5.0 -- Subcritical/Supercritical	22.30
22.6 FLDWAV Example 6.0 -- Free-Surface/Pressurized Flow	22.37
22.7 FLDWAV Example 7.0 -- Multiple Rivers, Levees	22.44
22.8 FLDWAV Example 8.0 -- Same as Example 2.0 Except with Metric Option	22.58
22.9 FLDWAV Example 9.0 -- Supercritical Flow Downstream of Dam	22.65
22.10 FLDWAV Example 10.0 – Two Dams	22.71

23. FLDWAV Model Program Structure	23.1
24. REFERENCES	24.1
25. INDEX	25.1
26. MATHEMATICAL NOTATION AND DEFINITION	26.1
27. ACKNOWLEDGEMENTS	27.1

NWS FLDWAV MODEL:
THEORETICAL DESCRIPTION by D.L. Fread
USER DOCUMENTATION by J.M. Lewis

Abstract

A generalized flood routing model, FLDWAV, has been developed by the National Weather Service (NWS). It replaces the NWS DAMBRK and DWOPER models since it will allow the utilization of their combined capabilities, as well as provide new hydraulic simulation features. FLDWAV is based on an implicit finite-difference solution of the complete one-dimensional Saint-Venant equations of unsteady flow coupled with an assortment of internal boundary conditions for simulating unsteady flows controlled by a wide spectrum of hydraulic structures. The flow may occur in a single waterway (channel/floodplain) or a system of interconnected waterways in which sinuosity effects are considered. The flow, which can range from Newtonian (water) to non-Newtonian (mud/debris, mine tailings) may freely change with time and location from subcritical to supercritical or vice versa, and from free-surface to pressurized flow.

Special modeling features include time-dependent dam breaches, multiple levee overtopping and crevasse, time-dependent gate controlled flows, assorted spillway flows, bridge/embankments, tidal flap gates, user-specified multiple routing techniques (dynamic-implicit/explicit, diffusion, level-pool) throughout the river system, and a real-time Kalman filter estimator for updating real-time predictions. FLDWAV can be automatically calibrated for a single channel or dendritic system of channels; calibration is achieved through an efficient automatic adjustment of the Manning n coefficient that varies with location and flow or water-surface elevation. The model provides an option for automatic selection of critical computational time and distance steps.

Parameter data is user-specified through a batch mode, and output is tabular and graphic. Input/output may be in English or metric units. FLDWAV can be used by hydrologists/engineers for a wide range of unsteady flow applications including real-time flood forecasting in a dendritic system of rivers, dam-breach analysis for sunny-day piping or overtopping associated with a Probable Maximum Flood, design of waterway improvements, floodplain inundation mapping, irrigation system design, debris flow inundation mapping, and storm sewer analysis/design.

FLDWAV is available as a stand-alone computer program for PC or HP-workstation computers, and is scheduled for January, 1999 availability as an operation within the NWS River Forecast System (NWSRFS) on HP-workstation computers.

NWS FLDWAV MODEL:

THEORETICAL DESCRIPTION by D.L. Fread

USER DOCUMENTATION by J.M. Lewis

November 28, 1998

1. INTRODUCTION

The National Weather Service (NWS) hydrologic services program provides accurate and timely hydrologic information to the general public. This includes flood forecasts, as well as day-to-day river forecasts which are used for water supply, navigation, irrigation, hydropower, reservoir flood control operations, recreation, and water quality interests. Thirteen River Forecast Centers (RFC^s) prepare the forecasts which are disseminated to the public throughout the United States via local Weather Forecast Offices (WFO^s).

Within the National Weather Service River Forecast System (NWSRFS), the runoff generated by rainfall-runoff models is aggregated into fairly large, well defined channels (rivers), and then transmitted downstream by routing techniques of the hydrologic or storage routing variety, e.g., the Lag and K technique (Linsley, et al., 1958). Although the hydrologic routing techniques function adequately in many situations, they have serious shortcomings when the unsteady flows are subjected to backwater effects due to reservoirs, tides, or inflows from large tributaries. When channel bottom slopes are quite mild, the flow inertial effects ignored in the hydrologic techniques also become important. Also, levee overtoppings/failures add complexities which are not handled by the hydrologic routing techniques; and highly transient flow from dambreaks which often greatly exceed the flood-of-record are not treated adequately by hydrologic routing.

To improve the routing capabilities within NWS forecasting procedures, the Hydrologic Research Laboratory (HRL) of the NWS Office of Hydrology developed dynamic wave routing models suitable for efficient operational use in a wide variety of applications involving the

prediction of unsteady flows in rivers, reservoirs, and estuaries. These models are based on an implicit (four-point, nonlinear) finite-difference solution of the complete one-dimensional Saint-Venant equations of unsteady flow.

1.1 Model Development

The Dynamic Wave Operational Model (DWOPER), developed in the early 1970's and enhanced in the early 1980's (Chow, et al., 1988; Fread, 1978a, 1978b, 1985b, 1992), is generalized for wide applicability to rivers of varying physical features, such as irregular geometry, variable roughness parameters, lateral inflows, flow diversions, off-channel storage, local head losses such as bridge contraction-expansions, lock and dam operations, and wind effects. It is suited for efficient application to dendritic river/floodplain systems or to channel networks consisting of bifurcations with weir-type flow into the bifurcated channel. Its features include the ability to use large time steps for slowly varying floods and to use cross sections spaced at irregular intervals along the river system. Limitations of DWOPER include its inability to automatically interpolate cross sections when needed; its inability to handle flows in the supercritical or mixed-flow regimes; its inability to model dam breaks and assorted reservoir outflow controls; and its limited levee capability. DWOPER is currently being implemented on rivers where backwater effects and mild bottom slopes are most troublesome for hydrologic routing methods. It is either in operational service or in the process of being implemented by RFC^s on the Upper and Lower Mississippi, Ohio, Columbia, Missouri, Illinois, Cumberland, Tennessee, Willamette, Sacramento, Grand, Des Moines, and Minnesota Rivers.

The Dam-Break Flood Forecasting Model (DAMBRK), developed in the mid-1970's and improved throughout the 1980's (Fread, 1977, 1985b, 1988, 1992), is a generalized model that can be used for real-time flood forecasting of dam-break floods and/or natural floods, dam-breach flood analysis for sunny-day piping or overtopping associated with the Probable Maximum Flood, floodplain inundation mapping for contingency dam-break flood planning, and design of waterway improvements. The DAMBRK model computes the outflow hydrograph from a dam due to spillway, overtopping and/or dam-breach outflows. The resulting floodwave is then routed through

the downstream channel/floodplain (valley) using the unsteady flow equations along with appropriate internal boundary equations representing downstream dams, bridges, weirs, waterfalls, and other man-made/natural flow controls. The model may also be used for a multitude of purposes by engineering planners, designers, and analysts who are concerned with possible future flood inundation mapping due to dam-break floods and/or reservoir spillway floods. DAMBRK can also be used for routing any user-specified flood hydrograph through reservoirs, rivers, canals, or estuaries as part of general engineering studies of waterways. Its principal limitation is its confinement to analyzing flow through a single waterway rather than a network of mutually interactive channels, e.g., dendritic (tree-type network of river, distributary network of irrigation canals, and estuarial network of waterways). Also, fixed arrays within the computer program for the number of time steps and number of cross sections severely limit the size of the river systems that can be modeled without breaking up the application into several datasets.

Since the mid-1980's, a comprehensive Flood Wave routing model (FLDWAV) has been undergoing development and testing (Fread and Lewis, 1988; Fread, 1992). This state-of-the-art model combines the capabilities of DWOPER and DAMBRK, and provides features not contained in either of these models. FLDWAV has undergone extensive testing (over 160 datasets) to ensure the same level of accuracy and stability as the DAMBRK and DWOPER models. It has also gone through two years of beta testing. The FLDWAV model will continue to undergo development improvements and testing by the NWS to increase its range of applicability and numerical robustness for more convenient usage.

1.2 Scope

Herein, the November 1998 version of FLDWAV is described. The governing equations are described, and new developments are delineated, information on model application difficulties along with suggested means of overcoming the difficulties are provided, some example applications are given, the user-specified data input description along with some examples are provided, and model output is described.

1.3 Summary Preview of FLDWAV

FLDWAV is a generalized flood routing (unsteady flow simulation) model. The governing equations of the model are the complete one-dimensional Saint-Venant equations of unsteady flow which are coupled with internal boundary equations representing the rapidly varied (broad-crested weir) flow through structures such as dams and bridge/embankments which can develop a user-specified time-dependent breach. Also, appropriate external boundary equations at the upstream and downstream ends of the routing reach are utilized. The system of equations is solved by an iterative, nonlinear, weighted four-point implicit finite-difference method. The flow may be either subcritical or supercritical or a combination of each varying in space and time from one to the other; fluid properties may obey either the principles of Newtonian (water) flow or non-Newtonian (mud/debris flows or the contents of a mine-tailings dam) flow. The hydrograph to be routed may be user-specified as an input time series, or it can be developed by the model via user-specified breach parameters (size, shape, time of development). The possible presence of downstream dams which control the flow and may be breached by the flood, bridge/embankment flow constrictions, tributary inflows, river sinuosity, levees located along the tributaries and/or downstream river, and tidal effects are each properly considered during the downstream propagation of the flood. FLDWAV also may be used to route mud and debris flows or rainfall/snowmelt floods using user-specified upstream hydrographs. High water profiles along the valley, flood arrival times, and discharge and stage (water-surface elevation) hydrographs at user-selected locations are standard model output. Model input/output may be in either English or metric (SI) units.

1.4 Comparison of FLDWAV to DAMBRK and DWOPER Models

The NWS FLDWAV model is a combination of the NWS DAMBRK and DWOPER models. Although these models are quite powerful, limitations exist that hinder their flexibility. Limitations of DWOPER include its inability to interpolate cross sections when needed, its inability to handle supercritical flow, its inability to model dam breaks and assorted reservoir outflow controls, and its limited levee capability. DAMBRK can only model single rivers; also, fixed arrays for the number of time steps and number of cross sections severely limit the size of river systems

that could be modeled without breaking up the problem into several datasets. FLDWAV includes the best capabilities of both models and a few enhancements that make it the model of choice.

1.4.1 Obsolete DAMBRK Capabilities

The following DAMBRK (Fread, 1988) capabilities are obsolete in FLDWAV: 1) All options (1-6,9,10) that involve storing a generated hydrograph and then routing it downstream (sequential method) have been eliminated. Under selected conditions, these options may not adequately account for submergence below the dam due to backwater effects. The simultaneous method (Options 11,12) can adequately model these situations. In situations where the flow regime switches between subcritical and supercritical, the mixed-flow algorithm will handle the transitions. The user will find less than a 3 percent difference in the results when comparing the two techniques on datasets with no backwater effects; 2) The cross-section smoothing option is not currently available in FLDWAV; and 3) The option to automatically create cross sections within the reservoir is not currently available in FLDWAV.

1.4.2 Obsolete DWOPER/NETWORK Capabilities

Although no capabilities of the DWOPER model have been eliminated in FLDWAV, the NETWORK option in DWOPER (Fread, 1983b) is not currently available. The NETWORK option allows bifurcated channels (islands, bypasses, etc.) to be simulated.

1.4.3 Current FLDWAV Capabilities Common to DAMBRK/DWOPER

The following capabilities have been retained in the FLDWAV model:

1. Variable Dimensioning - The input data structure has been arranged in a manner so that array sizes are determined internally based on the river system. This eliminates the problem of an insufficient number of time steps or number of cross sections.

2. Multiple Rivers - FLDWAV can model river systems that have a dendritic tree-type structure (n^{th} -order tributaries). The algorithm in DWOPER to model 1st-order tributaries was enhanced to handle n^{th} -order tributary systems. This capability is described in Sub-section 7.2.
3. Dam and Bridge/Embankment - All of the capabilities associated with dams and bridges have been retained. These capabilities are described in Sub-section 3.3.
4. Levee Option - Flows which overtop levees located along either or both sides of a main-stem river and/or its principal tributaries may be simulated within FLDWAV. This capability has been greatly enhanced compared to that within the DAMBRK and DWOPER models. This option is described in Sub-section 12.2.
5. Simultaneous Method of Computation - FLDWAV can route unsteady flows occurring simultaneously in a system of interconnected rivers. Any of the rivers may have one or more structures (dams, bridges, levees, etc.) which control the flow and which may breach if failure conditions are reached. These are described in Sub-sections 3.3 and 12.2.
6. Flow Regime - FLDWAV can handle subcritical, supercritical, or a combination of each, varying in space and time from one to another. A new computational scheme (LPI) has been developed to model mixed flow. Mixed flow and the LPI computational schemes are described in Section 5.
7. Boundary Conditions - The upstream boundary described in Sub-section 3.1 may be either a stage or discharge hydrograph for each river. The downstream boundary described in Sub-section 3.2 choices remain the same as those for DAMBRK and DWOPER. Although the downstream boundary on tributaries is a generated stage hydrograph, the KD parameter must be set to zero for these rivers. The KD=1 option is being reserved for an observed stage hydrograph which will allow diverging channels (e.g., branches of a river delta) to be modeled more directly. Currently these channels are modeled by specifying the downstream

end of the channel as the upstream boundary condition and by specifying the inflow hydrograph as negative flows which can then be interpreted as outflow.

8. Initial Conditions - The initial conditions described in Section 4 include the initial water-surface elevations (WSEL) and discharges at each of the read-in cross section locations. FLDWAV can start up in either a steady-state (not changing temporally) or an unsteady-state condition.

9. Computational Time Step - The initial computational time step may be read in or generated by the model. The model will determine the time to peak of each inflow hydrograph (upstream boundary) and divide the smallest value by 20. This value will be used throughout the run period until a dam breach failure mode is activated. The model will use the smallest value between failure time step(s) and the initial time step. Time step selection is described in Sub-section 13.2.

10. Roughness Coefficients - A Manning n table is defined for each channel reach bounded by gaging stations and is specified as a function of either water-surface elevation (h) or discharge (Q) according to a piece-wise linear relation with both the Manning n and the independent variable (h or Q) specified to FLDWAV in tabular form. Linear interpolation is used to obtain n for values of h or Q intermediate to the tabular values. Unlike DWOPER, the Manning n reaches are defined by their upstream-most section rather than their downstream-most section. To allow FLDWAV to function like DAMBRK, Manning n tables are duplicated internally such that there is a table at each reach between cross sections. The Manning n is described in Section 9.

11. Automatic Calibration - This option (Fread and Smith, 1978) allows the automatic determination of the Manning n so that the difference between computed water-surface elevations (stage hydrographs) and observed hydrographs is minimized. In areas where detailed cross sections may not be available, there is an option (Fread and Lewis, 1986) that will automatically adjust average sections (obtained from topographic maps) if required for

the calibrated Manning n values to lie within specified minimum and maximum n values. These options are described in Sub-sections 14.2 and 14.3.

12. Printer Output - Although the format may be slightly different, FLDWAV will display the same data (e.g., echo print of the input data, hydraulic information, summary of peak data, etc.) as the DAMBRK model.

13. Other Options - The following options are in FLDWAV and have not been altered from the original definitions in DAMBRK or DWOPER: low flow filter, pressurized flow, cross-section interpolation, floodplain option (sinuosity and conveyance), off-channel (dead) storage, robust computational features, local losses, wind effects, hydraulic radius option, lateral inflow/outflow, routing losses, and automatic time step increase for dam-break waves. These are respectively described in Sub-sections 13.1, 12.4, 8.3, 10.1-10.2, 8.2, 13.2, 2.1, 2.1, 2.2, 12.1, 12.3, and 11.2. Also, the metric option is retained in the FLDWAV model.

1.4.4 New Enhancements to FLDWAV

1. Graphical Output Display - A utility (FLDGRF) has been developed to display output data generated by the FLDWAV model. FLDGRF is a user friendly, menu-driven, DOS application which is written in C. The following information is displayed: peak profiles, hydrographs, cross sections, rating curves, and external boundary conditions. Water-surface elevations and/or discharges may be displayed at any cross section (input or interpolated). Multiple profiles and hydrographs may also be displayed. Actual cross sections may be displayed showing the peak conditions. Unlike FLDWAV, this utility is not portable to the Unix workstation environment. FLDGRF is described in Sub-section 21.2.

2. LPI Mixed-Flow Technique - The Local Partial Inertial (LPI) mixed-flow technique (Fread et al., 1996) improves the stability of the model when modeling through mixed-flow (subcritical/supercritical) situations. This technique is described in Sub-section 5.1.

3. Explicit Dynamic Routing - A characteristics-based upwind explicit scheme (Jin and Fread, 1997) has been added to FLDWAV to model instantaneous dam failures and very rapidly occurring failures (less than three minutes). This scheme is also applicable to the complicated flows in the mixed-flow regime. It is described in Sub-section 5.3.

4. Multiple Routing - FLDWAV has the capability of using multiple routing techniques in a river system. Currently, there are four routing techniques available: dynamic implicit, dynamic explicit, level pool (storage), and diffusion. Each reach between adjacent cross sections is assigned a routing technique via the user-specified KRCH parameter. The LPI computational scheme may also be applied to specific rivers.

5. Kalman Filter - A real-time Kalman filter estimator (Fread and Jin, 1993) has been added to FLDWAV. If a river has stage observations for more than two gaging stations, the Kalman filter may be turned on to update the predictions for each time step using observations. This option is applicable for real-time forecasting only. It is described in Sub-section 12.5.

6. At Time Series - This option allows the user to specify multiple computational time steps throughout the temporal range of the inflow hydrograph.

1.4.5 Future Enhancements to FLDWAV

The following enhancements are planned to be added in the next year after the November 1998 FLDWAV release:

1. FLDINP Utility - The interactive input program is a user friendly, menu-driven, Windows application that will allow the user to generate the data file required by the FLDWAV model. FLDINP will have graphics capabilities to allow the user to display hydrographs, cross sections, internal boundaries and tools to graphically modify cross sections.

2. NETWORK Option - The multiple channel option (NETWORK) that is currently in DWOPER will be incorporated into FLDWAV. This option allows the user to model channel bifurcations (islands).

The following options are also expected to be added to FLDWAV in subsequent releases: Muskingum-Cunge routing, mudflow/debris flow and multiple movable gates, routing flow through culverts and landslide generated waves.

2. SOLUTION OF THE BASIC EQUATIONS

The essential component of the FLDWAV model is the computational hydraulic routing algorithm which determines the extent and time of occurrence of flooding in one or more interconnected rivers (incised channel/floodplain) when subjected to unsteady flow (flood) hydrograph(s). The hydrograph is modified (attenuated, lagged, and distorted) as it is routed through the channel/floodplain due to the effects of floodplain storage, frictional resistance to flow, floodwave acceleration components, flow losses and gains, and downstream channel constrictions and/or flow control structures. Modifications to the flood wave are manifested as attenuation of the flood-peak magnitude, spreading-out or dispersion of the temporal varying flood-wave volume, and changes in the celerity (propagation speed) or travel time of the flood wave. If the river/valley contains significant storage volume such as a wide floodplain which becomes inundated, the flood wave (particularly a dam-breach flood wave) can be extensively attenuated as shown in Figure 2.1 and its time of travel greatly increased. Even when the channel/floodplain approaches that of a uniform rectangular-shaped section, the dam-break flood wave can experience appreciable attenuation of the flood peak and reduction in the wave celerity as the wave progresses through the channel/floodplain while a precipitation run-off generated flood wave experiences considerably less attenuation and celerity reduction.

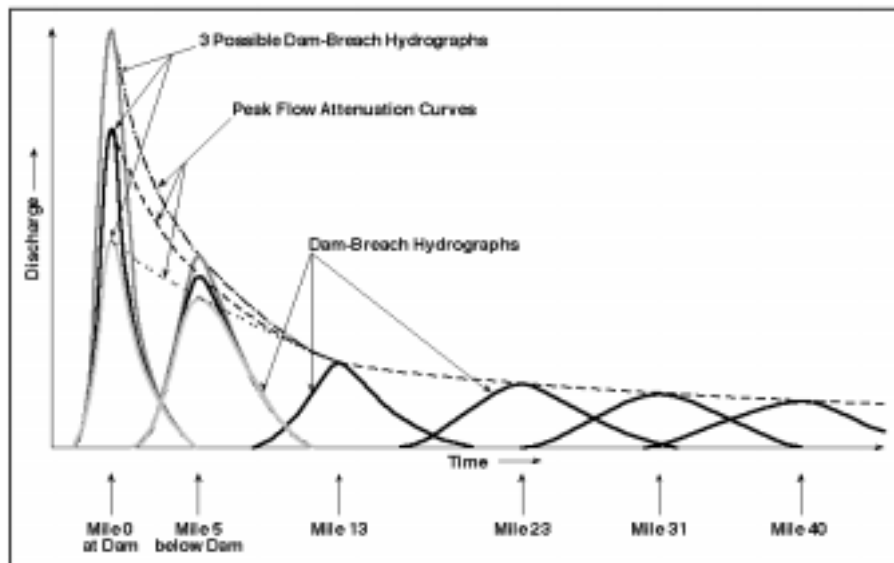


Figure 2.1 - Dam-Break Flood Wave Attenuation Along the Routing Reach.

There are two basic types of flood waves: runoff-generated waves (from either precipitation or snowmelt) and dam-break generated flood waves. The magnitude of the peak discharge of a dam-break wave is usually much greater than the runoff flood of record having occurred in the same river; although under extreme hydrologic conditions, runoff-generated waves may also exceed the flood of record. The above-record discharges make it necessary to extrapolate certain coefficients used in various flood routing techniques and make it impossible to fully calibrate the routing technique. Another distinguishing characteristic of dam-break floods is the very short duration time, and particularly the extremely short time from beginning of rise until the occurrence of the peak. This time to peak, in almost all instances, is synonymous with the period of breach formation time and therefore is in the range of a few minutes to about an hour. Runoff-generated waves tend to have time of rise periods ranging from a few hours to several weeks. The relatively rapid time to peak of the dam-break flood wave causes it to have acceleration components of a far greater significance than those associated with a runoff-generated flood wave.

There are two basic types of flood routing methods: the hydrologic and the hydraulic methods. (See Fread (1981a, 1985b) for a more complete description of the two types of routing methods.) The hydrologic methods usually provide a more approximate analysis of the progression of a flood wave through a river/valley reach than do the hydraulic methods. The hydrologic methods are used for reasons of convenience and economy. They are most appropriate, as far as accuracy is concerned, when the flood wave is not rapidly varying, i.e., the flood-wave acceleration effects are negligible compared to the effects of gravity and channel friction. Also, they are best used when backwater effects are negligible and when the flood wave is very similar in shape and magnitude to previous flood waves for which stage and discharge observations are available for calibrating the hydrologic routing parameters (coefficients).

For routing unsteady flood waves, a particular hydraulic method, known as the dynamic wave method based on the complete one-dimensional Saint-Venant unsteady flow equations, is chosen as the basic hydraulic routing algorithm for the FLDWAV model. This choice is based on its ability to provide more accuracy in simulating the unsteady flood wave than that provided by the hydrologic methods, as well as, other less complex hydraulic methods such as the kinematic-wave and the

diffusion-wave methods. Of the many available hydrologic and hydraulic routing techniques, only the dynamic wave method accounts for the acceleration effects associated with the dam-break wave and the influence of downstream unsteady backwater effects produced by channel constrictions, dams, bridge-road embankments, and tributary inflows. Also, the dynamic wave method is computationally feasible, i.e., the computational time can be made rather insignificant if advantages of certain "implicit" numerical solution techniques are utilized (Preissmann, 1961; Amein and Fang, 1970; Strelkoff, 1970; Chaudry and Contractor, 1973; Fread, 1973a, 1974a, 1974b, 1977, 1978a, 1978b, 1985b, 1992; Liggett and Cunge, 1975; Barkow, 1990).

The dynamic wave method is based on the complete one-dimensional equations of unsteady flow (Saint-Venant equations) which are used to route flood hydrograph(s) through a designated channel/floodplain and its tributaries. This method is based on an expanded version of the original equations developed by Barré de Saint-Venant (1871). When simulating record floods such as dam-break floods, the only coefficients that must be extrapolated beyond the range of past experience are the coefficients of flow resistance. When modeling dam-break floods, it has been shown (Fread, 1988) that this is not an extremely sensitive parameter in effecting the modifications of the flood wave due to its progression through the downstream channel/ floodplain. The Saint-Venant equations can be appropriately used to simulate abrupt waves such as the dam-break wave; this is a "through computation" method which does not provide special treatment for shock waves. This method does not isolate a single shock wave, should it occur, nor apply the shock equations to it while simultaneously using the Saint-Venant equations for all other portions of the flow. The FLDWAV model is primarily based on the complete Saint-Venant equations of unsteady flow.

2.1 Expanded Saint-Venant Equations

The equations of Saint-Venant, expressed in conservation form (Fread, 1974b), with additional terms for the effect of expansion/contractions (Fread, 1978a), channel sinuosity (DeLong, 1986, 1989) and non-Newtonian flow (Fread, 1988) consist of a conservation of mass equation, i.e.,

$$\frac{\partial Q}{\partial x} + \frac{\partial s_{co}(A+A_o)}{\partial t} - q = 0 \dots\dots\dots (2.1)$$

and a conservation of momentum equation, i.e.

$$\frac{\partial(s_m Q)}{\partial t} + \frac{\partial(\beta Q^2/A)}{\partial x} + gA \left(\frac{\partial h}{\partial x} + S_f + S_e + S_i \right) + L + W_f B = 0 \dots\dots\dots (2.2)$$

where Q is the discharge or flow (- if directed upstream), h is the water-surface elevation, A is the active cross-sectional area of flow, A_o is the inactive (off-channel storage) cross-sectional area, s_{co} and s_m are sinuosity factors after DeLong (1986, 1989) which vary with h , x is the longitudinal distance along the river(channel/floodplain), t is the time, q is the lateral inflow or outflow per lineal distance along the channel (inflow is positive and outflow is negative in sign), β is the momentum coefficient for velocity distribution, g is the acceleration due to gravity, S_f is the channel/floodplain boundary friction slope, S_e is the expansion-contraction slope, S_i is the additional friction slope associated with internal viscous dissipation of non-Newtonian fluids such as mud/debris flows, B is the active river topwidth at water-surface elevation h , and W_f is the effect of wind resistance on the surface of the flow.

The wind effect (W_f) is expressed as:

$$W_f = C_w V_{rw} |V_{rw}| \dots\dots\dots (2.3)$$

where C_w is the user-specified non-dimensional wind coefficient ($1 \times 10^{-6} \leq C_w \leq 3 \times 10^{-6}$), V_{rw} is the velocity of the wind relative to the velocity of the channel flow ($V_{rw} = V \pm V_w \cos \omega$) in which $V=Q/A$, V_w is the user-specified velocity of the wind (- if aiding the flow velocity), and ω is the user-specified acute angle between the wind direction and channel flow x -direction.

In Eq. (2.2), L is the momentum effect of lateral flow. This term (Strelkoff, 1969) has the following form: (1) lateral inflow, $L = -qv_x$, in which v_x is the component of the tributary flow velocity in the direction of the main river x -axis (lateral inflows other than dynamic tributaries are

assumed to be perpendicular to the main river such that $v_x=0$); (2) seepage lateral outflow, $L = -0.5qQ/A$; and (3) bulk lateral outflow (e.g. flow over a levee), $L = -qQ/A$. The boundary friction slope (S_f) in Eq. (2.2) is evaluated from Manning's equation for uniform, steady flow, i.e.,

$$S_f = \frac{n^2 |Q| Q}{\mu^2 A^2 R^{4/3}} = \frac{|Q| Q}{K^2} \dots\dots\dots (2.4)$$

in which n is the Manning coefficient of frictional resistance, μ is a units conversion factor 1.49 for English units and 1.0 for SI units, R is the hydraulic radius, and K is the flow conveyance factor. When the conveyance factor (K) is used to represent S_f , the river (channel/floodplain) cross-sectional properties are designated as left floodplain, channel, and right floodplain rather than as a single composite channel/floodplain section. Special orientation for designating left or right is not required as long as consistency is maintained. The conveyance factor is evaluated as follows:

$$K_\ell = \frac{\mu}{n_\ell} A_\ell R_\ell^{2/3} \dots\dots\dots (2.5)$$

$$K_c = \frac{\mu}{n_c} \frac{A_c R_c^{2/3}}{s_m^{1/2}} \dots\dots\dots (2.6)$$

$$K_r = \frac{\mu}{n_r} A_r R_r^{2/3} \dots\dots\dots (2.7)$$

$$K = K_\ell + K_c + K_r \dots\dots\dots (2.8)$$

in which the subscripts ℓ , c , and r designate left floodplain, channel, and right floodplain, respectively. The sinuosity factors (s_{co} and s_m) in Eqs. (2.1), (2.2), and (2.6) are cross-sectional area and conveyance weighted, respectively, according to the following relations:

$$s_{coJ} = \frac{\sum_{k=2}^{k=J} \Delta A_{\ell_k} + \Delta A_{c_k} s_{co_k} + \Delta A_{r_k}}{A_{\ell_J} + A_{c_J} + A_{r_J}} \quad J=2,3,\dots,NCS \dots\dots\dots (2.9)$$

$$s_{m_J} = \frac{\sum_{k=2}^{k=J} \Delta K_{\ell_k} + \Delta K_{c_k} s_{m_k} + \Delta K_{r_k}}{K_{\ell_J} + K_{c_J} + K_{r_J}} \quad J=2,3,\dots,NCS \quad \dots\dots\dots (2.10)$$

in which $\Delta A = A_{J+1} - A_J$, the sinuosity factor s_m represents the sinuosity factor for a differential portion of the flow between the J^{th} depth and the $(J+1)^{\text{th}}$ depth. Distances (Δx_i) between cross sections are measured along the mean flow path for the floodplain flow while distances (Δx_{c_k}) are measured along the meandering (sinuous) channel between the cross sections as shown in Figure 2.2. The sinuosity coefficients for the k^{th} depth are equivalent to: $s_{cok} = s_{mk} = \Delta x_{c_k} / \Delta x_i$. The sinuosity coefficients for the $J=1$ elevation remain the same as the user-specified value for that elevation.

The momentum coefficient for velocity distribution (β) is evaluated as follows:

$$\beta = \frac{(K_{\ell}^2/A_{\ell} + K_c^2/A_c + K_r^2/A_r)}{(K_{\ell} + K_c + K_r)^2/(A_{\ell} + A_c + A_r)} \quad \dots\dots\dots (2.11)$$

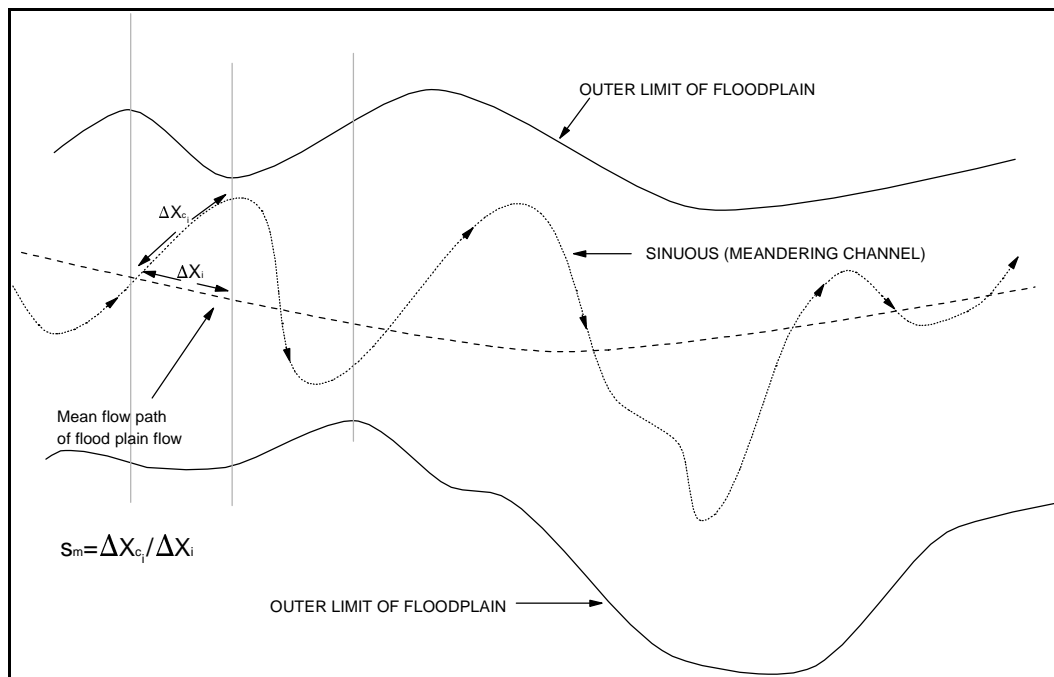


Figure 2.2 - Meandering River and Floodplain Showing Sinuosity (s_m)

where $\beta = 1.06$ when floodplain characteristics are not specified and the total cross section is treated as a composite section. The term (S_e) in Eq. (2.2) is defined as follows:

$$S_e = \frac{k_{ce} \Delta(Q/A)^2}{2g \Delta x} \dots\dots\dots (2.12)$$

in which k_{ce} is the user-specified expansion-contraction coefficient (Morris and Wiggert, 1972), and $\Delta(Q/A)^2$ is the difference in the term $(Q/A)^2$ at two adjacent cross sections separated by a distance Δx . A provision is made within FLDWAV to automatically change contraction to expansion coefficients and vice versa if the flow direction changes from downstream to upstream in which case the computed Q values are negative. The expansion ($k_{ce} = -0.05$ to -0.75) or contraction ($k_{ce} = 0.05$ to 0.4) coefficient is changed to k_n for reverse flows by using the relationship $k_n = -(2 k_{ce} + 0.1)$ if $k_{ce} > 0$, and $k_n = -(k_{ce} + 0.1)/2$ if $k_{ce} < 0$.

The term (S_i) in Eq. (2.2) is significant only when the fluid is quite viscous and severely non-Newtonian. It is evaluated for such non-Newtonian flow (Fread, 1988) as follows:

$$S_i = \frac{\kappa}{\gamma} \left[\frac{(b+2)Q}{AD^{b+1}} + \frac{(b+2)(\tau_o/\kappa)^b}{2 D^b} \right]^{1/b} \dots\dots\dots (2.13)$$

in which γ is the fluid's unit weight, τ_o is the fluid's yield strength, D is the hydraulic depth (A/B), $b=1/m$ where m is the power of the power function that fits the fluid's stress-strain properties as shown in Figure 2.3, and κ is the apparent viscosity or scale factor of the power function. In lieu of actual fluid stress-strain properties, mud/debris flow properties may be estimated from the percent concentration (by volume) of solids (c_v) in the fluid (O'Brien and Julien, 1984) as follows:

$$\kappa = 0.001357e^{16.81c_v} \dots\dots\dots (2.14)$$

$$\tau_o = 0.00886e^{13.11c_v} \dots\dots\dots (2.15)$$

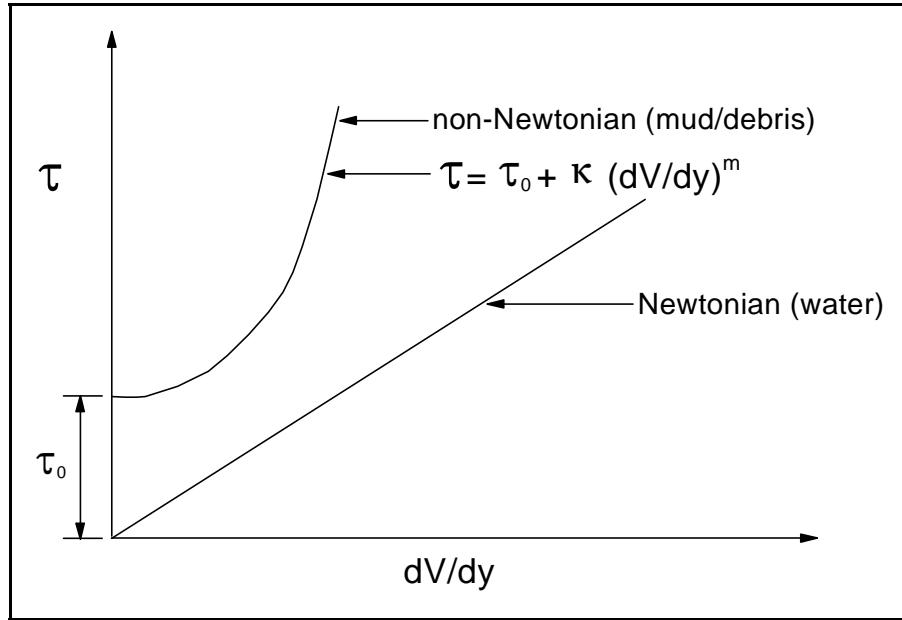


Figure 2.3 - Stress-Strain Power Relation for non-Newtonian Flow.

where κ and τ_0 have units $\text{lb. sec}^2/\text{ft}^2$ and lb/ft^2 , respectively, $e=2.718$ is the base of the natural logarithm, and c_v has ranges of 0.20-0.45 for mudfloods and 0.45-0.50 for mudflows. A user-specified option ($\text{MUD}>0$) in FLDWAV allows the term (S_i) to be considered, otherwise S_i is always assumed to be zero.

The active cross-sectional area (A) and inactive (off-channel storage) area (A_o) are obtained from hydrographic surveys and/or topography maps. They are user-specified in FLDWAV as a table of wetted topwidths (B_k) which vary with elevation (h_k) at selected cross sections along the channel/floodplain. The subscript $k=1,2,3,\dots,\text{NCS}$, where NCS is the user-specified maximum number of topwidths (must be the same for all cross sections). Within the model, the topwidth table is integrated using the trapezoidal rule to obtain a table of cross-sectional area versus elevation. Linear interpolation is used for intermediate elevations between the k^{th} and $k+1$ user-specified tabular points. Areas associated with elevations exceeding the maximum value as specified in the table are linearly extrapolated.

The Manning n_{i_k} coefficient is user-specified for each i^{th} reach between adjacent cross sections or adjacent gages and varies with elevation (h_{i_k}) or discharge (Q_{i_k}) according to user-

specified tabular values similar to the topwidths table. Linear interpolation is used for n values associated with intermediate elevations/flows between the k^{th} and $k+1$ tabular points. Values of n for elevations/flows exceeding the tabular values are not extrapolated; they are assigned the n value associated with the maximum elevation/flow.

2.2 Solution Technique for Saint-Venant Equations

The expanded Saint-Venant equations, Eqs. (2.1-2.2), constitute a system of nonlinear, partial differential equations with two independent variables, x and t , and two dependent variables, h and Q ; the remaining terms are either functions of x , t , h , and/or Q , or they are constants. These equations are not amenable to analytical solutions except in cases where the channel geometry and boundary conditions are uncomplicated and the nonlinear properties of the equations are either neglected or made linear. Eqs. (2.1-2.2) may be solved numerically by performing two basic steps. First, the partial differential equations are represented by a corresponding set of approximate finite-difference algebraic equations; and second, the system of algebraic equations is solved in conformance with prescribed initial and boundary conditions.

Eqs. (2.1-2.2) can be solved by either “explicit” or “implicit” finite-difference techniques (Liggett and Cunge, 1975). Explicit methods, although simpler in application, are restricted by mathematical stability considerations to very small computational time steps (on the order of a few seconds for most dam-break waves and a few minutes for run-off generated waves). Such small time steps cause the explicit methods to be very inefficient in the use of computer time. Implicit finite-difference techniques (Preissmann, 1961; Amein and Fang, 1970; Strelkoff, 1970), however, have no restrictions on the size of the time step due to mathematical stability; however, convergence considerations may require its size to be limited (Fread, 1974b). Although the implicit method is almost always preferred, a particular explicit method is provided as a user-specified option in FLDWAV in order to treat certain applications involving mixed (subcritical/supercritical) flows. This explicit option is described later in Sub-section 5.3.

Of the various implicit schemes that have been developed, the "weighted four-point" scheme first used by Preissmann (1961), and somewhat later by Chaudhry and Contractor (1973) and Fread (1974a, 1974b, 1978a) appears most advantageous since it can readily be used with unequal distance and time steps and its stability-convergence properties can be conveniently controlled. In the weighted, four-point implicit finite-difference scheme, the continuous x-t (space-time) region in which solutions of h and Q are sought, is represented by a rectangular net of discrete points shown in Figure 2.4. The net points are determined by the intersection of lines drawn parallel to the x- and t-axes. Those parallel to the t-axis represent locations of cross sections; they have a spacing of Δx_i , which need not be constant. Those parallel to the x-axis represent time lines; they have a spacing of Δt_j , which also need not be constant. Each point in the rectangular network can be identified by a subscript (i) which designates the x-position and a superscript (j) which designates the particular time line. The time derivatives are approximated by a forward-difference quotient centered between the i^{th} and $i+1$ points along the x-axis, i.e.,

$$\frac{\partial \Psi}{\partial t} = \frac{\Psi_i^{j+1} + \Psi_{i+1}^{j+1} - \Psi_i^j - \Psi_{i+1}^j}{2 \Delta t_j} \dots \dots \dots (2.16)$$

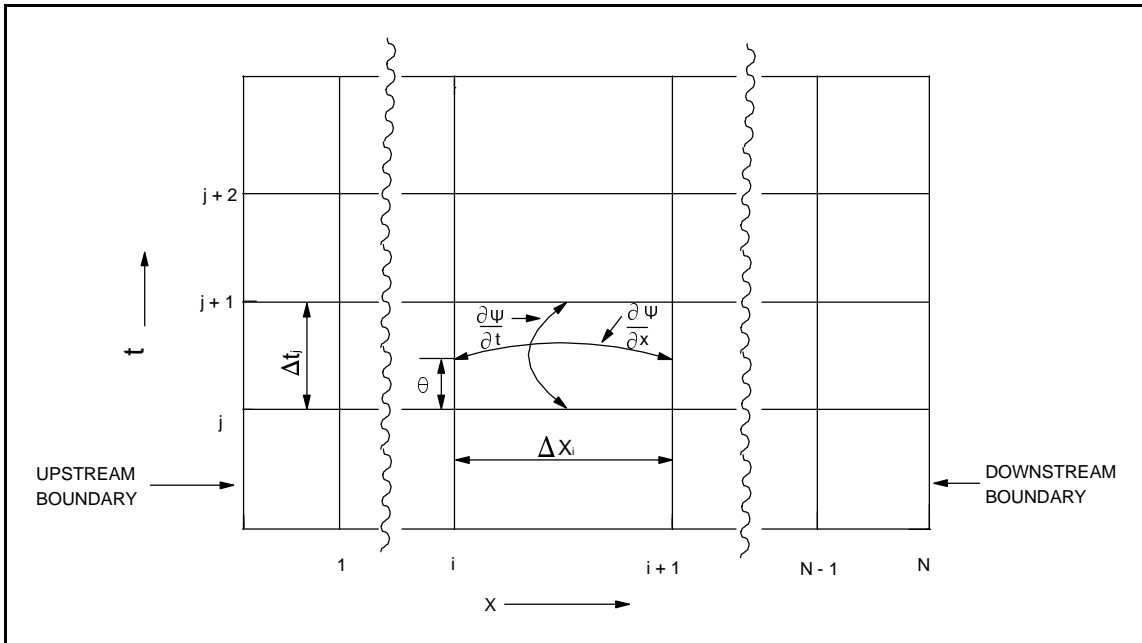


Figure 2.4 - Discrete x-t Solution Domain

where Ψ represents any variable (Q , h , A , A_o , s_{co} , s_m , etc.).

The spatial derivatives are approximated by a forward-difference quotient positioned between two adjacent time lines according to weighting factors of θ and $(1-\theta)$, i.e.,

$$\frac{\partial \Psi}{\partial x} = \theta \left[\frac{\Psi_{i+1}^{j+1} - \Psi_i^{j+1}}{\Delta x_i} \right] + (1-\theta) \left[\frac{\Psi_{i+1}^j - \Psi_i^j}{\Delta x_i} \right] \dots\dots\dots (2.17)$$

Variables other than derivatives are approximated at the time level where the spatial derivatives are evaluated by using the same weighting factors, i.e.,

$$\Psi = \theta \left[\frac{\Psi_i^{j+1} + \Psi_{i+1}^{j+1}}{2} \right] + (1-\theta) \left[\frac{\Psi_i^j + \Psi_{i+1}^j}{2} \right] \dots\dots\dots (2.18)$$

A θ weighting factor of 1.0 yields the fully implicit or backward difference scheme used by Baltzer and Lai (1968). A weighting factor of 0.5 yields the box scheme used by Amein and Fang (1970). The influence of the θ weighting factor on the accuracy of the computations was examined by Fread (1974b), who concluded that the accuracy tends to somewhat decrease as θ departs from 0.5 and approaches 1.0. This effect becomes more pronounced as the magnitude of the computational time step increases. Usually, a weighting factor of 0.55 to 0.60 is used so as to minimize the loss of accuracy associated with greater values while avoiding the possibility of a weak or pseudo instability noticed by Baltzer and Lai (1968), and Chaudhry and Contractor (1973) for θ values of 0.5; however, θ may be user-specified other than the recommended value of 0.55 to 0.60 via the F1 parameter in the FLDWAV model.

When the finite-difference operators defined by Eqs. (2.16-2.18) are used to replace the derivatives and other variables in Eqs. (2.1-2.2), the following weighted, four-point implicit, finite-difference equations are obtained:

$$\theta \left[\frac{Q_{i+1}^{j+1} - Q_i^{j+1}}{\Delta x_i} \right] - \theta q_i^{j+1} + (1-\theta) \left[\frac{Q_{i+1}^j - Q_i^j}{\Delta x_i} \right] - (1-\theta) q_i^j$$

$$+ \left[\frac{s_{co_i}^{j+1} (A+A_o)_i^{j+1} + s_{co_i}^{j+1} (A+A_o)_{i+1}^{j+1} - s_{co_i}^j (A+A_o)_i^j - s_{co_i}^j (A+A_o)_{i+1}^j}{2\Delta t_j} \right] = 0 \dots\dots\dots (2.19)$$

$$\left[\frac{(s_{m_i} Q_i)^{j+1} + (s_{m_i} Q_{i+1})^{j+1} - (s_{m_i} Q_i)^j - (s_{m_i} Q_{i+1})^j}{2\Delta t_j} \right] + \theta \left[\frac{(\beta Q^2/A)_{i+1}^{j+1} - (\beta Q^2/A)_i^{j+1}}{\Delta x_i} \right]$$

$$+ g \bar{A}^{j+1} \left(\frac{h_{i+1}^{j+1} - h_i^{j+1}}{\Delta x_i} + \bar{S}_f^{j+1} + S_e^{j+1} + \bar{S}_i^{j+1} \right) + L_i^{j+1} + (W_f \bar{B})_i^{j+1}$$

$$+ (1-\theta) \left[\frac{(\beta Q^2/A)_{i+1}^j - (\beta Q^2/A)_i^j}{\Delta x_i} + g \bar{A}^j \left(\frac{h_{i+1}^j - h_i^j}{\Delta x_i} + \bar{S}_f^j + S_e^j + \bar{S}_i^j \right) \right]$$

$$+ L_i^j + (W_f \bar{B})_i^j = 0 \dots\dots\dots (2.20)$$

where:

$$\bar{A} = \frac{A_i + A_{i+1}}{2} \dots\dots\dots (2.21)$$

$$\bar{S}_f = \left[\frac{n_i^2 \bar{Q} |\bar{Q}|}{\mu^2 \bar{A}^2 \bar{R}^{4/3}} \right] = \frac{\bar{Q} |\bar{Q}|}{\bar{K}^2} \dots\dots\dots (2.22)$$

$$\bar{Q} = \frac{Q_i + Q_{i+1}}{2} \dots\dots\dots (2.23)$$

$$\bar{R} = \frac{\bar{A}}{\bar{B}} \quad \text{or} \quad \bar{R} = \frac{\bar{A}}{\bar{P}} \dots\dots\dots (2.24)$$

$$\bar{B} = \frac{B_i + B_{i+1}}{2} \dots\dots\dots (2.25)$$

$$\bar{K} = \frac{K_i + K_{i+1}}{2} \dots\dots\dots (2.26)$$

$$\bar{P} = \frac{P_i + P_{i+1}}{2} \dots\dots\dots (2.27)$$

where: P_i is the wetted perimeter given by the following:

$$P_{i_1} = B_{i_1} \dots\dots\dots (2.28)$$

$$P_{i_k} = P_{i_{k-1}} + 2 \left[0.25 (B_{i_k} - B_{i_{k-1}})^2 + (h_{i_k} - h_{i_{k-1}})^2 \right]^{1/2} \quad (k=2,3,\dots) \dots\dots\dots (2.29)$$

The hydraulic radius (R) used in Eqs. (2.22, 2.24) is normally evaluated within FLDWAV as A/B or the hydraulic depth (D). This is satisfactory for almost all river channels since $A/B \approx A/P$, where P is the wetted perimeter. For very narrow, deep channels ($B < 10 D$) this approximation is not as good. Therefore, a user-specified option for $R = A/P$ is available in FLDWAV by providing a value of unity to the control parameter, KPRES. When this option is selected, the wetted perimeter (P) is computed from the user-specified topwidth (B_k) versus elevation (H_k) table according to Eqs. (2.28-2.29). The term (\bar{S}_i) is evaluated using Eq. (2.13) in which $D = \bar{R}$, $Q = \bar{Q}$, and $A = \bar{A}$.

The terms associated with the j^{th} time line are known from either the initial conditions or previous computations. The initial conditions refer to values of h_i^j and Q_i^j at each node along the x-axis for the first time line ($j=1$). The initial conditions are further described later in Section 4.

Eqs. (2.19-2.20) cannot be solved in an explicit or direct manner for the unknowns since there are four unknowns Q_i^{j+1} , h_i^{j+1} , Q_{i+1}^{j+1} , h_{i+1}^{j+1} and only two equations. However, if Eqs. (2.19-2.20) are applied to each of the (N-1) rectangular grids shown in Figure 2.4 between the upstream

and downstream boundaries, a total of $(2N-2)$ equations with $2N$ unknowns can be formulated. (N denotes the total number of nodes or cross sections.) Then, prescribed boundary conditions for subcritical flows, one at the upstream boundary and one at the downstream boundary, provide the necessary two additional equations required for the system to be determinate (same number of equations and number of unknowns). The boundary conditions are further described later in Section 3. The resulting system of $2N$ nonlinear equations with $2N$ unknowns is solved by a functional iterative procedure, the Newton-Raphson method (Amein and Fang, 1970).

Computations for the iterative solution of the nonlinear system are begun by assigning trial values to the $2N$ unknowns. Substitution of the trial values into the system of nonlinear equations yields a set of $2N$ residuals. The Newton-Raphson method provides a means for correcting the trial values until the residuals are reduced to a suitable tolerance level, near zero. This is usually accomplished in one or two iterations through use of linear extrapolation for the first trial values. If the Newton-Raphson corrections are applied only once, i.e., there is no iteration, the nonlinear system of difference equations degenerates to the equivalent of a quasi-linear, finite-difference formulation (Barkou, 1985) of the Saint-Venant equations which often will require smaller time steps than the nonlinear formulation (used in FLDWAV) for the same degree of numerical accuracy.

A system of $2N \times 2N$ linear equations relates the corrections to the residuals and to a Jacobian coefficient matrix composed of partial derivatives of each equation with respect to each unknown variable in that equation. The Jacobian (coefficient) matrix of the linear system has a banded structure as shown in Figure 2.5 which allows the system to be solved by a compact, quad-diagonal, Gaussian elimination algorithm (Fread, 1971, 1985a), which is very efficient with respect to computing time and storage. The required storage is reduced from $2N \times 2N$ to $2N \times 4$ and the required number of computational steps is greatly reduced from $16/3N^3 + 8N^2 + 14/3N$ to approximately $38N$. A more detailed treatment of the solution technique is given elsewhere by Fread (1978a, 1985b).

When flow is supercritical throughout the entire routing reach of channel/floodplain, the solution technique previously described can be somewhat simplified. Instead of a solution involving

2N x 2N equations, supercritical flow can be solved via a system of only 2x2 equations. The unknown h and Q at the upstream section are determined from the two boundary equations. Then, progressing from upstream to downstream in a cascading manner, Eqs. (2.19-2.20) are used to obtain h_{i+1} and Q_{i+1} at each section. Since Eqs. (2.19-2.20) are nonlinear with respect to h_{i+1} and Q_{i+1} , they are solved by the Newton-Raphson iterative technique applied to a system of two equations with two unknowns. For supercritical flow, this technique has been found to provide a somewhat more stable solution than one involving 2N x 2N equations (Traver, 1988). When the flow is a mixture of subcritical and supercritical in time and/or space, special user-specified techniques described later in Section 5 are used within FLDWAV.

a	a	0	0	0	0	0	0	0	0	0	0	0	0
a	a	a	a	0	0	0	0	0	0	0	0	0	0
a	a	a	a	0	0	0	0	0	0	0	0	0	0
0	0	a	a	a	a	0	0	0	0	0	0	0	0
0	0	a	a	a	a	0	0	0	0	0	0	0	0
0	0	0	0	a	a	a	a	0	0	0	0	0	0
0	0	0	0	a	a	a	a	0	0	0	0	0	0
.
.
0	0	0	0	0	0	0	0	0	a	a	a	a	0
0	0	0	0	0	0	0	0	0	a	a	a	a	0
0	0	0	0	0	0	0	0	0	0	0	a	a	a
0	0	0	0	0	0	0	0	0	0	0	a	a	a
0	0	0	0	0	0	0	0	0	0	0	0	a	a

Figure 2.5 - Jacobian Coefficient Matrix

3. BOUNDARY CONDITIONS

Unsteady flows usually occur because of the flow conditions at the upstream most location of the river reach for which FLDWAV is being used to simulate/forecast the flow changes through the routing reach. This is known as the upstream boundary condition. Each tributary that is being simulated using the Saint-Venant equations also has an upstream boundary condition. Also, at the most downstream location of the main river, another boundary condition also influences the flow behavior within the river reach being simulated. This is known as the downstream boundary condition.

3.1 Upstream Boundary

The upstream boundary shown in Figure 3.1 is required to obtain a solution of the Saint-Venant equations. In the FLDWAV model, this is either a user-specified discharge or water-surface elevation hydrograph, i.e.,

$$Q_1 = Q(t) \dots\dots\dots (3.1)$$

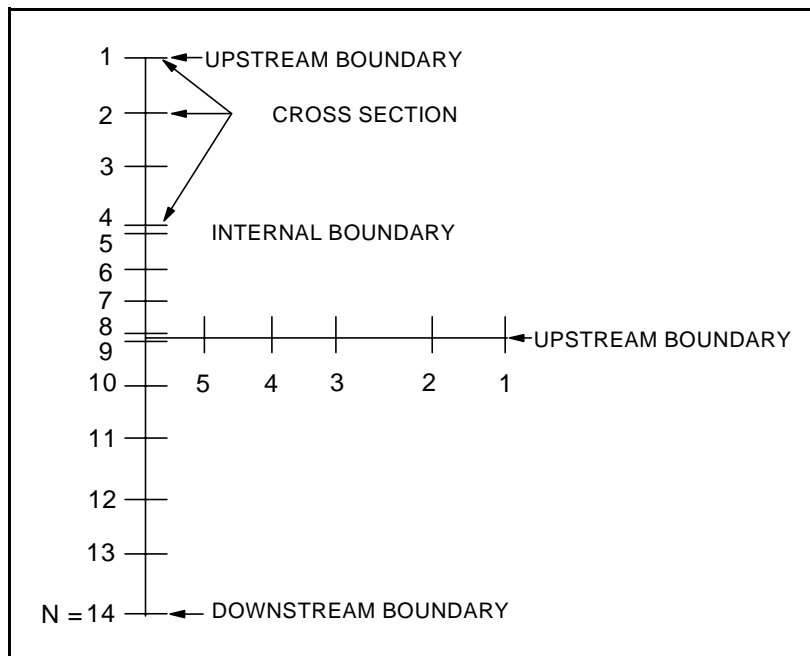


Figure 3.1 - Boundary Conditions

$$\text{or} \quad h_1 = h(t) \dots\dots\dots (3.2)$$

in which Q_1 is the flow at section 1 (the most upstream cross section), $Q(t)$ represents a time series of user- specified flow at each time (t), h_1 is the water-surface elevation (or stage) at section 1, and $h(t)$ represents a time series of user-specified water-surface elevation at each time (t). The hydrograph values, are user-specified at either constant or variable time intervals. Intermediate values are linearly interpolated from the table of discharge/water surface-elevation versus time. If the upstream flow/water-surface elevation is steady, i.e., it is constant for all time, the table has the same user-specified value for all times. Generally, the upstream value will not be zero. Also, the upstream hydrograph should be user-specified for the total duration of time that the Saint-Venant equations are to be solved. An upstream hydrograph must be user-specified at the upstream end of each river in the system.

When doing some modeling sensitivity studies, the inflow hydrograph may be user-specified within FLDWAV conveniently as a mathematical gamma function (Fread, 1974b), i.e.,

$$Q(t) = Q_o + (\rho - 1) \left(\frac{t}{T_p} \right)^{\frac{1}{\gamma' - 1}} e^{\left(\frac{1}{\gamma' - 1} \right) \left(1 - \frac{t}{T_p} \right)} \dots\dots\dots (3.3)$$

where Q_o is the initial base flow, T_p is the time from initial steady flow to the peak flow (Q_p), ρ is the ratio of Q_p to Q_o , γ' is the ratio (the time from initial steady flow to the center of gravity of the hydrograph/ T_p). If the inflow hydrograph is the water-surface elevation, the discharge information in Eq. (3.3) is replaced with the equivalent water-surface elevation information.

3.2 Downstream Boundary

The downstream boundary shown in Figure 3.1 is located at the downstream extremity of the most downstream routing reach of a single river or the main-stem river of a system of dendritic (tree-type) rivers. When the flow at the downstream boundary is subcritical, i.e.,

$$Fr_N = V_N / (gA_N/B_N)^{0.5} < 1 \dots\dots\dots (3.4)$$

where $V_N = Q_N / A_N$ and N designates the sequence number of the most downstream cross section, a known relationship between flow and depth or depth and time must be user-specified. Depending on the physical characteristics of the downstream section, the FLDWAV model allows the user to specify the appropriate one of the following six downstream boundary equations:

(1) Single-value rating:

$$Q_N^{j+1} = Q(h) \dots\dots\dots (3.5)$$

in which $Q(h)$ represents a user-specified tabular relation of Q and h .

(2) Generated dynamic loop-rating using the Manning equation with a dynamic energy slope term (S) computed by one of two user-selection options (Fread, 1973b, 1975, 1977):

$$Q_N^{j+1} = \frac{\mu}{n_N} A_N^{j+1} R_N^{j+1 2/3} S_{N-1}^{1/2} = K_N^{j+1} S_{N-1}^{1/2} \dots\dots\dots (3.6)$$

where:

$$S_{N-1} = \frac{h_{N-1} - h_N}{\Delta x_{N-1}} + \frac{(Q_N' - Q_N)}{0.5g (A_N + A_{N-1}) \Delta t} + \frac{(Q_{N-1}^2/A_{N-1} - Q_N^2/A_N)}{0.5g (A_N + A_{N-1}) \Delta x_{N-1}} \dots\dots\dots (3.7)$$

or

$$S_{N-1} = \frac{n_N^2 \bar{Q} \bar{Q}}{\mu^2 \bar{A} \bar{R}^{4/3}} \dots\dots\dots (3.8)$$

in which Q_N' is the discharge at time t^{j+1} and all other terms in the equation are at the j^{th} time ($t - \Delta t$), $\mu=1.49$ for English units and 1.0 for SI units, and \bar{A} , \bar{Q} , \bar{R} are reach average values for the $N-1$ reach according to Eqs. (2.21-2.25).

(3) Generated single-value rating in which Eq. (3.6) is used, but S is user-specified as the channel bottom slope in the vicinity of the N^{th} cross section.

(4) Critical flow rating that occurs at a waterfall or beginning of a short, steep rapids:

$$Q_N^{j+1} = \left[g \left(A_N^{j+1} \right)^3 / B_N^{j+1} \right]^{0.5} \dots\dots\dots (3.9)$$

(5) Water-surface elevation time series:

$$h_N^{j+1} = h(t) \dots\dots\dots (3.10)$$

in which $h(t)$ represents a user-specified time series of water-surface elevation at each time (t) at the N^{th} cross section.

(6) Discharge time series:

$$Q_N^{j+1} = Q(t) \dots\dots\dots (3.11)$$

in which $Q(t)$ represents a user-specified time series of discharge (flow) at each time (t) at the N^{th} cross section.

If channel control exists, i.e., the flow at section N is controlled by the channel properties, then either Eq. (3.5) or (3.6) can be selected. Eq. (3.5) is useful if an empirical $Q(h)$ relation is available which is essentially single-valued, i.e., for each water-surface elevation there is only one discharge. When a known $Q(h)$ relation does not exist, option (3) can be used; or when the relation is not single-valued, then the dynamic loop-rating, Eq. (3.6) may be used. The loop-rating allows two water-surface elevations to exist for each discharge value. On the rising limb of the hydrograph, the water-surface elevation is usually less than that which occurs for the same discharge on the recession limb. The magnitude (Δh_L) of the loop (the maximum difference between two water-surface elevations associated with the same discharge) is directly proportional to the rate of increase in water-surface elevation and inversely proportional to the invert slope of the channel. Thus for the

rapidly rising hydrographs associated with dam-break floods, the loop-rating is more likely to be significant; although if the channel slope is quite steep (say, 150 ft/mi or greater), the loop will probably be less than 0.5 feet. On the other hand, slowly changing hydrographs along mildly sloping rivers (less than 5 ft/mi) may also produce significant loops. The user can estimate the magnitude of the loop (Fread, 1973b, 1975) with the following:

$$\Delta h_L = \bar{Q} \bar{n} / (\mu \bar{B}) \left[\frac{1}{(S_0 - a)^{0.3}} - \frac{1}{(S_0 + a)^{0.3}} \right] \dots \dots \dots (3.12)$$

where:

$$a = 0.5 \delta h \bar{n} / (S_0^{1/2} \bar{D}^{2/3}) \dots \dots \dots (3.13)$$

in which $D=A/B$ is the hydraulic depth (ft), S_0 is the channel bottom slope (ft/ft) or water-surface slope at low flow, δh is the rate of rise of the water elevation (ft/sec), the bar (-) over the variables (Q , n and B) represents the average value for each, and Δh_L is the magnitude of the loop (ft).

Dynamic loops are judged to be significant when $\Delta h_L > 1$ foot.

The dynamic loop-rating, Eq. (3.6), may be subject to numerical instability when the channel bottom slope S_0 is less than about one ft/mi. In this situation, the S term as computed by Eq. (3.7) may be user-specified to be computed by Eq. (3.8) which yields more stable results than those using Eq. (3.7). If the solution remains unstable, the downstream boundary can be relocated a sufficient distance further downstream of the original downstream boundary location and Eq. (3.6) with $S=S_0$ can be user-specified. Errors in Q and h due to the alternate use of a single-value rating (which is not subject to numerical problems) are increasingly damped-out as the downstream boundary is moved further and further downstream from the vicinity of the original boundary location where computed Q and h values are of interest. A channel control boundary, Eq. (3.5) or (3.6) should not be located where changes in flow further downstream can affect the flow at the chosen boundary location, e.g., just upstream of where a significant tributary flow enters, or within the backwater effect of a bridge, dam, or tidal fluctuation.

A user-specified water-surface elevation time series may be used when the downstream boundary is located in a wide estuary or bay where the water-surface elevation is controlled only by the tidal fluctuation and not by the flow emanating from the upstream routing reach. This requires that the boundary be located far enough into the estuary or bay that the incoming flow does not appreciably raise the water surface at that chosen location. Also, this boundary condition can be used when the channel terminates into a large lake whose level is not appreciably influenced by the incoming flow. In this case, the water-surface elevation is user-specified as a constant value for all time during the simulation. When modeling dendritic river systems, the downstream boundary on each tributary is a water-surface elevation time series automatically generated by FLDWAV as the average water-surface elevation at the confluence of the tributary with the other river.

A single-value rating, Eq. (3.5), may also be used when the downstream boundary is a dam where the total flow through the dam is controlled by the water-surface elevation occurring immediately upstream of the dam and not by the water elevation downstream of the dam due to tailwater submergence conditions affecting spillway or gated outflows.

3.3 Internal Boundaries

There can be structures such as dams, bridges, or waterfalls (short rapids) along a waterway (channel/floodplain) where the Saint-Venant equations are not applicable. At these internal locations (boundaries) shown in Figure 3.1, the flow is rapidly varied (spatially) rather than gradually varied as necessary for the applicability of the Saint-Venant equations. Empirical water-surface elevation-discharge relations such as that for weir flow can be utilized for simulating rapidly-varying flow. In FLDWAV, unsteady flows are routed along the waterway including locations of rapidly-varying flow by utilizing internal boundaries. At internal boundaries, cross sections are user-specified for the upstream and downstream extremities of the short reach of waterway encompassing the rapidly-varying flow. The short reach length between the two cross sections can be any value from approximately zero to the actual measured distance. Since, as with any other Δx reach, two equations (the Saint-Venant equations) are required, the internal boundary- Δx reach also requires two equations. The first of the required equations represents the conservation of mass with

negligible time-dependent storage and lateral flow, and the second is an empirical, spatially-rapidly-varied flow equation representing weir, orifice, critical flow, etc. The internal boundary equations are:

$$Q_i = Q_{i+1} \dots\dots\dots (3.14)$$

$$Q_i = Q_s + Q_b \dots\dots\dots (3.15)$$

in which Q_s and Q_b are the spillway and breach flow, respectively. The breach flow (Q_b) will be treated later in Section 6. In this way, the flows Q_i and Q_{i+1} and the elevations h_i and h_{i+1} are in balance with the other flows and elevations occurring simultaneously throughout the entire flow system which may consist of additional dams or bridges which are treated as additional internal boundary conditions via Eqs. (3.14-3.15). In fact, FLDWAV can simulate the progression of a dam-break flood or any other type of unsteady flow through an unlimited number of dams and/or bridges in any combination located sequentially along the main-stem river or its tributaries. Any of the dams or bridge-embankments can breach if they are sufficiently overtopped relative to user-specified criteria.

3.3.1 Dams

A dam can have several components that pass (emit) discharge, including spillways, gates, and turbines (Fread, 1988). Figure 3.2 shows a typical dam which can be modeled within FLDWAV. Flow may pass through the structure via any of these components as well as over the top of the dam. In the event of failure, flow may also pass through the breach which is formed in the failure process. A dam may be considered an internal boundary defined by a short Δx_i reach between sections i and $i+1$ in which the flow is governed by Eqs. (3.14-3.15). In Eq. (3.14), the spillway flow (Q_s) is computed from the following expression:

$$Q_s = Q_{\text{spillway}} + Q_{\text{gate}} + Q_{\text{dam}} + Q_t \dots\dots\dots (3.16)$$

where Q_{spillway} , Q_{gate} , Q_{dam} , and Q_t represent flow through the respective components.

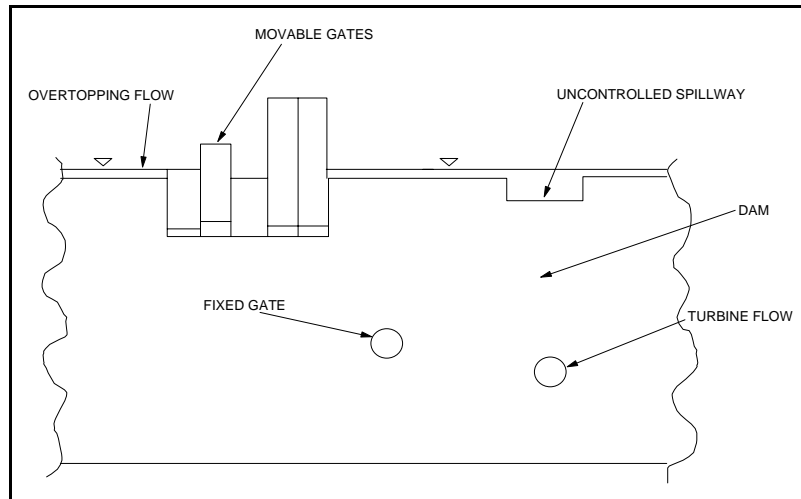


Figure 3.2 - Front-View of Dam with Discharge Components.

3.3.1.1 Uncontrolled Spillways

Uncontrolled spillway flow which passes through the dam and can be represented as weir flow (e.g. emergency spillway or main spillway). The flow can be represented by either an empirical head-discharge rating curve similar to Eq. (3.5) which is user-specified, or automatically generated using the following:

$$Q_{\text{spillway}} = k_{\text{sp}} c_{\text{sp}} L_{\text{sp}} (h - h_{\text{sp}})^{1.5} \dots \dots \dots (3.17)$$

in which c_{sp} is the user-specified uncontrolled spillway discharge coefficient, $(h - h_{\text{sp}})$ is the computed head, h_{sp} is the user-specified uncontrolled spillway crest elevation, L_{sp} is the user-specified spillway length, and k_{sp} is a automatically computed submergence correction factor ($0 \leq k_{\text{sp}} \leq 1$) for tailwater effects, i.e.,

$$k_{\text{sp}} = 1 - 27.8 \left(\frac{h_{\text{tw}} - h_{\text{sp}}}{h - h_{\text{sp}}} - 0.67 \right)^3 \dots \dots \dots (3.18)$$

where h_{tw} and h are the tailwater and reservoir pool elevations, respectively. Only one spillway can be simulated at a particular dam. If more that one spillway exists at a single dam structure, they can be combined into a single empirical rating curve. The limitation of combining multiple spillways is

that the submergence correction may be inaccurate since Eq. (3.18) is based on a single spillway crest elevation.

3.3.1.2 Fixed Gate(s)

Several gates may exist in a dam. When the gates are fixed, the flow through a fixed-gated spillway is computed using the following:

$$Q_{gate} = \sqrt{2g} c_g A_g (h-h_g)^{0.5} \dots\dots\dots (3.19)$$

where A_g is the user-specified gate flow area (fixed in time), c_g is the user-specified fixed-gated spillway discharge coefficient ($0.5 \leq c_g \leq 0.75$), $(h-h_g)$ is the computed head, and h_g is the user-specified center-line elevation of the gated spillway or it is the automatically computed tailwater elevation if the latter is greater. If several gate openings share a common gate sill, they can be combined into one gate and user-specified as an averaged fixed-gate opening. The fixed-gated spillway flow can also be represented as a table of head versus discharge values.

3.3.1.3 Movable Gate

The gate flow may also be user-specified as a function of time via a movable-gate option. Time-dependent, movable-gate flow (Wortman, 1983; Fread, 1988) can be simulated with the FLDWAV model by specifying the movable-gate height (H_g) above the user-specified gate sill elevation (h_g) and the width of gate opening (W_g). H_g and W_g are user-specified as functions of time. The gate flow may be either orifice flow and/or weir flow. Weir flow occurs if the gate is not submerged sufficiently or as overtopping flow (Q_{og}) when the reservoir water-surface elevation is sufficiently above the top of the dam (h_d) which is assumed within FLDWAV to be coincident with the top of the gate in its closed position. Time-dependent orifice gate flow (Q_g) is computed as follows:

$$Q_{\text{gate}} = \sqrt{2g} C_o W_g H_g (\hat{h} - 0.5 H_g)^{0.5} + Q_{\text{og}} \quad \text{if } \hat{h} > 1.2 H_g \dots\dots\dots (3.20)$$

where:

$$C_o = \frac{0.712}{W_g} \left[W_d - 2 (0.02 W_d/40 + 0.1) \hat{h}_d \right] (\hat{h}/\hat{h}_d)^{0.1} \quad 0.40 \leq C_o \leq 0.71 \dots\dots\dots (3.21)$$

$$\hat{h} = h - h_g \dots\dots\dots (3.22)$$

$$Q_{\text{og}} = 3.1 W_g (h - h_d - H_g)^{1.5} \quad \text{if } h > h_d + H_g \dots\dots\dots (3.23)$$

otherwise, $Q_{\text{og}} = 0$. If the tailwater elevation (h_{tw}) is greater than $h_g + 0.5 H_g$, then $(\hat{h} - 0.5 H_g)$ in Eq. (3.20) is replaced by the differential head across the gate, i.e., $h - h_{\text{tw}}$. Time-dependent weir flow (Q_{gate}) through the gate is computed as follows:

$$Q_{\text{gate}} = Q_d \left[1 - (1 - H_g/\hat{h})^{1.5} \right] (\hat{h}/\hat{h}_d)^{1.6} \quad \text{if } H_g \leq \hat{h} \leq 1.2 H_g \dots\dots\dots (3.24)$$

where:

$$Q_d = 3.9 k_g \left[W_d - 2 (0.02 W_d/40 + 0.1) \hat{h}_d \right] \hat{h}_d^{1.5} \dots\dots\dots (3.25)$$

$$\hat{h} = h - h_g \dots\dots\dots (3.26)$$

$$\hat{h}_d = h - h_g \quad \text{at } t = 0 \dots\dots\dots (3.27)$$

$$W_d = W_g \quad \text{maximum for all time (t)} \dots\dots\dots (3.28)$$

$$Q_{\text{gate}} = Q_d (\hat{h}/\hat{h}_d)^{1.6} \quad 0 < \hat{h} < H_g \dots\dots\dots (3.29)$$

$$k_g = 1.0 - 27.8 \left[(h_{\text{tw}} - h_g)/\hat{h} - 0.67 \right]^3 \quad \text{if } (h_{\text{tw}} - h_g)/\hat{h} > 0.67 \dots\dots\dots (3.30)$$

otherwise $k_g = 0$ ($0 \leq k_g \leq 1$). There will be some error in the computed flow when the gate is narrow, i.e., small W_g relative to H_g . The term \hat{h}_d is the initial ($t=0$) value for \hat{h} . Transition from orifice flow to weir flow may produce a slight discontinuity.

3.3.1.4 Average Multiple-Movable Gates

Time-dependent, movable-gate flow may also be computed for multiple gates. The technique described in Section 3.3.1.3, which assumes that there is only one gate, may be used. The user must manipulate the multiple gate openings to obtain an average gate which represents the setting of the multiple movable gates.

3.3.1.5 Dam Overtopping Flow

Flow over the top of the dam may be computed using the following:

$$Q_{\text{dam}} = k_d c_d L_d (h - h_d)^{1.5} + Q_b \dots\dots\dots (3.31)$$

where h_d is the user-specified height (elevation) of dam crest, k_d is a submergence correction for tailwater effects computed with Eq. (3.17) with h_{sp} replaced by user-specified h_d , c_d is the user-specified discharge coefficient for flow over the crest of the dam, L_d is the user-specified length of the dam crest less L_s and the length of the gates located along the dam crest (L_d may also vary with h according to a user-specified table of L_d versus h ; this allows for dam crests which are not level). The last term (Q_b) is the dam breach outflow and is described later in Section 6.

3.3.1.6 Turbine Flow

Turbine flow (Q_t) usually represents a constant flow which is head independent; however, it may also be variable with time. Since FLDWAV requires the initial condition to have a non-zero minimum flow, the Q_t parameter may also be used to pass a minimum flow through the dam when the initial pool elevation is below any spillway crests or gate sill elevations such that spillway and/or gate flows are zero.

3.3.2 Bridges

Highway/railway bridges and their associated earthen embankments (as shown in Figure 3.3) which are located anywhere along the routing reach may be treated also as internal boundary conditions. Eqs. (3.14-3.15) are used at each bridge; the term Q_s in Eq. (3.14) is computed by the following expression (Fread, 1988):

$$Q_s = \sqrt{2g} C A_{br} (h_i - h_{i+1} + V_i^2/2g - \Delta h_f)^{1/2} + cc_u L_u k_u (h_i - h_{cu})^{3/2} + cc_\ell L_\ell k_\ell (h_i - h_{cl})^{3/2} \dots (3.32)$$

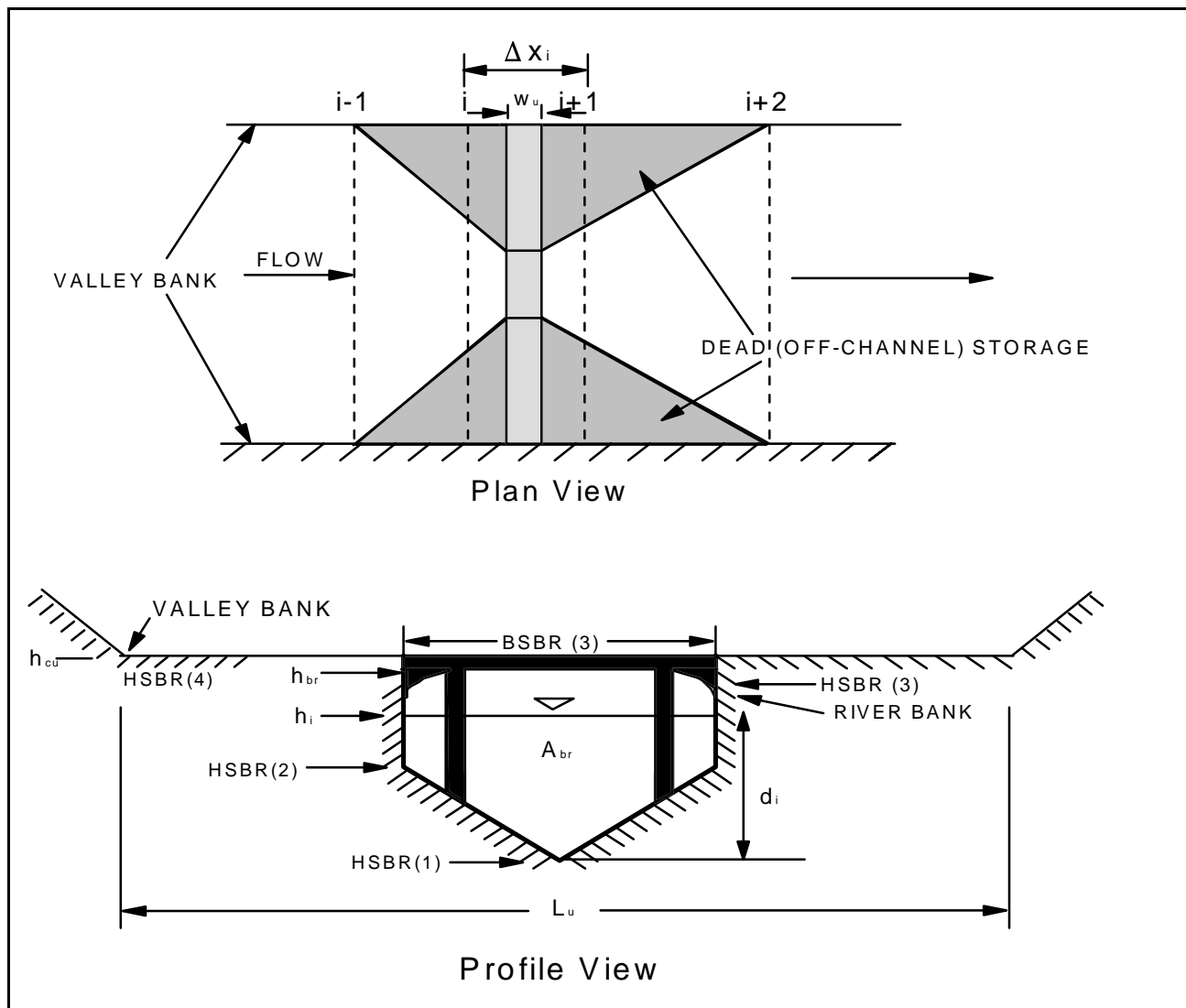


Figure 3.3 - Schematic of Bridge

in which,

$$k_u = 1.0, \quad \text{if } h_{ru} \leq 0.76 \quad \dots\dots\dots (3.33)$$

$$k_u = 1.0 - c_u(h_{ru} - 0.76)^3, \quad \text{if } h_{ru} > 0.76 \quad \dots\dots\dots (3.34)$$

$$c_u = 133(h_{ru} - 0.78) + 10, \quad \text{if } 0.76 < h_{ru} \leq 0.96 \quad \dots\dots\dots (3.35)$$

$$c_u = 400(h_{ru} - 0.96) + 34, \quad \text{if } h_{ru} > 0.96 \quad \dots\dots\dots (3.36)$$

$$h_{ru} = (h_{i+1} - h_{cu})/(h_i - h_{cu}) \quad \dots\dots\dots (3.37)$$

$$cc_u = 3.02(h_u - h_{cu})^{0.015}, \quad \text{if } 0 < h_u \leq 0.15 \quad \dots\dots\dots (3.38)$$

$$cc_u = 3.06 + 0.27(h_u - 0.15), \quad \text{if } h_u > 0.15 \quad \dots\dots\dots (3.39)$$

$$h_u = (h_i - h_{cu})/w_u \quad \dots\dots\dots (3.40)$$

$$\Delta h_f = \Delta x_i (Q_{br}/\bar{K}_i)^2 \quad \dots\dots\dots (3.41)$$

$$Q_{br} = \sqrt{2g} C A_{br} (h_i - h_{i+1} + V_i^2/2g)^{1/2} \quad \dots\dots\dots (3.42)$$

$$V = Q_i/A_i \quad \dots\dots\dots (3.43)$$

in which C is a user-specified coefficient of bridge flow which accounts for piers, alignment, etc. (Chow, 1959), A_{br} is the cross-sectional flow area of the bridge opening at section i+1 (downstream end of bridge) which is user-specified via a tabular relation of wetted topwidth versus elevation, h_{cu} is the user-specified elevation of the upper embankment crest, h_i is the water-surface elevation at section i (slightly upstream of bridge), h_{i+1} is the water-surface elevation at section i+1 (slightly downstream of the bridge), V is the velocity of flow within the bridge opening, L_u is the user-specified length of the upper embankment crest perpendicular to the flow direction including the length of bridge at elevation h_{cu} (L_u may be user-specified as a tabular relation with elevation), k_u is the computed submergence correction factor for flow over the upper embankment crest, and w_u is the user-specified width (parallel to flow direction) of the crest of the upper embankment. In Eq. (3.32), the terms with an (ℓ) subscript refer to a lower embankment crest, and these terms are defined by Eqs. (3.33-3.40) in which the (u) subscripts are replaced with (ℓ) subscripts. Eqs. (3.33-3.40) were developed from basic information on flow over road embankments as reported by the U.S. Dept. of

Transportation (1978). When the bridge opening becomes submerged, C in Eqs. (3.32) and (3.42) is replaced by C' for orifice flow according to the following:

$$C' = c_o C \quad \dots\dots\dots (3.44)$$

$$\text{where: } c_o = 1.0 - (r - 0.09) \quad \text{if } 0.09 \leq r \leq 0.31 \quad \dots\dots\dots (3.45)$$

$$\text{otherwise, } c_o = 1.0, \quad \dots\dots\dots (3.46)$$

$$\text{and } r = (h_i - h_{br})/d_i \quad \dots\dots\dots (3.47)$$

in which h_{br} is the user-specified elevation of the bottom of the bridge deck, and d_i is the computed flow depth at section i located slightly upstream of the upstream face of the bridge. The FLDWAV model creates a table of A_{br} from user-specified tabular values of the width (BSBR) of the bridge opening versus elevation (HSBR); the highest user-specified elevation for the table is h_{br} and at this elevation the width of the bridge opening must be zero, while the next lower elevation (say 0.01 ft lower) is associated with the total width of the bridge opening.

The cross section designated by $i+1$ should represent the cross section slightly downstream of the bridge opening; the cross-section properties include the active portion of the channel closely related to the constricted bridge opening, and the cross section properties also include the off-channel storage portions as shown in Figure 3.3. A contraction coefficient (k_{ce}) should be user-specified for the Δx_{i-1} reach upstream of cross section i , and an expansion coefficient should be user-specified for the Δx_{i+1} reach downstream of cross section $i+1$.

3.3.3 Waterfalls or Rapids

If a short reach of the river contains a waterfall or steep rapids which will not be completely submerged at high flows due to downstream backwater effects, the FLDWAV model can simulate the critical flow through the falls or rapids by considering them to be an internal boundary represented by a dam. A rating is used for the spillway flow where h_{sp} specifies the invert elevation of the upstream or control section of the channel at the beginning of the falls or rapids. The user-

specified rating table of discharge versus water-surface elevation may be computed by the user from the following equation for critical flow through the waterfall or the short rapids:

$$Q = (gA^3/B)^{0.5} \dots\dots\dots (3.48)$$

3.3.4 Lock and Dams

A river system may include small dams with manually controlled gates to pass the river flow in such a way as to maintain certain water-surface elevations on the upstream side of the dam. Usually associated with the dam is a lock for allowing navigation of river craft and barges past the dam. FLDWAV can accommodate any number of lock and dam installations within the river system being simulated.

During normal operations (non-flood conditions), the gates control the flow and create a backwater condition upstream of the gates and dam, which produces water elevations sufficiently high to accommodate the navigation. The lock and dam is modeled in FLDWAV for normal flow conditions by treating the lock and dam as an internal boundary condition where Eq. (3.14) is used along with the following equation:

$$h_i^{j+1} - h_{pt} = 0 \dots\dots\dots (3.49)$$

in which h_i^{j+1} is the computed water-surface elevation just upstream of the lock/dam and h_{pt} is the user-specified target pool elevation just upstream of the dam that the dam operator attempts to maintain by adjusting the gates. The target-pool elevation is user-specified as either a constant value or a time series of values.

During high flows, the gates become unable to control the flow and the dam becomes a “run-of-the-river dam” which is partially to completely submerged. In FLDWAV, this condition is determined when the tailwater elevation exceeds a user-specified critical tailwater elevation, h_{ct} . Also, during this condition, the Δx_i reach through the internal boundary is modeled using the Saint-

Venant finite-difference Eqs. (2.19-2.20) with the Manning n for this reach having unusually large values to reflect the relatively large head-loss across the dam represented by the S_f term in Eq. (2.20). Another user-specified time series of gate control switches $IG(t)$ allows the FLDWAV model to override the critical tailwater criterion and force the reach to be modeled by the Saint-Venant equations. This option is useful for certain movable (collapsible) “wicket-type” dams.

4. INITIAL CONDITIONS

In order to solve the Saint-Venant unsteady flow equations, the state of the flow (h_i and Q_i) must be known at all cross sections ($i=1,2,3,\dots,N$) at the beginning of the simulation ($t=0$). This is known as the initial conditions of the flow. The initial conditions may be either a steady or unsteady flow condition. In the unsteady state condition, the initial conditions are known and the h_i and Q_i at each i^{th} cross section are user-specified. These stages and discharges may be user-estimated values, or computed values saved from a previous unsteady flow simulation. In the steady state condition, the FLDWAV model assumes the flow to be steady, nonuniform flow with the flow at each cross section initially computed as:

$$Q_i = Q_{i-1} + q_{i-1} \Delta x_{i-1} \quad , \quad i=2,3,\dots,N \quad \dots\dots\dots (4.1)$$

where Q_1 is the known steady discharge at $t=0$ at the upstream boundary, and q_i is any user-specified lateral inflow at $t=0$ from tributaries existing between the user-specified cross sections spaced at intervals of Δx along the valley. Tributaries may be dynamic rivers which will be modeled using the unsteady flow equations, or local lateral inflows which must be user-specified as one or more time series. If the local lateral inflows are relatively small (say less than a few percent) compared to the expected maximum flood, they may be omitted in the simulation. Discharges at $t=0$ are usually assumed to be nonzero, i.e., an initially dry downstream channel is not usually simulated in FLDWAV. An exception to this must be used when mud/debris flows are routed in very flat sloping channels. A nonzero initial flow for non-mud/debris flow is not an important restriction, especially when maximum flows and peak stages are of paramount interest in flood forecasting/analyses. However, when modeling regular water low flows, it is important to maintain a sufficient base flow to prevent numerical instability when solving the Saint-Venant finite-difference Eqs. (2.19-2.20).

The water-surface elevations (h_i) associated with the steady flow also must be determined at $t=0$. The user may specify known h_i values at various locations along the routing reach (e.g., reservoir pool elevation behind a dam). The remaining elevations will be generated by FLDWAV.

If the flow is subcritical, this is accomplished by using the iterative Newton-Raphson method to solve the following backwater equation for h_i (Fread and Harbaugh, 1971):

$$(Q^2/A)_{i+1} - (Q^2/A)_i + g\bar{A}_i \left(h_{i+1} - h_i + \Delta x_i \bar{S}_f + \Delta x_i \bar{S}_i \right) = 0 \quad \dots\dots\dots (4.2)$$

in which \bar{A} , \bar{S}_f , and \bar{S}_i are defined by Eqs. (2.21), (2.22), and (2.13), respectively. Eq. (4.2) is a simplified form of the momentum Eq. (2.2) where the first term is taken as zero for steady flow; and L and W_f are assumed to be zero. The computations proceed in the upstream direction ($i = N, N-1, \dots, 3, 2, 1$). The starting water-surface elevation (h_N) may be user-specified, or obtained from the user-specified downstream boundary condition for either a discharge of Q_N (Eq. (3.6) or Eq. (3.9)) or the elevation h_N at $t=0$, Eq. (3.10). When the generated dynamic loop-rating, Eq. (3.6), is used as the downstream boundary, there can be some numerical difficulties due to errors associated with a computed h_N . The Manning equation with a constant energy slope term (S), i.e.,

$$Q_N = \mu/n_N A_N R_N^{2/3} S^{1/2} = K_N S^{1/2} \quad \dots\dots\dots (4.3)$$

is used to compute h_N . Eq. (4.3) is solved iteratively for h_N using the Newton-Raphson method. The energy slope (S) is approximated by using the channel bottom slope (S_o) associated with the most downstream Δx_{N-1} reach; however, this may not be a sufficiently accurate approximation resulting in an erroneous value computed by Eq.(4.3) for h_N which then produces subsequent errors in the computed values for h_i via Eq. (4.2). The erroneous initial conditions result in fluctuations in the discharges and elevations as the Saint-Venant finite-difference Eqs. (2.19-2.20), are applied. Thus, it may appear that some unsteady flows are occurring in the vicinity of the downstream boundary long before the floodwave actually has reached that location; these arise as the Saint-Venant solution attempts to correct the erroneous initial conditions. This type of numerical noise may be minimized or possibly eliminated by a judicious change in the invert elevations of the two most downstream cross sections such that another value of S_o is used to better approximate S . The true initial energy slope (S) can be estimated from the first run of FLDWAV wherein it is the stabilized water surface slope in the vicinity of the downstream boundary obtained after several time steps and before the

arrival of the floodwave. Another numerical problem occurs when the value for S_o , used to approximate S in Eq. (4.3), is negative due to the invert at section $N-1$ being less than that at section N . A warning message is printed when this situation is encountered. This problem can be overcome by the user adjusting the invert elevations of the two most downstream sections so that S_o is positive, i.e.,

$$S_o = (h_{N-1} - h_N)/\Delta x_{N-1} > 0 \dots\dots\dots (4.4)$$

If the flow is supercritical, the computations for h_i proceed from upstream to downstream ($i = 1, 2, 3, \dots, N-1, N$). In this case, Eq. (4.2) is also used, but to compute h_{i+1} . The starting water-surface elevation (h_1) is obtained by using Eq. (4.3) with N replaced by 1 and Eq. (4.4) with N replaced by 2. Additional details concerning the solution of Eq. (4.2) can be found elsewhere (Fread, 1985b).

Whether the initial conditions are user-specified or automatically generated within FLDWAV, the unsteady flow equations are solved for several time steps using the initial conditions together with boundary conditions which are held constant during several computational time steps. This allows the errors in the initial conditions to dampen out which results in the initial conditions being more nearly error free when the actual simulation commences and transient boundary conditions are used. If the initial conditions represent an unsteady state, this “warm-up” procedure must not be used. Also, if the downstream boundary is a tide, the warm-up procedure must not be used since the effect of the tide would be dampened. To obtain a proper set of initial conditions for this situation, the user should assume constant inflow hydrographs and run FLDWAV (without the warm-up) for a few tidal cycles. The initial conditions for the actual simulation would be the water-surface elevations and discharges computed at the end of simulating the few tidal cycles.

5. MIXED (SUBCRITICAL/SUPERCritical) FLOW

Since FLDWAV is a generalized flood routing model, it must be applicable to rivers in both the subcritical and supercritical flow regimes. However, some rivers experience “mixed-flow”, i.e., the flow regime changes back and forth between subcritical and supercritical flow within the period of simulation and/or in space, i.e., at various locations along the channel. The complexity of “mixed flow” is most frequently encountered in dam-break applications of FLDWAV. The four-point implicit solution used in FLDWAV for the Saint-Venant equations is not applicable to such transition flows passing through critical depth. In FLDWAV, the flow regime must be user-specified as subcritical, supercritical, or mixed flow. The Froude number (F_r) can be used to determine if the flow is subcritical or supercritical; however, a more convenient “a priori” predictor for the user is:

$$S_c = 77000 n^2/D^{1/3} \dots\dots\dots (5.1)$$

in which S_c is the critical slope (ft/mi), n is the Manning coefficient, and D is the estimated hydraulic depth (A/B). The required accuracy of D as used in Eq. (5.1) can be somewhat relaxed since it is raised to the $1/3$ power which tends to dampen differences in the value used for D . The required accuracy of D as used in Eq. (5.1) can be somewhat relaxed since it is raised to the $1/3$ power which tends to dampen differences in the value used for D . Comparison of S_c with the channel bottom slope (S_m , ft/mi) is a good approximate indicator (S_m is a major component of the dynamic energy slope, S) of the type of flow, i.e.,

$$S_m > S_c \quad \text{supercritical flow} \dots\dots\dots (5.2)$$

$$S_m < S_c \quad \text{subcritical flow} \dots\dots\dots (5.3)$$

Eqs. (5.2-5.3) are only indicators since the instantaneous dynamic energy slope (S) which is not known a priori is the true determining factor as to whether the flow is subcritical or supercritical.

An inspection of Eq. (5.1) indicates the magnitude of S_c is directly and strongly dependent on n while inversely and weakly dependent on D . Hence, usually overbank flow with increased flow resistance due to trees, etc. require steeper slopes for supercritical flow to occur than flow within the channel bank (bankfull) with smaller flow resistance even though D is greater for the higher flows. Also, from Eq. (5.1) it is evident that a moderate increase in the n value may cause the flow to change from supercritical to subcritical. In many applications, the flow may be supercritical for low flows within bankfull and then may change to subcritical flow as the flow increases and inundates the floodplain. Another common situation encountered when applying the FLDWAV model is when the user-specified roughness coefficient is essentially constant for all flow depths and the bottom slope is such that the low flows are subcritical while high flows become supercritical as D increases with increasing flows. Therefore, in many applications, elimination of the mixture of subcritical/supercritical flow could be accomplished by making minor changes in the estimated n values, yet within the bounds of uncertainty inherently associated with the n values. In other situations, if supercritical flow occurred only in a few isolated short, steep reaches, these could be modeled via a critical flow rating of discharge versus elevation; and each short reach could be considered an internal boundary or dam with a rating curve based on critical flow through the upstream section of the steep reach. For situations where mixed flow must be modeled, FLDWAV has three techniques which can be selected by the user. These are described in the following three subsections.

5.1 Local Partial Inertia (LPI) Technique

When modeling unsteady flows, the complete (dynamic) Saint-Venant equations when solved using the four-point implicit numerical scheme tends to be less numerically stable than the diffusion (zero inertia, i.e., the first two terms in Eq. (2.2) are neglected) routing technique for certain mixed flows, especially in the near-critical range of the Froude number ($F_r \approx 1$) or mixed flows with moving supercritical/subcritical interfaces. It has been observed that the diffusion routing technique which eliminates the two inertial terms (the first two terms) in the momentum equation produces stable numerical solutions for flows where F_r is in the range of critical flow ($F_r=1.0$). To take advantage of the diffusion method's stability and retain the accuracy of the dynamic method, a technique (Fread

et al., 1996) termed Local Partial Inertial (LPI), is utilized in which a numerical filter (σ) modifies the extent of contribution of the inertial terms in the momentum equation such that its properties vary from dynamic to diffusion.

In the LPI technique, the momentum equation, Eq. (2.2), is modified by a numerical filter, σ , so that the inertial terms are partially or altogether omitted in some situations. The modified equation and numerical filter are:

$$\sigma \left[\frac{\partial(s_m Q)}{\partial t} + \frac{\partial(\beta Q^2/A)}{\partial x} \right] + gA \left(\frac{\partial h}{\partial x} + S_f + S_e + S_i \right) + L + W_f B = 0 \quad \dots\dots\dots (5.4)$$

$$\sigma = \begin{cases} 1.0 - F_r^m & (F_r \leq 1.0; \quad m \geq 1) \\ 0 & (F_r > 1.0) \end{cases} \quad \dots\dots\dots (5.5)$$

in which the power m is a user-specified constant, usually $3 \leq m \leq 5$. Figure 5.1 shows the variation of σ with F_r and with the power (m). The σ numerical filter, which depends on F_r , has a variation that ranges from a linear function to the Dirac-delta function. Since the Froude number is determined at each computational point for each time, σ is a “Local” parameter. Therefore, portions of the routing

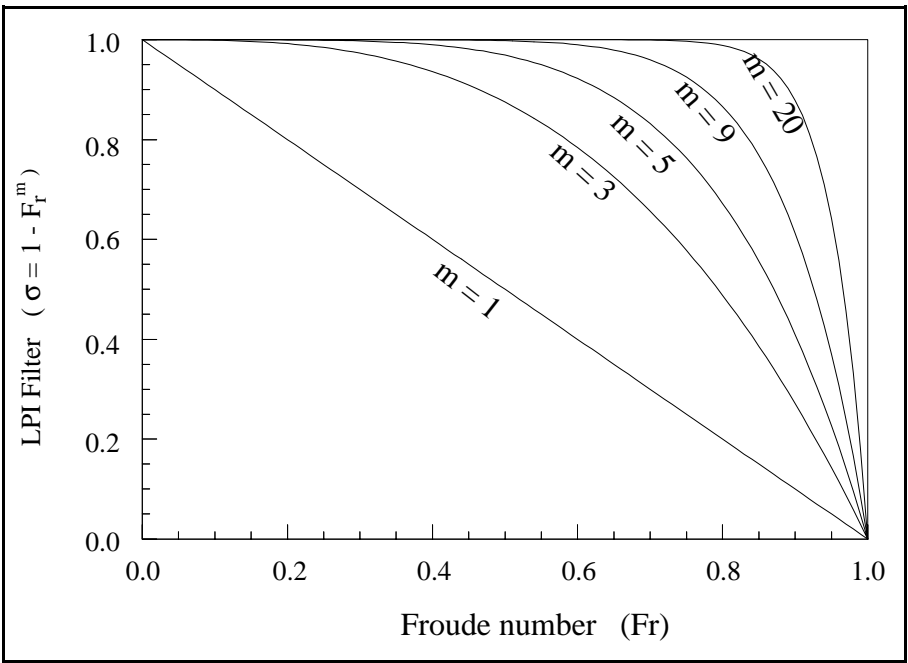


Figure 5.1 - The LPI Filter (σ).

reach with low Froude numbers will be modeled with all or essentially all of the inertial terms included, while those portions with F_r values in the vicinity of critical flow will be modeled with “Partial Inertial” effects included; and supercritical flow ($F_r > 1$) will be modeled with no inertial effects. It is found that smaller values of the power (m) tend to stabilize the solution in some cases while larger values of m provide more accuracy. By using the σ filter, the FLDWAV model automatically changes from a dynamic model to a diffusion model as F_r approaches 1.0 and takes advantage of the stability of the diffusion model for those flows with F_r near the critical value of 1.0. Previously, a simple inertial filter ($1-F_r^2$) was proposed (Havnø and Brorsen, 1986); however, it was not “localized” nor its error properties analyzed.

The error properties of the LPI technique, which totally or partially omit the inertial terms of the momentum equation, have been theoretically analyzed and numerically tested (Fread et al., 1996). It has been shown that the proportional contribution of the inertial terms, noted as IT (which is the inertial terms divided by the water-surface slope), to the total momentum equation depends on the flow Froude number and another dimensionless parameter, ϕ . The term, IT, can be shown to be related to the Froude number (F_r) and ϕ as follows:

$$IT = \frac{\left[\frac{\partial(s_m Q)}{\partial t} + \frac{\partial(\beta Q^2/A)}{\partial x} \right]}{gA \partial h / \partial x} = \frac{-0.5 F_r^2}{1 + 1.5 \phi F_r^3} \dots \dots \dots (5.6)$$

where:

$$\phi = \frac{n^2 g^{3/2} y^{1/6}}{\mu \partial y / \partial t} \dots \dots \dots (5.7)$$

in which n is the Manning's resistance coefficient, y is the flow depth, and λ is the constant in Manning's equation ($\mu=1.49$ for English system of units and $\mu=1.0$ for SI units). The new parameter (ϕ), reflects the flow's unsteadiness and hydraulic condition. Further analysis (Fread, Jin, and Lewis, 1996) has shown that IT is a very small term (usually less than 4% of the total momentum equation) and that IT decreases rapidly as the ϕ value increases and F_r approaches 1.0; therefore, Eq. (2.2) is very closely approximated by Eq. (5.4) in most unsteady flow conditions.

Figures 5.2 and 5.3 show some test results of the computational errors for the LPI technique. The errors are considered as differences between the results of using the complete momentum equation (dynamic routing) and the results of using the LPI modified equation, Eq. (5.4). Numerical experiments compared the results from both methods for a broad range of unsteady flow conditions, and two kinds of errors were examined. The error E_{pk} (%), as shown in Figure 5.2, is the maximum normalized error in the computed peak profiles; the error E_{rms} (%), as shown in Figure 5.3, is the normalized root-mean-square (RMS) error in the computed hydrographs. These results show that the

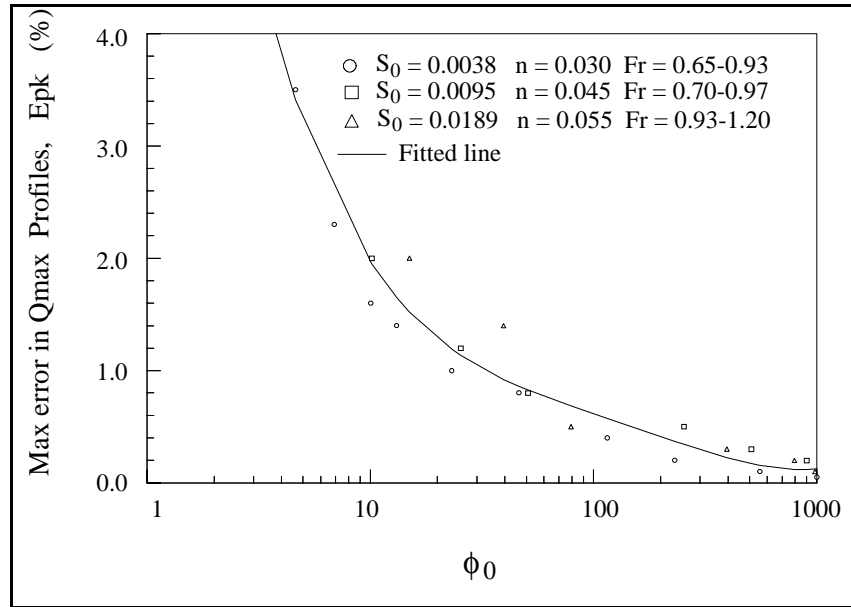


Figure 5.2 - Errors in the Computed Peak Flow.

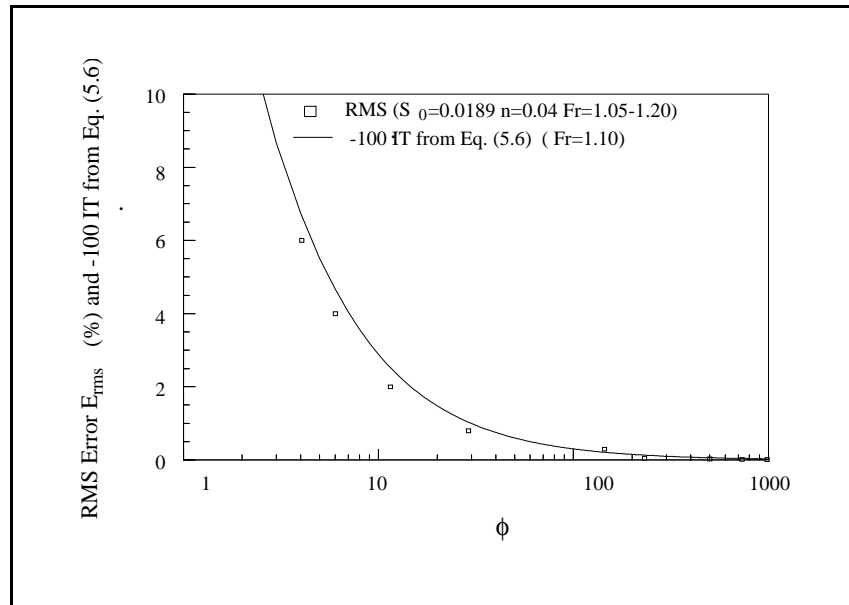


Figure 5.3 - RMS Errors of Computed Hydrographs.

overall errors in using the LPI technique are very small (less than 2%) for almost all flow conditions ($\phi > 10$) and less than 6% for very special flow situations ($5 \leq \phi \leq 10$) which are only applicable for near instantaneous large dam-failure induced floods in channels of very flat bed slopes, $S_o < 0.0003$. The LPI technique for mixed flows is user-specified by setting the input parameter, MIX(J)=5.

5.2 Mixed-Flow Algorithm

The FLDWAV model provides a second method (user-specified) for treating the problem of mixed flow. It consists of an algorithmic procedure (Fread, 1983b, 1985b, 1988) which automatically subdivides the total routing reach into sub-reaches in which only subcritical or supercritical flow occurs. The transition locations where the flow changes from subcritical to supercritical or vice versa are treated as boundary conditions thus avoiding the application of the Saint-Venant equations to a transition flow reach. The mixed-flow algorithm consists of two components, one for obtaining the initial condition of discharge and water-surface elevation at $t=0$ and another which functions during the unsteady flow solution. The mixed-flow algorithm increases computer run times by about 20 percent.

The mixed-flow algorithm initial condition component, which is similar to that described by Molinas and Yang (1985), uses the same method of determining the initial flow at each cross section as described previously in Section 4. The water elevations are obtained by the following algorithm: (1) normal and critical depths are obtained for each section -- the section is designated subcritical if normal depth is greater than critical depth or it is designated supercritical if normal depth is less than critical depth after a check is made to see if downstream elevations created by a dam may drown-out the supercritical depths existing upstream; (2) commencing at the downstream boundary, a backwater solution proceeds from a known elevation (dependent on the downstream boundary condition at $t=0$) in an upstream direction until supercritical flow occurs, or if supercritical flow occurs at the downstream boundary, the computations proceed in the downstream direction from the normal depth at the upstream-most section of all contiguous sections having supercritical flow; (3) when internal boundaries, such as a dam, are encountered, the user-specified water elevations occurring at $t=0$ for each reservoir are used for the backwater solution, or if a bridge is encountered, Eq.

(3.32) is solved iteratively until the correct value of h_i is determined from known values of Q_i and h_{i+1} ; bridges are allowed to exist within a supercritical reach; however, dams must have at least two upstream sections having subcritical flow; (4) steps (2) and (3) are repeated as necessary until the water-surface elevations for all sections have been obtained. The initial condition component is also used along with the LPI optional technique for treating mixed flows.

The time-dependent component of the mixed-flow algorithm uses the Froude number of the estimated flow occurring at each cross section to group contiguous sections into subcritical sub-reaches and supercritical sub-reaches. Contiguous sections with a Froude number less than or equal to 0.95 are grouped into subcritical sub-reaches, and those with a Froude number greater than or equal to 1.05 are grouped into supercritical sub-reaches. Those sections with Froude numbers between 0.95 and 1.05 are considered critical sections. However, isolated critical sections that are surrounded by subcritical sections are grouped with a subcritical sub-reach, while isolated critical sections amongst supercritical sections are grouped with a supercritical sub-reach. The upstream and downstream limits of the subcritical/supercritical reaches are noted and used to determine the range over which the Saint-Venant finite-difference Eqs. (2.19-2.20) are applied. During a Δt time step, the solution commences with the most upstream sub-reach and proceeds sub-reach by sub-reach in the downstream direction. The upstream and downstream boundary conditions for each sub-reach are selected according to the following algorithm: (1) if the most upstream reach is subcritical, the upstream boundary is given by either Eq.(3.1) or Eq.(3.2) and the downstream boundary is Eq. (3.8) since flow must pass through critical when the next downstream sub-reach is supercritical; (2) if the most upstream reach is supercritical, the upstream boundary is given by both Eq.(3.1) and Eq.(3.6) in which the subscript N is replaced by 1, and a downstream boundary is not required for the supercritical reach since flow disturbances created downstream of the supercritical reach cannot propagate upstream into the supercritical reach; (3) if an inner sub-reach (a sub-reach which is neither the most upstream nor the most downstream sub-reach) is supercritical, the following equations are used for the two upstream boundary equations:

$$Q_i = Q'(t) \dots\dots\dots (5.8)$$

$$h_i = h'(t) \dots\dots\dots (5.9)$$

in which $Q'(t)$ is the most recently computed flow at the last cross section of the upstream subcritical sub-reach, and $h'(t)$ is the computed critical water-surface elevation of the downstream-most (critical section) of the upstream subcritical sub-reach; (4) if an inner sub-reach is subcritical, Eq. (5.8) is used for the upstream boundary in which $Q'(t)$ represents the computed flow at the last section of the upstream supercritical sub-reach, and the critical flow, Eq. (3.13), is used as the downstream boundary; (5) if the most downstream sub-reach is subcritical, Eq. (5.8) is used for the upstream boundary condition, and the downstream boundary condition is appropriately selected from Eqs. (3.5-3.11) by the user; (6) if the most downstream sub-reach is supercritical, Eqs. (5.8-5.9) are used as the upstream boundary equations, and no downstream boundary is required.

A hydraulic jump occurs between the last section of a supercritical sub-reach and the first section of the adjacent downstream subcritical sub-reach, although an equation for such is not directly used. To account for the possible upstream movement of the jump the following procedure is utilized before advancing to the next time step: (1) the subcritical elevation (h_e) is extrapolated to the adjacent upstream supercritical section; (2) the sequent water-surface elevation of the adjacent upstream supercritical section is iteratively computed via the numerical bi-section method applied to the following sequent elevation equation:

$$\frac{Q^2}{gA} + \bar{z}A - \frac{Q'^2}{gA'} - \bar{z}'A' = 0 \dots\dots\dots (5.10)$$

in which \bar{z} is the distance from the water surface to the center of gravity of the wetted cross section, A is the wetted area, Q is the computed flow at the section, and the superscript (') represents variables associated with the sequent elevation (h') while the variables with no superscript are associated with the supercritical elevation; (3) if the sequent elevation (h') is greater than the extrapolated elevation (h_e), the jump is not moved upstream; however, if $h' \leq h_e$, the jump is moved upstream section by section until $h' > h_e$.

To account for the possibility of the jump moving downstream (if it did not move upstream), the following procedure is utilized before advancing to the next time step: (1) starting at the most upstream section of the subcritical sub-reach, the supercritical elevation is computed using Eq. (4.2),

and its sequent elevation (h') is computed by applying the iterative bi-section method to Eq. (5.10);
(2) using the most recently computed subcritical elevation (h), if $h \geq h'$, the jump is not moved downstream; however, if $h < h'$, the jump is moved downstream section by section until $h \geq h'$.

Sub-reaches wherein the flow is essentially near-critical can cause some numerical difficulties when the mixed-flow algorithm is used to locate possible movement of the jump. In those cases, it is recommended to not allow the jump to move by the user selecting MIXF=4. When MIXF=2 or MIXF=3, the mixed-flow algorithm allows for possible movement of the hydraulic jump. Use of MIXF=3 rather than MIXF=2 is recommended for greater numerical robustness of the mixed-flow algorithm wherein the θ weighting factor in the Saint-Venant finite-difference equations, Eqs. (2.19-2.20), is set to 1.0 for the supercritical reaches only; otherwise, it is always defaulted to a value of 0.6 unless otherwise user-specified via the F1 input parameter. Also, when MIXF=3, the jump is allowed to move only if the Froude number is greater than 2.0.

Smaller computational distance steps (Δx_i) are required in the vicinity of the transition reaches between subcritical and supercritical flow. This is particularly required both upstream and downstream of a critical flow section to avoid numerical difficulties. Smaller Δx_i reaches also will enable more accurate location of hydraulic jumps. A very convenient feature for controlling the computational distance step size can be user-selected within FLDWAV and is described later in Subsection 11.1.

During the computation of initial conditions for such mixed flows in which the flow changes from subcritical to supercritical between cross sections i and $i+1$, the movement of a hydraulic jump from the position determined by comparison of normal and critical elevations is not considered. However, since the FLDWAV model can solve the Saint-Venant equations to improve the initial conditions before the unsteady solution commences, the jump at $t=0$ is allowed to move upstream or downstream from its original location via the technique described previously in the time-dependent component of the mixed-flow algorithm.

A reservoir, which has a sufficiently steep slope for supercritical flow to occur in its upper reaches as the reservoir pool is significantly lowered by a dam-breach outflow, may be treated as entirely subcritical flow by assigning sufficiently large Manning n values for the lower elevations of each reservoir cross section. The required n values can be determined via Eqs. (5.1-5.3). User-specification of such n values in the lower portions of the reservoir generally will not significantly affect the computed outflow hydrographs.

5.3 Characteristics-Based Upwind Explicit Routing

It has been observed that the four-point implicit scheme, using the mixed-flow technique previously described, has difficulties when solving the Saint-Venant equations for some near-instantaneous, very large dam-break induced flood waves which often produce a moving supercritical-subcritical mixed-flow interface.

One of the techniques developed in the FLDWAV model to simulate flows with strong shocks (near instantaneous dam-break waves) or subcritical/supercritical mixed flows is a characteristics-based upwind explicit numerical scheme (Jin and Fread, 1997). To construct the explicit scheme, the Saint-Venant equations are transformed into a conservation form of mass and momentum, i.e.

$$\frac{\partial(A+A_0)}{\partial t} + \frac{\partial Q}{\partial x} - q = 0 \quad \dots\dots\dots (5.11)$$

$$\frac{\partial Q}{\partial t} + \frac{\partial(\frac{Q^2}{A} + P_1)}{\partial x} + gA(S_f + S_e) - P_2 + L + W_f B = 0 \quad \dots\dots\dots (5.12)$$

in which

$$P_1 = g \int_{h_b}^h A(x, \xi) d\xi; \quad P_2 = g \int_{h_b}^h \frac{\partial A(x, \xi)}{\partial x} d\xi \quad \dots\dots\dots (5.13)$$

where h_b is the elevation of the channel bed at location x , and ξ is a dummy variable for the integration. The state variables in the conservation form of the basic equations, are now $(A+A_o)$ and Q , while the most useful variable is water surface elevation, h . However, it is easy to obtain h from the numerical solutions of $(A+A_o)$, according to the cross-sectional data of tabular values of channel wetted active and inactive top widths versus water surface elevation by a reverse table look-up. Also, the state variable integral functions, P_1 and P_2 in Eq.(5.13), can be determined during the computations by using P_1 versus h and P_2 versus h tables at any h_j (the j^{th} h in the B versus h table) and interpolating when h is between h_j and h_{j+1} . The P_1 and P_2 tabular values are computed by following:

$$P_{1,j+1} = P_{1,j} + A_j (h_{j+1} - h_j) + \frac{1}{6} (2B_j + B_{j+1}) (h_{j+1} - h_j)^2 \quad \dots \quad (5.14)$$

$$P_{2,j+1} = P_{2,j} + \frac{\partial A_j}{\partial x} (h_{j+1} - h_j) + \frac{1}{6} \left(\frac{\partial B_{j+1}}{\partial x} + 2 \frac{\partial B_j}{\partial x} \right) (h_{j+1} - h_j)^2 \quad \dots \quad (5.15)$$

in which $P_1=0$ and $P_2=0$ for $j=1$.

The principle of an upwind, explicit scheme is to use a one-sided, finite-difference approximation for the space derivative, according to the time dependent local characteristic velocities. The two local characteristic velocities corresponding to the two characteristic directions are defined as follows:

$$\lambda_i = \frac{Q}{A} \pm \sqrt{\frac{gA}{B}} = v \pm c \quad (i=1,2) \quad \dots \quad (5.16)$$

in which $i=1$ for $v+c$ and $i=2$ for $v-c$; $v=Q/A$ is the local cross-sectional average velocity and $c=\sqrt{gA/B}$ is the local dynamic wave velocity. Based on local time-dependent Froude number $(F_r = v/\sqrt{gA/B})$, four switch functions are assigned to these characteristic directions to represent their contribution to downstream direction (identified by $+$) or upstream direction (identified by $-$) as followings:

$$\hat{\lambda}_1^+ = 1; \quad \hat{\lambda}_1^- = 0; \quad \hat{\lambda}_2^+ = 0; \quad \hat{\lambda}_2^- = 1 \quad (F_r < 1, \text{ subcritical}) \dots\dots\dots (5.17)$$

and

$$\hat{\lambda}_1^+ = 1; \quad \hat{\lambda}_1^- = 0; \quad \hat{\lambda}_2^+ = 1; \quad \hat{\lambda}_2^- = 0 \quad (F_r > 1, \text{ supercritical}) \dots\dots\dots (5.18)$$

The derivative terms with respect to x in Eqs.(5.11 and 5.12) are split into two parts, with each corresponding to a local characteristic direction, by splitting its Jacobian vector into two parts in terms of a split normalized Jacobian matrix. From this, an upwind scheme can be constructed based on that matrix (Jin and Fread, 1997). A final scheme can be expressed in the form of the following algebra equations:

$$\begin{aligned} & \frac{(A+A_0)_i^{j+1} - (A+A_0)_i^j}{\Delta t_j} + (\hat{G}_1^+)_i^j \frac{Q_i^j - Q_{i-1}^j}{\Delta x_{i-1}} + (\hat{G}_1^-)_i^j \\ & + (\hat{G}_2^+)_i^j \left[\frac{(\frac{Q^2}{A} + P_1)_i^j - (\frac{Q^2}{A} + P_1)_{i-1}^j}{\Delta x_{i-1}} \right] + (\hat{G}_2^-)_i^j \left[\frac{(\frac{Q^2}{A} + P_1)_{i+1}^j - (\frac{Q^2}{A} + P_1)_i^j}{\Delta x_i} \right] - q_i^j = 0 \quad \dots\dots (5.19) \end{aligned}$$

$$\begin{aligned} & \frac{Q_i^{j+1} - Q_i^j}{\Delta t_j} + (\hat{G}_3^+)_i^j \frac{Q_i^j - Q_{i-1}^j}{\Delta x_{i-1}} + (\hat{G}_3^-)_i^j \frac{Q_{i+1}^j - Q_i^j}{\Delta x_i} + (\hat{G}_4^+)_i^j \left[\frac{(\frac{Q^2}{A} + P_1)_i^j - (\frac{Q^2}{A} + P_1)_{i-1}^j}{\Delta x_{i-1}} \right] \\ & + (\hat{G}_4^-)_i^j \left[\frac{(\frac{Q^2}{A} + P_1)_{i+1}^j - (\frac{Q^2}{A} + P_1)_i^j}{\Delta x_i} \right] + [gA(S_f + S_e) - P_2 + L + W_f B]_i^j = 0 \quad \dots\dots\dots (5.20) \end{aligned}$$

in which the components of the normalized Jacobian matrix are defined by the following:

$$\hat{G}_1^+ = -\frac{v}{c} \left(\frac{\hat{\lambda}_1^+ - \hat{\lambda}_2^+}{2} \right) + \left(\frac{\hat{\lambda}_1^+ + \hat{\lambda}_2^+}{2} \right) \dots\dots\dots (5.21)$$

$$\hat{G}_1^- = -\frac{v}{c} \left(\frac{\hat{\lambda}_1^- - \hat{\lambda}_2^-}{2} \right) + \left(\frac{\hat{\lambda}_1^- + \hat{\lambda}_2^-}{2} \right) \dots\dots\dots (5.22)$$

$$\hat{G}_2^+ = \frac{1}{c} \left(\frac{\hat{\lambda}_1^+ - \hat{\lambda}_2^+}{2} \right) \dots\dots\dots (5.23)$$

$$\hat{G}_2^- = \frac{1}{c} \left(\frac{\hat{\lambda}_1^- - \hat{\lambda}_2^-}{2} \right) \dots\dots\dots (5.24)$$

$$\hat{G}_3^+ = \frac{(c^2 - v^2)}{c} \left(\frac{\hat{\lambda}_1^+ - \hat{\lambda}_2^+}{2} \right) \dots\dots\dots (5.25)$$

$$\hat{G}_3^- = \frac{(c^2 - v^2)}{c} \left(\frac{\hat{\lambda}_1^- - \hat{\lambda}_2^-}{2} \right) \dots\dots\dots (5.26)$$

$$\hat{G}_4^+ = \frac{v}{c} \left(\frac{\hat{\lambda}_1^+ - \hat{\lambda}_2^+}{2} \right) + \left(\frac{\hat{\lambda}_1^+ + \hat{\lambda}_2^+}{2} \right) \dots\dots\dots (5.27)$$

$$\hat{G}_4^- = \frac{v}{c} \left(\frac{\hat{\lambda}_1^- - \hat{\lambda}_2^-}{2} \right) + \left(\frac{\hat{\lambda}_1^- + \hat{\lambda}_2^-}{2} \right) \dots\dots\dots (5.28)$$

Since the values of the state variables, $A+A_0$ and Q , are known at all computational nodes at time t_j , values for all interior nodes at time t_{j+1} can be directly computed from the Eqs. (5.19 - 5.20)

In order to obtain solutions for the upstream and downstream boundaries, two additional equations are needed. They are derived by integrating the continuity equation, Eq.(5.11), for the first reach ($i=1$) and the last reach ($i=N-1$) over one time step as follows:

$$\int_{t^j}^{t^{j+1}} \int_{x_i}^{x_{i+1}} \left[\frac{\partial Q}{\partial x} + \frac{\partial(A+A_0)}{\partial t} - q \right] dx dt = 0 \dots\dots\dots (5.29)$$

which written in finite-difference form becomes:

$$\Delta t_j [Q_{i+1}^{j+1} + Q_{i+1}^j - Q_i^{j+1} - Q_i^j] + \Delta x_i [(A + A_0)_{i+1}^{j+1} + (A + A_0)_i^{j+1} - (A + A_0)_{i+1}^j - (A + A_0)_i^j] - 2\bar{q}\Delta x_i \Delta t_j = 0 \quad \dots\dots\dots (5.30)$$

in which $i=1$ for the upstream boundary and $i=N-1$ for the downstream boundary (N is the total number of computational cross-sections). Also, Eq.(5.30) can be applied to upstream and downstream reaches of a hydraulic structure (internal boundary such as a dam or bridge), together with an appropriate internal boundary equation representing the relationship between flow through the structure and water surface elevations both upstream and downstream of the structure, as previously described in the Section 3.2.

Unlike unconditionally stable implicit schemes, most explicit schemes are restricted to the Courant-Friedrich-Lewy (CFL) condition for numerical stability. For the upwind scheme presented herein, the CFL condition can be written as follows:

$$\Delta t \leq C_n \min\left(\frac{\Delta x}{v+c}\right)_i \quad (C_n \leq 1.0) \quad \dots\dots\dots (5.31)$$

in which C_n is the Courant number, and $\min (\Delta x/v+c)_i$ represents the minimum value of this ratio for all Δx_i reaches. A large value of C_n (0.9-1.0) can be used for simple prismatic channels. C_n has to be reduced to 0.5-0.8 for complicated channel geometry such as rapid expansions and contractions, rapid changes in slope, channel cross sections with wide floodplains, or a large portion of off-channel storage due to an increased effect of the source terms (all terms other than the derivative terms) in Eqs.(5.11, 5.12). In the FLDWAV model, options are provided to input either Δt or C_n .

Because the numerical stability requirement of the explicit scheme restricts the time step to a Courant condition, the explicit scheme requires smaller computational time steps than the implicit scheme which is unconditionally stable; therefore, for most applications, it requires more computational time. In Figure 5.4, the ratio of computational time of the explicit scheme to the computational time of the implicit scheme is plotted as a function of the routed hydrograph's time of rise (T_r). It can be seen that the explicit scheme needs much more computation time when modeling slowly-rising flood waves, while it (when applied to simple prismatic channels) is equal to

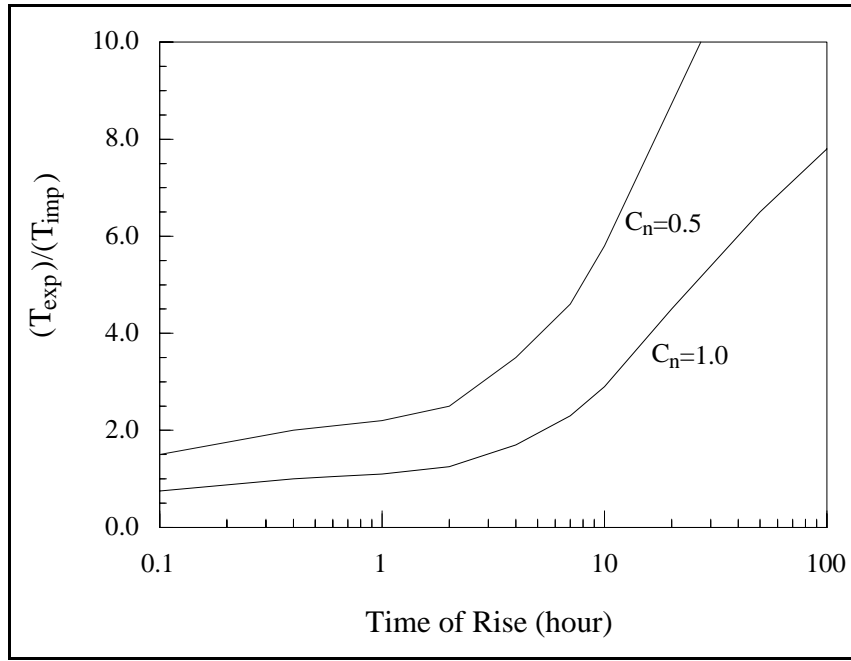


Figure 5.4 - Ratio of Required Computation Time of Implicit and Explicit Schemes.

or more time efficient than the implicit scheme for very fast-rising waves of about 0.5 hour or smaller time of rise, T_r .

In the FLDWAV model, an implicit-explicit multiple dynamic routing option is available to allow the user to select a different scheme for any subreach within the entire routing reach. The upwind, explicit algorithm, when combined with the four-point implicit scheme, enables only those portions of an entire river system being modeled to utilize the advantages of accuracy and stability of an explicit method for sharp waves or nearly critical flows, while minimizing the effect of its greater computational requirement by using the implicit algorithm for other reaches of the river system where nearly critical flows do not occur. Figure 5.5 is a schematic illustration of the multiple dynamic routing capability within the FLDWAV model. The explicit scheme is used for a subreach from x_a to x_b , and the four-point implicit scheme is used for a subreach from x_b to x_c .

The time step (from t_j to t_{j+1}) for the implicit scheme is Δt_i , and the explicit scheme has a downstream boundary condition for the first routing subreach. The connecting cross section in this multiple routing, therefore, must be located where the channel shape has little change, and the

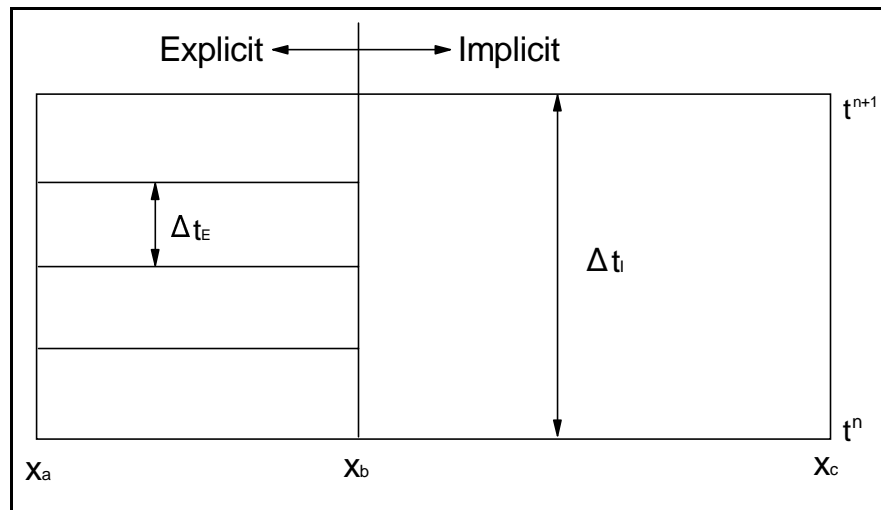


Figure 5.5 - Implicit-Explicit Multiple Routing.

backwater effects from any downstream dam, bridge, or other cross-sectional constriction are insignificant. The first routing subreach is computed for one implicit time step, and the downstream subreach can be computed using the computed discharge from the first subreach as its upstream boundary condition. Also, the implicit scheme may be used in an upstream subreach and the explicit scheme used in the downstream subreach.

6. DAM-BREACH MODELING

Dams, bridge embankments, and levees all have the potential for failure. The breach is the opening formed in the structure as it fails. User-specified breach parameters Fread (1998) and a description of the reservoir (cross sections or storage-elevation curve) will enable FLDWAV to compute the outflow hydrograph in the same manner as previously in DAMBRK (Fread, 1988).

6.1 Breach Outflow

The breach outflow (Q_b) is computed as broad-crested weir flow (Fread, 1977, 1988, 1989b), i.e.,

$$Q_b = c_v k_s \left[3.1 b_i (h - h_b)^{1.5} + 2.45 z (h - h_b)^{2.5} \right] \dots \dots \dots (6.1)$$

in which c_v is a small computed correction for velocity of approach, b_i is the computed instantaneous breach bottom width as described later by Eq. (6.9), h is the computed elevation of the water surface just upstream of the structure, h_b is the computed elevation of the breach bottom which is assumed to be a function of the breach formation time (τ) as described later by Eq. (6.8), z is the user-specified side slope of the breach, and k_s is the computed submergence correction due to the downstream tailwater elevation (h_t), i.e.,

$$k_s = 1.0 - 27.8 \left[\frac{h_t - h_b}{h - h_b} - 0.67 \right]^3 \quad \text{if } (h_t - h_b)/(h - h_b) > 0.67 \dots \dots \dots (6.2)$$

otherwise, $k_s = 1.0$. Eq. (6.2) was developed from a graphical representation by Venard (1954). The velocity of approach correction factor (c_v) is computed from the following (Brater, 1959):

$$c_v = 1.0 + 0.023 \frac{Q_b^2}{\left[B_d^2 (h - h_{bm})^2 (h - h_b) \right]} \dots \dots \dots (6.3)$$

in which B_d is the reservoir width at the dam and h_{bm} is the user-specified final (terminal) elevation of the breach bottom. If the breach is formed by piping, z is assumed zero (rectangular shape) and Eq. (6.1) is replaced by an orifice equation, i.e.,

$$Q_b = 4.8 A_p (h - \bar{h})^{1/2} \dots\dots\dots (6.4)$$

where:

$$A_p = 2b_i (h_p - h_b) \dots\dots\dots (6.5)$$

in which h_p is the user-specified center-line elevation of the pipe, and $\bar{h} = h_p$ or $\bar{h} = h_{tw}$ if $h_{tw} > h_p$ in which h_{tw} is the tailwater surface elevation just downstream of the dam. The breach flow automatically ceases to be orifice flow and becomes broad-crested weir flow when the reservoir elevation (h) lowers sufficiently and/or the pipe enlarges sufficiently that:

$$h < 3 h_p - 2 h_b \dots\dots\dots (6.6)$$

6.2 Breach Parameter Selection

The actual failure mechanics are not well understood for either earthen or concrete dams. In earlier attempts to predict downstream flooding due to dam failures, it was usually assumed that the dam failed completely and instantaneously. Investigators of dam-break flood waves such as Ritter (1892), Schocklitsch (1917), Re (1946), Dressler (1954), Stoker (1957), and Sakkas and Strelkoff (1973) assumed the breach encompasses the entire dam and that it occurs instantaneously. Others, such as Schocklitsch (1917) and Army Corps of Engineers (1960), have recognized the need to assume partial rather than complete breaches; however, they assumed the breach occurred instantaneously. The assumptions of instantaneous and complete breaches were used for reasons of convenience when applying certain mathematical techniques for analyzing dam-break flood waves. These assumptions are somewhat appropriate for concrete arch dams, but they are not appropriate for earthen dams and concrete gravity dams. In FLDWAV the breach is always assumed to develop over a finite interval of time (τ) and will have a final size determined by a terminal bottom width

parameter (b) and various shapes depending on another parameter (z) as shown in Figure 6.1. Such a parametric representation of the breach is utilized in FLDWAV for reasons of simplicity, generality, wide applicability, and the uncertainty in the actual failure mechanism. This approach to the breach description follows that used by Fread and Harbaugh (1973) and by Fread (1977, 1985b, 1988, 1989b, 1998).

The shape parameter (z) identifies the side slope of the breach, i.e., 1 vertical: z horizontal. The range of z values is from 0 to somewhat larger than unity. Its value depends on the angle of repose of the compacted and wetted materials through which the breach develops. Rectangular, triangular, or trapezoidal shapes may be user-specified by using various combinations of values for z and b , e.g., $z=0$ and $b>0$ produces a rectangle, and $z>0$ and $b=0$ yields a triangular-shaped breach. The terminal width b is related to the average width of the breach (\bar{b}) by the following:

$$b = \bar{b} - zh_d \dots\dots\dots (6.7)$$

The model assumes the breach bottom width starts at a point (see Figure 6.1) and enlarges at a linear or nonlinear rate over the failure time (τ) until the terminal bottom width (b) is attained and the breach bottom has eroded to the terminal elevation h_{bm} . If τ is less than one minute, the width of the breach bottom starts at a value of b rather than zero; this represents more of a collapse failure than an erosion failure. The bottom elevation of the breach (h_b) is simulated as a function of time (τ)

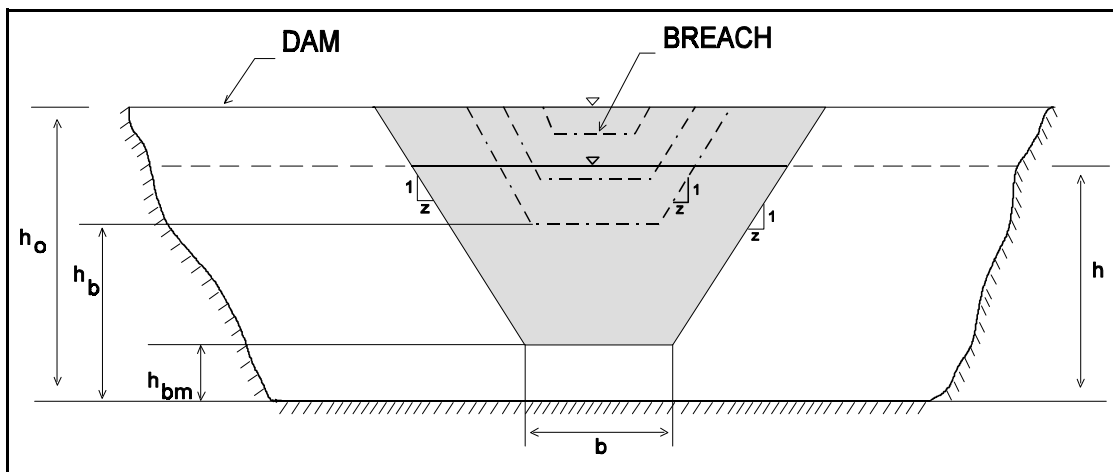


Figure 6.1 - Front View of Dam Showing Formation of Breach.

according to the following:

$$h_b = h_d - (h_d - h_{bm}) \left(\frac{t_b}{\tau} \right)^{\rho_o} \quad \text{if } 0 < t_b \leq \tau \dots\dots\dots (6.8)$$

in which h_{bm} is the final elevation of the breach bottom which is usually, but not necessarily, the bottom of the reservoir or outlet channel bottom, t_b is the time since beginning of breach formation, and ρ_o is the parameter specifying the degree of nonlinearity, e.g., $\rho_o=1$ is a linear formation rate, while $\rho_o=2$ is a nonlinear quadratic rate; the range for ρ_o is $1 \leq \rho_o \leq 4$; however, the linear rate is usually assumed. The instantaneous bottom width (b_i) of the breach is given by the following:

$$b_i = b \left(\frac{t_b}{\tau} \right)^{\rho_o} \quad \text{if } 0 < t_b \leq \tau \dots\dots\dots (6.9)$$

During the simulation of a dam failure, the actual breach formation commences when the reservoir water-surface elevation (h) exceeds a user-specified value, h_f . This feature permits the simulation of an overtopping of a dam in which the breach does not form until a sufficient amount of water is flowing over the crest of the dam to erode the downstream face of the dam sufficiently for the actual breach failure to commence wherein the upstream face of the dam begins to erode thus providing an increased area of opening for more flow to pass the dam. (Refer to Sub-section 6.2.2 for a further description of the breaching process.) A piping failure may also be simulated by specifying the initial centerline elevation (h_p) of the piping failure. Another feature in FLDWAV allows the user to specify the breach initiation time, the time interval after beginning of simulation until the breach begins to form. This is an alternative to the use of h_f as the overtopping elevation at which failure commences. Still, another feature in FLDWAV is the ability to limit the breach formation to the uncontrolled and/or gated spillway section of the dam.

6.2.1 Concrete Dams

Concrete gravity dams tend to have a partial breach as one or more monolith sections formed during the construction of the dam are forced apart and over-turned by the escaping water through the

breach. The time for breach formation is in the range of a few minutes. It is difficult to predict the number of monoliths which may be displaced or fail; however, by using the FLDWAV model and making several separate applications wherein the parameter b representing the combined lengths of assumed failed monoliths is varied in each, the resulting reservoir water-surface elevations can be used to indicate the extent of reduction of the loading pressures on the dam. Since the loading diminishes as b is assumed to increase, a limiting safe loading condition which would not cause further failure may be estimated. Concrete arch dams tend to fail completely and are assumed to require only a few minutes for the breach formation. The shape parameter (z) is usually assumed zero for concrete gravity or arch dams.

6.2.2 Earthen Dams

Earthen dams which exceedingly outnumber all other types of dams do not tend to completely fail, nor do they fail instantaneously. The fully formed breach in earthen dams tends to have an average width (\bar{b}) in the range $(0.5h_d \leq \bar{b} \leq 8h_d)$ where h_d is the height of the dam. The middle portion of this range for \bar{b} is supported by the summary report of Johnson and Illes (1976) and the upper range by the report of Singh and Snorrason (1982). Breach widths for earthen dams are therefore usually much less than the total length of the dam as measured across the valley. Also, the breach requires a finite interval of time (τ) for its formation through erosion of the dam materials by the escaping water. The time of failure (for overtopping and not including the breach initiation time which does not affect the rate of breach formation and breach discharge) may be in the range of a few minutes to usually less than an hour depending on the height of the dam, the type of materials used in construction, the extent of compaction of the materials, and the magnitude and duration of the overtopping flow of the escaping water. The time of failure as used in FLDWAV is the duration of time between the first breaching of the upstream face of the dam until the breach is fully formed. For overtopping failures, the beginning of breach formation is after the downstream face of the dam has eroded away, and the resulting crevasse has progressed back across the width of the dam crest to reach the upstream face. A piping failure occurs when initial breach formation takes place at some point below the top of the dam due to erosion of an internal channel through the dam by the escaping water. The time of failure is usually considerably longer for piping than an overtopping failure since

the upstream face is slowly being eroded in the very early phase of the piping development. As the erosion proceeds, a larger and larger opening is formed; this is eventually hastened by caving-in of the top portion of the dam. Values of $\rho_o \geq 2$ are appropriate for simulating piping initiated breaches. Poorly constructed coal-waste slag piles (dams) which impound water tend to fail within a few minutes and have an average breach width in the upper range of the earthen dams mentioned above.

Some statistically derived predictors for \bar{b} and τ have been presented in the literature, i.e., MacDonald and Langridge-Monopolis (1984) and Froelich (1987, 1995). From Froelich's work in which he used the properties of 43 breaches of dams ranging in height from 15 to 285 ft with all but 6 between 15 and 100 ft, the following predictive equations can be obtained:

$$\bar{b} = 9.5 k_o (V_r h_d)^{0.25} \dots\dots\dots (6.10)$$

$$\tau = 0.59 V_r^{0.47} / h_d^{0.9} \dots\dots\dots (6.11)$$

in which \bar{b} is average breach width (ft), τ is time of failure (hrs), $k_o = 0.7$ for piping and 1.0 for overtopping, V_r is the reservoir volume (acre-ft), and h_d is the height (ft) of water over the breach bottom which is usually about the height of the dam. Standard error of estimate for \bar{b} was ± 94 ft which is an average error of ± 54 percent of \bar{b} , and the standard error of estimate for τ was ± 0.9 hrs which is an average error of ± 70 percent of τ .

Another means of determining the breach properties is the use of physically-based breach erosion models. Cristofano (1965) attempted to model the partial, time-dependent breach formation in earthen dams; however, this procedure requires critical assumptions and specification of unknown critical parameter values. Also, Harris and Wagner (1967) used a sediment transport relation to determine the time for breach formation, but this procedure requires specification of breach size and shape in addition to two critical parameters for the sediment transport relation. More recently, Ponce and Tsivoglou (1981) presented a rather computationally complex breach erosion model which coupled the Meyer-Peter and Muller sediment transport equation to the one-dimensional differential equations of unsteady flow (Saint-Venant equations) and sediment conservation. They compared the

model's predictions with observations of a breached landslide-formed dam on the Mantaro River in Peru. The results were substantially affected by the judicious selection of the Manning n , a breach width-flow relation parameter, and a coefficient in the sediment transport equation.

Fread (1984a, 1985a, 1989b) developed a breach erosion model (BREACH) for earthen dams. It substantially differs from the previously mentioned models. It is a physically-based mathematical model which predicts the breach characteristics (size, shape, time of formation) and the discharge hydrograph emanating from a breached earthen dam. The earthen dam may be man-made or naturally formed by a landslide. The model is developed by coupling the conservation of mass of the reservoir inflow, spillway outflow, and breach outflow with the sediment transport capacity of the unsteady uniform flow along an erosion-formed breach channel. The bottom slope of the breach channel is assumed to be essentially that of the downstream face of the dam. The growth of the breach channel is dependent on the dam's material properties (D_{50} size, unit weight, friction angle, cohesive strength). The model considers the possible existence of the following complexities: (1) core material having properties which differ from those of the outer portions of the dam; (2) the necessity of forming an eroded ditch along the downstream face of the dam prior to the actual breach formation by the overtopping water; (3) the downstream face of the dam can have a grass cover or be composed of a material of larger grain size (cobble stones, rip-rap, etc.) than the outer portion of the dam; (4) enlargement of the breach through the mechanism of one or more sudden structural collapses of portions of the dam where breaching occurs due to the hydrostatic pressure force exceeding the resisting shear and cohesive forces; (5) enlargement of the breach width by collapse of the breach sides according to slope stability theory; and (6) initiation of the breach via piping with subsequent progression to a free-surface breach flow. The outflow hydrograph is obtained through a time-stepping iterative solution that requires only a few seconds for computation. The BREACH model is not subject to numerical stability or convergence difficulties. The BREACH model's predictions have been favorably compared with observations of a piping failure of the man-made Teton Dam in Idaho, the piping failure of the man-made Lawn Lake Dam in Colorado, and an overtopping activated breach of a landslide-formed dam in Peru. Model sensitivity to numerical parameters is minimal; however, it is sensitive to the internal friction angle of the dam's material and the extent of grass cover when simulating man-made dams and to the cohesive strength of the material composing landslide-formed

dams. In the three test cases, a fairly extensive variation of cohesion and internal friction angle produced less than ± 20 percent variation in the breach properties. The BREACH model has not been directly incorporated into FLDWAV to discourage its indiscriminate use, since it should be used judiciously and with caution; it is intended to be an auxiliary method for determining the breach parameters and should be used in conjunction with statistical and range of magnitude data from historical breaches.

Another way of checking the reasonableness of the breach parameters (\bar{b} and τ) is to use the following equations:

$$Q_p^* = 370 (V_r h_d)^{0.5} \dots\dots\dots (6.12)$$

$$Q_p = 3.1 \bar{b} \left(\frac{C}{\tau + C/\sqrt{h_d}} \right)^3 \dots\dots\dots (6.13)$$

in which Q_p^* and Q_p are the expected peak discharge (cfs) through the breach, V_r and h_d are the reservoir volume (acre-ft) and height (ft) of dam, respectively, and $C = 23.4 A_s \bar{b}$ in which A_s is the surface area (acres) of the reservoir at the top of the dam. Eq. (6.12) was developed by Hagen (1982) for historical data from 14 dam failures and provides a maximum envelope of all 14 of the observed discharges. Eq. (6.13) was developed by Fread (1981) and is used in the NWS Simplified Dam Break Model, SMPDBK (Wetmore and Fread, 1984; Fread, 1988). After selecting \bar{b} and τ , Eq. (6.13) can be used to compute Q_p which then can be compared with Q_p^* from Eq. (6.12). Thus, if $Q_p \gg Q_p^*$, (\gg means much, much larger) then either \bar{b} is too large and/or τ is too small; however, if $Q_p \ll Q_p^*$, then either \bar{b} is too small and/or τ is too large. Eq. (6.12) over-estimates the peak discharges for each of 21 historical dam failures (including the previously mentioned 14 failures) by an average of 130 percent. Eq. (6.13), although used in the NWS SMPDBK (Simplified Dam-Break model) it is not used in FLDWAV, has been found to yield peak discharges within 5-10 percent of those produced in FLDWAV when equivalent values of \bar{b} and τ are utilized in Eq. (6.13) and in Eqs. (6.8-6.9) within FLDWAV.

6.3 Breach Parameter Sensitivity

Selection of breach parameters before a particular breach forms, i.e., in the absence of observations, introduces a varying degree of uncertainty in the downstream flooding results produced by the FLDWAV model; however, errors in the breach description and thence in the resulting peak outflow rate are damped-out as the flood wave advances downstream. Using FLDWAV, it has been observed that large variations in Q_p at the dam can be damped-out as the flood peak advances farther and farther downstream. The extent of damping is related to the size of the downstream floodplain; the wider the floodplain, the greater will be the extent of damping. Sensitivity tests on the breach parameters are best determined using the FLDWAV model and then comparing the variation in simulated flood peaks at critical downstream locations. In this way, the real uncertainty (that which effects the locations of concern) in the breach parameter selections will be determined.

For conservative forecasts (for contingency planning or real-time warnings) which err on the side of larger flood waves, values for b and z should produce an average breach width (\bar{b}) in the uppermost range for a certain type of dam. Failure time (τ) should be selected in the lower range to produce a maximum outflow. Of course, in real-time forecasting of dam-break floods, observational estimates of \bar{b} and τ should be used when available to update forecasts when response time is sufficient as in the case of forecast points many miles downstream of the breached dam. Flood wave travel rates are often in the range of 2-10 miles per hour. Accordingly, response times for some downstream forecast points may therefore be sufficient for updated forecasts to be issued.

Eq. (6.13) can be used quickly and conveniently to test the sensitivity of \bar{b} and τ for a specific reservoir having properties of V_r , h_d , and A_s . For example, using Eq. (6.13) for a moderately large reservoir ($V_r = 250,000$ acre-ft, $h_d = 260$ ft, $A_s = 2,000$ acres), it can be shown that Q_p varies in proportion as \bar{b} varies, however, Q_p only varies by less than 1/5 of the variation in τ . Although for a fairly small reservoir ($V_r = 500$ acre-ft, $h_d = 40$ ft, $A_s = 10$ acres), it can be shown, using Eq. (6.13), that Q_p varies less than 20 percent for a variation in \bar{b} of 50 percent while Q_p varies about 40 percent for a variation in τ of 50 percent. Thus, it can be generalized, that, for large reservoirs Q_p is quite

sensitive to \bar{b} and rather insensitive to τ , while for very small reservoirs Q_p is somewhat insensitive to \bar{b} and fairly sensitive to τ .

7. RIVER SYSTEMS

Flow routing is often required in natural waterways (streams, rivers, reservoirs, estuaries) as well as man-made channels (canals, ditches, storm drains) which are linked together forming a network of waterways/channels. The configuration may be dendritic (tree-type) and/or looped (islands, parallel channels connected by bypasses, etc.). The implicit formulation of the Saint-Venant equations is well-suited from the standpoint of accuracy for simulating unsteady flows in a network of channels since the response of the system as a whole is determined within a certain convergence criterion for each time step. However, a network of channels presents complications in achieving computational efficiency when using the implicit formulation. Equations representing the conservation of mass and momentum at the confluence of two channels produce a Jacobian matrix (Figure 2.5) in the Newton-Raphson method with elements (Fread, 1985b) which are not contained within the narrow band along the main diagonal of the matrix. The column location of the elements within the Jacobian depends on the sequence numbers of the adjacent cross-sections at the confluence. The generation of such “off-diagonal” elements produces a “sparse” matrix containing relatively few non-zero elements. Unless special matrix solution techniques are used for the sparse matrix, the computational time required to solve the matrix by conventional matrix solution techniques is so great as to make the implicit method unfeasible. The same situation also occurs for the linearized implicit methods which must also solve a system of linear equations similar to the Jacobian. FLDWAV contains an algorithm with an efficient computational treatment of dendritic (tree-type) channel networks.

7.1 Single River

When modeling a single river (Figure 7.1) using FLDWAV, the external boundary conditions must first be established. The upstream boundary must be selected at a location such that it is independent of the downstream conditions (e.g., a generated or observed discharge hydrograph, driven by upstream conditions). The downstream boundary is usually selected at a location that is independent of flow conditions below the boundary (e.g., backwater effects from storm surges, tides, large tributary inflows, reservoirs, bridge/natural channel constrictions). A rating curve is used to

represent channel control. Also, events which are being simulated using historical data may have a downstream boundary that is influenced by downstream phenomena. The downstream boundary under these conditions can be represented by a known time series.

After the routing reach is established by the boundary locations, cross sections are obtained to represent the reach. Cross section locations can be measured from upstream to downstream e.g., starting at a dam and continuing downstream; or cross sections can be measured from downstream to upstream, e.g., starting at the mouth of the river and continuing in the upstream direction. The cross sections must be numbered sequentially from upstream to downstream as shown in Figure 7.1. The initial conditions at each cross section are next established at each cross section. The Saint-Venant equations and boundary equations (external and internal) are then solved simultaneously using the four-point nonlinear implicit technique. The system of equations is solved iteratively using the Newton-Raphson technique until the maximum errors in water-surface elevations and discharges at any cross section are less than the user-specified tolerances. The first estimates for the water-surface elevations and discharges are extrapolated from values at the previous two time steps.

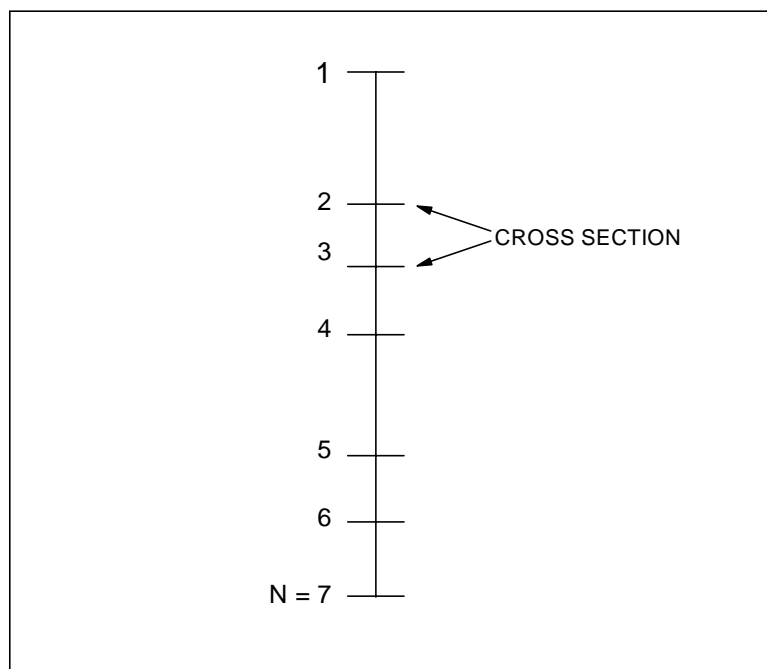


Figure 7.1 - Schematic of Single River with Numbered Cross Sections

7.2 Dendritic River Systems

Although the implicit formulation of the unsteady flow equations is well-suited for simulating unsteady flows in a system of rivers, particular care must be given to maintain the necessary solution efficiency as mentioned previously with regards to the matrix solution technique of the Newton-Raphson procedure. To accomplish this, a special solution procedure (the relaxation algorithm) is available within FLDWAV to simulate a system of dendritic (tree-type) channels.

7.2.1 Relaxation Solution Algorithm

During a time step, the relaxation algorithm as described by Fread (1973a) solves the Saint-Venant equations first for the main-stem river and then separately for each tributary of the dendritic network. The tributary flow at each confluence is treated as lateral flow (q) which is estimated when solving Eqs. (2.1-2.2) for each river. Each tributary flow depends on its upstream boundary condition, lateral inflows along its reach, and the water elevation at the confluence (downstream boundary for the tributary) which is obtained during the simulation of the main-stem river. Due to the interdependence of the flows in the main-stem river and its tributaries, the following iterative or relaxation algorithm (Fread, 1973a, 1985b) is used:

$$q^* = \alpha q + (1 - \alpha)q^{**} \quad \dots\dots\dots (7.1)$$

in which q is the computed tributary flow at each confluence, q^{**} is the previous estimate of q , q^* is the new estimate of q , and α is a weighting (relaxation) factor ($0 < \alpha \leq 1$). Convergence is attained when q is sufficiently close to q^{**} , i.e., $|q^* - q^{**}| < \epsilon_Q$.

The acute angle (ω_t) that the tributary makes with the main-stem river or another tributary is a user-specified parameter. This enables the inclusion of the momentum effect of the tributary inflow via the term ($L = -qv_x$) as used in Eq. (2.2) and Eq. (2.20). The velocity of the tributary inflow is given by:

$$v_x = (Q/A)_N \cos \omega_t \quad \dots\dots\dots (7.2)$$

in which N denotes the last cross section of the tributary just before it enters the main-stem river or another tributary.

A dendritic system containing 1st and higher-order tributaries (Figure 7.2) may be modeled within FLDWAV using this algorithm. The FLDWAV model requires the user to supply the following information for each tributary: ω_t , α , ϵ_Q , and the cross-section location along the main-stem river or tributary immediately upstream of the tributary confluence (NJUN(j) where j=2,3,...,JN in which JN=1+total number of tributaries). If, in addition to these parameters, the user specifies the

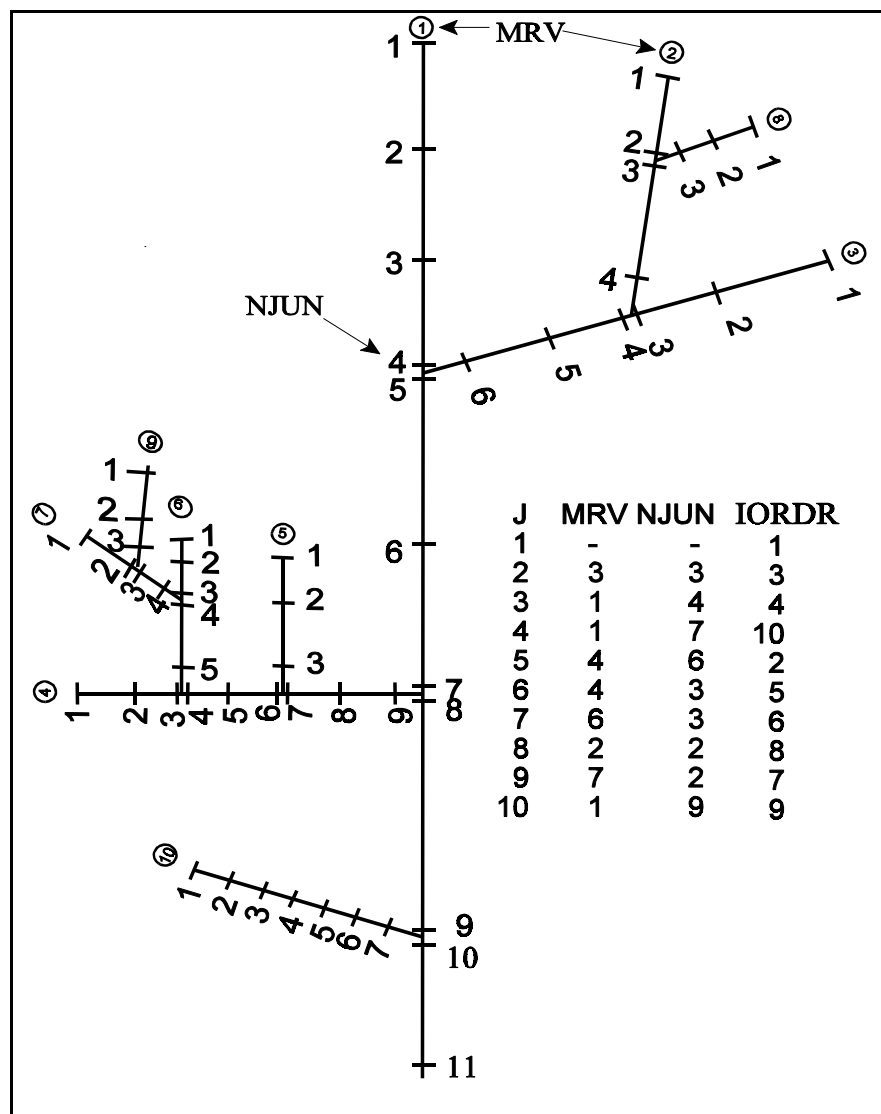


Figure 7.2 - Dendritic River System Backwater Algorithm for Spatial Conditions.

number of the river into which the tributary flows (MRV(j)), the relaxation algorithm may be used, without modification, to model river systems containing nth-order tributaries. The main-stem river is always numbered 1 while the tributaries are numbered 2,3,...,JN.

7.2.2 Initial Conditions for Dendritic River System

In dendritic river systems, the initial conditions, if not user-specified, may be generated by assuming steady flow in the system and adding the inflow from each flow successively starting with the n^{th} -order tributary and proceeding downstream to the main-stem river. Backwater computations (Lewis, et. al, 1996) commence with the water-surface elevation at the downstream boundary of the main-stem river and proceed to the upstream location on each river according to the order number (i.e., main stem, all 1st-order tributaries, ..., all n^{th} -order tributaries) as shown in Figure 7.2. The parameter, MRV, is user-specified and represents the number of the river into which tributaries discharge. The parameter, NJUN, is also user-specified and represents the number of the cross section immediately upstream of where a tributary junctions with river number MRV. J represents the river number and IORDR is automatically computed by the algorithm in Figure 7.3.

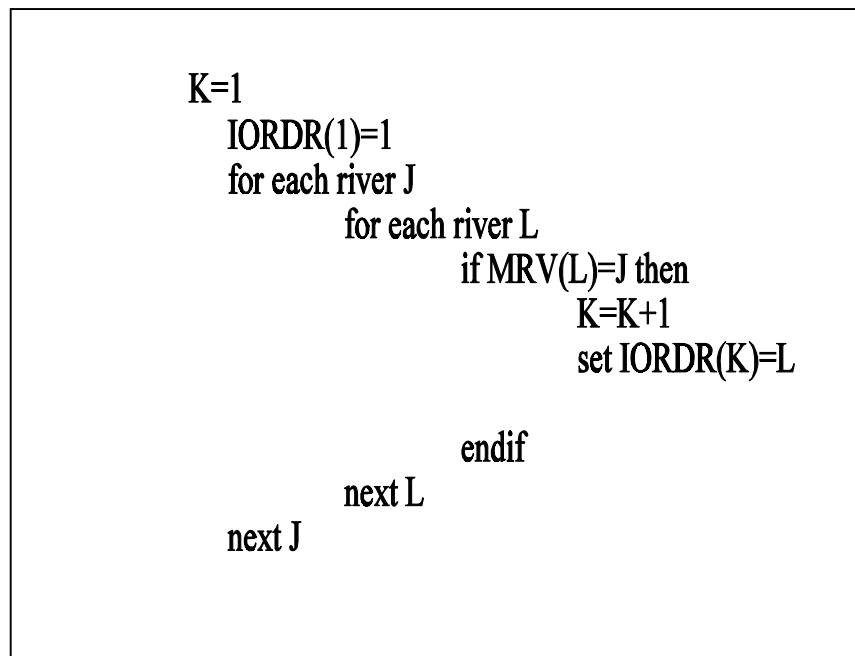


Figure 7.3 - Algorithm for Backwater Computational Order of Rivers.

When computing the initial discharges, the computational order of rivers is the reverse of that needed for backwater computations. The relaxation technique allows the flexibility of adding tributaries to the system in any order without affecting the numbering scheme of the original river system.

8. CROSS SECTIONS

Much of the uniqueness of a specific flow routing application using FLDWAV is captured in the cross sections located at selected points along the channel or waterway as shown in Figure 8.1(a).

8.1 Active Sections

That portion of the channel cross section in which flow is conveyed or in which the velocity in the x-direction is non-negligible, is called the active section. Active cross-sectional area is represented by the term (A) in the Saint-Venant equations. (2.1-2.2). Cross sections may be of regular or irregular geometrical shape. As indicated in Figure 8.1(b), each cross section is described by tabular values of channel topwidth (B_i) and water-surface elevation (h_i) which constitute a piece-wise linear relationship. Generally about 4 to 12 sets of topwidths and associated elevations provide a sufficiently accurate description of the cross section. Area (A_i)-elevation (h_i) tables are automatically generated initially within FLDWAV from the user-specified topwidth-elevation data. During the solution of the Saint-Venant equations, any areas or widths associated with a particular water-surface elevation are linearly interpolated from the tabular values. Cross sections at gaging station locations are generally used as computational points. Other computational points at which cross sections are described are also user-specified at locations along the river where significant cross-sectional or flow-resistance changes occur or at locations where major tributaries enter. The spacing of cross sections can range from a few hundred feet to a few miles apart. Typically, cross sections are spaced farther apart for large rivers than for small streams, since the degree of variation in the cross-sectional characteristics is greater for the small streams. It is essential that the selected cross sections, with the assumption of linear variation between adjacent sections, represent the volume that is available to contain the flow along the waterway.

In addition to the consideration of cross-sectional variation in the selection of Δx reaches, the solution accuracy is also affected by the choice of Δx . For best accuracy, the maximum reach length (Δx_m , mi) is related to Δt_n (hr) by the Courant condition as follows:

$$\Delta x_m \leq \hat{c} \Delta t_h \quad \dots\dots\dots (8.1)$$

in which \hat{c} is the kinematic or bulk wave speed (mi/hr) of the essential characteristic of the unsteady flow such as the mid-point of the hydrograph. The bulk wave speed (\hat{c}) may be initially estimated from Eq. (11.10) or from observed flows via Eq.(11.11), and the time step (Δt_h) is selected according to Eq. (11.14-11.17). Since \hat{c} can vary with distance along the channel because of variation of channel bottom slope, hydraulic roughness, peak discharge and associated velocity, Δx_m may not be constant along the channel.

In some applications, particularly the routing of flood waves in large rivers with gradually varying cross sections, the number of required cross sections can be reduced by using a distance-weighted average section whose width is so computed that it replaces several (varying from a few to more than 50) intervening cross sections and yet conserves the volume within the reach. The distance-weighting equation to obtain the average width is given by the following:

$$\overline{B}_k = 0.5[(B_i + B_{i+1}) \Delta d_i + (B_{i+1} + B_{i+2}) \Delta d_{i+1} + \dots + (B_{I-1} + B_I) \Delta d_{I-1}] / \sum_1^I \Delta d_i \quad \dots\dots\dots (8.2)$$

n which \overline{B}_k is the distance-weighted width for a particular k^{th} depth of flow, B_i is width of the i^{th} section along a reach having a total of (I') sections to be averaged, and Δd_i is the distance between the individual sections. The total reach length ($\sum \Delta d_i$) of Eq. (8.2) must be less than Δx_m of Eq. (8.1).

8.2 Inactive (Dead) Off-Channel Storage Sections.

There can be portions of a cross section where the flow velocity in the x-direction is negligible relative to the velocity in the active portion. The inactive portion is called off-channel (dead) storage, and it does not convey flow in the downstream x-direction; it is represented by the term (A_o) in the Saint-Venant conservation of mass Equation (1.1). The judicious use of off-channel storage enables the one-dimensional Saint-Venant equations to approach the capabilities of two-dimensional unsteady flow equations for certain applications as described herein.

Every cross section must have an active area (A_k); however, a cross section need not have an inactive area (A_{o_k}). The presence of inactive area is subjectively determined by discerning those portions of a cross section where large eddies may occur and the flow is not directed in the downstream direction. Therein, the flow is temporarily stored as the water elevation rises to inundate those portions of the cross section, yet little if any quantity of flow is conveyed to other sections located further downstream.

Off-channel storage is often associated with contracting and expanding sections. Streamlines tend to be more flexible as flow contracts, hence less off-channel storage is associated with a contracting reach than with an expanding reach where large eddies are easily formed by the streamlines as they gradually expand from a contracted section to a wider downstream section.

Another instance of off-channel storage occurs when flow temporarily stores within the downstream reaches of a tributary which connects to the river through which the flood is being routed via the Saint-Venant equations (Figure 8.1(a)). In this case, the off-channel storage width (BO) is zero or nonexistent at a section on the river coincident with the upstream bank (floodplain boundary) of the tributary, and also the BO is zero at a section of the routed river coincident with the downstream bank of the tributary. However, a section located along the river and midway between the other two sections does have an off-channel storage width (BO). This value may be determined from the following relation:

$$BO_k = 2 (43560) Sa_k / L \dots\dots\dots (8.3)$$

in which the subscript k designates the particular elevation (h_k) within the cross section (the elevation is usually associated with topographic contour elevations), Sa_k represents the surface area (acres) of that portion of the tributary which would be inundated at the k^{th} elevation due to the backwater pool caused by the flow in the river, L is the length (ft) of the reach along the routed river bounded by the two banks (upstream and downstream) of the connecting tributary, and BO_k is the width (ft) of the off-channel portion of the cross section along the routed river and coincident with the middle of the tributary. Of course, if flow is occurring in the tributary due to runoff from its upstream

drainage basin, then that portion of the tributary section needed to convey this flow should not be included in the determination of BO_k , i.e., only those elevations exceeding that required to convey the tributary flow should be used to compute Sa_k in Eq. (8.3). When off-channel storage areas are used in the Saint-Venant equations, it is implied that as the water-surface elevation rises at the center of the river cross section, that same elevation is attained within the computational time step interval throughout limits of the specified off-channel storage area associated with that section. This may be quite erroneous when the tributary has an extremely mild slope which extends for many miles upstream. It may be roughly approximated that the backwater effects of the routed river flows will propagate up the tributary at the celerity of small disturbances (local dynamic wave velocity), i.e.,

$$c = \sqrt{g \bar{D}_t} \dots\dots\dots (8.4)$$

in which c is the local dynamic wave velocity (ft/sec), g is the gravity acceleration constant, and \bar{D}_t is the average hydraulic depth (ft) along the tributary within the backwater reach ($\hat{c}\Delta t$) of the tributary. The actual reach of tributary used in Eq. (8.3) to determine Sa_k should not greatly exceed the backwater reach ($c\Delta t$). If it does, then too much of the routed river flow is stored within the tributary.

Another type of off-channel storage is a ponding area or an embayment (see Figure 8.1) located along the river where water is stored therein but is not conveyed downstream along with the flow in the river. The connection between the ponding area and the river may be either a short conveyance channel or a broad-crested weir (sill). If the connecting channel/sill is rather narrow, then off-channel storage should be determined via Eq. (8.3); however, if the connecting channel/sill is very wide, then the BO_k values may be determined by direct measurement of the storage pond widths in the direction perpendicular to the river.

Thus, within FLDWAV, dead or off-channel storage areas (A_o) can be used to effectively account for embayments, ravines, or tributaries which connect to the flow channel but do not pass flow and serve only to store the flow. Another effective use of off-channel storage is to model a heavily wooded flood plain which temporarily stores a portion of the flood waters passing along the waterway. In each of these cases, the use of zero velocity for the portion of the flood waters

contained in the dead storage areas results in a more realistic simulation of the actual flow than using an average velocity derived from the main flow channel area (A) and the dead storage area (A_o). The off-channel storage cross-sectional properties are described in the same way as the active cross-sectional areas, i.e., for each section, a table of top widths (BO_k) and elevations (h_k) is user-specified. A table of area (A_{o_k}) -elevation (h_k) is created within FLDWAV, and intermediate storage top widths (BO) or areas (A_o) are linearly interpolated from the two tables as required during the computations.

Another type of off-channel storage is associated with levee-protected floodplains. When a floodplain is separated from the river by a levee that is parallel to the river, the portion of the floodplain below the crest elevation of the levee may be approximated as off-channel storage via a technique, “cave-in-the-bank”, as illustrated in Fig 8.2. The volume (acre-ft) within a Δx_i (ft) reach along the river is designated herein as V_f and the levee crest elevation as h_ℓ (ft). The off-channel storage width (BO_k) may be computed by the user of FLDWAV for an elevation ($h_\ell + \hat{d}/2$) by the following relation:

$$BO_k = 2 (43560) V_f / (\hat{d} \Delta x_i) \dots\dots\dots (8.5)$$

in which \hat{d} is an estimated differential elevation (ft) approximated as the necessary rise in the water-surface elevation (h) above the levee crest (h_ℓ) during which the volume V_f is filled by flow leaving the river via the broad-crested weir which has an average depth above the levee crest of $\hat{d}/2$ during the interval of time for filling the V_f volume. The BO_k values associated with the elevations h_ℓ and

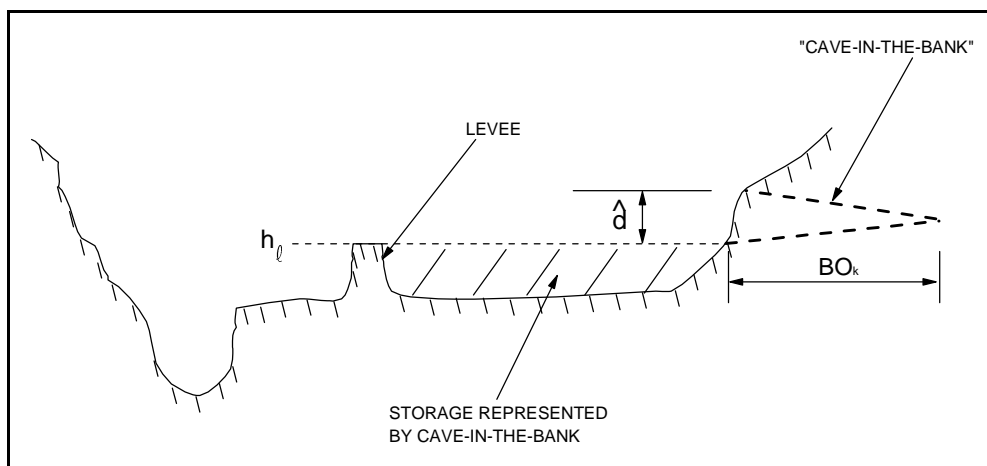


Figure 8.2 - Floodplain Storage Treated by the “Cave-in-the-bank” Off-Channel Storage Technique.

$h_t + d$ are specified as zero. The estimation of \hat{d} is not simple; for best results, it requires an iterative application of the FLDWAV model. As a first estimate for \hat{d} , the following may be used:

$$\hat{d} = 0.037(V_f \delta_h)^{0.4} \dots \dots \dots (8.6)$$

where δ_h is the rate of rise (ft/hr) in the river stage in the vicinity of the elevation of h_t .

8.3 Cross-Section Interpolation

Within FLDWAV is a user-selected option to automatically generate additional cross sections between any two adjacent user-specified cross sections. The properties of the additional cross sections are linearly interpolated. Both active and inactive (off-channel storage) cross-sectional properties are generated via the interpolation procedure. Generation of the additional cross sections enables the computational distance step (Δx_i) used to solve the finite-difference Saint-Venant equations, Eqs. (2.19-2.20), to be smaller than the distance step separating the original user-specified cross sections. The original distance steps are determined by considerations for properly specifying the river/valley volume via the cross sections with an assumption of linear variations between user-specified sections. Thus, the river/floodplain sections are located at narrow and wide sections with linear variation from one to the other. Original specified cross sections are also selected according to special features that need to be described, e.g., bridges, dams, locations where significant changes in the channel bottom slope or the Manning n occur, locations where lateral inflow/outflow occur, and locations where information about the simulated flood wave is desired.

The option for interpolation of cross sections requires adherence to the following criteria when specifying the cross sections: (1) all cross sections should have the same number of topwidths; (2) if possible, the bankfull (top of incised river channel) topwidth should be in the same relative position of the topwidth table for all cross sections, e.g., the second topwidth (BO_2) should represent the bankfull width for all sections.

The computational distance step (Δx_i) is controlled within FLDWAV by the parameter (DXM_i) which is user-specified for each (i^{th}) original distance step between user-specified cross sections. The relation of DXM_i (mi) to Δx_i (ft) is simply $\Delta x_i = 5280 DXM_i$ in which DXM is the computational reach length (mi), and Δx_i is the computational distance step (ft). Criteria for specifying DXM_i are given in a following Sub-section 11.1.

If interpolated cross sections are created between two adjacent user-specified cross sections and lateral inflows or computed outflows as described in a following Sub-section 12.1, the following provisions automatically occur: (1) for lateral inflows, the inflow is made to occur entirely within the most upstream (Δx_i) computational distance step within the original reach between user-specified sections; (2) for computed lateral outflows, the computed outflow occurs for each of the computational distance steps (Δx_i), each having the same crest elevation (h_i) as user-specified for the original reach between specified cross sections; and (3) for computed outflow to floodplain compartments, the computed flow occurs for each of the (Δx_i) computational distance steps, each having the same levee crest elevation (h_i) as user-specified for the original reach.

9. SELECTION OF MANNING n

Manning n is used to describe the resistance to flow due to channel roughness caused by sand/gravel bed-forms, bank vegetation and obstructions, bend effects, and circulation-eddy losses. The Manning n is user-defined for each channel reach between user-specified cross-sections or a river reach bounded by cross sections with gaging stations. The Manning n is user-specified as a function of either stage or discharge according to a piece-wise linear relation with both n and the independent variable (h or Q) user-specified in FLDWAV in tabular form. Linear interpolation is used to obtain n for values of h or Q intermediate to the tabular values.

Simulation results are often very sensitive to the Manning n. Although in the absence of necessary data (observed stages and discharges), n can be estimated; however, best results are obtained when n is adjusted to reproduce historical observations of stage and discharge. The adjustment process is referred to as calibration. This may be either a trial-error process or an automatic iterative procedure available within FLDWAV. The automatic calibration feature is described later in Sub-section 14.2.

Alternatively, the friction effects can be represented by channel conveyance (K) which may be user-specified in FLDWAV as a tabular function of water elevation. Conveyance is related to the Manning n and cross-sectional properties, i.e.

$$K = \mu AR^{2/3}/n \dots\dots\dots (9.1)$$

The use of K rather than the Manning n has an advantage in applications where the cross-section consists of an in-bank portion and a rather wide, flat floodplain. The hydraulic radius (R) can be somewhat mathematically discontinuous when the water surface expands onto the floodplain. This discontinuity can be treated by specifying conveyance as a function of elevation which is mathematically much smoother in the vicinity of the discontinuity. This provides more realistic flows and helps to avoid numerical problems during the computations.

Selection of the Manning n should reflect the influence of bank and bed materials, channel obstructions, irregularity of the river banks, and especially vegetation. The Manning n varies with the magnitude of flow (Fread, 1989a). As the flow increases and more portions of the bank and overbank become inundated, the vegetation located at these elevations causes an increase in the resistance to flow. The latter may cause the n values to vary considerably with flow elevation, i.e., the n value may be considerably larger for flow inundating the floodplain than for flow confined within the channel bank. This is due to the presence of field crops, weeds, brush, scattered trees, or thick woods located in the floodplain. Also, the n value may be larger for small floodplain depths than for larger depths. This can be due to a flattening of the brush, thick weeds, or tall grass as the flow depths and velocities increase. This effect may be reversed in the case of thick woods where, at the greater depths, the flow impinges against the branches having leaves rather than only against the tree trunks. Seasonal influences (leaves and weeds occur in summer but not in winter) may also affect the selection of the Manning n .

The n values may also decrease with increasing discharge when the increase in the overbank flow area is relatively small compared to the increase of flow area within the banks, as the case of wide rivers with levees situated closely along the natural river banks, or when floods remain confined within the channel banks.

Changing (time-dependent) conditions can result in different n values for the same flow; these are: (a) change of season which affects the extent of vegetation, (b) change of water temperature which affects bed-forms in some alluvial rivers, (c) ice cover effects, and (d) man-made channel changes such as drift removal, channel straightening, bank stabilization, or paving.

Basic references for selecting the Manning n may be found in Chow (1959) and Barnes (1967). Also, some other reports should be considered in selecting n values, i.e., Arcement and Schneider (1984) for wooded floodplains and Jarrett (1984, 1985) for relatively steep ($0.002 \leq S_o \leq 0.040$) streams with gravel/cobble/boulder beds. Both of these also provide general methodologies quite similar to that given by Chow (1959) for selecting the n value to account for the various factors previously mentioned. Arcement and Schneider (1984) also consider the effects of urbanization of

the floodplain. Another methodology which estimates the Darcy friction factor (f) for floodplain flows is described by Walton and Christenson (1980). The Darcy f is related to the Manning n as follows (Fread, 1988):

$$n = 0.0926 f^{0.5} D^{0.17} \dots\dots\dots (9.2)$$

The flow observations used in developing the Manning n predictive methodologies have been confined to floods originating from rainfall/snowmelt-runoff. The much greater magnitude of a dam-break flood produces greater velocities and results in the inundation of portions of the floodplain never before inundated. The higher velocities will cause additional energy losses due to temporary flow obstructions formed by transported debris which impinge against some more permanent feature along the river such as a bridge or other man-made structure. The dam-break flood is much more capable than the lesser runoff-generated flood of creating and transporting large amounts of debris, e.g., uprooted trees, demolished houses, vehicles, etc. Therefore, the Manning n values often need to be increased in order to account for the additional energy losses associated with the dam-break flows such as those due to the temporary debris dams which form and then disintegrate when backwater depths become too great. The extent of the debris effects, of course, is dependent on the availability and amount of debris which can be transported and the existence of man-made or natural constrictions where the debris may impinge behind and form temporary obstructions to the flow.

The uncertainty associated with the selection of the Manning n and the resulting error in the Manning n can be quite significant for dam-break floods due to: (1) the great magnitude of the flood produces flow in portions of floodplains which were never before inundated; this necessitates the selection of the n value without the benefit of previous evaluations of n from measured elevation/discharges or the use of calibration techniques for determining the n values; (2) the effects of transported debris can alter the Manning n . Although the uncertainty of the Manning n may be large, this effect is considerably damped or reduced during the computation of the water surface elevations. For example, a 20 percent change in the Manning n resulted in less than a 5 percent change in the flood depths associated with the Teton dam-break flood. (Fread, 1988).

10. FLOODPLAINS

10.1 Composite Option or Conveyance Option

The friction slope (S_f) may be evaluated by two different methods as indicated by Eq. (2.4) or Eq. (2.22). The first method (composite option) directly utilizes composite (average of channel and floodplain) values of the Manning n , A , and R while the second method indirectly uses separate Manning n , A , and R values for the channel and left and right portions of the floodplain (Figure 10.1).

In the composite option (the first expression for S_f in Eqs. (2.4 and 2.22), the A and R values are for the total active flow portion of the river/valley section, i.e., the channel, and left and right floodplains. The Manning n is for the total active flow river/valley section. It can be estimated for each (k^{th}) topwidth (B_k) and associated elevation (h_k) by the following:

$$n_k = (n_{c_k} B_{c_k} + n_{l_k} B_{l_k} + n_{r_k} B_{r_k}) / (B_{c_k} + B_{l_k} + B_{r_k}) \dots\dots\dots(10.1)$$

in which the subscripts (c, l, r) represent the channel, left floodplain, and right floodplain, respectively. The Manning n that is user-specified for each k^{th} elevation is the effective n value for all flow beneath each k^{th} elevation, i.e., the n_k value represents the depth integrated effective n value for the total flow occurring when the k^{th} elevation is reached by the surface-water elevation (h_k)

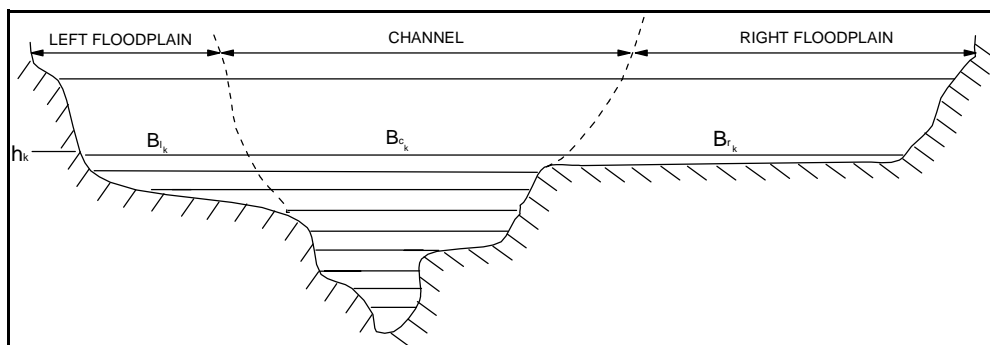


Figure 10.1 - Cross Section Showing Incised Channel and Floodplain.

associated with that particular flow condition. The concept of a depth integrated Manning n is also used in the conveyance option.

In the second method, (conveyance (K) option which uses the second expression for S_f in Eqs. (2.4 and 2.22)), the conveyances for each portion of the total cross section are computed initially within FLDWAV via Eqs. (2.5-2.7), and then the total conveyance for a particular section is obtained by summing the separate conveyances as in Eq. (2.8). The conveyance option is activated when the user assigns the control parameter (KFLP) a value of unity. Assigning KFLP a zero value results in the composite representation of S_f .

An advantage in using the conveyance option is the elimination of numerical convergence difficulties associated with the composite option for S_f ; this occurs when the cross-sectional geometry consists of an incised channel and a very wide and flat floodplain. In this case, the derivative (dB/dh), which is necessary to evaluate when using the Newton-Raphson iterative technique to solve the Saint-Venant equations, is not well-defined (it abruptly changes in value) in the vicinity of the top of the channel bank at the beginning of the overbank (floodplain) portion of the river/valley; here the topwidth greatly increases with a small increase in elevation. However, the total conveyance function, which also varies with elevation, is well behaved, i.e., the slope dK/dh is more smoothly varying in the vicinity of the top of bank whereas the slope dB/dh is somewhat discontinuous in this same region. The selection of the conveyance option requires the separate user-specification of the topwidths and n values for each of the portions of the total cross section, i.e., channel, left floodplain, and right floodplain. The left and/or the right floodplain properties (B and n) may be user-specified as zero values if there is no floodplain or portion thereof for a particular cross section.

10.2 Sinuosity Factors Associated with Floodplains

A meandering or sinuous channel within a floodplain provides a longer flow path than that provided by the floodplain as shown in Figure 2.2. This effect is simulated in FLDWAV via the sinuosity factors (s_{co} and s_m) in Eqs. (2.1-2.2) or Eqs.(2.19-2.20). The cross sections are designated via a mileage parameter (XS) which is measured along the mean flow-path through the floodplain. The

sinuosity factors which are always ≥ 1.0 represent the ratio of the flow-path distance along the meandering channel to the mean flow-path distance (XS) along the floodplain. A single sinuosity factor is user-specified for each top width elevation (h_k) for each i^{th} reach between two adjacent user-specified cross sections; the sinuosity factor tends to decrease for elevations extending above the top of bank. For those elevations used to describe the topwidth at bankfull elevation and below, the sinuosity factor is as previously defined; however, at elevations above bankfull, the sinuosity factor for each layer of flow between user-specified elevations is decreased. This trend is continued until for those flow layers, say 5 to 10 feet above bankfull, the user-specified sinuosity factor is reduced to unity which indicates that the floodplain flow has fully captured the upper layers of flow directly above the channel. The sinuosity factor may be user-specified as either 1.0 or 0.0 for FLDWAV; if user-specified as 0.0, it is automatically set to unity for all elevations. This represents a straight river with no meanders. When the conveyance option is not used, i.e., $KFLP = 0$, the sinuosity factors are not user-specified; however, they are then automatically set to unity within FLDWAV.

The sinuosity factor as used in the finite-difference, Saint-Venant equations, Eqs. (2.19-2.20), is depth-weighted within FLDWAV according to Eqs. (2.9-2.10). The depth weighting is treated differently for the conservation of mass Eq. (2.1) or Eq. (2.19) and for the momentum Eq. (2.2) or Eq. (2.20). This gives rise to the fact that the single user-specified sinuosity factor (s_k) for each k^{th} elevation of flow (corresponding to each h_k elevation associated with each user-specified topwidth B_k), is actually represented as two distinct sinuosity factors, s_{co_k} for the conservation of mass equation and s_{m_k} for the conservation of momentum equation. However, the user specifies only one sinuosity factor for each h_k elevation. The depth-weighting results in a sinuosity factor which only approaches unity, even for the upper elevations associated with large floodplain flows. This occurs since the total flow is still comprised of the relatively small flow within bankfull which follows the meandering channel, as well as the larger portion of the total flow which follows the floodplain flow-path.

11. COMPUTATIONAL PARAMETER SELECTION

It is critical for successful applications of FLDWAV that appropriate computational parameters for distance steps (Δx_i) and time steps (Δt_j) be used in the computational solution of the numerical Saint-Venant equations (2.19-2.20). Generally, unsuccessful (aborted runs or runs with too much numerical error in the solutions) occur when Δx_i (ft) and/or Δt_j (sec) are too large. However, specifying too small values for Δx_i and Δt_j require more computational resources (storage and execution time). To avoid either of these extremes the following guidelines are provided, and specific capabilities within FLDWAV for implementing these are described.

11.1 Selection of Computational Distance Steps

It is most important that computational distance steps (Δx_i , ft) in the finite-difference Saint-Venant equations, Eqs. (2.19-2.20), be properly selected via the parameter (Δx_m) or (DXM_i , mi) in order to avoid computational difficulties and to achieve an acceptable level of numerical accuracy. When the computational distance step chosen is too large, the resulting truncation error (the difference between the true solution of the partial differential Saint-Venant equations (2.1-2.2), and the approximate solution of the finite-difference Saint-Venant equations, Eqs. (2.19-2.20)) may be so large that the computed solutions of h_i and Q_i are totally unrealistic, e.g., the computed flow depths have negative values. This causes an execution of the FLDWAV program to abort since a negative depth or cross-sectional area is raised to a power which is necessary when computing the friction slope (S_f) via Eq. (2.22). Large truncation errors can also cause irregularities in the computed hydrograph as manifested by spurious spikes in the rising and/or falling limbs. Three criteria are used to select the computational distance steps.

The first of the criteria is related to contracting/expanding cross sections. Samuels (1985) found that the four-point implicit difference scheme used in FLDWAV theoretically requires the following criteria be satisfied within any computational distance step:

$$0.635 < A_{i+1}/A_i < 1.576 \dots\dots\dots (11.1)$$

Basco (1987) found from numerical experimental studies using the NWS DAMBRK model (Fread, 1988) that the factor 0.635 should be increased to 0.70, and the factor 1.576 could be increased to 2.00. Within FLDWAV, the following algorithm automatically selects the computational distance step (Δx_i) such that the above contraction/expansion criterion, Eq. (11.1), is conservatively satisfied:

$$DXM_i = L/M \dots\dots\dots (11.2)$$

where:

$$M = 1 + 2 |A_i - A_{i+1}|/\hat{A} \dots\dots\dots (11.3)$$

$$\hat{A} = A_{i+1} \quad \text{if } A_i > A_{i+1} \quad (\text{contraction}) \dots\dots\dots (11.4)$$

$$\hat{A} = A_i \quad \text{if } A_i < A_{i+1} \quad (\text{expansion}) \dots\dots\dots (11.5)$$

in which L is the original distance step (mi) between user-specified cross sections and M is rounded to the nearest smaller integer which represents the new number of computational distance steps within the original distance step.

The second of the three criteria is the following:

$$DXM_i \leq \hat{c} T_r/M \dots\dots\dots (11.6)$$

in which DXM_i is the computational distance step (mi), \hat{c} is the kinematic or bulk wave velocity (mi/hr), T_r is the time of rise (hr) of the routed hydrograph (time interval between the significant beginning of increased discharge and the peak of the discharge hydrograph as illustrated in Figure 11.1), and $5 \leq M \leq 40$ (default within FLDWAV is $M = 20$). Eq. (11.6) was first developed empirically in the late 1970's, and later Fread and Lewis (1993) provided a theoretical foundation for

this critical equation, especially for rapid-rising flood waves such as dam-break waves. The selection of the time step is discussed in the next Sub-section. The kinematic or bulk wave velocity (\hat{c}) for most unsteady flows, including dam-break floods, that propagate through a river/valley can be approximated by the kinematic wave velocity, i.e.,

$$\hat{c} \approx 0.68 K_w V \dots\dots\dots (11.7)$$

where K_w is approximately 1.4 for most natural channels but is more accurately given by the following:

$$K_w = 5/3 - 2/3 A (dB/dy)/B^2 \dots\dots\dots (11.8)$$

and V is computed from the Manning equation, i.e.,

$$V = \mu/n R^{2/3} S_o^{1/2} \dots\dots\dots (11.9)$$

Also, the kinematic wave speed (\hat{c}) in mi/hr can be “roughly” estimated by the following:

$$\hat{c} \approx 2 S m^{1/2} \dots\dots\dots (11.10)$$

in which $S m$ is the river bottom slope (ft/mi).

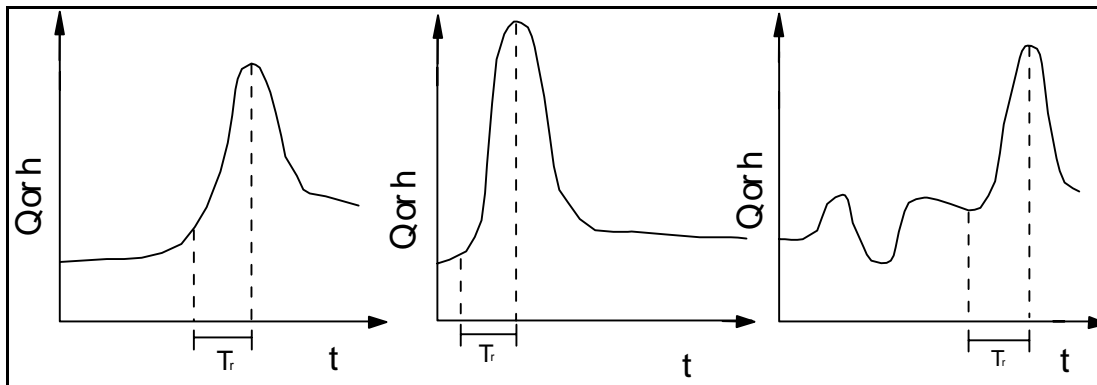


Figure 11.1 - Time of Rise (T_r) for Various Hydrographs.

If observed hydrographs from historical floods are available along the routing reach and if the hydrograph routing application is similar to the historical flood, \hat{c} may be accurately determined from two hydrographs at different locations along the river. This is accomplished by dividing the distance ΔL between the two locations along the river by the difference in the times of occurrence of the peak (T_p) of the observed hydrograph at each i^{th} location, i.e.,

$$\hat{c} = \Delta L / (T_{p_{i+1}} - T_{p_i}) \quad \dots\dots\dots (11.11)$$

Since the bulk wave speed (\hat{c}) can vary along the river, DXM may not be constant along the river. Therefore, the capability to have a particular DXM_i value for each i^{th} reach between user-specified cross sections along the river is provided within FLDWAV. Three options are provided for selecting the computational distance step (DXM_i). They are: (1) the DXM_i value is zero, and the value used in the routing computations is the difference between two adjacent user-specified cross-section locations determined within FLDWAV; (2) DXM_i is determined by the user of FLDWAV for each i^{th} reach using Eqs. (11.6-11.9) or Eq. (11.10), and a negative sign (-) preceding the first value signals the model to bypass the automatic computation of DXM_i ; and (3) DXM_i is user-specified with a positive value which signals the model to automatically compute DXM_i and print it out, while still using the user-specified value for the routing if it is smaller. If DXM_i is non-zero, this value is used in computation; however, the value will be compared to an automatically determined value within FLDWAV using the minimum value obtained from Eqs. (11.2, 11.6, 11.10, 11.12, 11.13) and if the minimum value thus obtained is less than the user-specified DXM_i value, a warning message will be printed suggesting the minimum value be used in a future run. When the FLDWAV model automatically computes the DXM_i value, the wave speed (\hat{c}) is determined via the technique described by Fread (1987a), and Wetmore and Fread (1984), which is used in the NWS Simplified Dam-Break model (SMPDBK). This technique computes the maximum dam-breach outflow using Eq. (6.13) and then routes the peak through the downstream river/valley using dimensionless routing relationships which were previously developed via the NWS DAMBRK model (based on the Saint-Venant equations) for a myriad of scenarios consisting of various sizes of dams, reservoirs, breaches, downstream valleys, and different valley slopes and roughness factors. This technique neglects backwater effects from downstream natural constrictions and dams or bridges. Hence, when

downstream backwater effects may be significant, the computed wave speed used in option (1) or (3) may result in computed DXM_i values somewhat smaller than those obtained from Eq. (11.6) if a more accurate wave speed were used.

In routing applications other than dam-break floods, option (1) should not be used; rather, option (2) should be used with the user specifying the DXM values between each of the user-specified cross sections by utilizing Eqs. (11.6-11.10) to compute each DXM_i value. Once a FLDWAV solution has been obtained, better values of DXM_i conforming to Eq. (11.6) may be used in subsequent solutions since \hat{c} can be obtained from computed hydrographs using Eq. (11.11).

The third criterion (Fread, 1988) for selecting the computational distance step (DXM_i) is related to significant changes in the channel bottom slope (S_m , ft/mi). Wherever the channel bottom slope (S_{m_i}) abruptly changes, smaller computational distance steps, say $1/5$ to $1/2$ of those required by the second criteria, Eq. (11.6), are automatically determined. Also, wherever the flow changes from subcritical to supercritical or vice versa, the computational distance step (DXM_i) should be smaller. The FLDWAV model automatically determines computational distance steps according to the following approximations: If $S_{m_i} > 30$ ft/mi and $S_{m_i}/S_{m_{i+1}} > 2$ ft/mi, then

$$DXM_i = 0.5(S_{m_{i+1}}/S_{m_i}) \dots\dots\dots (11.12)$$

If $S_{m_i} < 30$, $S_{m_{i+1}} > 30$, and $S_{m_{i+1}}/S_{m_i} > 2$, then

$$DXM_i = 0.5(S_{m_i}/S_{m_{i+1}}) \dots\dots\dots (11.13)$$

Abrupt changes in bottom slope where computational distance steps are too large not only cause numerical difficulties when solving the numerical Saint-Venant equations, Eqs. (2.19-2.20) but also cause numerical difficulties when solving Eq. (4.2) to obtain the initial water-surface elevations.

The options (1) and (3) to automatically compute the DXM_i values should not be relied on for all situations. Judicious selection of DXM_i values by the user provides a means for intelligent use of the FLDWAV model for unusual or complex applications.

11.2 Selection of Computational Time Steps

Equally important to the computational distance steps (Δx_i) are the computational time steps (Δt_j). Their proper selection prevents the occurrence of numerical difficulties due to excessive truncation errors in the finite-difference approximate solution of the Saint-Venant equations. Also, if the computational time steps are too large, the user-specified hydrograph or the hydrograph generated by the breaching of the dam will not be accurately characterized, i.e., if the time steps are too large, the peak of the hydrograph can be ignored as the time steps (Δt_j) step through and actually bypass the hydrograph peak. To ensure small truncation errors and to properly treat the hydrograph peak, the following criteria are used within FLDWAV: (1) the selected time step Δt_j is evenly divisible into the smaller of either the time of rise of the user-specified hydrograph or the time of failure (τ) of the breach; usually the latter is sufficiently small such as to also cause the Δt_j time step to coincide with the peak of the user-specified hydrograph; (2) the time of rise (T_r) of the user-specified hydrograph or the time of failure (τ) of the breach is divided by a factor (M'), where $6 \leq M' \leq 40$; usually a value of 20 is sufficiently large to produce computational time steps sufficiently small so as to minimize truncation errors.

Within the FLDWAV model, there is an option to automatically select the computational time step when the user-specified parameter DTHM is 0.0. In this option, the model uses the following computational time step (Δt_h) in units of hrs:

$$\Delta t_h = T_r / M' \dots\dots\dots (11.14)$$

in which the subscript j designates the particular time line from 1 to the total number of time lines used during the simulation, T_r is the time of rise of the user-specified hydrograph, and $M'=20$ until the breach is just about to begin to form. Thereafter, the time step is given by

$$\Delta t_h = \tau / M' \dots\dots\dots (11.15)$$

in which τ is the breach time (hr) of formation and $M'=20$. If there is only one dam being simulated, then the computational time step is allowed to automatically increase as the time of rise of the breach hydrograph (τ) increases due to dispersion (spreading-out of the hydrograph shape) of the wave as it propagates downstream. In applications with two or more dams, the time step is not allowed to increase as the wave propagates downstream; however, in Eq. (11.15) the minimum τ for any of the dams which have commenced their breach formation is used to compute Δt_h .

When DTHM (hr) is user-specified as a positive value equal to the computational time step size, i.e., $DTHM > 0$, the FLDWAV model uses this computational time step throughout the period of simulation. When DTHM is user-specified with a negative sign (-) preceding its value, Eqs. (11.14-11.15) are used to determine the computational time step with $M' = |DTHM|$; this allows the user to have some control over the size of the variable time step.

Another parameter (TFI) can also be user-specified to allow control of the time step size. In this case, DTHM (hr) is user-specified as the computational time step size which is used by the FLDWAV model until the simulation time exceeds the user-specified value of TFI (hr), at which time the model uses Eq. (11.14-11.15) to compute the new computational time step.

Another option within FLDWAV allows a user-specified time series of time steps (Δt_h). In this option the user can specify what time step can be used for various intervals of time throughout the computational run of the FLDWAV model.

When selecting the computational time step, Eqs. (11.14-11.15) can be used along with a suitable value of M' . Also, a theoretical relation for the computational time step (Fread and Lewis, 1993) may be used in selecting DTHM. This relation is:

$$\Delta t_h \leq T_r / M' \dots\dots\dots (11.16)$$

where:

$$M' = 2.67[1 + \mu'n^{0.9}/(q^{0.1}S_o^{0.45})] \dots\dots\dots (11.17)$$

in which Δt_h is the computational time step (hrs), T_r is the time of rise of the flood wave (hrs) or the time (hr) of failure (τ) for a breached dam, $\mu' = 3.97$ (3.13 SI units), n is the Manning friction coefficient, q (ft^3/sec per ft of river width, B_k) is the peak flow per unit river width, and S_o is the river bottom slope (ft/ft). Using typical values for S_o , n , and q provides a range of M' values generally not exceeding $6 \leq M' \leq 30$. Thus, Eq. (11.14) with $M' = 20$, is the same as Eq (11.16).

Generally, with a smaller computational time step, there is a smaller truncation error if Eq. (11.6) is used to select the computational distance step) and there is less chance for the occurrence of numerical difficulties; however, the smaller the time step, the smaller the distance step must be, and this results in considerably more computer time needed to obtain the solution. In fact, halving the time step requires halving the distance step which then quadruples the required computer time. Thus, there is always a trade-off between accuracy or an absence of numerical difficulties and the required expenditure of computational time.

It is recommended that first the computational time step (Δt_h) is either user-specified or computed automatically within the FLDWAV model. Then, the computational distance step (Δx_i), i.e. DXM_i , is either user-specified or computed automatically within the model via Eq. (11.6).

12. OTHER MODELING CAPABILITIES

FLDWAV provides additional flow modeling capabilities. These are: lateral flows, levee overtopping and/or crevasse flows, flow losses, pressurized flows and a real-time Kalman filter updating technique. A description of each of these capabilities follows.

12.1 Lateral Flows

User-specified unsteady or steady (constant with time) flows associated with tributaries (that are not treated as separated rivers for which the flows in those rivers are dynamically routed) can be added to the unsteady flow along the routing reach. This is accomplished via the term (q) in Eq. (2.1) and the term (L) in Eq (2.2); however, since the lateral flow is assumed in FLDWAV to enter perpendicular to the main-stem river flow, L becomes zero since v_x is zero in this case. If tributaries are dynamically routed, the same approach of using q in Eq (2.1) and L in Eq (2.2) is utilized, but in this case the angle that the tributary flow enters the river is user-specified as shown in Figure 12.1. This enables FLDWAV to model the dynamic tributaries in a very accurate manner. The total tributary flow which is a known function of time, i.e., $Q(t)$ which is a user-specified time series, is distributed along a single Δx_i sub-reach, i.e., $q(t) = Q(t)/\Delta x_i$. Backwater effects of the

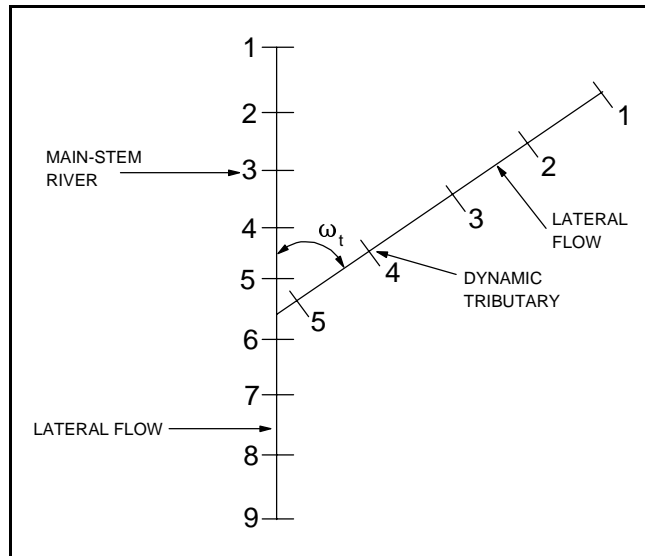


Figure 12.1 - Schematic of River System Showing Dynamic Tributary and Lateral Flows.

routed flow on the tributary flow are ignored. Known outflows can be simulated by using a negative sign with the user-specified $Q(t)$. Linear interpolation is used to provide flow values at times other than those of the user-specified time series. Numerical difficulties in solving the Saint-Venant equations sometimes arise when the ratio of lateral inflow to channel flow, q_i/Q_i , is too large; this can be overcome by increasing Δx_i for this particular sub-reach.

Outflows which occur as broad-crested weir flow over a levee or natural crest of the watershed boundary may be simulated within the FLDWAV model. This capability is described in the next Sub-section 12.2.

12.2 Levee Overtopping/Crevasse Flows and Floodplain Interactions

Flows which overtop levees located along either or both sides of a main-stem river and/or its principal tributaries may be simulated within FLDWAV. The overtopping flow is considered lateral outflow ($-q$) in Eqs. (2.1-2.2), and is computed as broad-crested weir flow. Four options shown in Figure 12.2 exist within FLDWAV for simulating the interaction of the overtopping flow with the receiving floodplain area, i.e., (1) the floodplain is ignored, (2) cave-in-the-bank, (3) the

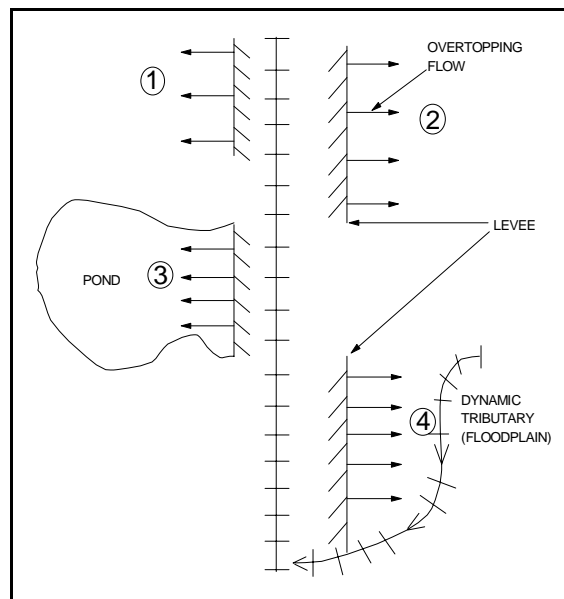


Figure 12.2 - Levee Overtopping Flow Interacting with the Receiving Floodplain.

floodplain is treated as a storage or ponding area, and (4) the floodplain is treated as a tributary and its flow is simulated using the Saint-Venant equations (2.1-2.2).

The first option simply ignores the presence of the floodplain. The levee-overtopping broad-crested weir flow is computed according to the following:

$$q_i^{j+1} = S_g c_{\ell_i} k_{s_i} (\bar{h}_i - h_{c_i})^{3/2} \dots\dots\dots (12.1)$$

where k_s , the submergence correction factor, is assumed for this option to be unity, c_{ℓ} is the user-specified weir discharge coefficient ($2.6 \leq c_{\ell} \leq 3.2$ for US units and $1.4 \leq c_{\ell} \leq 1.8$ for SI units), h_{c_i} is the user-specified levee-crest elevation, \bar{h}_i is the average computed water-surface elevation of the river, between the i^{th} and $i+1$ cross-sections, i.e.,

$$\bar{h}_i = (h_i^{j+1} + h_{i+1}^{j+1})/2 \dots\dots\dots (12.2)$$

The + or - direction of the flow is given by S_g as follows:

$$S_g = 0 \quad \text{if} \quad \bar{h}_i \leq h_{c_i} \quad \text{and} \quad h_{fp} \leq h_{c_i} \dots\dots\dots (12.3)$$

$$S_g = m(\bar{h}_i - h_{fp})/(\bar{h}_i - h_{c_i}) \quad \text{if} \quad \bar{h}_i > h_{c_i} \quad \text{and/or} \quad h_{fp} > h_{c_i} \dots\dots\dots (12.4)$$

in which $m = -1$ for computations pertaining to the river, $m = 1$ for computations pertaining to the floodplain, h_{fp} is the computed water-surface elevation of the floodplain.

The second option treats the floodplains as inactive storage modeled as “cave-in-the-bank”. This method was described previously in Section 8.2.

The third option treats the receiving floodplain as a storage or ponding area having a user-specified storage-elevation relationship. This option is well-suited if the receiving floodplain area is divided into separate compartments by additional levees or road-embankments located perpendicular

to the river and its levees. The flow transfer from the river to the floodplain as well as the flow from a floodplain compartment to an adjacent upstream or downstream compartment is simulated via broad-crested weir flow with submergence correction; flow reversals can occur when dictated by the water-surface elevations within adjacent compartments, which are computed by the storage equation. The floodplain water-surface elevations are computed via a storage (level-pool) routing equation ,i.e.,

$$S_{ii}^{j+1} = S_{ii}^j + 0.5 \left(\sum q_{ii}^{j+1} + \sum q_{ii}^j \right) / (43560 \Delta t^j) \quad \dots\dots\dots (12.5)$$

in which

$$Q_{ii} = \sum_{i=L_1}^{i=L_2} q_i \Delta x_i \quad \dots\dots\dots (12.6)$$

where the subscript (ii) is the sequential number of the floodplain compartment, L_1 represents the first (upstream) $i^{th} \Delta x_i$ river reach associated with the ii^{th} floodplain and L_2 represents the last (downstream) $i^{th} x_i$ river reach associated with the ii^{th} floodplain compartment. Also, h_i^{j+1} can be obtained by a table look-up of S (acre-ft) vs. h from the user-specified storage- elevation table for the ii^{th} floodplain compartment. The overtopping broad-crested weir flow is corrected for submergence effects if the floodplain water-surface elevation exceeds sufficiently the levee crest elevation. In fact, the overtopping flow may reverse its direction if the floodplain water-surface elevation exceeds the river water-surface elevation. The submergence effects are simulated by computing k_s in Eq. (12.1) as follows:

$$k_s = 1.0 \quad \text{if } h_r \leq 0.67 \quad \dots\dots\dots (12.7)$$

$$k_s = 1.0 - 27.8 (h_r - 0.67)_3 \quad \text{if } h_r > 0.67 \quad \dots\dots\dots (12.8)$$

in which,

$$h_r = (h_{fp} - h_{c_i}) / (\bar{h}_i - h_{c_i}) \quad \dots\dots\dots (12.9)$$

in which k_s is the submergence correction factor similar to that used for internal boundaries (dams),

h_{c_i} is the levee-crest elevation, \bar{h}_i is the water-surface elevation of the river between the i^{th} and $i+1^{th}$ cross sections, and h_{fp} is the water-surface elevation of the ii^{th} floodplain. Flow in the floodplain can affect the overtopping flows via the submergence correction factor, k_s .

In the fourth option the floodplain is treated as a tributary of the river and the Saint-Venant equations (2.1-2.2) are used to determine its flow and water-surface elevations; the overtopping levee flow is considered as lateral inflow (q) in Eqs. (2.1-2.2), however, the term (L_i) in Eq (2.2) is computed as $L_i = -q\overline{Q}/\overline{A}$ (see Eqs. (2.21) and (2.23)) for the levee overtopping flow leaving the river and L_i is assumed in FLDWAV to be zero for the floodplain (being treated as a tributary) since the overtopping flow is assumed in FLDWAV to enter the floodplain perpendicular to the floodplain flow direction and hence, $v_x = 0$.

In each option the levee may also experience a time dependent crevasse (breach) along a user-specified portion of its length. In this situation the flow exiting the river and entering the floodplain is multiplied by the ratio $L_b/\Delta x_i$ in which L_b is the user-specified length of the levee crevasse or breach and Δx_i is the sub-reach in which the crevasse occurs. During the breaching process the breach bottom elevation commences at the levee crest elevation (h_{c_i}) and proceeds linearly downward to a user-specified lower elevation ($h_{b_{ii}}$) during a user-specified time interval. The broad-crested weir flow Eq. (12.1) is used for computing the breach (crevasse) flow.

12.3 Routing Losses Due to Floodplain Infiltration or Depression Storage

Often in the case of very large floods including dam-break floods, where the extremely high flows inundate considerable portions of overbank or floodplain, a measurable loss of flow volume occurs. This is due to infiltration into the relatively dry overbank material and flood detention storage losses due to topographic depressions and/or water trapped behind field irrigation levees. Such losses of flow may be taken into account via the term q in Eq. (2.1) The loss induced lateral flow (q) as developed by Jin and Fread (1996) is as follows:

$$q = \frac{e^{-(x-x_1/x_2-x_1)^{\alpha'}} \alpha' (Q-Q_0)}{(1+x-x_1/x_2-x_1)^{\alpha'} \alpha' (x_2-x_1)} \dots\dots\dots (12.10)$$

in which Q_0 is the initial flow at $t=0$, x_1 is the upstream beginning location of the flow loss, x_2 is downstream ending location of the flow loss, x is any distance between x_1 and x_2 , α' is the ratio of the flow volume loss to the total active flow (α' may be - for loss and + for flow volume gain), α' is user-

specified and its value is determined by iterative trial using FLDWAV, and e' is a user-specified parameter which selects the pattern (see Figure 12.3) of the change in total active volume. Eq. (12.10) which is a user-specified option to be used within FLDWAV determines the loss-induced or gain-induced lateral flow (q) as a function of local discharge for any user-specified amount of loss, α' , between any two cross sections x_1 and x_2 along the routing reach. The sensitivity of the e' parameter for flow volume change $[QV(x)/QV(x_1)]$ between x_1 and x_2 is demonstrated in Figure 12.3 for a set value of $\alpha' = -0.2$.

12.4 Pressurized Flow

The FLDWAV model may be used to simulate unsteady flows which can change from free-surface flow to pressurized flow from one section to another and/or as the flow changes with time. When the flow, passing through a section of closed conduit of any shape, completely submerges the section; the flow properties change from those of free-surface to pressurized flow. In the latter type of flow, disturbances in the flow are propagated at velocities many times greater than those for free-surface flow. A technique which enables the Saint-Venant equations to properly simulate pressurized

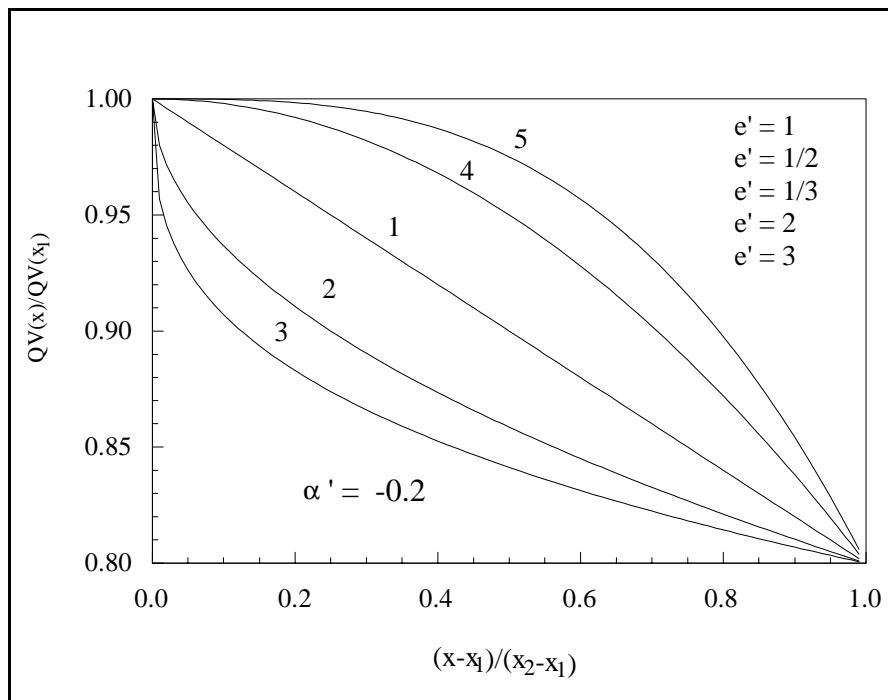


Figure 12.3 - Change in Total Active Volume, QV.

flow is included within FLDWAV. It follows the method first described by Cunge and Cunge and Wegner (1964) and described by Fread (1984b) for application of the Saint-Venant equations to unsteady flows in a network of storm sewers. In this method, closed conduits are user-specified by a table of topwidth versus elevation in a manner similar for open channels such as rivers, except when the topwidth diminishes to zero at the top of the closed conduit it is actually user-specified to have a very small topwidth (b^*) which extends vertically upward for at least one or more feet as shown in Figure 12.4. Within FLDWAV this topwidth is extrapolated for elevations larger than the last user-specified elevation; hence, the extrapolated topwidth is always b^* for all elevations since the last two user-specified topwidths are each b^* . Thus, by expressing the topwidth table in this manner for closed conduits, the Saint-Venant equations properly simulate either free-surface or pressurized flow. The local dynamic wave celerity (c) of disturbances sensed by the Saint-Venant equations is given by the following:

$$c = \sqrt{g A/B} \dots\dots\dots (12.11)$$

in which $B = b^*$ for flows in which the free-surface water elevations extend above the top of the closed conduit, as is the case for pressurized flow. Of course, B represents the actual wetted topwidth for those sections experiencing free surface flow. An inspection of Eq. (12.10) shows that c may become quite large as B becomes very small. The value of b^* may be obtained from Eq. (12.10) if c

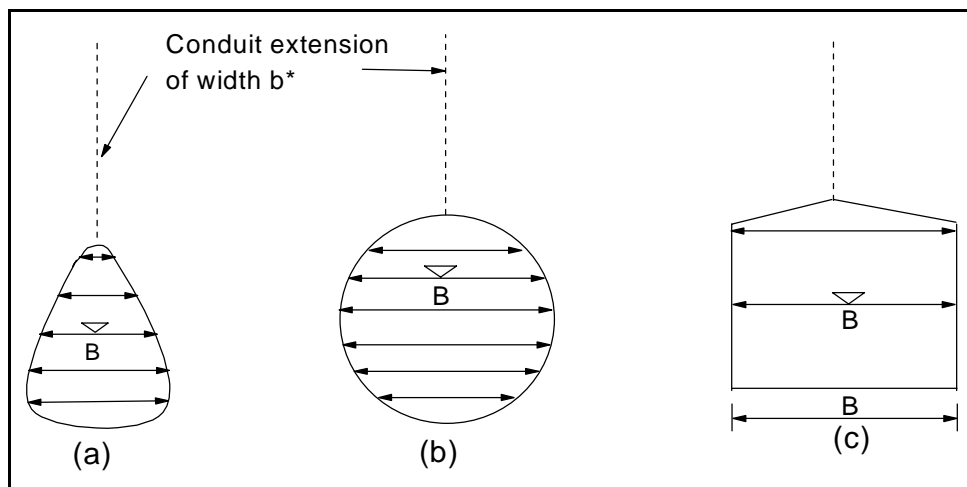


Figure 12.4 - Cross-Sections for Closed Conduits: (a) Irregular Shape, (b) Circular, (c) Rectangular.

for pressurized flow is known from previous observations, or b^* can be computed from conduit and water properties as delineated by Fread (1984b). Thus, in FLDWAV, flows may be simulated which are always free surface in some reaches where the sections are open while in other reaches with closed conduit sections, the flow may be initially pressurized or with time change from free surface to pressurized flow and vice versa.

12.5 Kalman Filter

The numerical solutions of the Saint-Venant equations provide deterministic predictions to the unsteady flows. In order to account for the effect of uncertainties in the parameters, initial and boundary conditions, and to make use of the real-time observations of the water stages in the routing reach to correct the predictions and to adapt the model to changing physical circumstances using the on-line information of the real-time observations, a Kalman filter technique is available as a user-specified option in the FLDWAV model for real-time river forecasting (Fread and Jin, 1993).

Eqs. (2.1-2.2), along with two boundary conditions, are transformed into a system of discrete, implicit nonlinear equations as represented by Eqs. (2.19-2.20). In order to account for the uncertainties existing in the mathematical equations, boundary and initial conditions, as well as the model parameters such as the Manning n , this deterministic dynamic system can be transformed into a stochastic dynamic system by including an additional random noise process, i.e. a Gaussian white noise process. Eqs. (2.19-2.20) thus can be rewritten in a stochastic sense (in vector form) as:

$$f(\mathbf{Y}^{j+1}, \mathbf{Y}^j, t^{j+1}, t^j) = \mathbf{W}^j \quad \dots \dots \dots (12.12)$$

in which \mathbf{Y} is a vector representation of the system state variables, i.e. $\mathbf{Y} = \mathbf{Y}(Q_1, Q_2, h_1, h_2, \dots)$, the \mathbf{W} is the Gaussian white noise process with user-specified statistical features. Similarly, the on-line observations of the river discharges and/or stages can also be expressed by an equation with inclusion of a random noise process to account for the errors in the observed data. Based on these two stochastic dynamic equations, the Kalman filter technique provides an algorithm to use the new observations to update or correct the predictions of the state variable, \mathbf{Y} , for the time t^j , and then the updated solutions are used as initial conditions for the prediction at the next time, t^{j+1} . The Kalman

filter technique therefore provides a stochastic method to make optimal use of the real-time on-line observations.

It has been shown (Fread and Jin, 1993) that the use of the Kalman filter can improve the flood predictions for large-river flood waves (time of the rise (T_r) of the flood wave is longer than a day); however, negligible improvements are obtained for more fast rising waves including tidal generated waves when the forecast lead-times are greater than 4 hrs.

The Kalman filter is activated in FLDWAV by the user-specified parameter KFTR=1. It is used for real-time operational river forecasting applications and the observed data (discharge and/or stage time series) must be user-specified as input to FLDWAV.

13. ROBUST COMPUTATIONAL FEATURES

There are two features within the FLDWAV model that help maintain computational robustness and prevent numerical difficulties in addition to the previously mentioned subcritical/supercritical algorithm (Section 5), conveyance representation of the friction slope (S_f) (Sub-sections 2.1 and 10.1), and distance and time step selection criteria (Section 11). Many simulations which would normally abort are computed successfully because of the following two computational features.

13.1 Low-Flow Filter

The first feature is a "safety net" or numerical low-flow filter (Fread, 1988) which prevents computed values of h_i and Q_i from retaining values which are not possible according to a limiting assumption of the type of hydrographs that may be user-specified and/or created within FLDWAV and which are routed via the Saint-Venant equations. Under this assumption, all hydrographs are not allowed to have flow values less than the initial flow at $t=0$. Thus, any computed flow or elevation during the simulation that is smaller than the initial flow or elevation at each i^{th} section is considered to be erroneous due to the truncation error in the approximate Saint-Venant difference solution. Such computed flows or elevations are set to their previous value before the last computations were made. This prevents the retention of critical errors in depth and flow in the vicinity of a rapidly rising wave front such as associated with dam-break waves or any sudden discharge releases from reservoirs. These errors are usually manifested as flows and elevations which are less than the initial flow through (on) which the steep wave propagates. In fact the erroneous elevations may even be lower than the channel bottom elevation and cause the computer simulation to abort as a negative area or hydraulic radius is raised to a power such as in the friction slope computation given by Eq. (2.22). These errors usually can be controlled by proper selection of the computational distance and time steps; however, the low-flow filter permits somewhat larger computational steps which provide savings in computer simulation time and storage. The numerical filter or safety net may be decommissioned by a user-specified parameter $F1I = 0.50$. This will allow the following hydraulic phenomena to occur: (1) the user-specified hydrograph or generated breach hydrograph can have

flows that are less than the initial flow at $t=0$, and (2) the computed flows may reverse direction and propagate upstream, in which case the flows have negative (-) values.

13.2 Automatic Time Step Reduction

The second feature (Fread, 1988) within FLDWAV that assists in providing computational robustness is the automatic reduction in the computational time step when the numerical solution of the finite-difference, Saint-Venant equations fails to converge within ITMAX (usually user-specified as 9) iterations. If nonconvergence occurs, i.e., if at any computational section either ϵ_{h_i} or ϵ_{Q_i} are greater than their respective allowable tolerances, then the computation is repeated with a reduced time step of $1/2$ of the original time step; subsequently at $1/8$, then at $1/16$, if nonconvergence persists. If nonconvergence still occurs, then the θ weighting factor is increased by 0.2 and the computations repeated with computational time step of one-half the original time step. This is repeated until θ is equal to 1.0 at which time the computations proceed to the next full time step assuming the most recently computed values are correct although convergence was not attained. Such a final nonconvergent solution is allowed to occur a total of 5 times during a simulation run. If the maximum allowable of 5 final nonconvergent solutions is exceeded during the run, the run automatically stops and all numerical/graphical output up to that point in the computation is available for inspection (viewing or printing). If at any time during the previously described iteration procedure convergence is attained, the computations proceed to the next time level using a time step equal to the difference between the original and that which caused convergence and a θ weighting factor of 0.6 unless user-specified via the F1 parameter. At any time during the computations, if nonconvergence occurs and the time step is reduced, this can be printed out to notify the user of this situation ($JNK \geq 5$, where JNK is an output control parameter). This does not constitute an invalid solution; on the contrary, a successful solution is attained whenever the time step is advanced forward in time with the solutions of h_i and Q_i obtained in less than the allowable ITMAX iterations. Often, computational difficulties can be overcome via one or two time step reductions. However, if the solution advances forward in time with nonconvergence occurring, and the θ value has been increased to a value of one, then the solution is suspect, and all h_i and Q_i should be closely examined at that particular time line to see if the results appear reasonable. Usually, if final nonconvergence occurs, i.e., the θ factor has

been increased to a value of one, the simulation should be repeated with appropriate data modifications, e.g., the computational distance steps should be adjusted to more closely satisfy Eq. (11.6).

14. MODEL CALIBRATION

Routing results are often sensitive to the values of the Manning n . Best results are obtained when n is adjusted to reproduce historical observations of discharge and water-surface elevations. The adjustment process is referred to as “calibration”. There are two calibration approaches described herein, (1) a trial-error approach and (2) a user-selected automatic approach.

14.1 Manning n by Trial-Error

The Manning n for the range of flows associated with previously observed floods may be selected via a trial-and-error calibration methodology. With observed stages and flows, preferably continuous hydrographs from a previous large flood, the FLDWAV model can be used to determine the n values as follows: (1) use the observed flow hydrograph as the upstream boundary condition and select an appropriate downstream boundary (an observed stage hydrograph at the downstream boundary could be used if available); (2) estimate the Manning n values throughout the routing reach; (3) obtain computed h and Q from the solution of the Saint-Venant equations; (4) compare the computed elevations with the observed elevations at the upstream boundary and elsewhere; (5) if the computed elevations are lower than the observed, increase the estimated n values; or if the computed elevations are higher than the observed, decrease the estimated n values; (6) repeat steps (3) and (4) until the computed and observed elevations are approximately the same. The final n values are sufficient for the range of flows used in the calibration; however, the n values for those flow elevations exceeding the observed must be estimated as previously discussed in Section 9. The calibrated n values, however, provide an initial estimate from which the unknown n values may be extrapolated or ultimately approximated.

14.2 Manning n by Automatic Calibration Option

The Manning n may be obtained for unsteady flows by a user-specified option for an automatic calibration procedure (Fread and Smith, 1978).

14.2.1 Basic Formulation.

An elementary reach of channel between two gaging stations where stage (water-surface elevation) h'_A and discharge Q'_A are measured at the upstream station and stage only h'_B is measured at the downstream station is shown in Figure 14.1. Eqs. (2.1-2.2) or (2.19-2.20) describe the unsteady flow within the elementary reach. The initial conditions of stages and discharges at all computational nodes along the reach A-B must be user-specified as well as the boundary conditions at the extremities of the reach. The upstream boundary condition is a known discharge hydrograph, i.e.,

$$Q_A = Q'_A(t) \quad \dots\dots\dots (14.1)$$

which is the same as Eq. (3.1); and the downstream boundary condition is a known stage hydrograph, i.e.

$$h_B = h'_B(t) \quad \dots\dots\dots (14.2)$$

which is the same as Eq. (3.9). Also, all lateral inflows or outflows contained within the reach A-B must be known.

By specifying the known discharge hydrograph at the downstream boundary, any flow disturbances occurring downstream of the reach A-B that could affect the flow within reach A-B such

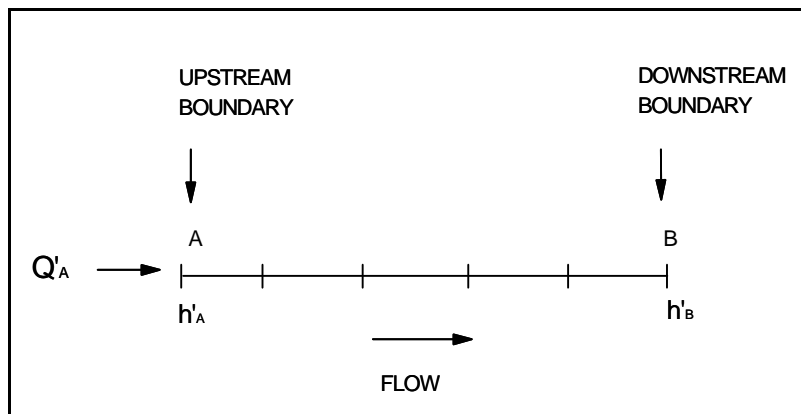


Figure 14.1 - Schematic of Elementary Channel Reach A-B.

as backwater from tributary inflow or tidal effects that could influence the flow within reach A-B are effectively considered.

The n value is considered to be an integrated value throughout the reach A-B, i.e., n is not considered to vary with distance between the two gaging stations. However, n may vary with stage or discharge, and this variation can be described as a continuous piece-wise linear function as shown in Figure 14.2. The discharge is expressed as an average discharge throughout reach A-B. The total range of possible discharges is divided into a number ($j=1,2,3,...J$) of strata. Each stratum is associated with a break-point (change of slope of the $n(\bar{Q})$ function) in the $n(\bar{Q})$ piece-wise linear function.

From inspection of Eq. (2.3) it is apparent that n is a function of both Q and h ; therefore, in order to determine a unique $n(\bar{Q})$ function for reach A-B, the discharge in the reach as well as the stage must be user-specified. The two boundary conditions given by Eqs. (14.1-14.2) provide the necessary combination of Q and h to allow a unique determination of n .

14.2.2 Optimization Algorithm.

In order to determine the appropriate $n(\bar{Q})$ function for reach A-B, a trial $n(\bar{Q})$ function is selected, and Eqs. (2.19-2.20) are solved subject to the user-specified boundary conditions, Eqs. (14.1-14.2). An optimal $n(\bar{Q})$ function is sought which will minimize the bias (the absolute value of the sum of the differences between the computed stages, h_A , and the measured stages, h'_A , at the upstream boundary).

The overall objective function chosen for minimization is

$$\min \phi_T = \left| \sum_{j=1}^J \phi_j \right| \dots\dots\dots (14.3)$$

in which
$$\phi_j = \frac{1}{M_j} \sum_{j=1}^{M_j} h_A - h'_A \dots\dots\dots (14.4)$$

in which M_j denotes the total number of stages associated with discharges within the j^{th} discharge stratum as shown in Figure 14.2.

In order to determine the appropriate correction to each stratum of the $n(\bar{Q})$ function, it is desirable to work with an objective function for each stratum, i.e., ϕ_j as defined by Eq. (14.4). However, since

$$\left| \sum_{j=1}^J \phi_j \right| \leq \sum_{j=1}^J |\phi_j| \dots\dots\dots (14.5)$$

the overall objective function, ϕ_T , will be minimized by minimizing each ϕ_j . The objective function for the j^{th} stratum, ϕ_j , may also be expressed in the following functional form:

$$\min \phi_j \{ h_{A_j} [n_j(Q_j)] \} = 0 ; j=1,2,\dots,J \dots\dots\dots (14.6)$$

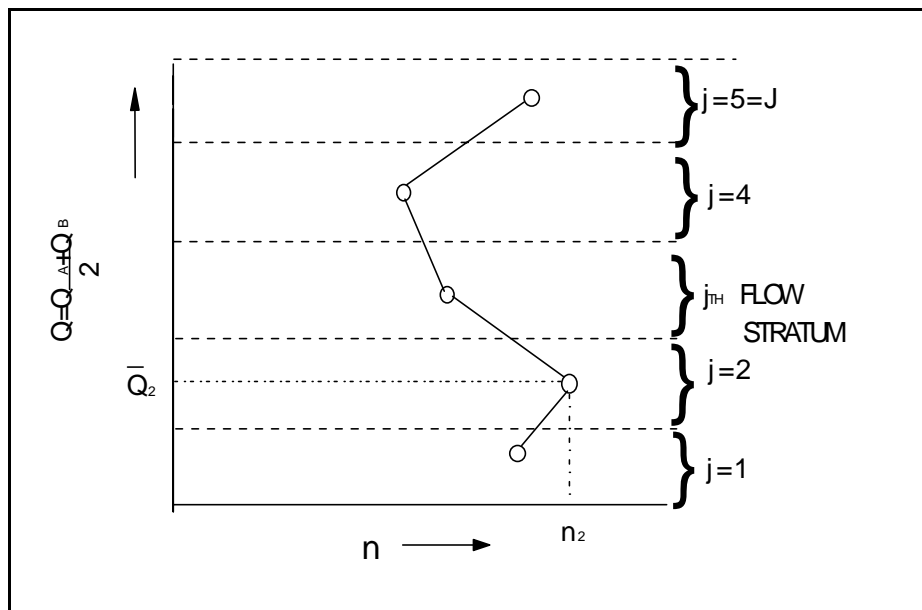


Figure 14.2 - Typical Functional Relational for Channel Reach A-B.

in which ϕ_j is a function of the computed and measured stages (h_A and h'_A) associated with discharges in the j^{th} stratum as indicated in Eq. (14.4). Stages are also functions of the Manning n at the j^{th} stratum, and the Manning n is a function of the average discharge \bar{Q} within reach A-B.

An equivalent form of Eq. (14.6) is given by the following:

$$\phi_j[h_A[n_j(Q_j)]] = 0; j=1,2,...,J \quad \dots\dots\dots (14.7)$$

By expressing Eq. (14.3) or Eq.(14.7) in the form of Eq. (14.7), a gradient-type modified Newton-Raphson algorithm can be applied to determine the improved $n(\bar{Q})$ functions so as to minimize ϕ_j . The modification of the Newton-Raphson algorithm consists of the replacement of the continuous derivative with a finite-difference derivative. Thus, upon applying the modified Newton-Raphson algorithm to Eq. (14.7), the following expression is obtained for determining the improved n_j trial value:

$$n_j^{k+1} = n_j^k - \frac{\phi_j^k(n_j^k - n_j^{k-1})}{\phi_j^k - \phi_j^{k-1}}; k \geq 2; j=1,2,...,J \quad \dots\dots\dots (14.8)$$

in which the k^{th} superscript denotes the number of iterations. Eq. (14.8) can only be applied for the second and successive iterations because of the $k-1$ terms in the numerical derivative portion of Eq. (14.8). Therefore, the first iteration is made using the following algorithm:

$$n_j^{k+1} = n_j^k \left(1.00 - 0.01 \phi_j^k / |\phi_j^k| \right); k=1; j=1,2,...,J \quad \dots\dots\dots (14.9)$$

in which a small percentage change in the Manning n is made in the correct direction as determined by the term $-(\phi_j^k / |\phi_j^k|)$. The convergence properties of Eq. (14.8) are quadratic. Usually convergence is obtained within $3 \leq k \leq 5$ iterations. Convergence is obtained when either of the following inequalities is satisfied:

$$\phi_T^k = \frac{1}{J} \sum \phi_j^k < \epsilon \quad \dots\dots\dots (14.10)$$

$$\phi_T^k \geq \phi_T^{k-1} \quad \dots\dots\dots (14.11)$$

in which ϵ is a user-specified convergence criterion; an ϵ of 0.001 ft (0.0003 m) has been found to be a sufficiently small value.

The quality of the first trial (starting) values, n_j^1 , for the $n(\bar{Q})$ function influences the required number of iterations. If the starting values deviate from the optimal values by too great a margin, Eq. (14.8) will not converge. This is easily remedied by assuming new starting values and repeating the procedure. Starting values may simply be judicious guesses or they may be estimated from the following application of the Manning equation using the water-surface slope as a better approximation of the true energy slope than the conventional river bottom slope (S_o):

$$n_j^1 = \frac{1}{M_j} \sum \mu \frac{AR^{2/3}}{\bar{Q}} \left(\frac{h'_A - h'_B}{|x_A - x_B|} \right)^{1/2} \quad \dots\dots\dots (14.12)$$

in which M_j is the number of stage-discharge observations in the j^{th} stratum (range) of discharge values, \bar{Q} is the average discharge between locations x_A and x_B , and A and R are the average cross section area and hydraulic radius, respectively.

From the preceding theory, an optimization algorithm can be formulated for determining the optimal $n(\bar{Q})$ function of an elementary reach A-B; it consists of the following steps:

- Step 1. Initial values of the $n(\bar{Q})$ function are computed from Eq. (14.12) or are simply estimated.
- Step 2. Eqs. (2.1-2.2) are solved by a finite-difference technique creating Eqs. (2.19-2.20) subject to the boundary conditions, Eqs. (14.1-14.2), and the user-specified initial conditions and lateral inflows. The objective function, Eq. (14.3), is then determined for each stratum of

discharges in the $n(\bar{Q})$ function using the computed and observed stages at the upstream boundary.

Step 3. Improved values of the $n(\bar{Q})$ function are obtained from Eq. (14.9) for the first iteration only and from Eq. (14.8) for the second and succeeding iterations.

Step 4. The objective function is evaluated and compared to see if it is less than a small user-specified ϵ value for convergence. If it satisfies either inequality, Eqs. (14.10-14.11), the optimal $n(\bar{Q})$ function has been determined; otherwise, return to step 2.

14.2.3 Decomposition of River System.

A river system consisting of either multiple reaches or multiple reaches and tributaries may be decomposed in such a way that the preceding optimization algorithm for an elementary reach A-B may be applied reach-by-reach to the entire river system. The decomposition of a river system into elementary reaches for which optimal n values may be obtained reach-by-reach greatly simplifies the optimization problem and allows the calibration process to be accomplished in a most efficient manner.

First, consider the multiple-reach system shown in Figure 14.3 with the gaging stations at cross-section locations A, B, C, and D. Discharge is observed at A and stages are observed at A, B, C, and D. This multiple-reach system may be decomposed into three elementary reaches as shown in Figure 14.4. The upstream reach A-B is treated first. Using the observed discharge, Q_A , and the observed stage, h_B , as the upstream and downstream boundaries, respectively, the unsteady flow Eqs. (2.19-2.20) are solved with a starting $n(\bar{Q})$ function either assumed or estimated from Eq. (14.12). The objective function that is to be minimized is the bias at point A, i.e., $\phi_A = h_A - h'_A$. Eqs. (14.8-14.9) are used to obtain improved values of n while simultaneously minimizing ϕ_A .

As previously mentioned, any flow affecting reach A-B is accounted for by the upstream boundary condition, Q_A , while anything occurring downstream of point B which might affect the flow

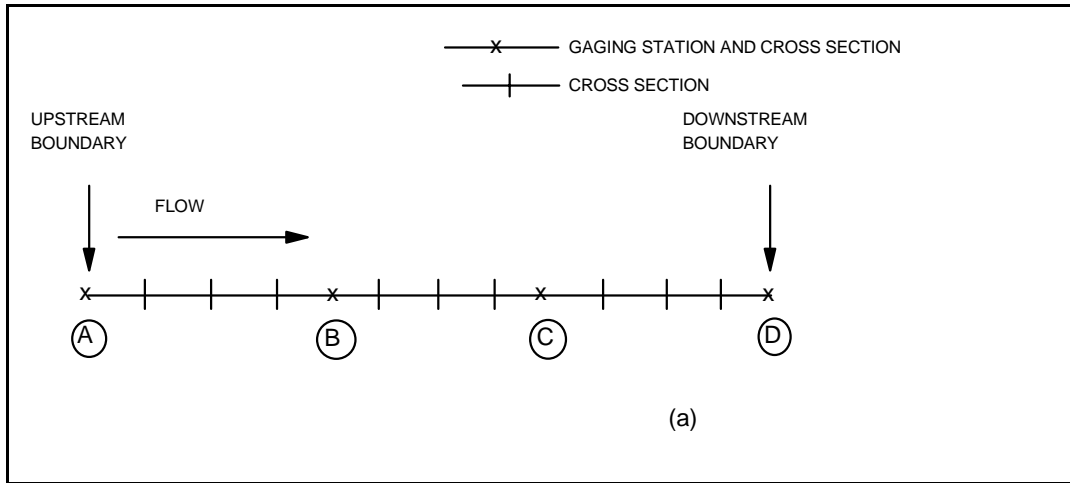


Figure 14.3 - Schematic of Multiple-Reach River System A-B-C-D.

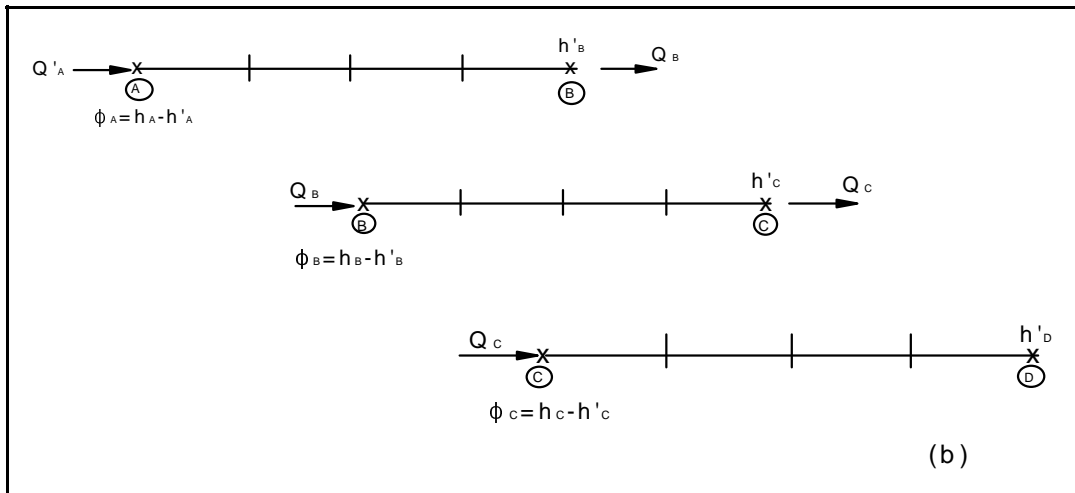


Figure 14.4 - Schematic of Decomposed Multiple-Reach River System A-B-C-D.

in A-B is taken into account by the downstream boundary condition of the observed stage, h_B . Once the optimal $n(\bar{Q})$ function is obtained for reach A-B, the computed discharge, Q_B , is then used as the upstream boundary condition for reach B-C. In this way, the optimization process can proceed reach-by-reach in the downstream direction.

Next, consider the multiple-reach system with a tributary as shown in Figure 14.5 with gaging stations at points A, B, C, and D. Discharge is observed at the upstream points on each river, i.e., at points A and D. This river system may be decomposed into three elementary reaches as shown

Diagram illustrating a river reach for water quality modeling. The main stem is represented by a horizontal line with five cross-sections marked with 'X' and labeled (A), (B), (E), and (C) in circles. Section (D) is a tributary joining the main stem between (B) and (E). Arrows indicate flow direction: upstream to downstream along the main stem, and downstream into the tributary. Labels include 'UPSTREAM BOUNDARY' at (A), 'DOWNSTREAM BOUNDARY' at (C), 'FLOW' with arrows, and 'MAIN STEM' and 'TRIBUTARY'.

14.9

starting $n(\bar{Q})$ function are then solved. Improved n values are obtained from Eqs. (14.8-14.9) so as to minimize the bias ϕ_T at D. The computed discharge at E coincident with the optimal $n(\bar{Q})$ function obtained from Eq. (14.8) is saved for use as lateral inflow q when optimizing reach B-C. Next, the multiple reach system (A-B and B-C) is treated, starting with the first upstream reach A-B. Then, when reach B-C is optimized, the effect of the tributary flow Q_E over the small Δx reach containing the confluence as shown in Figure 14.6 is properly considered.

The decomposition principle can be used on a multiple-reach system with any number of tributaries. However, it is limited to river systems of dendritic configuration. An interconnecting system (network with islands, bifurcations, etc.) of channels is not amenable to the approach presented herein.

The basic formulation of the calibration procedure as described previously requires both discharge and stage observations. The observed discharges are required as an upstream boundary condition and the observed stages required as a downstream boundary condition. The objective function for determining the optimal $n(\bar{Q})$ function is composed of both computed and observed stages at the upstream boundary. This approach of using observed upstream stages-discharges and downstream stages is well-suited for most applications on large rivers where stage observations are much more plentiful than discharge observations. Actually, when multiple reaches are treated, only observed stages are required at all gaging points other than the most upstream station where observed discharges also are required. Also, lateral inflows should be known for best calibration results, particularly if the lateral flow is significant.

14.3 Cross Sections by Automatic Option

A methodology has been developed (Fread and Lewis, 1986) for determining the optimal parameters of dynamic routing models thereby eliminating costly and time-consuming preparation of detailed cross-sectional data. The methodology utilizes (1) approximate cross-sectional properties represented by separate power functions for channel and floodplain, and (2) a very efficient optimization algorithm for determining the Manning n as a function of either stage or discharge

previously described in Sub-section 14.2. Essential data required for implementing the methodology are stage hydrographs at both ends of each routing reach and a discharge hydrograph at the upstream end of each river. The methodology is applicable to multiple routing reaches along main-stem rivers and their tributaries. Optimal n values may be constrained to fall within a specified min-max range for each routing reach. Specific cross-sectional properties at key locations, e.g., bridges, dams, unusual constrictions, also can be utilized within the optimization methodology. The methodology was tested on 1,275 miles (2051 km) of major rivers and their principal tributaries in the U.S. with good results (Fread and Lewis, 1987); the average root-mean-square error was 0.44 ft (0.13 m) or 2.9 percent of the change in stage.

Dynamic routing is usually applied when there is a substantial amount of cross-sectional data available to characterize the cross-sectional area (A) and top width (B) as known functions of h . This requires the existence of detailed hydrographic survey information and topographical maps, as well as considerable time consuming effort by hydrologists to reduce the basic cross-section information to the form of cross-sectional area (A) and top width (B) as specified tabular functions of h . In order to eliminate the necessity for using detailed cross-sectional data which is often unavailable, a very powerful and computationally efficient parameter optimization methodology which utilizes minimal cross-sectional information was developed for flood forecasting. Also, this methodology can be used advantageously by hydrologists concerned with unsteady flow prediction in waterways where detailed cross-sectional data is prohibitively expensive to obtain.

Data normally required to calibrate a dynamic routing model are: 1) cross-sectional area (A) and width (B) as a function of water surface elevation (h) for sections representative of the routing reach, 2) the Manning n which may vary with either water-surface elevation or discharge throughout the routing reach, 3) observed discharge and stage hydrographs at the upstream end of the routing reach, and either a stage or discharge hydrograph at the downstream extremity of the routing reach.

To avoid the costly and time-consuming tasks of gathering detailed cross-section data and then reducing the data into tables of top width (B) and water elevation (h), simple approximations are used to represent an average cross-section within each routing reach. A power function,

$$B = k Y_c^{m_c} \dots\dots\dots (14.13)$$

is used for the channel and another power function,

$$B_f = k_f Y_f^{m_f} \dots\dots\dots (14.14)$$

is used for the floodplain. The parameters k_c , m_c , k_f , m_f are estimated from 1) topographical maps, 2) visual inspection of a few easily accessible cross-sections, and/or 3) a few available cross-sections of the river. The shape parameter (m_c) can be easily computed, i.e.,

$$m_c = (\log B_2 - \log B_1) / (\log Y_2 - \log Y_1) \dots\dots\dots (14.15)$$

in which B_2 and Y_2 are the estimated bank-full width and depth and B_1 and Y_1 are estimates of an intermediate width and depth. The scaling parameter (k_c) is computed from the basic power function, i.e., $k_c = B/Y_c^{m_c}$. Similarly the shape and scaling parameters for the floodplain can be computed from estimates of the floodplain widths and depths. Sometimes it is appropriate simply to estimate the shape parameter, i.e., rectangular-shape ($m=0$), parabolic shape ($m=0.5$), triangular shape ($m=1.0$) or ∇ -shapes ($m>1$). The parameter optimization methodology which has been programmed as an integral option within the FLDWAV routing model allows the k and m parameters to be specified directly or to be computed by the program from the specified B and Y values for each routing reach.

When unusual cross-sections exist in a routing reach, e.g., at a bridge, dam or some natural constriction, those cross-section's top width and elevation tables may be specified; they each remain distinct from the average section described by the two power functions.

A parameter optimization algorithm within FLDWAV iteratively determines the best value for the Manning n which is allowed to vary with h or Q for each reach of waterway bounded by water level recorders. An objective function defined as the difference between the computed and observed upstream stage hydrographs for several ranges of flow is minimized by a Newton-Raphson technique (Fread and Smith, 1978; Fread, 1985a) previously described in Sub-section 14.2. A numerical

derivative is used in lieu of the analytical derivative for the rate of change of the objective function with respect to the change in the Manning n as previously delineated by Eq. (14.8). With starting values for n via Eq. (14.12) which is based on an assumption of steady flow or simply using a reasonable estimate, convergence to an optimal set of $n(Q)$ values is obtained in three to four iterations, i.e., the optimal n relation with h or Q for the reach of water bounded by known stage hydrographs can be obtained within three to four evaluations of the objective function; an evaluation consists of routing the flood hydrograph through the reach and comparing computed and observed upstream stage values. An option in FLDWAV allows the hydrologist to estimate a range of minimum and maximum n (n_{\min} and n_{\max}) values within which the optimal n values must reside. When the optimal values are outside the specified min-max range, the cross section is automatically reduced or increased sufficiently to allow the next optimization to yield Manning n values within the allowable range using the following:

$$F_{\text{new}} = F_{\text{old}} * \frac{n_{\max}}{n} * 0.99 \quad \text{if } n > n_{\max} \quad \dots\dots\dots (14.16)$$

$$F_{\text{new}} = F_{\text{old}} * \frac{n_{\min}}{n} * 1.01 \quad \text{if } n < n_{\min} \quad \dots\dots\dots (14.17)$$

where F is the cross section property (B , K) for the next (new) and previous (old) guesses, n_{\max} is the user-specified maximum allowable Manning n and n in Eq. (14.16) is the maximum n value obtained during the calibration of n . In Eq. (14.17), n_{\min} is the user-specified minimum allowable Manning n , and n is the minimum n value obtained during the calibration of n .

The optimization algorithm can be applied to multiple routing reaches, commencing with the most upstream reach and progressing reach-by-reach in the downstream direction. An observed discharge hydrograph is used as an upstream boundary condition for the most upstream reach. Then, the discharges computed at the downstream boundary using the optimal Manning n values are stored internally by the program and used as the upstream boundary condition for the next downstream reach. Dendritic river systems are automatically decomposed into a series of multiple-reach rivers.

Tributaries are optimized before the main-stem river and their flows are added to the main stem as lateral inflow(s).

The optimal n values obtained via the parameter optimization methodology presented herein is limited to expected applications where the maximum discharges do not greatly exceed those used in the optimization. Also, the methodology is best suited for applications where flood predictions are primarily required at locations along the waterway where level recorders exist. Unless detailed cross-sectional information at significant constriction or expansions is utilized in the optimization methodology, the cross sections throughout each routing reach should be generally uniform.

15. OTHER ROUTING TECHNIQUES

15.1 Diffusion Routing

A user-specified option is provided within FLDWAV to utilize a simplified distributed routing model, known as the diffusion wave (zero-inertia) model. It is based on Eq. (2.1) along with an approximation of the momentum equation that omits the first two terms, the inertial terms, in Eq. (2.2), i.e.,

$$gA \left(\partial h / \partial x + S_f + S_{ec} + S_i \right) + L_i + W_f B = 0 \quad (15.1)$$

The diffusion simplified routing model considers backwater effects; however, its accuracy is also deficient for very fast rising hydrographs, such as those resulting from dam failures, hurricane storm surges, or rapid reservoir releases, which propagate through mild to flat sloping waterways with medium to small Manning n . The range of application (with expected modeling errors less than 5 percent) for the diffusion models, including the Muskingum-Cunge model, is given by the following (Fread, 1983a, 1992):

$$T_r S_o^{0.7} n^{0.6} / q_o^{0.4} \geq \Psi \quad (15.2)$$

in which $\Psi=0.0003$ for English units and $\Psi=(0.00075)$ for SI units.

For example, to check if diffusion routing would produce results with less than 5% numerical error compared to the complete Saint-Venant Eqs. (2.1-2.2) for an application in which the time of rise (T_r) of the hydrograph is 24 hr, the Manning n is 0.030, the channel bottom slope (S_o) is 2.3 ft/mile or 0.00043 ft/ft, the average discharge is 25,000 cfs and the average wetted top width is 300 ft such that $q_o=25000/300=83.3$ ft²/sec. Therefore, inserting these values in Eq. (15.2) yields 0.0022 which is greater than 0.0003; thus, the routing errors will be less than 5%. However, if $S_o = 0.8$ ft/mi and $T_r = 6$ hr, Eq (15.2) yields a value of 0.00026 and the expected error using diffusion routing

would exceed 5%. This indicates that diffusion routing is less applicable for very flat rivers with unsteady flows that are fast rising , i.e. $T_r < 6$ hrs.

Within FLDWAV, the diffusion routing option uses a modified form of Eq. (2.20), i.e.,

$$\begin{aligned} & \theta \left[g\bar{A}^{j+1} \left(\frac{h_{i+1}^{j+1} - h_i^{j+1}}{\Delta x_i} + \bar{S}_{f_i}^{j+1} + S_{e_i}^{j+1} + \bar{S}_i^{j+1} \right) + L_i^{j+1} + (W_f \bar{B})_i^{j+1} \right] \\ & + (1-\theta) \left[g\bar{A}^j \left(\frac{h_{i+1}^j - h_i^j}{\Delta x_i} + \bar{S}_{f_i}^j + S_{e_i}^j + \bar{S}_i^j \right) + L_i^j + (W_f \bar{B})_i^j \right] = 0. \end{aligned} \quad \dots\dots\dots (15.3)$$

15.2 Level-Pool Routing

Often, unsteady flow routing in reservoirs can be approximated by a simple level-pool routing technique. This is acceptable for routing in reservoirs which are not excessively long and in which the inflow hydrograph is not rapidly changing with time, as determined from Figure 15.1 (Fread et al., 1988; Fread, 1992).

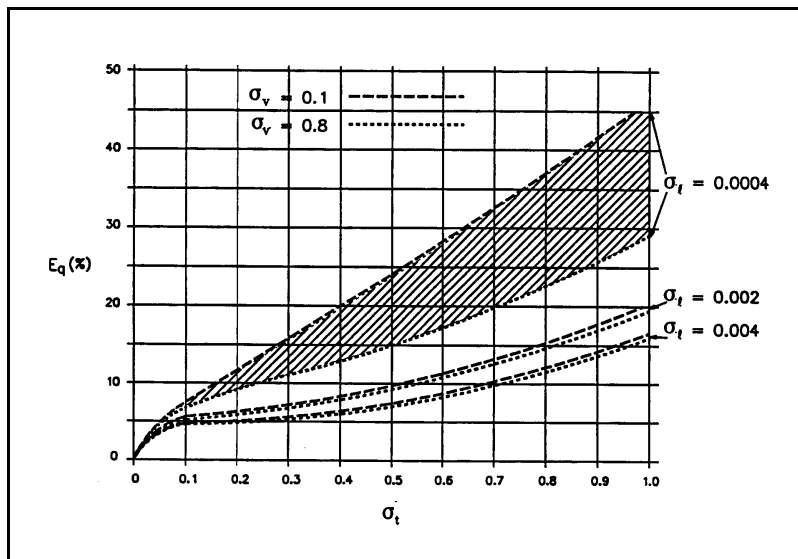


Figure 15.1 - Level Pool routing Error When Compared to Dynamic Routing.

The error (E_q) of level-pool routing compared with dynamic routing is determined in Figure 15.2 by using three dimensionless parameters $\sigma_l = D_r/L_r$, $\sigma_v = \text{inflow hydrograph volume/reservoir volume}$, and $\sigma_t = L_r/(3600 T_r \sqrt{gD_r})$ in which $D_r = \text{average hydraulic depth (ft) of the reservoir}$, $L_r = \text{length of reservoir (ft)}$, and $T_r = \text{time of rise (hr) of inflow hydrograph}$.

The simple level-pool routing technique which is based on the principle of conservation of mass, i.e.,

$$Q_i(t) - Q_{i+1}(t) = dS/dt \quad \dots\dots\dots (15.4)$$

in which inflow (Q_i) and outflow (Q_{i+1}) are functions of time (t), and the storage (S) is a function of the water-surface elevation (h) which changes with time (t). The reservoir is assumed always to have a horizontal water surface throughout its length, hence level-pool ($h_i = h_{i+1}$). Also, Q is assumed to be a function only of $h(t)$ which is the case for reservoirs with uncontrolled overflow spillways such as the ogee-crested, broad-crested weir, and morning-glory types. Gate controlled spillways which also affect Q can be included in level-pool routing if the gate setting (height of the gate bottom above the gate sill) is a predetermined (user-specified) function of time, since the outflow is a function of h and the extent of gate opening. Reservoirs, in which the dam fails and produces a breach outflow hydrograph, can also be included in the level-pool routing approach.

The finite-difference approximation to Eq.(15.4) is given by the following:

$$Q_i^{j+1} - Q_{i+1}^{j+1} + 43560 \overline{S}_{a_i} \Delta h_{i+1}^{j+1} / \Delta t_j = 0 \quad \dots\dots\dots (15.5)$$

where:

$$\overline{S}_{a_i} = (S_{a_i}^j + S_{a_i}^{j+1})/2 \quad \dots\dots\dots (15.6)$$

$$\Delta h_{i+1}^{j+1} = h_{i+1}^{j+1} - h_{i+1}^j \quad \dots\dots\dots (15.7)$$

A second equation must be used for level-pool routing. It expresses the fact that the reservoir water-surface elevation is level (horizontal), i.e.,

$$h_i - h_{i+1} = 0 \quad \dots\dots\dots (15.8)$$

In level-pool routing using Eqs. (15.5) and (15.8), the i^{th} cross section is located at the upstream end of the reservoir and the $i+1^{\text{th}}$ cross section is located immediately upstream of the dam. Also, two additional internal boundary equations (as described in Sub-section 3.3) are used to govern the flow through the dam, between the $i+1$ and $i+2$ cross sections.

16. LIMITATIONS OF FLDWAV

For some applications, the FLDWAV model is subject to limitations due to its governing equations, and also due to the uncertainty associated with some of the parameters used within the model.

16.1 Governing Equations

The governing equations within FLDWAV for routing hydrographs (unsteady flows) are the one-dimensional Saint-Venant equations. There are some instances where the flow is more nearly two-dimensional than one-dimensional, i.e., the velocity of flow and water-surface elevations vary not only in the x-direction along the river/valley but also in the transverse direction perpendicular to the x-direction. Neglecting the two-dimensional nature of the flow can be important when the flow (particularly dam-break floods) first expands onto an extremely wide and flat floodplain after having passed through an upstream reach which severely constricts the flow. In many cases, where the wide floodplain is bounded by rising topography, the significance of neglecting the transverse velocities and water-surface variations is confined to a transition reach in which the flow changes from one-dimensional to two-dimensional and back to one-dimensional along the x-direction. In this case, the use of radially defined cross sections along with judicious off-channel storage widths can minimize the two-dimensional effect neglected within the transition reach. The radial cross sections appear in plan-view as concentric circles of increasing diameter in the downstream direction which is considered appropriate for radial flow expanding onto a flat plane. Also, the cross sections must gradually become perpendicular to the x-direction for the reach downstream of the transition reach. Where the very wide, flat floodplain appears unbounded, the radial representation of the cross sections is at best only an approximation which varies from reality the farther from the constricted section and the greater the variability of the floodplain topography and friction. Other applications of the one-dimensional Saint-Venant equations within the FLDWAV model include: (1) very wide lakes, estuaries, or bays in which the computed velocities are required to be accurate for sediment modeling or other transport modeling applications and (2) very wide floodplains with very complex overbank flows controlled by a complicated pattern of road embankments and levees and flow bifurcations.

16.2 Fixed-Bed Assumption

The high velocity flows associated with dam-break floods can cause significant scour (degradation) of alluvial channels. This enlargement in channel cross-sectional area is neglected in FLDWAV since the equations for sediment transport, sediment continuity, dynamic bed-form friction, and channel bed armoring are not included among the governing equations. The significance of the neglected alluvial channel degradation is directly proportional to the channel/floodplain conveyance ratio, since the characteristics of most floodplains, along with their much lower flow velocities, cause much less degradation within the floodplain. As this ratio increases, the degradation could cause a significant lowering of the water-surface elevations until the flows are well within the recession limb of the dam-break hydrograph; however, in many instances this ratio is fairly small and remains such until the dam-break flood peak has attenuated significantly at locations far downstream of the dam, and where this occurs the maximum flow velocities also have attenuated. However, narrow channels with minimal floodplains are subject to overestimation of water elevations due to significant channel degradation. The effect of alluvial fill (aggradation) associated with the recession limb of the dam-break hydrograph and that occurring in the floodplain are considered to have relatively small effects on the peak flood conditions.

16.3 Manning n Uncertainty

The uncertainty associated with the selection of the Manning n can be quite significant for dam-break floods due to: (1) the great magnitude of the flood produces flow in portions of floodplains which have been very infrequently or never before inundated; this necessitates the selection of the n values without the benefit of previous evaluations of n from measured elevation/discharges or the use of calibration techniques for determining the n values; (2) the effects of transported debris can alter the Manning n . Although the uncertainty of the Manning n values may be large, this effect is considerably damped or reduced during the computation of the water-surface elevations. Fread (1981) derived the following relation (based on the Manning equation) between the error or uncertainty in the Manning n and the resulting flow depth, i.e.,

$$d_e/d = (n_e/n)^{b'} \dots\dots\dots (16.1)$$

$$\text{in which } b' = 3/(3m+5) \dots\dots\dots (16.2)$$

in which d_e is the flow depth (ft) associated with an erroneous n_e value, d is the flow depth (ft) associated with the correct n value, and m is a cross section shape factor (the exponent in the width-depth power function), i.e., $m = 0$ for rectangular sections, $m = 0.5$ for parabolic, $m = 1$ for triangular, and $1 < m < 3$ for channels with floodplains (the wider and more flat the floodplain, the greater the m value). Since for channels with wide floodplains ($m = 2$), the exponent b' in Eq. (16.2) is equal to 0.27; and from an inspection of Eq. (16.1) it is evident that the difference between d_e and d is substantially damped relative to the difference between n_e and n . In fact, if $n_e/n = 1.5$, then $d_e/d = 1.12$, which illustrates the degree of damping. Thus for rivers with wide floodplains, the uncertainty in the Manning n value results in considerably less uncertainty in the flow depths.

The propagation speed (c) of the floodwave is related to the uncertainty in the Manning n according to the following:

$$\hat{c}_e/\hat{c} = (n_e/n)^{2b'/3-1} \dots\dots\dots (16.3)$$

in which c_e is the propagation speed (mi/hr) associated with an erroneous n_e value. If $n_e/n = 1.5$, then $c_e/c = 0.72$, which indicates less damping than that associated with Eq. (16.1). Thus errors in the Manning n affect the rate of propagation more than the flow depth, but in each instance the error of the flow is not proportional to the n_e error, but rather the flow error is damped.

When the range of possible Manning n values is fairly large for dam-break flood applications, it is best to perform a sensitivity test using the FLDWAV model to simulate the flow, first with the lower estimated n values and then a second time with the higher estimated n values. The resulting high water profiles computed along the river/valley for each simulation represent an envelope of possible flood peak elevations within the range of uncertainty associated with the estimated n values.

16.4 Dam-Break Floods

Dam-break floods with a large amount of transported debris may accumulate at constricted cross sections such as bridge openings where it acts as a temporary dam and partially or completely restricts the flow. At best, the maximum magnitude of this effect, i.e., the upper envelope of the flood-peak elevation profile can be approximated by using the FLDWAV model to simulate the blocked constriction as a downstream dam having an estimated elevation-discharge relation approximating the gradual flow stoppage and the later rapid increase due to the release of the ponded waters when the debris dam is allowed to breach.

The uncertainty associated with the breach parameters, especially \bar{b} and τ , also cause uncertainty in the flood peak elevation profile and arrival times. The best approach is to perform a sensitivity test using minimum, average, and maximum values for \bar{b} and τ . As mentioned previously in Sub-section 2.3, the maximum flood is usually produced by selecting the maximum probable \bar{b} and minimum probable τ , whereas the minimum flood is produced by using the minimum \bar{b} and maximum τ values. The differences in flood-peak properties (flow, elevation, time of arrival) at each section downstream of the dam due to variations in the breach parameters reduces in magnitude or is damped as the dam-break flood propagates through the downstream river/valley.

16.5 Volume Losses

There is uncertainty associated with volume losses incurred by the dam-break flood as it propagates downstream and inundates large floodplains where infiltration and detention storage losses may occur. Such losses are difficult to predict and are usually neglected, although they may be significant. Again, a sensitivity test may be performed using estimated α values in Eq. (12.9). The conservative approach is to neglect such losses, unless very good reasons justify their consideration, e.g., observed losses associated with previous large floods in the same floodplain.

17. MODEL TESTING

The FLDWAV has been tested in numerous actual applications of both real-time routing of runoff-generated floods, and in non-real-time dam-break flood forecasting. Also over 150 hypothetical dam-break applications and real-time flood routing applications were used to test the model using output from the DAMBRK and DWOPER models, respectively, to determine if the FLDWAV model was appropriately comparable to the previously much tested DAMBRK and DWOPER models.

The FLDWAV model has been tested with satisfactory results on at least five historical dam-break floods to determine its ability to reconstitute observed downstream peak stages, discharges, and travel times. Dam-break floods that have been used in the testing of the FLDWAV algorithms are the 1976 Teton Dam, the 1972 Buffalo Creek coal-waste dam, the 1889 Johnstown Dam, the 1977 Toccoa (Kelly Barnes) Dam, and the Laurel Run Dam floods. The FLDWAV algorithms were also tested on several historical floods on major rivers in the U.S. including the 1969 hurricane storm surge up the lower Mississippi River system, 1970 flood on the Ohio-Mississippi River system, 1993 flood on the Mississippi-Illinois-Missouri River system, and the 1997 flood on the Red River of the North at Grand Forks. Only two dam-break floods (the Teton and the Buffalo Creek floods), and two real-time river floods (the 1969 flood on the lower Mississippi River and the 1970 flood on the Ohio-Mississippi River system) are described to illustrate some of the FLDWAV model's capabilities and simulation accuracies.

17.1 Teton Dam Flood

The Teton Dam, a 300 ft high earthen dam with a 3,000 ft long crest and 250,000 acre-ft of stored water, failed on June 5, 1976, killing 11 people, making 25,000 homeless, and inflicting about \$400 million in damages to the downstream Teton-Snake River Valley. Data from a Geological Survey Report by Ray, et al. (1976) provided observations on the approximate development of the breach, description of the reservoir storage, downstream cross sections and estimates of Manning n approximately every 5 miles, indirect peak discharge measurements at two sites, rating curves at two

sites, flood-peak travel times, and flood-peak elevations. The inundated area was as much as 9 miles in width about 16 miles downstream of the dam (Figure 17.1). The following breach parameters were used in FLDWAV to reconstitute the downstream flooding due to the failure of Teton Dam: $\tau = 1.43$ hrs, $b = 81$ ft, $z = 1.04$, $h_{bm} = 0.0$, $h_f = h_d = h_o = 261.5$ ft. They were obtained from the BREACH model (Fread, 1984a, 1987a). The time of failure τ as obtained by solving Eq. (6.13) for τ with Q_p , \bar{b} , h_d computed by the BREACH model. Eq. (6.13) can be rearranged to compute τ as follows:

$$\tau = C \left[(3.1 \bar{b}/Q_p)^{1/3} - 1/h_d^{0.5} \right] \dots\dots\dots (17.1)$$

in which $Q_p = 2,200,000$ cfs, $\bar{b} = 353$ ft, and $C = 23.4$ (1936 acres)/ \bar{b} . Cross-sectional properties were used at 12 locations along the 60-mile reach of the Teton-Snake River Valley below the dam. Five topwidths were used to describe each cross section. The downstream valley consisted of a narrow canyon (approx. 1,000 ft. wide) for the first 5 miles and thereafter a wide valley. Manning n values ranging from 0.028 to 0.047 were provided from field estimates by the Geological Survey.

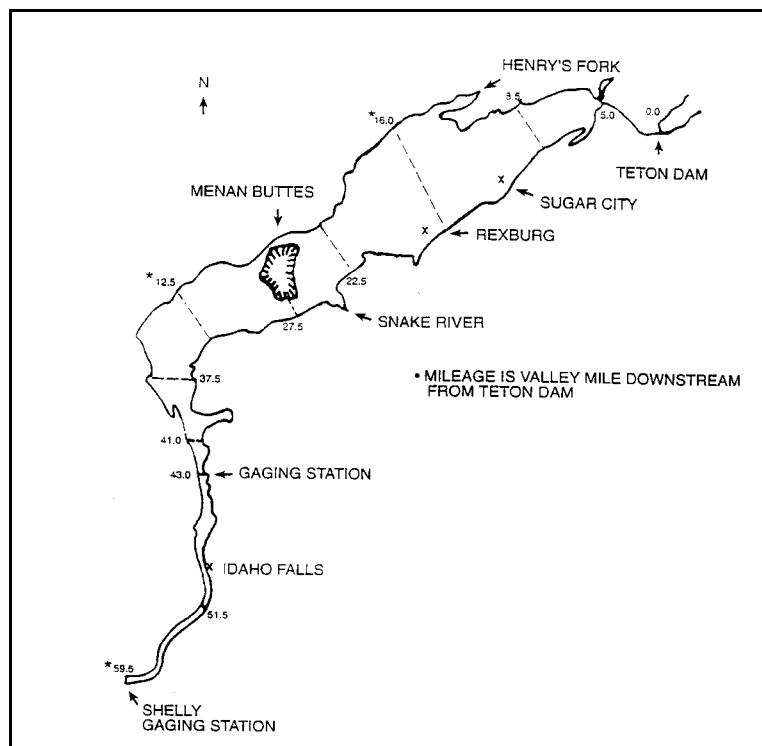


Figure 17.1 - Teton Dam Study Area.

DXM values between cross sections were assigned values that gradually increased from 0.5 miles near the dam, to a value of 1.4 miles near the downstream boundary at the Shelly gaging station (valley mile 59.5 downstream from the dam). The reservoir surface area-elevation values were obtained from Geological Survey topographic maps. The downstream boundary was assumed to be channel flow control as represented by a loop-rating curve given by Eq. (3.6).

The computed outflow hydrograph is shown in Figure 17.2. It has a peak value of 2,183,000 cfs, a time to peak of 1.43 hrs, and a total duration of significant outflow of about 6 hrs. This peak discharge is about 30 times greater than the flood of record at Idaho Falls. The temporal variation of the computed time-integrated outflow volume compared within 3 percent of observed as shown in Figure 17.3. In Figure 17.4, a comparison is presented of Teton reservoir outflow hydrographs computed via reservoir storage (level-pool) routing and reservoir dynamic (Saint-Venant equations) routing. Since the breach of the Teton Dam formed gradually over approximately a one hour interval, a steep negative wave did not develop. Also, the inflow to the reservoir was insignificant. For these reasons, the reservoir surface remained essentially level during the reservoir drawdown and the dynamic routing yielded almost the same outflow hydrograph as the level-pool routing technique.

The computed peak discharge values along the 60-mile downstream valley are shown in Figure 17.5 along with four observed values (two by indirect measurement; two by rating curves) at

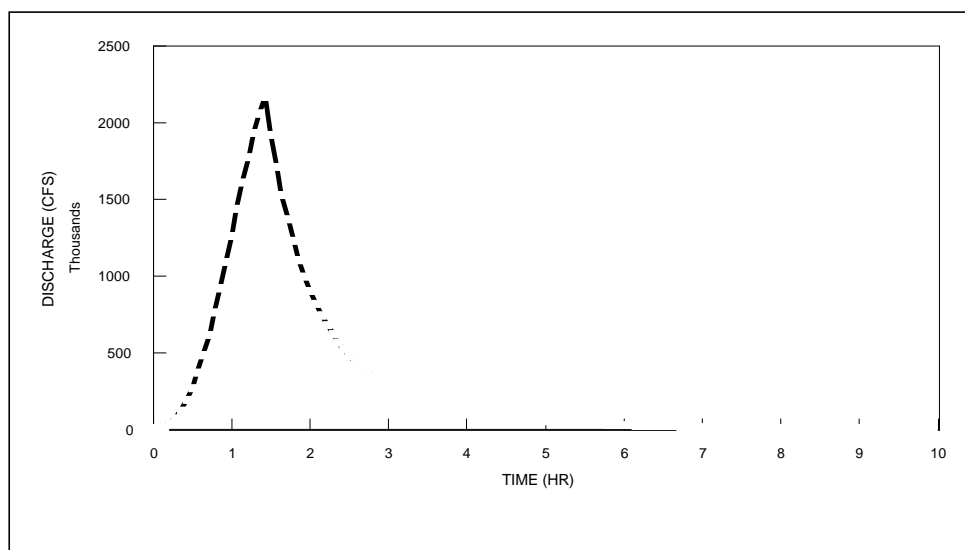


Figure 17.2- Teton Breach Outflow Hydrograph.

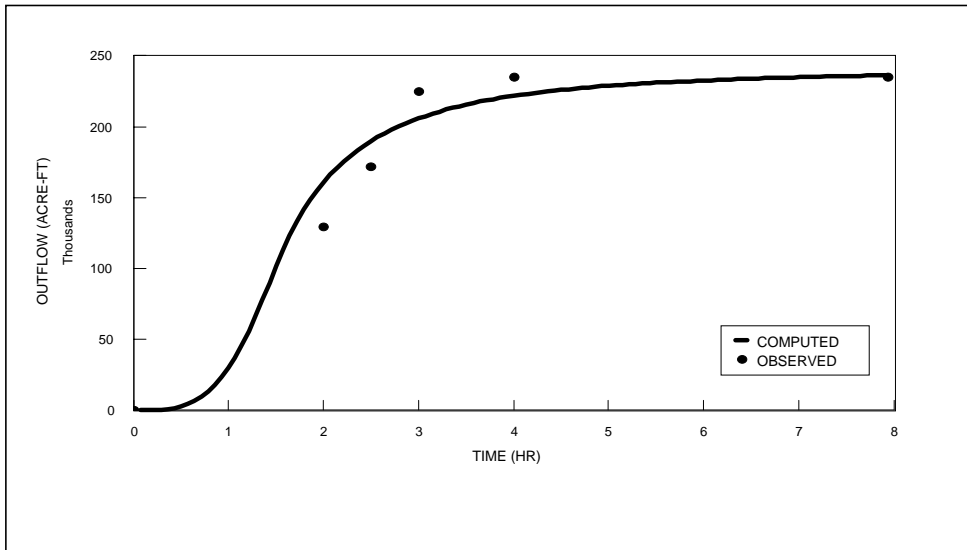


Figure 17.3 - Outflow Hydrograph From Teton Dam Failure.

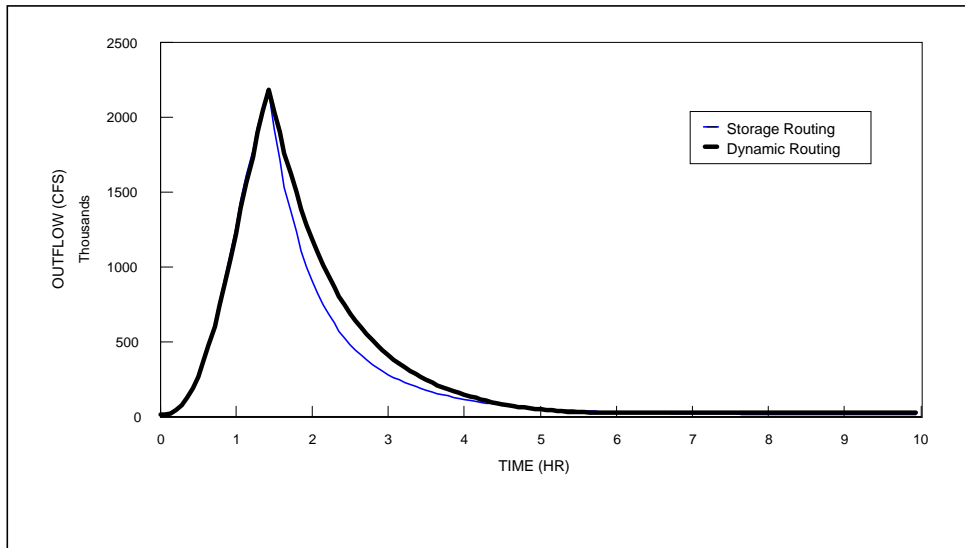


Figure 17.4 - Outflow Volume From Teton Dam.

miles 2.0, 8.5, 43.0, and 59.5. The average absolute difference between the computed and observed values is 5.2 percent. Most apparent is the extreme attenuation of the peak discharge as the flood wave propagates through the valley. Two computed curves are shown in Figure 17.5; one in which no losses were assumed, i.e., using Eq. (12.10) with $\alpha' = 0$ and $e' = 1$; and a second in which the total volume losses of about 30 percent and an active volume loss of 50 percent ($\alpha' = -0.5$) and were accounted for in the routing via the q term in the Saint-Venant Eqs. (2.1-2.2). Losses were due to infiltration and detention storage behind irrigation levees.

The a priori selections of the breach parameters (τ and b) cause the greatest uncertainty in forecasting dam-break flood waves. The sensitivity of downstream peak discharges to reasonable variations in τ and b are shown in Figure 17.6. Although there are large differences in the discharges (+63 percent to -30 percent) near the dam, these rapidly diminish in the downstream direction. After 8.5 miles the variation is about ± 18 percent, and after 22 miles the variation has further diminished to about ± 5 percent. The tendency for extreme peak attenuation and rapid damping of differences in the peak discharge is accentuated in the case of Teton Dam due to the presence of the very wide downstream valley. Had the narrow canyon extended all along the 60-mile reach to Shelly, the peak

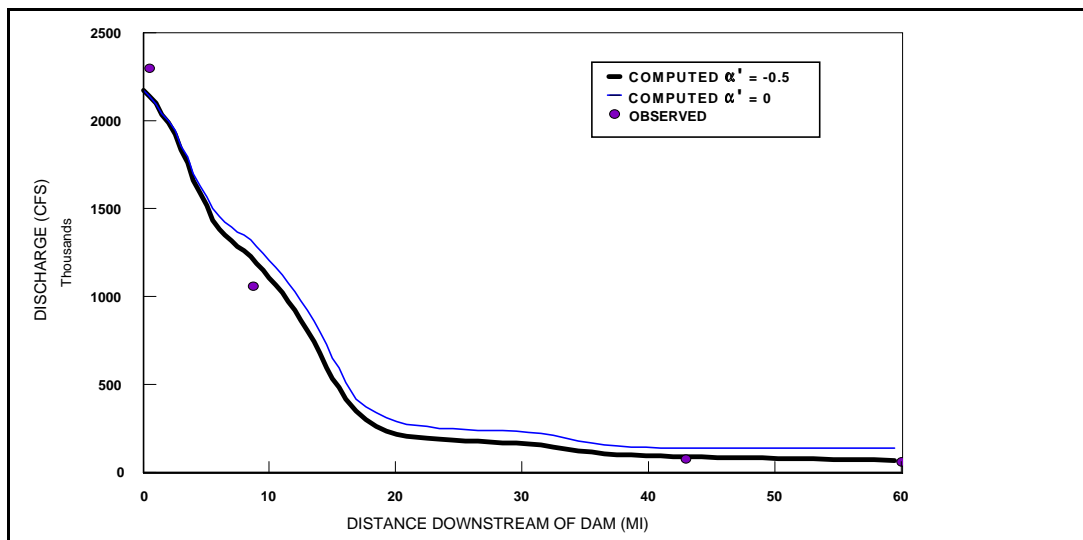


Figure 17.5 - Profile of Peak Discharge From Teton Dam Failure

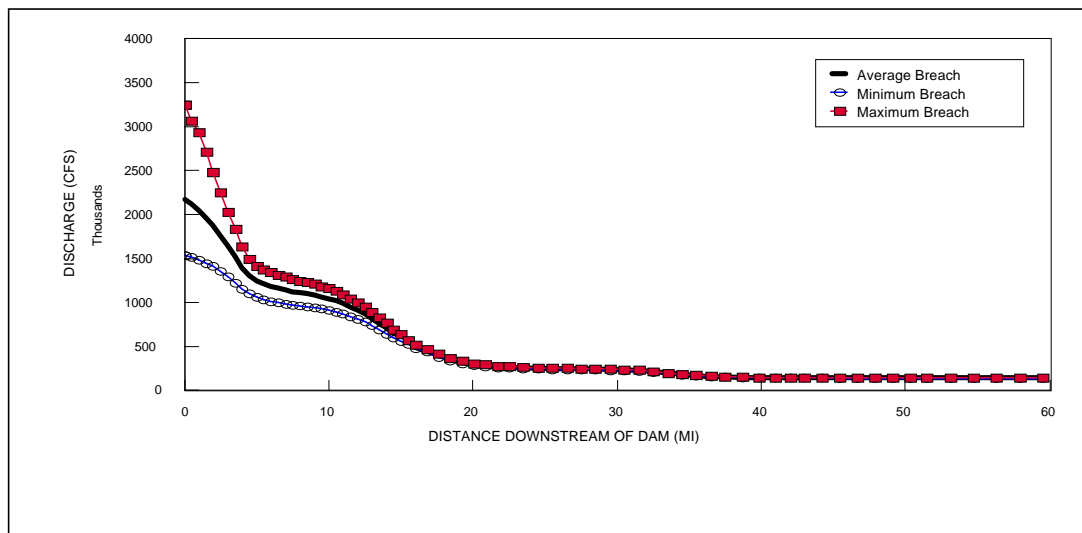


Figure 17.6 - Profile of Peak Discharge From Teton Dam Failure Showing Sensitivity of Various Input Parameters.

discharge would not have attenuated as much and the differences in peak discharges due to variations in τ and \bar{b} would be more persistent. In this instance, the peak discharge would have attenuated to about 750,000 cfs rather than 142,000 cfs as shown in Figure 17.6, and the differences in peak discharges at mile 59.5 would have been about ± 18 percent as opposed to 1 percent as shown in Figure 17.6. Computed peak elevations compared favorably with observed values, as shown in Figure 17.7. The average absolute error is 1.9 ft., while the average arithmetic error is +0.8 ft.

The computed flood-peak travel times and three observed values are shown in Figure 17.8. The differences between the computed and observed travel times at mile 59.5 are about 5 percent for the case of using the estimated Manning n values and about 13 percent if the n values are arbitrarily increased by 20 percent.

As stated previously in Section 14, the Manning n must be estimated, especially for the flows above the flood of record. The sensitivity of the computed water elevations and discharges of the Teton flood due to a substantial change (20 percent) in the Manning n is found to be as follows:

- (1) 0.3 ft in computed peak water surface elevations or about 1 percent of the maximum flow depths,
- (2) 13 percent deviation in the computed peak discharges, (3) 0.5 percent change in the total attenuation of peak discharge incurred in the reach from Teton Dam to Shelly, and (4) 13 percent change in the flood-peak travel time at Shelly. These results indicate that the Manning n has little

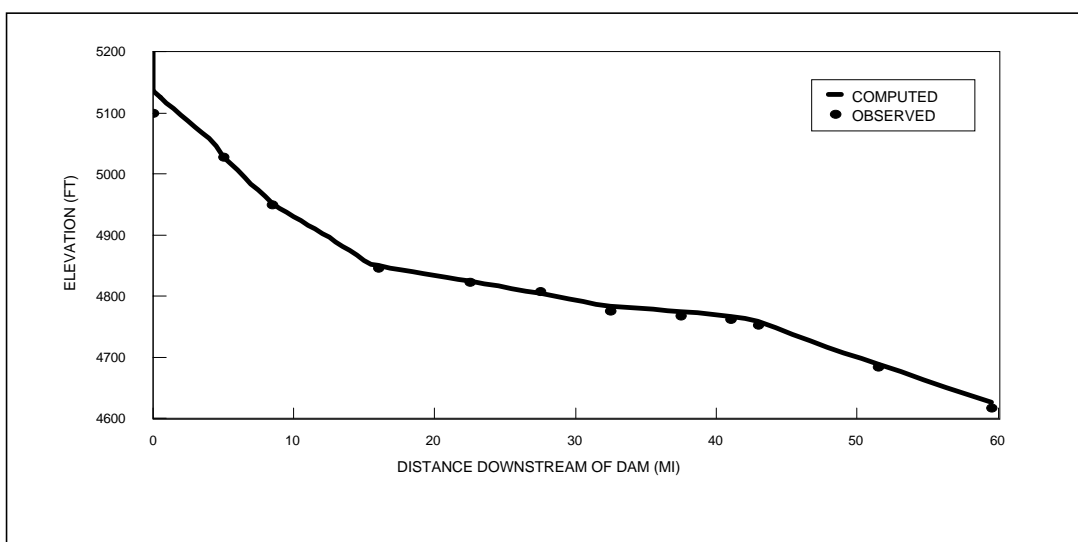


Figure 17.7 - Profile of Peak Flood Elevation From Teton Dam Failure.

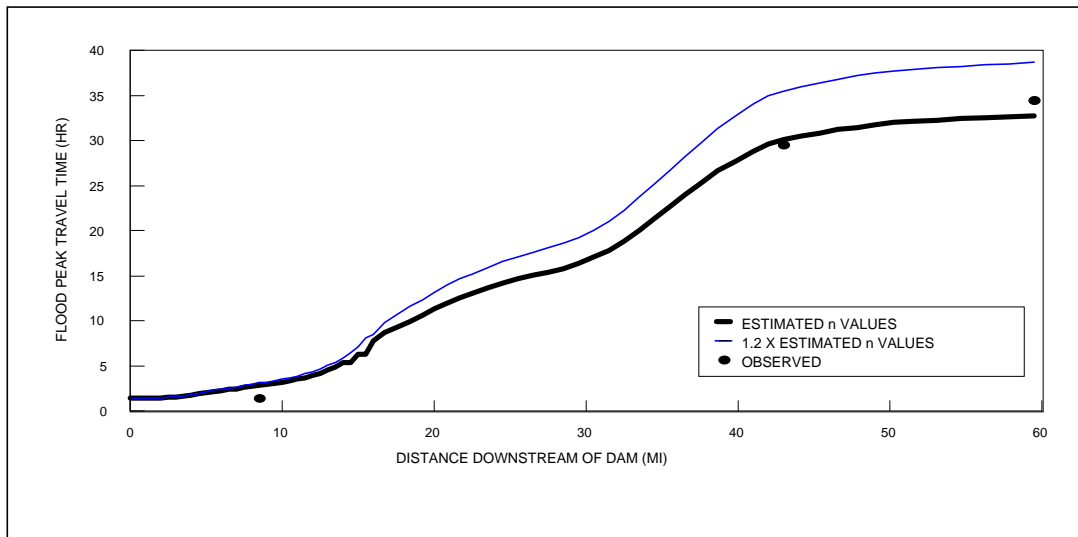


Figure 17.8 - Travel Time of Flood Peak From Teton Dam Failure.

effect on peak elevations or depths; however, the travel time is affected by more than one-half of the percentage change in the n values.

A typical simulation of the Teton flood as described above involved 73 Δx reaches, 55 hrs of prototype time, and an initial time step (Δt) of 0.072 hrs which automatically increased gradually to 0.1025 hrs. Such a simulation run required only 6 seconds run time on a PC (300 MHz Pentium).

17.2 Buffalo Creek Flood

The FLDWAV model was also applied to the failure of the Buffalo Creek coal-waste dam which collapsed on the Middle Fork, a tributary of Buffalo Creek in southwestern West Virginia near Saunders (Figure 17.9). The dam failed very rapidly on February 26, 1972, and released about 500 acre-ft of impounded waters into Buffalo Creek valley, causing the most catastrophic flood in the state's history with the loss of 117 lives, 500 homes, and property damage exceeding \$50 million. Observations were available on the approximate development sequence of the breach, the time required to empty the reservoir, indirect peak discharge measurements at four sites, approximate flood-peak travel times, and flood-peak elevations (Davies, et al., 1972). Cross sections and first

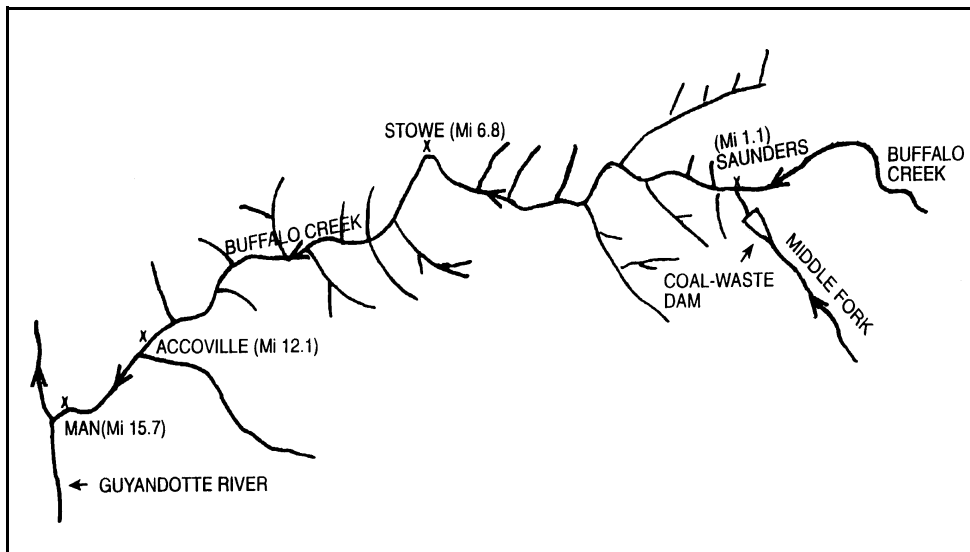


Figure 17.9 - Schematic of Buffalo Creek Study.

estimates of the Manning n values were taken from a report on routing dam-break floods by McQuivey and Keefer (1975).

The time of failure was estimated to be in the range of 5 minutes and the reservoir took only 15 minutes to empty according to eyewitnesses' reports. The following breach parameters were used: $\tau = 0.083$ hrs, $b = 290$ ft, $z = 0.0$, $h_{bm} = 0.0$ ft, $h_f = h_d = h_o = 44.0$ ft. Cross-sectional properties were specified for eight locations along the 15.7 mile reach from the coal-waste dam to below the community of Man at the confluence of Buffalo Creek with the Guyandotte River. The downstream valley widened from the narrow width (approximately 100 ft) of the Middle Fork to about 400-600 feet width of the Buffalo Creek valley. Minimum DXM_i values were gradually increased from 0.10 mile near the dam to 0.8 mile near Man at the downstream boundary. The reservoir area-elevation values were obtained from Davies, et al., (1972).

The 15.7 mile reach consisted of two distinct sloping reaches; one was approximately 4 miles long, with a very steep channel bottom slope (84 ft/mi), and the second extended on downstream approximately 12 miles, with an average bottom slope of 40 ft/mi. Subcritical flow prevailed throughout the routing reach for selected Manning n values of 0.060.

The reservoir storage routing option was used to generate the outflow hydrograph shown in Figure 17.10. The computations indicated the reservoir emptied of its contents in approximately 15 minutes which agreed closely with the observed emptying time. The indirect measurements of peak discharge at miles 1.1, 6.8, 12.1, and 15.7 downstream of the dam are shown in Figure 17.11. The average absolute difference between the computed and observed values is 11 percent. Again, as in the Teton Dam flood, the flood peak was greatly attenuated as it advanced downstream. Whereas the Teton flood was attenuated by 78 percent in the first 16 miles, of which 11 miles included the wide, flat valley below the end of the Teton Canyon, the Buffalo Creek flood was confined to a relatively

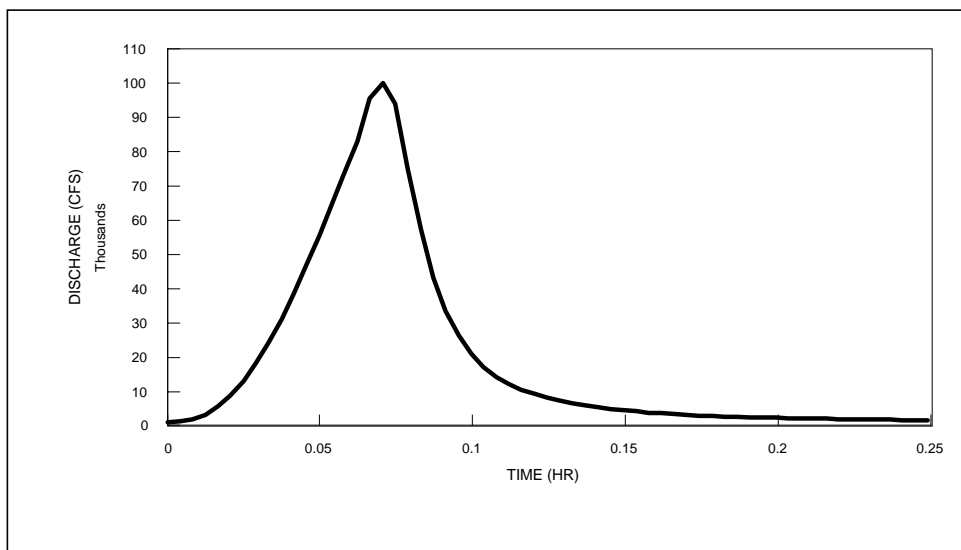


Figure 17.10 - Buffalo Creek Breach Outflow Hydrograph.

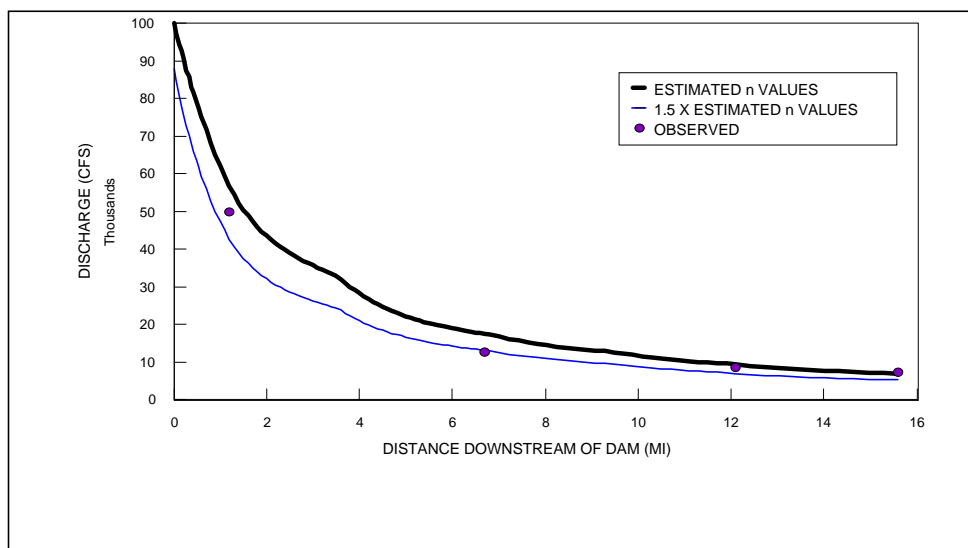


Figure 17.11 - Profile of Peak Discharge From Buffalo Creek Failure.

narrow valley, but was attenuated by 92 percent in the same distance. The more pronounced attenuation of the Buffalo Creek flood was due to the much more rapid breach formation time and the much smaller volume of its outflow hydrograph compared with that of the Teton flood.

In Figure 17.11, the computed discharges agree favorably with the observed. There are two curves of the computed peak discharge in Figure 17.11; one is associated with n values of 0.06 and the other with n values of 0.090. Comparison of computed flood travel times with the observed are shown in Figure 17.12 for 0.060 n values and for the 0.090 n values. It should be noted that the two computed curves in Figure 17.11 are not significantly different, although the n values differ by a factor of 1.50. Again, as in the Teton application, the n values influence the time of travel (Figure 17.12) much more than the peak discharge (Figure 17.11). The selected n values appear to be appropriate for dam-break waves in the near vicinity of the breached dam where extremely high flow velocities uproot trees and transport considerable sediment and boulders (if present), and generally result in large energy losses.

A profile of the observed peak flood elevations downstream of the Buffalo Creek coal-waste dam is shown in Figure 17.13. The average absolute error is 2.1 feet and the average arithmetic error is -0.9 foot.

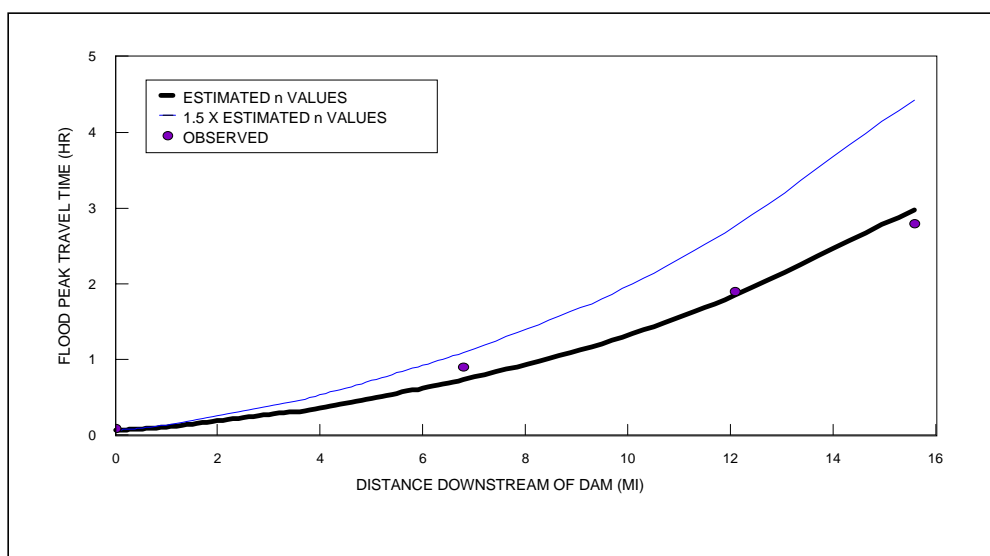


Figure 17.12 - Travel Time of Flood Peak From Buffalo Creek Failure.

Sensitivities of the computed downstream peak discharges to reasonable variations in the selection of breach parameters (τ , b , and z) are shown in Figure 17.14. The resulting differences in the computed discharges diminish in the downstream direction. Like the Teton dam-break flood wave, errors in forecasting the breach are damped-out as the flood advances downstream.

A typical simulation of the Buffalo Creek flood involved 198 Δx reaches, 3.0 hours of prototype time, use of the reservoir storage routing option, and time step of 0.008 hour for the sub-critical downstream reach. Computation time for a typical simulation run was 7 seconds on a PC (300 MHz Pentium).

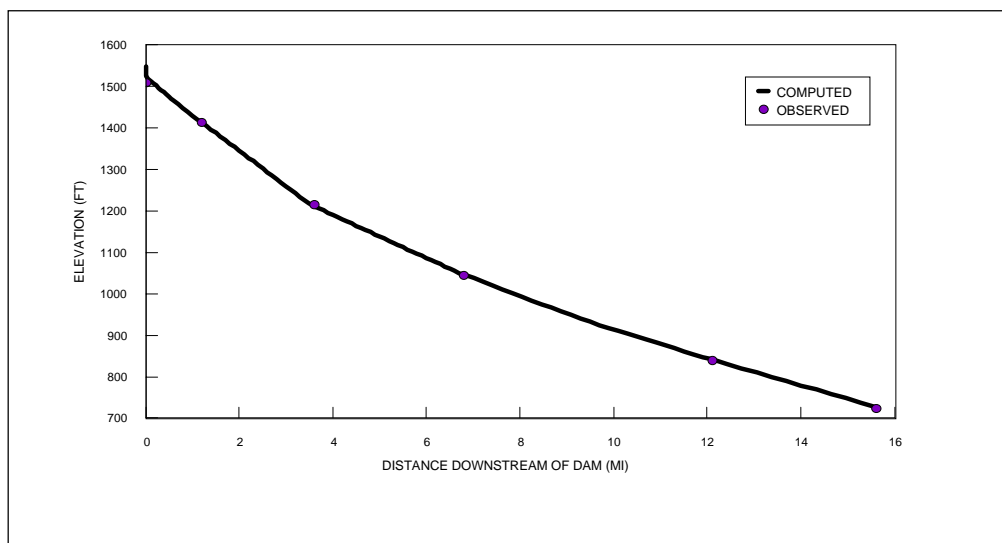


Figure 17.13 - Profile of Peak Flood Elevation From Buffalo Creek Failure.

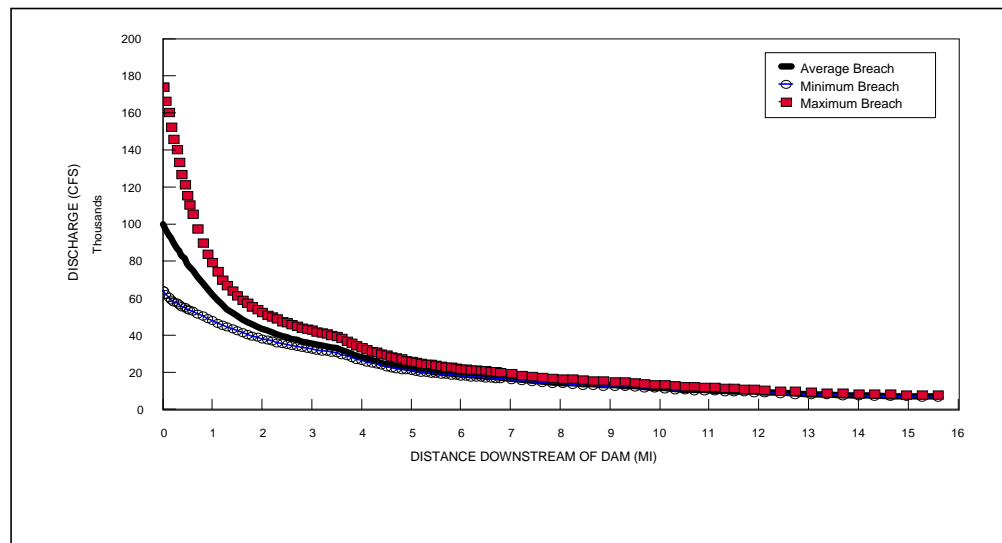


Figure 17.14 - Profile of Peak Discharge From Buffalo Creek Failure Showing Sensitivity of Various Input Parameters.

17.3 Lower Mississippi River System

FLDWAV was applied to a 291.7 mi reach of the Lower Mississippi River from Red River Landing to Venice, shown schematically in Figure 17.15 (Fread, 1974a, 1978b). Six intermediate gaging stations at Baton Rouge, Donaldsonville, Reserve, Carrollton, Chalmette, and Pt. A La Hache were used to evaluate the simulations.

This reach of the lower Mississippi is contained within levees for most of its length, although some overbank flow occurs along portions of the upper 70 mi. Throughout this reach, the alluvial river meanders between deep bends and relatively shallow crossings; the sinuosity coefficient is 1.6. The low flow depth varies from a minimum of 30 feet at some crossings to a maximum depth of almost 200 feet in some bends. The average channel bottom slope is a very mild 0.034 ft/mi. The discharge varies from low flows of about 100,000 cfs to flood discharges of over 1,200,000 cfs for the

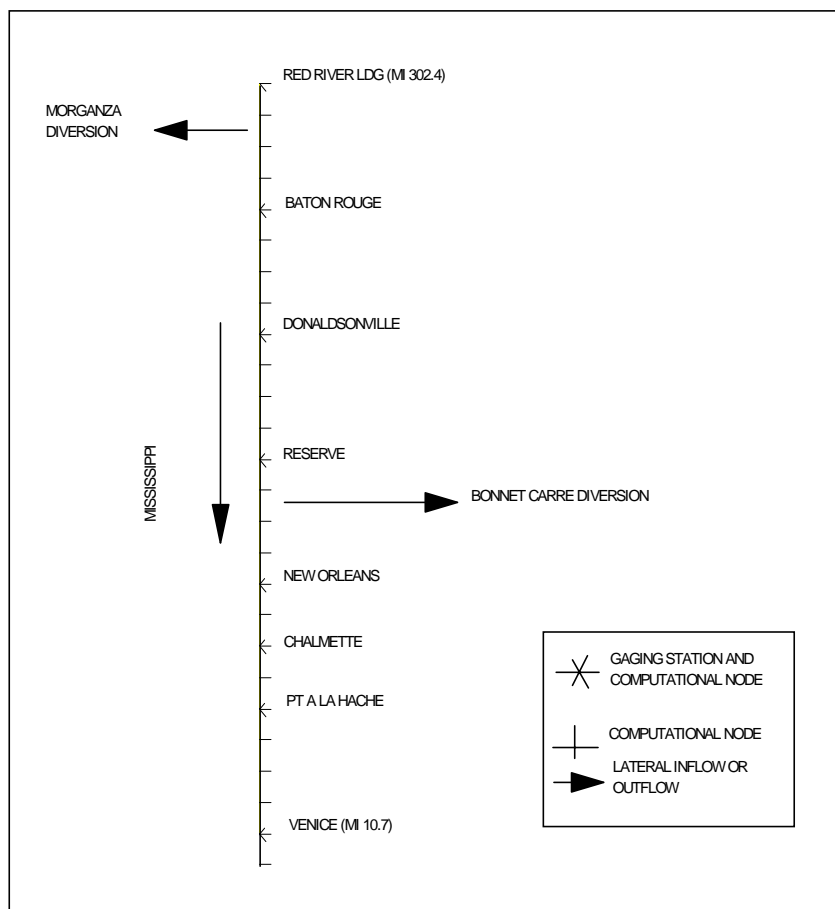


Figure 17.15 - Schematic of Lower Mississippi River.

applications presented herein. A total of 25 cross-sections located at unequal intervals ranging from 5-20 miles were used to describe the 291.7 mi reach.

The reach was first automatically calibrated by FLDWAV for the 1969 spring flood. Time steps of 24 hours were used. Then, using the calibrated set of Manning n vs. discharge for each reach bounded by gaging stations, the 1969 flood was simulated using stage hydrographs for upstream and downstream boundaries at Red River Landing and Venice, respectively. The simulated stage hydrographs at the six intermediate gaging stations are compared with the observed in Figures 17.16-17.21. The RMS error was used as a statistical measure of the accuracy of the calibration. The RMS error varies from 0.14-0.37 ft with an average value of 0.25 ft. Verification of the calibration was achieved by using the calibrated n - Q functions for floods occurring from 1959-1971 as shown in Table 17.1. The overall average RMS error for all stations for all floods was 0.47 ^{ft}. This error represents only about a 2.8 percent variance in the total change in stage during the flood. Peak discharges ranged from 750,000 cfs to 1,220,000 cfs.

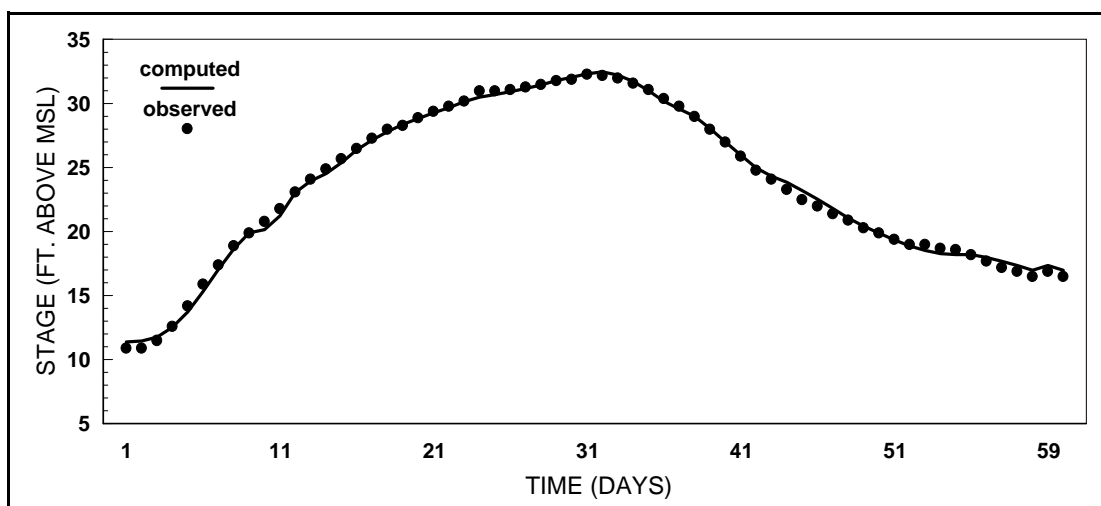


Figure 17.16 - Observed vs. Simulated Stages at Baton Rouge for 1969 Flood.

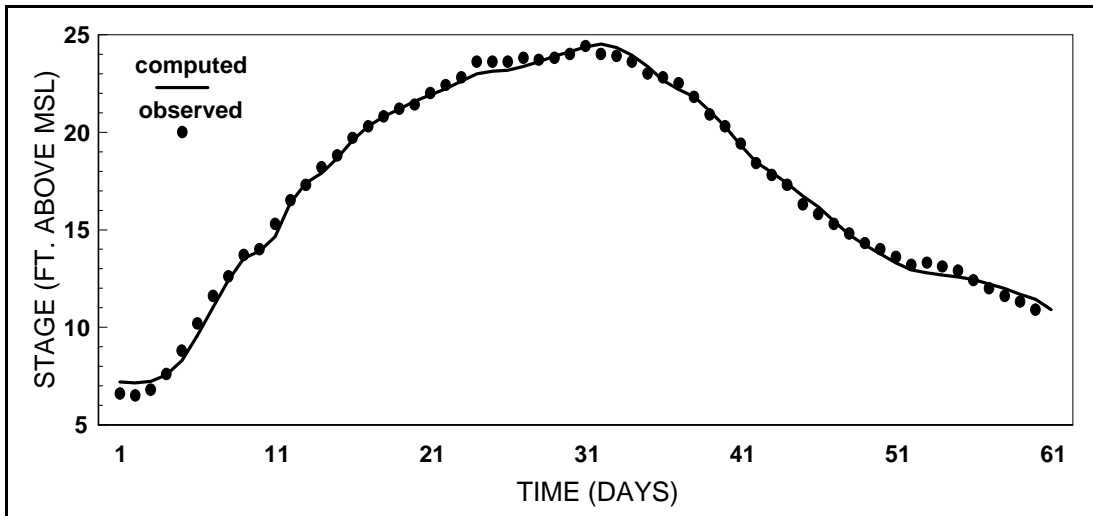


Figure 17.17 - Observed vs. Simulated Stages at Donaldsonville for 1969 Flood

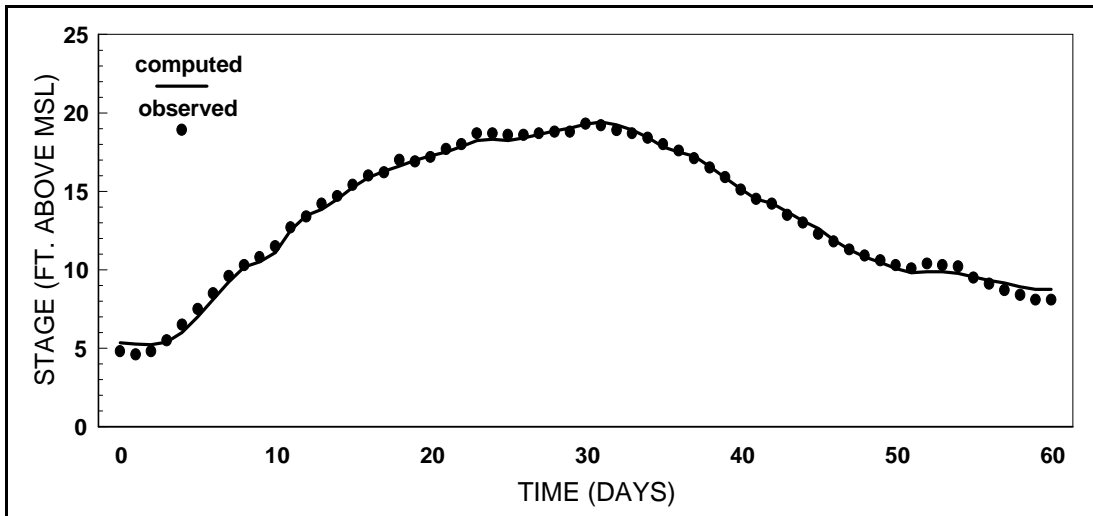


Figure 17.18 - Observed vs. Simulated Stages at Reserve for 1969 Flood.

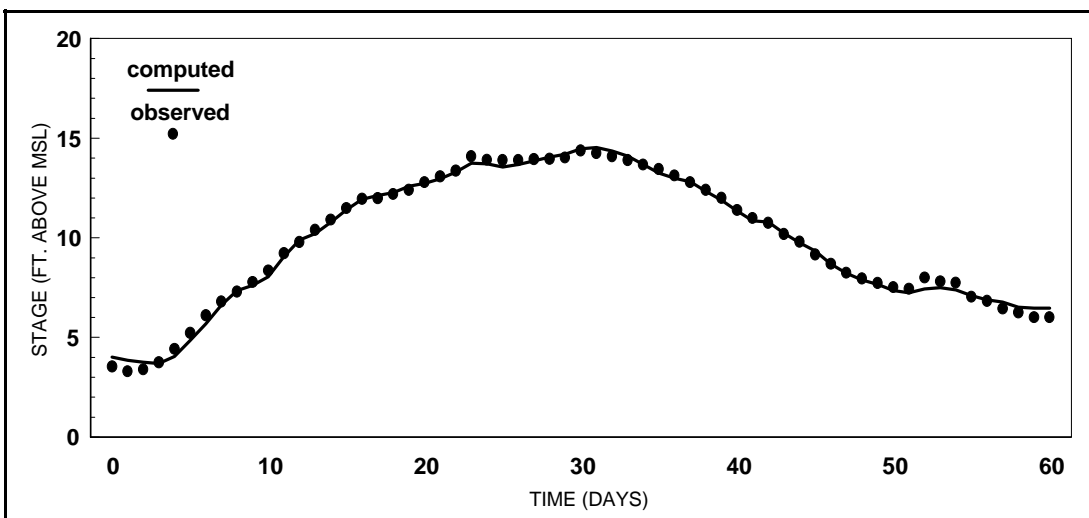


Figure 17.19 - Observed vs. Simulated Stages at Carrollton for 1969 Flood.

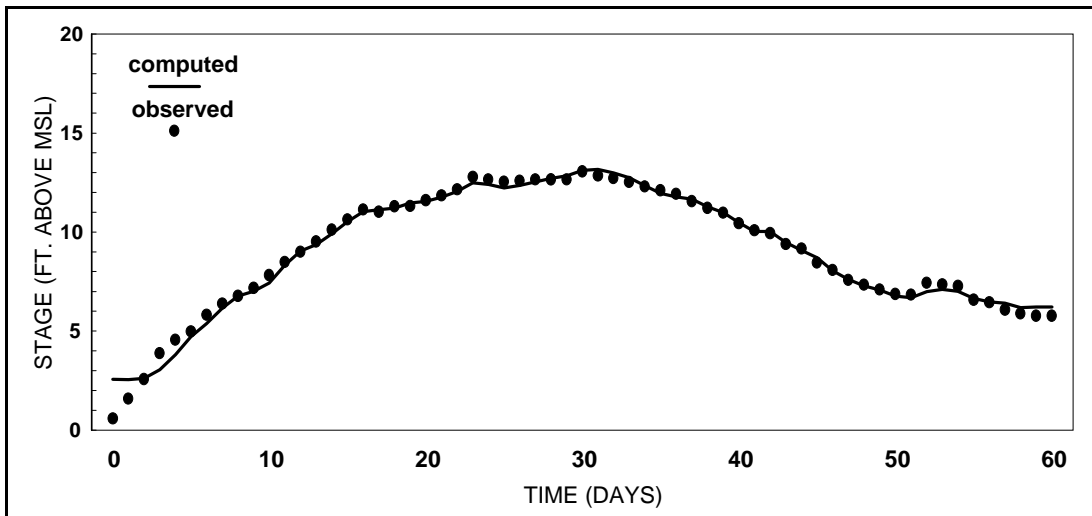


Figure 17.20 - Observed vs. Simulated Stages at Chalmette for 1969 Flood.

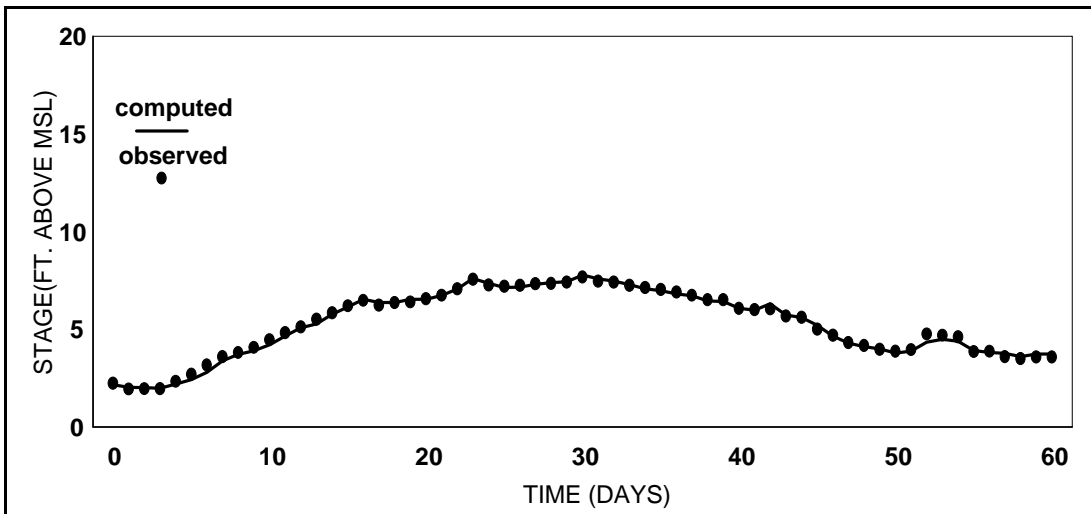


Figure 17.21 - Observed vs. Simulated Stages at Pt. A La Hache for 1969 Flood.

Table 17.1 - Summary of Flood Simulations in Lower Mississippi River (Red River Landing to Venice) for the Years 1959-1971.

<u>Year</u>	<u>Average RMS Error (ft)</u>	<u>Peak Discharge (1,000 cfs)</u>
1959	.62	750
1960	.31	850
1961	.47	1,220
1962	.61	1,155
1963	.38	960
1964	.51	1,140
1965	.44	1,040
1966	.38	1,090
1967	.38	700
1968	.36	980
1969*	.25	1,065
1970	.91	1,080
1971	.46	940
* Calibrated		

17.4 Mississippi-Ohio-Cumberland-Tennessee (MOCT) River System

A dendritic river system consisting of 393 miles of the Mississippi-Ohio-Cumberland-Tennessee (MOCT) River system (Fread, 1978b) was simulated using FLDWAV. A schematic of the river system is shown in Figure 17.22. Eleven intermediate gaging stations located at Fords Ferry, Golconda, Paducah, Metropolis, Grand Chain, Cairo, New Madrid, Red Rock, Grand Tower, Cape Girardeau, and Price Landing were used to evaluate the simulation.

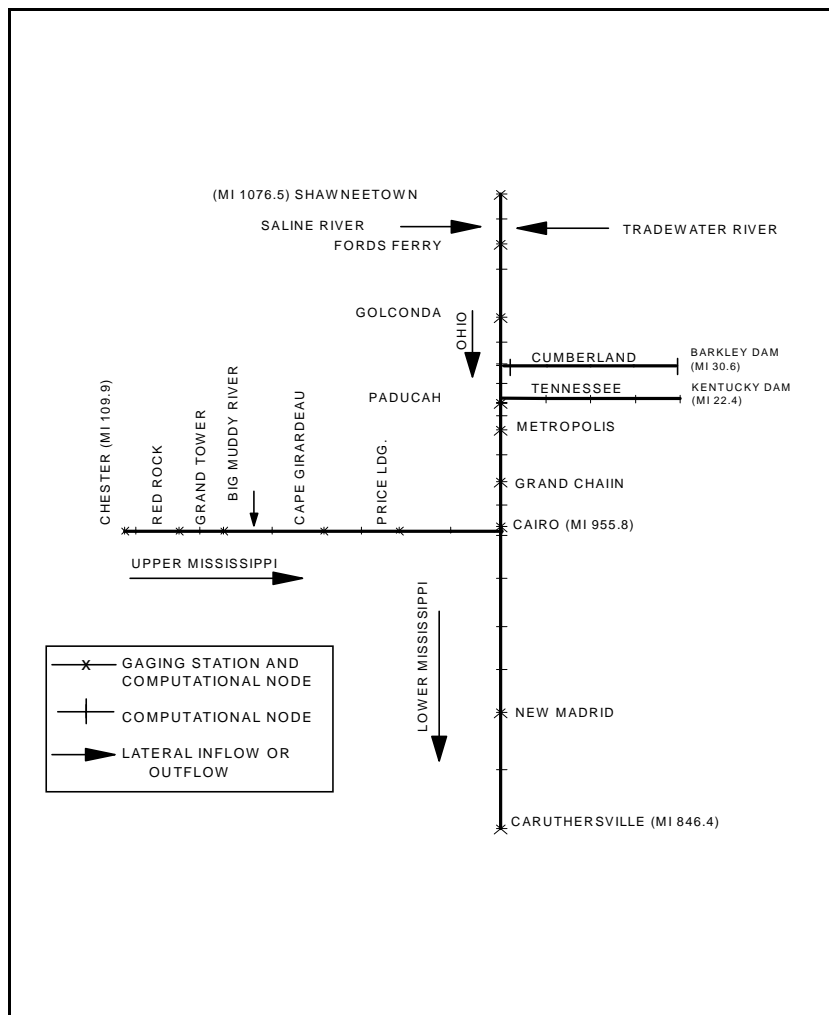


Figure 17.22 - Mississippi-Ohio-Cumberland-Tennessee (MOCT) River System.

In applying FLDWAV to this system, the main-stem river is considered to be the Ohio-Lower Mississippi segment with the Cumberland, Tennessee, and Upper Mississippi considered as first-order tributaries. The channel bottom slope is mild, varying from about 0.25 to 0.50 ft/mi. Each branch of the river system is influenced by backwater from downstream branches. Total discharge through the system for the applications described herein varied from low flows of approximately 120,000 cfs to flood flows of 1,700,000 cfs. A total of 45 cross-sections located at unequal intervals ranging from 0.5-21 miles were used to describe the MOCT river system.

The MOCT system was calibrated to determine the n-Q function for each of 15 reaches bounded by gaging stations. Time steps of 24 hours were used. About 3 seconds of Pentium300 CPU time were required by FLDWAV to perform the calibration. The flood of 1970 was used in the automatic calibration process. The average RMS error for all 15 reaches was 0.60 ft. A typical comparison of observed and simulated stages for the Cairo and Cape Girardeau gaging stations is shown in Figure 17.23 and Figure 17.24. Verification of the calibrated n-Q functions was made for the flood of 1969 which yielded an average RMS error of 0.70 ft for all gaging stations. This error represents only about a 3.0 percent variance of the total change in stage during the flood

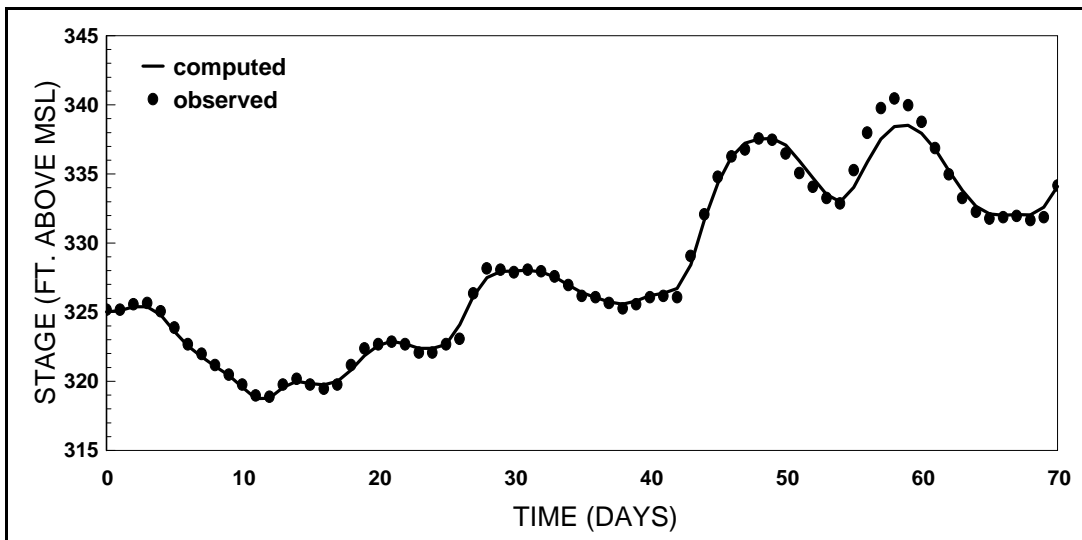


Figure 17.23 - Observed vs. Simulated Stages at Cape Girardeau for 1970 Flood.

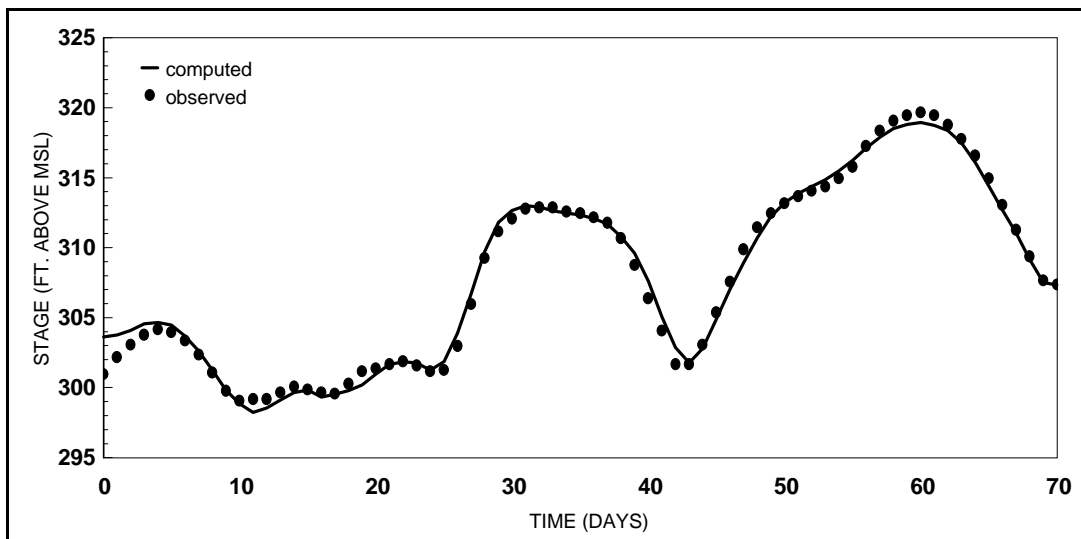


Figure 17.24 - Observed vs. Simulated Stages at Cairo for 1970 Flood.

18. DAM-BREAK FLOOD FORECASTING USING FLDWAV

The NWS FLDWAV model represents the current understanding of dam failures Fread (1998) and the utilization of hydrodynamic theory to predict the dam-break wave formation and the downstream progression. As stated in Sub-section 1.1, FLDWAV replaces the NWS DAMBRK model, and like DAMBRK, has wide applicability; it can function with various levels of input data ranging from rough estimates to complete data specification; the required data is readily accessible; and it is economically feasible to use.

18.1 Dam and Reservoir Considerations

The FLDWAV model consists of two conceptual parts, namely (1) a description of the dam failure mode, i.e. the temporal and geometrical description of the breach (Sub-section 6.1); and (2) a hydraulic computational algorithm for determining the hydrograph of the outflow through the breach as affected by the breach description, reservoir inflow, reservoir storage characteristics, spillway outflows, and downstream tailwater elevations; and routing of the outflow hydrograph through the downstream valley in order to account for the changes in the hydrograph due to valley storage, frictional resistance, downstream bridges or dams (Section 2). The model also determines the resulting water surface elevations (stages) and flood-wave travel times.

The primary breach parameters needed are the breach width and the time of failure of the dam. Breach parameters may be determined based on the rules of thumb described in Sub-section 6.2.1 for concrete dams and Sub-section 6.2.2 for earthen dams. Other dam types (e.g., rockfill, slag pile, masonry, stone) may behave more like earthen dams but adjustments should be made based on the dam material (e.g., a masonry dam may fail faster and more completely than an earthen dam). These rules of thumb are based on an average breach width; however, the shape of the breach may also be considered in FLDWAV. A general rule of thumb is to allow an earthen dam to breach with shape parameter, $z = 1.0$ and a concrete arch dam to breach with shape parameter, $z = 0$. The average breach width and time of failure may also be determined from Eqs. (6.10) and (6.11) which are based on the dam height and volume of the reservoir. As stated in Sub-section 6.2.2, the NWS BREACH

model may also be used to determine the breach parameters which will be entered into FLDWAV. A sensitivity study of the breach parameters (Sub-section 16.4) should be done to determine the effect of each parameter on the breach outflow. Eq. (6.13) may be used to compute the outflow in the sensitivity study.

In FLDWAV, the dam outflow hydrograph is a function of the method used for routing the flow through the reservoir. As stated in Sub-section 15.2, reservoirs which are not excessively long and in which the inflow hydrograph is not rapidly changing with time may be modeled using level-pool routing. In this case, the reservoir is described with a surface area vs. elevation table. Reservoirs for which level-pool routing is not applicable, are usually modeled in FLDWAV using dynamic routing. For dynamic routing, the reservoir is described using cross sections. Figure 15.1 may be used to help determine the applicability of the level-pool routing method on a particular reservoir. Currently, level pool-routing may only be used in the upstream reservoir. Subsequent downstream reservoirs are modeled using dynamic routing.

The FLDWAV model will route the outflow hydrograph through the channel/valley and determine the water-surface elevations, discharges, maximum velocities, and travel times along the routing reach. Hydrographs and peak flow and water-surface elevation profiles are generated using FLDWAV.

18.2 Dam-Break Simulation Numerical Difficulties

The FLDWAV model is capable of handling very complex routing reaches (e.g. mixed subcritical/supercritical flow, bridges, other dams, irregular cross sections, levees, channel networks, etc). These complexities may sometimes contribute to modeling difficulties. The following is a list of some difficulties encountered when using FLDWAV for dam-break flood forecasting and suggestions on how handle the difficulties.

1. Data errors: Review the model echo-output which represents what was specified as input to the model. The current (November 1998) version of the FLDWAV model does not check the input for erroneous data. In many cases the user may have mis-typed a parameter value which may cause problems later on. Be sure every cross section has the same number of topwidth-elevation values.
2. Starting with too complex of a problem: Simplify the problem to start; and then add complexities one or two at a time. For example, if the problem has variable geometry and roughness, two bridges, and levees on both sides of the river:
 - first, use prismatic geometry and constant roughness, no bridges or levees;
 - second, use variable geometry and variable roughness, no bridges or levees;
 - then, add one bridge, and then the other bridge; and
 - finally, add the levees.
3. Subcritical/Supercritical flow: Use the LPI technique (Sub-section 5.1) with $m=5$ (increased stability may be obtained by decreasing m towards a value of 1).
4. Expanding/Contracting cross sections: Increase the number of cross sections in the vicinity of the expansion/contraction by decreasing the DXM and allowing FLDWAV to linearly interpolate between existing cross sections. Note that reducing the distance interval may require decreasing the time step. Also, be sure to specify expansion/contraction coefficients.
5. Wide, flat overbank (floodplain): If feasible, use the floodplain option (Section 10) instead of the composite channel option for handling cross sections. If the composite channel is used, allow a portion of the cross sectional area to be off-channel storage (Section 8).
6. Distance interval, time interval is too large: Reduce the intervals as described in Section 11.

19. REAL-TIME FORECASTING USING FLDWAV

The NWS River Forecast System (NWSRFS) is an ensemble of computer models used to forecast river conditions in our Nation's rivers. The individual computer models are called operations. Currently, the DWOPER operation is the only dynamic routing operation in NWSRFS. As stated in Sub-section 1.1, dynamic routing is primarily used on rivers which are influenced by backwater conditions and on rivers with structures (dams, bridges, lock and dams, waterfalls, etc.) that make it difficult to use storage routing techniques. The FLDWAV operation will replace the DWOPER operation. It may be utilized to provide real-time forecasts of discharges, water-surface elevations, and velocities at specified locations along a river and its dynamic-modeled tributaries.

In order to implement the FLDWAV operation for real-time forecasting, the following tasks must be performed: 1) identify the river system and the data necessary to run the model; 2) calibrate the model; 3) define the operational forecast components; 4) define the initial conditions; and 5) run the model operationally. A description of each task follows. Difficulties encountered using dynamic routing in real-time are also discussed.

19.1 The River System and Required Data

A river system consisting of one or more rivers is defined by its boundary conditions, gaging stations (forecast points), lateral/tributary flows, and cross section topography. The dynamic rivers must be identified. Rivers which are influenced by backwater conditions, and/or rivers with very flat bottom slopes (less than about 2-3 ft/mi), and/or have rapidly varying temporal changes in the flow should be routed dynamically. All other rivers may be treated as lateral (local) inflows (Sub-section 12.1). Local flows should include both gaged and ungaged flow. These local flows are forecast values. The hydrograph (time series) for each local flow and for the inflow to each dynamic river described in the river system must be stored in the NWSRFS processed database or generated prior to running the FLDWAV operation. Time series are defined by an identifier, data type, and time step which are all described in the NWSRFS Users Manual.

To capture the widest range of flow, three floods should be calibrated: the flood of record to capture the maximum flood condition, a minimum flood to capture the low-flow condition, and a normal flood. The first two floods should be calibrated. The normal flood should be simulated to verify or determine how well the model will perform on an independent data set. This is an indicator of how well the model will perform in the forecast mode.

An upstream boundary location must be identified on each tributary which will be routed dynamically. The upstream boundary (Sub-section 3.1) should be such that it is not influenced by downstream backwater conditions. Usually the upstream boundary condition is a discharge time series which is currently being forecast (QINE or SQIN data type as defined in the NWSRFS Users Manual). Since the river system must be calibrated, observed discharges must also be available at this location (QIN or RQOT data type).

The downstream boundary (Sub-section 3.2) on tributaries is a stage time series generated within FLDWAV. The downstream boundary on the main river must be located such that it may be determined in the forecast mode. Typically the downstream boundary is either an empirical single-valued rating curve or a generated loop rating curve. In the case of tidal rivers, the downstream boundary must reflect the tidal conditions. On the Columbia River, the observed tide stage time series (TID data type) is blended with the National Ocean Survey (NOS) simulated tide stage which is forecast for the entire year (STID data type). On the lower Mississippi River, cross sections are extended several miles into the Gulf of Mexico and a stage time series (SSTG data type) with a value of 0 ft-msl is used. In cases of hurricane storm surges on the lower Mississippi River, the SLOSH model (Jelesnianski, 1972, 1978) is used externally to forecast the tidal surge. This time series (SSTG data type) is stored in the NWSRFS processed database and used as the downstream boundary condition.

Lock and dams (Sub-section 3.3.4) are modeled as internal boundary conditions. Pool and tailwater elevation time series (PELV and TWEL data types), and gate control switches (GTCS data type) are needed to model the lock and dams. The tailwater elevation time series is used only for calibration purposes.

Gaging station locations are where observed stage data is available. The reach between adjacent gages is the Manning n reach (Section 9). The roughness coefficients are usually a function of discharge (Q). The object of the calibration (Section 14) is to generate a table of n vs Q within each of the Manning n reaches such that the observed stages at each gage can be reproduced. Forecast points are those locations having a gage which the NWS is responsible for issuing a forecast. All gages may not be forecast points.

Cross sections (Section 8) are used to describe the channel/valley. They should be located along the river such that they adequately define the topography (e.g., expansions and contractions, flood storage, etc.) The distance between cross sections should obey the Courant condition for model stability (Eq. 8.1). Cross sections should be marked on USGS 7.5 minute topographic maps such that the line that represents the cross section is perpendicular to the direction of flow. For major rivers, the US Army Corps of Engineers is a good source of surveyed cross section data. If survey sections are unavailable, the floodplain portion of the section can be obtained from USGS topographic maps by measuring the distance (top width) between the same topographic (topo) contours (elevation) on either side of the river. This portion of the section may also be obtained from DEM data if it is available. In the absence of surveyed data, the channel portion of the cross section may have to be estimated based on the technique described in Sub-section 14.3. If additional cross sections are to be generated by automatic interpolation, it is important to remember that the number of topwidths used to describe the cross sections must be the same for all sections, and that the bank-full top width must be the same sequential number in the topwidth-elevation table for all cross sections (e.g. if bank-full topwidth is the third value in the topwidth-elevation table for one section, then it should be the third topwidth for all sections).

19.2 Calibration Procedure

In order to produce an acceptable forecast using FLDWAV, the model must first be calibrated by adjusting the roughness coefficients until the computed and observed stages match at each gage. A detailed description of the calibration process is described in Section 14. The following steps represent the calibration procedure.

1. Select an appropriate reach to calibrate, one that is bounded by gaging stations.
2. Select the observed floods to be used in the calibration.
3. Determine the lateral flows.
4. Gather appropriate data (boundary hydrographs, observed stage hydrographs at gages, topographic maps, cross sections, dam information, etc.).
5. Plot profiles of channel invert, minimum and maximum water-surface elevations, and flood stage.
6. Prepare the cross sections in the FLDWAV format.
7. Prepare FLDWAV data set.
8. Calibrate the FLDWAV data set (observed stages at gaging stations) for the minimum flood using the automatic calibration procedure.
9. Manually adjust (fine tune) the n values.
10. Using the best set of n values, use the FLDWAV model to simulate the flows at locations where observed flows are available; and compare the simulated and observed flows.
11. Repeat steps 6-10 for the maximum observed flood.
12. Simulate an intermediate flood and compare stages and flows.
13. Determine the minimum (smallest) flow that the model will allow.
14. Increase the maximum flood hydrograph by 50%-100% and simulate to insure cross sections and n tables are adequately defined beyond the flood of record.
15. Calibration is done! Add as an operation to NWSRFS.

19.3 Operational Forecast Using FLDWAV Operation in NWSRFS

A basin may be divided into several sub-basins. A segment is a group of operations used to describe the process of moving water through a sub-basin to its outlet. A typical segment includes a rainfall/runoff model, a unit graph operation, a routing operation, a rating curve operation to convert

discharge to stage, and an operation to display the results. Since the FLDWAV operation may encompass several sub-basins (and sometimes, an entire basin), no other operations (except an operation to display the results) are usually included in the segment. In most cases, the inflows and local flows entering the FLDWAV segment have been computed external to the FLDWAV segment. A group of segments used to describe a basin is called a forecast group. A group of forecast groups which share common initial conditions (carryover) is a carryover group.

The input to NWSRFS is defined by a segment definition (SEGDEF). The segment definition contains a description of all of the time series and all operations used in the segment along with the carryover for each operation. The FLDWAV model is Operation No. 55 in NWSRFS. A description of the parameters and format of the FLDWAV operation is in Sub-section V.3.3 of the NWSRFS User's Manual. Except for hydrograph (time series) information, the input structure in the operational version of FLDWAV model is the same as the stand-alone version as defined in this FLDWAV document. All of the time series used in the river system (inflows, local flows, observed stages) must be defined in the NWSRFS processed database. If an empirical rating curve is used, it must be defined in the NWSRFS parametric database via the DEF-RC command. After the segment has been successfully defined, the forecast group (FGDEF) and carryover group (CGDEF) must be defined respectively. A detailed description of SEGDEF, DEF-RC, FGDEF, and CGDEF is found in sub-section VI.3.4B of the NWSRFS User's Manual.

The correct initial conditions (carryover) are critical to effective real-time forecasting using FLDWAV. In FLDWAV, the carryover consists of the initial water surface elevations and discharges at each cross section (including interpolated cross sections); initial flow at each lateral flow point; and initial pool elevations and gate control switches at each dam location. When a carryover group is initially defined, the carryover in the segment definition is stored for each date specified in the CGDEF. Carryover for a maximum of ten dates may be stored in the parametric database. Each time FLDWAV is run, carryover data are updated for the specified dates.

Once the carryover group has been defined, a forecast run may be executed. In NWSRFS an input file must be created which contains Hydrologic Command Language (HCL) data. A detailed

description of the HCL is found in sub-section VI.5.2 of the NWSRFS User's Manual. The primary HCL commands needed to run FLDWAV include a beginning run time (STARTRUN), an ending runtime (ENDRUN), and the command to save carryover (SAVETDY(1)). The SAVETDY(1) command indicates that carryover will be updated at each date in the carryover list as well as the current date. When the maximum number of carryover date is being used, the oldest date is dropped so that the current date may be stored.

The results of a successful FLDWAV run include computed water-surface elevations (h), discharges (Q), and velocities (V) at specified locations along the river. Although discharges and water-surface elevations may be displayed internally within the FLDWAV operation, the information (Q, h, V) must be stored in the processed database so that it may be retrieved for future use by other operations. The mechanism to store the information is the output time series. By identifying the time series name, data type, and time step, the output time series will be written to the processed data base.

19.4 Real-Time Forecasting Numerical Difficulties

Model stability may be a problem when running FLDWAV in real-time especially during low flow periods. To prevent the model from terminating abnormally, a minimum-flow filter is specified on each river such that whenever the computed discharge is less than a specified minimum flow, the minimum flow is used. There are times when the model may abnormally terminate due to non-convergence (i.e. an adequate solution to the Saint-Venant Equations was not found within the user-specified number of iterations, automatic fix-ups (Section 13.2) were unsuccessful, and the results were extrapolated based on data at the previous time step more than six times). When this occurs, the FLDWAV simulation will stop computing and fill the rest of the time series with constant values (stages, discharges, velocities) equal to the last computed values. In many cases non-convergence is due to the model not being adequately calibrated or the time step or distance step may not be set properly (Section 11).

20. FLDWAV MODEL INPUT

The FLDWAV model requires an input file created by the user. Documentation of the data input structure for the FLDWAV model is given in this Section 20. The data is free formatted, i.e., numbers are separated by spaces or commas. Unlike the DAMBRK and DWOPER models which have fixed formatted input structures, all parameter values required by FLDWAV must be entered. Parameters that would normally be left blank must be entered as zero values. Decimal points are required only if the value being entered contains a decimal. Although there is no card coding, the user may add comments for each data group prior to entering the data for the group. In lieu of comments, the user may enter a blank line prior to each data group. A blank line or comment line **must** be entered before each data group except data groups 0-1 and 0-2. **Note: Data sets for the Beta version of FLDWAV will not run on this version (November 1998) of FLDWAV without modification because additional parameters have been added.**

20.1 Input Data Structure and Data Variable Definition for FLDWAV Model

<u>Data Group</u>	<u>Variable Name</u>	<u>Contents</u>
0-1*	MSG	Description of the data set. A maximum of 20 lines are allowed, the last line must be EOM. Each line may have a maximum of 80 characters.
0-2*	DESC	Type of output display. For echo print of the input parameters, enter "NODESC" For a description of the model parameters, enter "DESC".
1*	EPSY	Depth tolerance in Newton-Raphson Iteration scheme (0.001-1.0 ft). A good value is 0.01 ft.
	THETA	Acceleration factor in solving tributary junction problem (0.5-1.0). Varies with each problem. A good first choice is 0.8.

* Input data group required for any simulation.

** Input data group required for any dambreak simulation

DG Abbreviation for Data Group

<u>Data Group</u>	<u>Variable Name</u>	<u>Contents</u>
	F1	θ weighting factor (0.5-1.0) in finite difference technique. A good value is 0.6.
	XFACT	Factor to convert units describing the location of the computation points along the routing reach to feet; e.g., if units are in miles, XFACT=5280. When using metric units, this factor converts the units to meters: e.g., if units are in km, XFACT=1000.
	DTHYD	Time interval (hrs) of all input hydrographs. If time interval is not constant, set DTHYD=0.
	DTOUT	Time interval (hrs) of all output hydrographs. If running in stand-alone mode (not a part of NWSRFS), set DTHYD=0.
	METRIC	Parameter indicating if input/output is in English (METRIC=0) or Metric (METRIC=1) units. All computations within FLDWAV are done in English units; only the input/output may be displayed in metric units. See Table 20.1 for units conversion information.
2*	JN	Total number of rivers in the system being routed simultaneously.
	NU	Number of values associated with observed hydrographs.
	ITMAX	Maximum number of iterations allowed in the Newton-Raphson Iteration scheme for solving the system of nonlinear equations. If ITMAX=1, the nonlinear formulation degenerates into a linear formulation, and no iterations are required in the Newton-Raphson iteration procedure. A good value is 10.
	KWARM	Number of time steps used for warm-up procedure. If KWARM=0, no warm-up is done. If KWARM>0, the model assumes steady-state initial conditions and will solve the routing equations KWARM times without incrementing the time. A good value is 2.

TABLE 20.1. English/Metric Equivalents

<u>Property</u>	<u>English Unit</u>	<u>Metric Unit</u>	<u>Conversion Factor (English to Metric)</u>
Time	hr	hr	
Length	ft	m	1/3.281
Length	mile	km	1.6093
Flow	ft ³ /sec	m ³ /sec	1/35.32
Area	ft ²	m ²	1/10.765
Surface Area	acres	km ²	1/247.1
Volume	acre-ft	10 ⁶ m ³	1/810.833
Weir Coef.	ft ^{1/2} /sec	m ^{1/2} /sec	1/1.811
Unit Weight	lb/ft ³	N/m ³	157.1
Shear Strength	lb/ft ²	N/m ²	47.88
Viscosity (Dynamic)	lb sec/ft ²	N sec/m ²	47.88
Manning n	English and Metric are same		
<u>Note:</u>	Although the documentation refers to English units only, the metric option is fully functional. This table should be used to determine comparable units and to convert the recommended values to metric units.		

<u>Data Group</u>	<u>Variable Name</u>	<u>Contents</u>
	KFLP	Parameter indicating the use of the floodplain (conveyance) option. If KFLP=0, no floodplain (composite channel used); if KFLP=1, floodplain used with conveyance (K) generated; if KFLP>2, floodplain used with K values read in, and KFLP is the number of points in the conveyance table.
	NET	Parameter indicating the use of the channel network option. If NET=0, the network option is not used and a dendritic tree-type system is modeled using the relaxation algorithm. The network option is currently unavailable; set NET=0.
	ICOND	Parameter indicating the type of initial conditions. If running in stand-alone mode (not a part of NWSRFS), set ICOND=0.

<u>Data Group</u>	<u>Variable Name</u>	<u>Contents</u>
	IFUT(3)	Future parameters; enter four zero values for future enhancements.
3*	NYQD	Number of sets of stage-discharge values in empirical rating curve at downstream boundary.
	KCG	Number of data points in spillway gate control curve of gate opening (GHT) vs. time (TGHT) (DG-38,DG-39). If no movable gates in the system, set KCG = 0.
	NCG	Maximum number of gates on any dam in the system with multiple movable gates (ICG=2, DG-27). If no movable gates in the system, set NCG=0.
	KPRES	Parameter indicating method of computing hydraulic radius (R). If KPRES=0, then $R=A/B$ where A is cross-sectional area and B is channel topwidth; if KPRES=1, then $R=A/P$ where P is wetted perimeter.
4*	NCS	Number of values in table of topwidth (BS) vs. elevation (HS). This value applies to all cross sections in the river system.
	KPL	Parameter indicating what information will be plotted. If KPL=0, nothing is plotted; if KPL=1, stage hydrographs are plotted; if KPL=2, discharge hydrographs are plotted; if KPL=3, both are plotted. This parameter has nothing to do with the FLDGRF utility.
	JNK	Parameter indicating if hydraulic information will be printed. If JNK=0, nothing will be printed; if JNK>0 various hydraulic information will be printed; if JNK<0, various hydraulic information will be printed for specified reaches during automatic calibration (NP<0, DG-5). See Table 2 for description of debug output. A good value is JNK=4 or 5.
	KREVRS	Parameter indicating use of the low flow filter. If KREVRS=0, the low flow filter is activated causing the water surface elevations (WSELs) and discharges not to go below

<u>Data Group</u>	<u>Variable Name</u>	<u>Contents</u>
		the initial condition; if KREVRS=1, the low flow filter is off, and reverse flow is allowed.
	NFGRF	Parameter indicating if FLDGRF data will be generated. If NFGRF=0, the data will be generated; if NFGRF=1, the data will not be generated.
5*	IOBS	Parameter indicating if observed data are available at gaging stations. If IOBS=0, no data available; if IOBS=1, data is available; if IOBS=-1, a mathematical function is used to describe the inflow hydrograph.
	KTERM	Parameter indicating if the terms in equation of motion will be printed as special information. If KTERM=0, they will not be printed; if KTERM=1, they will be printed. Normally use KTERM=0.
	NP	Parameter indicating if Automatic Calibration option is used. If NP=0, calibration is not used; if NP=-1, automatic calibration of the roughness coefficient (n) is done; if NP=-4, automatic calibration of n using average cross sections is done.
	NPST	Parameter indicating the first value in the computed stage hydrograph which will be used in the statistics needed in the automatic calibration option to determine the Manning n. If NPST=0, the first value of observed stage hydrograph will be used. If NP=0, set NPST=0.
	NPEND	Parameter indicating the last value in the computed stage hydrograph which will be used in the statistics needed in the automatic calibration option to determine the Manning n. If NPEND=0, the last value of observed stage hydrograph will be used. If NP=0, set NPEND=0.
	SKIP DG-6 IF JNK \geq 0	
6	TDBG1	Time at which additional debug information begins.
	TDBG2	Time at which additional debug information ends.

<u>Data Group</u>	<u>Variable Name</u>	<u>Contents</u>
	JNKDBG	Debug switch (JNK, DG-4) for additional information. Refer to Table 2 for available debug.
	JDBG1	First river at which additional debug information will be applied.
	JDBG2	Last river at which additional debug information will be applied.
	LDBG1	First reach at which debug information will be applied during calibration. If NP=0 (DG-5), set LDBG1=0.
	LDBG2	Last reach at which debug information will be applied during calibration. After this reach has been calibrated, the model will stop. If NP=0 (DG-5), set LDBGZ=0.
	MCMDDBG	First iteration during calibration at which debug information will be printed. If NP=0 (DG-5), set MCMDDBG=0.
7*	TEH	Time (hours) at which routing computations will terminate.
	DTHII	Initial computational time step. If DTHII>0, a constant time step is used; if DTHII=0, a variable time step is used based on the inflow hydrographs and dam failure times. If DTHII<0, an array of time steps (NDT values) will be read in where $NDT= DTHII $.
	DTHPLT	Time step (hours) at which computed/observed hydrograph data are stored for plotting or printing. If DTHPLT=0, then DTHPLT is set equal to DTHII.
	FRDFR	Window for critical Froude number in mixed-flow algorithm. The default value is 0.05.
	DTEXP	Computational time step (hr) for explicit routing. If DTEXP>0, then a constant time step is used. If DTEXP<0, then a variable time step is used based on the Courant number (C_n) where $ DTEXP =C_n$. If explicit routing is not used, set DTEXP=0.

<u>Data Group</u>	<u>Variable Name</u>	<u>Contents</u>
	MDT	Divisor for determining the time step ($\Delta t = t_p / \text{MDT}$). A good value is 20 for subcritical flow or 40 for supercritical flow. If a constant time step is read-in ($\text{DTHII} \neq 0$), set $\text{MDT} = 0$.
	SKIP DG-8 & DG-9 IF TIME STEP ARRAY IS NOT USED ($\text{DTHII} \geq 0$)	
8	DTHIN(K)	Computational time step to be used until time TDTIN(K). K index goes from 1 to NDT (DG-7).
9	TDTIN(K)	Time at which DTHIN(K) is no longer used. K index goes from 1 to NDT (DG-7).
10*	NLEV	Total number of cross-section reaches in the system that have levees.
	DHLV	The difference in the maximum and minimum crest elevations along the reach (this is sometimes useful to prevent numerical problems with sudden large outflows when the levee is first overtopped. If $\text{NLEV} = 0$, set equal to zero.
	DTHLV	Computational time step to be used during levee overtopping/failure. If $\text{NLEV} = 0$, set equal to zero.
	SKIP DG-11 IF NO LEVEES IN THE SYSTEM ($\text{NLEV} = 0$).	
11	NJFM(K)	Sequence number of river from which levee overtopping/failure flow is passed from reach K.
	NIFM(K)	Sequence number of reach along the river with levee flow passing into reach NITO(K).
	NJTO(K)	Sequence number of river or pond receiving flow from levee overtopping/failure in reach K.
	NITO(K)	Sequence number of the reach along the river receiving flow from reach NIFM(J). If the receiving channel is a pond (i.e., level pool routing done), set $\text{NITO}(K) = 0$. The number of

<u>Data Group</u>	<u>Variable Name</u>	<u>Contents</u>
		ponds (NPOND) is generated by summing all NITO(K)=0 values.
		REPEAT DG-11 FOR EACH LEVEE REACH, K=1,NLEV
12*	NBT(J)	Total number of actual cross sections on river J.
	NPT(1,J)	Beginning cross-section number (after interpolation) on river J for which debug information will be printed.
	NPT(2,J)	Final cross-section number (after interpolation) on river J for which debug information will be printed.
	MRV(J)	Number of river into which river J flows. Omit this field for main river (J=1). Note that tributary (J-1) is river J.
	NJUN(J)	Sequence number of cross section immediately upstream of tributary (J-1) confluence (this section coincides with the upstream extremity of the small subreach which is equivalent in length to the tributary width). Omit this field for main river (J=1).
	ATF(J)	Acute angle (degrees) that tributary J makes with the main river at the confluence. Omit this field for main river (J=1).
	EPQJ(J)	Discharge tolerance in Newton-Raphson Iteration scheme in main river (J=1) or in Tributary Iteration Scheme (J>1).
	COFW(J)	Coefficient of wind stress (1.1E-06 to 3.0E-06) on river J.
	VWIND(J)	Wind velocity (ft/sec) on river J; (+) if directed upstream; (-) if directed downstream.
	WINAGL(J)	Acute angle (degrees) that wind makes with the channel axis of river J.
		REPEAT DG-12 FOR EACH RIVER, J=1,JN

<u>Data Group</u>	<u>Variable Name</u>	<u>Contents</u>
13*	KU(J)	Parameter indicating the type of upstream boundary condition being specified for the main river and tributaries; if KU(J)=1, a stage hydrograph or if KU(J)=2, a discharge hydrograph is the upstream boundary condition.
	KD(J)	Parameter indicating the type of downstream boundary condition being specified for the main river; if KD(J)=1, a stage hydrograph is the downstream boundary condition (in the case of tributaries, KD(J) where J goes from 2 to JN is always equal to zero); if KD(1)=2, a discharge hydrograph is the downstream boundary condition; if KD(1)=3, a single-valued rating curve of discharge as a function of stage is the boundary condition; if KD(1)=4, a looped rating curve is generated based on Manning's equation where the friction slope is computed based on the momentum equation; if KD(1)=5, normal flow computed from Manning's equation is the downstream boundary condition; if KD(1)=7, a looped rating curve is generated where the friction slope is computed based on conveyance; if KD(1)=1 and NYQD>0, a single-valued rating curve in which Q is a function of the computed water surface minus the read-in value of STN.
	NQL(J)	Total number of lateral flows on river J.
	NGAGE(J)	Total number of observed hydrographs along river J (routing reach) which will be compared with computed hydrograph; also, denotes total number of stations for which computed values will be plotted.
	NRCM1(J)	Total number of Manning n reaches on each river.
	NQCM(J)	Total number of values in the Manning n table. Also, denotes whether Manning n is a function of WSEL (NQCM(J)>0) or discharge (NQCM(J)<0). If NQCM(J)=0, Manning n is a function of WSEL and the number of table values is equal to NCS.
	IFUT(4)	Future parameters; enter four zero values for future enhancements.
REPEAT DG-13 FOR EACH RIVER, J=1,JN		

<u>Data Group</u>	<u>Variable Name</u>	<u>Contents</u>
14*	MIXF(J)	Parameter indicating the flow regime in river J. If MIXF(J)=0, river J has subcritical flow; if MIXF(J)=1, river J has supercritical flow; if MIXF(J)>1, there is a mixture of subcritical and supercritical flow throughout river J at varying times; if MIXF(J)=2, the hydraulic jump can move upstream or downstream; if MIXF(J)=3, the hydraulic jump moves only if the Froude number exceeds 2; if MIXF(J)=4, the hydraulic jump is stationary; if MIXF(J)=5, a modified implicit technique (LPI) is used to solve mixed flows.
	MUD(J)	Parameter indicating the use of the mud/debris flow option on river J. If MUD(J)=0, dynamic routing of non-mudflow (water) will be done; if MUD(J)=1, dynamic routing of mudflow will be done.
	KFTR(J)	Parameter indicating the use of Kalman Filter option on river J. If KFTR(J)=0, switch is off; if KFTR(J)=1, switch is on. Kalman filter can be turned on to update the forecast if river J has stage observations for more than 2 gaging stations.
	KLOS(J)	Parameter indicating the computation of volume losses in river J. If KLOS(J)=0, the losses will not be computed; if KLOSS(J)=1, the losses will be computed.
	IFUT(6)	Future parameters; enter six zero values for future enhancements.
	REPEAT DG-14 FOR EACH RIVER, J=1,JN	
	SKIP DG-15 IF LPI TECHNIQUE IS NOT USED IN SYSTEM (ALL MIXF(J) \neq 5)	
15	KLPI(K)	Power (m) used in the LPI technique. Values range from 1 to 10 where m=10 approaches the fully dynamic technique and m=1 approaches the diffusion technique. K index goes from 1 to the number of rivers using the LPI technique. A good value is 5.
	SKIP DG-16 IF MUDFLOW OPTION IS NOT USED IN SYSTEM (ALL MUD(J) = 0)	

<u>Data Group</u>	<u>Variable Name</u>	<u>Contents</u>
16	UW1(J)	Unit weight (lb/ft ³) of mud/debris fluid on river J.
	VIS1(J)	Dynamic viscosity (lb-sec/ft ²) of mud/debris fluid on river J.
	SHR1(J)	Initial yield stress of shear strength (lb/ft ²) of mud/debris fluid on river J.
	POWR1(J)	Exponent in power function representing the stress-rate of strain relation on river J; if Bingham plastic is assumed for fluid, set POWR1(J)=1.0.
	IWF1(J)	Parameter indicating dry bed routing on river J. If IWF1(J)=0, the base flow at t=0 will be used all along the routing reach; if IWF1(J)>0, wave front tracking will be used where the wave front velocity (V_w) is a function of the channel velocity (V); if IWF1(J)=1, $V_w = V_{N-4}$; if IWF1(J)=2, $V_w = K_w V_{N-4}$; if IWF1(J)=3, $V_w = V_{max}$, where V_{max} is the maximum velocity in the channel reach, N is the current location of the wave front, and K_w is the kinematic wave factor.

REPEAT DG-16 FOR EACH RIVER WITH MUDFLOW (MUD(J)>0, J=1,JN)

SKIP DG-17 IF VOLUME FLOW LOSSES ARE NOT COMPUTED IN SYSTEM (ALL KLOS(J) = 0)

17	XLOS(1,J)	Beginning location of the reach(s) where flow loss will occur on river J.
	XLOS(2,J)	Ending location of the reach(s) where flow loss will occur on river J.
	QLOS(J)	Percentage of the loss in terms of total active flow amount; (-) for loss and (+) for gain.
	ALOS(J)	Loss distribution coefficient for river J (0.3-3.0). For a linear loss distribution, set ALOS(J)=1.

REPEAT DG-17 FOR EACH RIVER WITH VOLUME FLOW LOSSES (KLOS(J)>0, J=1,JN)

<u>Data Group</u>	<u>Variable Name</u>	<u>Contents</u>
18*	XT(I,J)	Location of station or cross section where computations are made (units can be anything since XFACT converts these units to ft); I index goes from 1 to NBT(J).
19*	DXM(I,J)	Minimum computational distance step between cross sections. If DXM(I,J) is less than the distance between two adjacent cross sections read in, then intermediate cross sections are created within the program via a linear interpolation procedure. I index goes from 1 to NBT(J)-1.
20*	KRCHT(I,J)	Parameter indicating routing method or internal boundary condition in each reach. See Table 20.2 for a description of each type. I index goes from 1 to (NBT(J)-1).
REPEAT DG-18 - DG-20 FOR EACH RIVER, J=1,JN		
SKIP DG-21 - DG-25 IF NLEV = 0		
21	HWLV(L)	Elevation (ft msl) of top of levee, ridge line, etc. where weir-flow occurs. Elevation is average throughout Δx reach where weir flow occurs; also if flow through a pipe, -HWLV(L) is the invert elevation of pipe.
	WCLV(L)	Weir-flow discharge coefficient for Δx reach where weir-flow (inflow or outflow) may occur. Coefficient ranges from 2.6 to 3.2; if there is a pipe connection (WCLV(L)<0), the weir coefficient is equal to $ C_{d1} * \text{discharge loss coefficient} * \text{max area of pipe}$.
	TFLV(L)	Time (hr) from start of levee failure (crevasse) until the opening or breach is its maximum size. Set TFLV(L)=0 if the levee does not fail.
	BLVMX(L)	Final width (ft) of levee crevasse which is assumed to have a rectangular shape (200-1000 ft). Set BLVMX(L)=0 if the levee does not fail.

TABLE 20.2. Routing Methods and Internal Boundaries

<u>KRCHT(I,J)</u>	<u>Definitions</u>
0	Implicit Dynamic Routing
1	Implicit (Diffusion) Routing
4	Level Pool Routing
5	Explicit Dynamic Routing (Upwind)
6	Implicit (Local Partial Inertial) Routing
10	Dam
11	Dam + $Q=f(Y)$
21	Dam + $Y=f(Q)$
12	Dam + $Q=f(YY)$
14	Dam + Multiple Movable Gates $C=f(Y,HG,FR)$
15	Dam + Average Movable Gates (Corps of Engineers Type)
28	Lock and Dam
35	Bridge
<u>Variable Definitions</u>	
	Q=flow
	Y=pool elevation
	YY=tailwater elevation
	HG=centerline of gate
	C=gate coefficient
	FR=Froude number

<u>Data Group</u>	<u>Variable Name</u>	<u>Contents</u>
	HFLV(L)	Elevation (ft msl) of water surface when levee starts to fail. Set HFLV(L)=0 if the levee does not fail.
	HLVMN(L)	Final elevation (ft msl) of bottom of levee crevasse. Set HLVMN(L)=0 if the levee does not fail.
	SLV(L)	Slope of levee L. This parameter is used to interpolate levee reaches.
	SKIP DG-22 IF LEVEE HAS NO DRAINAGE PIPE ($WCLV(L) \geq 0$)	
22	HPLV(L)	Centerline elevation (ft msl) of flood drainage pipe (with flood gate).

<u>Data Group</u>	<u>Variable Name</u>	<u>Contents</u>
	DPLV(L)	Diameter (ft) of flood drainage pipe.
	REPEAT DG-21 & DG-22 FOR EACH LEVEE REACH, L=1,NLEV	
	SKIP DG-23 - DG-25 IF NO PONDS EXIST (NITO(L)>0, L=1,NLEV)	
23	HPOND(L)	Initial water surface elevation (ft) of storage pond L in levee option.
24	SAPOND(K,L)	Surface area (acres) of storage pond L corresponding to elevation HSAP in the area-elevation curve. These values should be entered from the top of the pond (maximum elevation) to the bottom. K index goes from 1 to 8. If less than 8 values are needed to describe the pond, set the remaining values to zero.
25	HSAP(K,L)	Elevation (ft msl) corresponding to SAPOND in the area elevation curve. These values should be entered from the top of the pond (maximum elevation) to the bottom. K index goes from 1 to 8. If less than 8 values are needed to describe the pond, set the remaining values to zero.
	REPEAT DG-23 - DG-25 FOR EACH POND, L=1,NPOND	
	SKIP DG-26 - DG-49 IF NO INTERNAL BOUNDARIES IN THE SYSTEM (ALL KRCHT VALUES < 10)	
	SKIP DG-26 - DG-43 IF INTERNAL BOUNDARY K IS NOT A DAM (KRCHT(K,J) <10 or KRCHT(K,J) > 30)	
	**SKIP DG-26 & DG-27 IF INTERNAL BOUNDARY K IS NOT A RESERVOIR (KRCHT(K,J)≠4 OR [KRCHT(1,J) <10 or KRCHT(1,J) > 30])	
26	SAR(L,K,J)	Surface area (acres) of reservoir behind dam at elevation HSAR(L,K,J). Values should be read in starting at the top of the reservoir to the bottom of the reservoir. L index goes from 1 to 8; if less than 8 values are needed to describe the reservoir, set the remaining values to zero.

<u>Data Group</u>	<u>Variable Name</u>	<u>Contents</u>
27	HSAR(L,K,J)	Elevation (ft msl) at which reservoir surface area SAR(L,K,J) is defined. Values should be read in starting at the top of the reservoir to the bottom of the reservoir. L index goes from 1 to 8; if less than 8 values are needed to describe the reservoir, set the remaining values to zero.
28**	LAD(K,J)	Reach number corresponding to location of dam K.
	HDD(K,J)	Elevation (ft msl) of top of dam.
	CLL(K,J)	Length (ft) of the dam crest less the length of the uncontrolled spillway and gates. If CLL(K,J) is entered as a negative value, the length of the dam crest is variable with elevation.
	CDOD(K,J)	Discharge coefficient for uncontrolled weir flow over the top of the dam (2.6-3.1).
	QTD(K,J)	Discharge (cfs) through turbines. This flow is assumed constant from start of computations until the dam is 1/4 breached; thereafter, QTD(K,J) is assumed to linearly decrease to zero when 1/2 breached; QTD(K,J) may also be considered leaking or constant spillway flow. If this flow is time-dependent, QTD(K,J) is entered with any negative value and the time series for QTD(K,J) is specified.
	ICHAN(K,J)	Parameter indicating if channel conditions at dam K will switch from manual control (e.g., lock and dam controlled by the lockmaster) to channel control (i.e., unsteady flow equations). If no channel control, set ICHAN(K,J)=0; if channel control switch is allowed, set ICHAN(K,J)=1.
IF DAM IS REPRESENTED BY A RATING CURVE ONLY, SET ALL VALUES IN DG-28 TO ZERO EXCEPT LAD(K,J)		
29**	ICG(K,J)	Parameter indicating type of movable gate structure. If ICG(K,J)=0, no movable gates exist; if ICG(K,J)=1, movable gates exist using an average gate opening; if ICG(K,J)=2, multiple movable gates exist with independent gate openings.

<u>Data Group</u>	<u>Variable Name</u>	<u>Contents</u>
	HSPD(K,J)	Elevation (ft msl) of uncontrolled spillway crest. If no spillway exists, let HSPD(K,J)=0.
	SPL(K,J)	Crest length (ft) of uncontrolled spillway. If no spillway exists, let SPL(K,J)=0.
	CSD(K,J)	Discharge coefficient of uncontrolled spillway. If CSD(K,J)<0, the failure starts in the spillway at its crest and failure is confined to a length of the spillway. If no spillway exists, let CSD(K,J)=0. If spillway is represented by an empirical rating curve, let CSD(K,J)=0. Note that only one empirical rating is allowed at the dam. If several rating curves exist at the dam, they should be combined and entered as one rating curve.
	HGTD(K,J)	Elevation (ft msl) of center of gate openings for average moveable gates.
	CGD(K,J)	Discharge coefficient for gate flow (0.60-0.80) times the area of the gates (sq-ft). If no gate exists, let CGD(K,J)=0. If gates are represented by an empirical rating curve, let CGD(K,J)=0. Note that only one empirical rating is allowed at the dam. If several rating curves exist at the dam, they should be combined and entered as one rating curve. If average moveable gate option is used and submergence effects are expected, an empirical rating curve with built in submergence should be used.
IF DAM IS REPRESENTED BY A RATING CURVE ONLY, SET ALL VALUES IN DG-29 TO ZERO EXCEPT HSPD(K,J)		

SKIP DG-30 & DG-31 IF THE DAM CREST LENGTH IS CONSTANT
(CLL(K,J) > 0.1)

30	HCRESL(L,K,J)	Elevation (ft msl) associated with variable length of dam crest, CRESL(L,K,J), for dam. Values should be read in starting at the minimal crest elevation to the maximum elevation. L index goes from 1 to 8; if less than 8 values are needed to describe the dam crest, set the remaining values to zero.
----	---------------	--

<u>Data Group</u>	<u>Variable Name</u>	<u>Contents</u>
31	CRESL(L,K,J)	Variable length (ft) of dam crest for a given elevation, HCRESL(L,K,J). L index goes from 1 to 8; if less than 8 values are needed to describe the dam crest, set the remaining values to zero.
SKIP DG-32 & DG-33 IF THE TURBINE FLOW IS CONSTANT ($QTD(K,J) \geq 0$.)		
32	QTT(L,K,J)	Variable discharge (cfs) through the turbines; this flow is time dependent. L index goes from 1 to NU (DG-2).
33	TQT(L,K,J)	Time (hrs) associated with discharge through turbines , QTT(L,K,J). L index goes from 1 to NU (DG-2_
SKIP DG-34 & DG-35 IF NO RATING CURVE IS GENERATED FOR THE SPILLWAY OR GATE STRUCTURE ($KR \neq 11,21,12,22,13,23,14,16,17$)		
34	RHI(L,K,J)	Head (ft) above spillway crest or gate center. Head is associated with spillway or gate flow (RQI(L,K,J) in rating curve. L index goes from 1 to 8; if less than 8 values are needed to describe the rating curve, set the remaining values to zero.
35	RQI(L,K,J)	Discharge (cfs) of spillway or gate rating curve corresponding to RHI(L,K,J). L index goes from 1 to 8; if less than 8 values are needed to describe the rating curve, set the remaining values to zero.
SKIP DG-36 - DG-39 IF NO MULTIPLE MOVABLE GATES ($KR \neq 14$)		
36	NG(K,J)	Number of movable gates in dam K.
37	GSIL(L,K,J)	Elevation (ft-msl) of the bottom of gate L.
	GWID(L,K,J)	Width of gate opening on gate L.

<u>Data Group</u>	<u>Variable Name</u>	<u>Contents</u>
38	TGHT(I,L,M,J)	Time (hrs) associated with gate opening GHT(L,K,J). I index goes from 1 to KCG.
39	GHT(I,L,M,J)	Distance (ft) from bottom of gate to gate sill, GSIL(L,K,J). This distance is time dependent and is associated with the time array TGHT(I,L,K,J); I index goes from 1 to KCG.
REPEAT DG-37 - DG-39 FOR EACH MOVABLE GATE, L=1,NG(K,J)		
SKIP DG-40 - DG-43 IF INTERNAL BOUNDARY IS NOT A LOCK AND DAM (KR \neq 28)		
40	PTAR(K,J)	Elevation (ft-msl) of water surface in headwater pool at upstream face of lock and dam; this elevation is considered the target pool elevation; the lock-master controls the flow through the dam via gates to maintain the pool elevation at this target elevation.
41	CHTW(K,J)	Elevation (ft-msl) of water surface in tailwater pool at downstream face of lock and dam; this elevation is considered the elevation at which the lock-master can no longer control the flow through the dam, and the flow becomes channel control; usually this elevation will be equal to or slightly less than the target pool elevation.
42	POLH(L,K,J)	Target pool elevation (same as PTAR(K,J)) for each time step; if 0.0 is read in, then PTAR(K,J) is used for POLH(L,K,J). L index goes from 1 to NU. These elevations are associated with the inflow hydrograph time array, T1(L,J).
SKIP DG-43 IF LOCK AND DAM WILL NEVER SWITCH TO CHANNEL CONTROL (ICHAN(K,J)=0)		
43	ITWT(L,K,J)	Parameter indicating if gates control the flow; if ITWT(L,K,J)=0, flow is controlled by the gates; if ITWT(L,K,J)=1, flow is not controlled by the gates, e.g., the entire dam is removed as in the case of the low lift dams on

<u>Data Group</u>	<u>Variable Name</u>	<u>Contents</u>
		the Lower Ohio River and the flow becomes channel controlled. L index goes from 1 to NU. These gate control switches are associated with the inflow hydrograph time array, T1(L,J).
	SKIP DG-44 - DG-46 IF INTERNAL BOUNDARY IS NOT A BRIDGE (KR \neq 35)	
44	LAD(K,J)	Reach number corresponding to location of bridge K.
	EMBEL2(K,J)	Crest elevation (ft msl) of uppermost portion of road embankment.
	EMBW2(K,J)	Crest length (ft) of uppermost portion of road embankment (including bridge opening) measured across valley and perpendicular to flow.
	EMBEL1(K,J)	Crest elevation (ft msl) of lower portion (emergency overflow) road embankment. If nonexistent, set EMBEL1(K,J)=0.
	EMBW1(K,J)	Crest length (ft) of lower portion of road embankment measured across valley and perpendicular to flow. If nonexistent, set EMBW1(K,J)=0.
	BRGW(K,J)	Width of top of road embankment as measured parallel to flow.
	CDBRG(K,J)	Coefficient of discharge of flow through bridge opening (see: Chow, <u>Open Channel Hydraulics</u> , pp. 476-490).
45	BRGHS(L,K,J)	Elevations (ft msl) associated with widths of bridge opening; the brige opening should be closed by setting the last BRGHS(L,K,J) slightly higher than the previous value; start at invert and proceed upwards. L index goes from 1 to 8; if less than 8 values are needed to describe the bridge opening, set the remaining values to zero.

<u>Data Group</u>	<u>Variable Name</u>	<u>Contents</u>
46	BRGBS(L,K,J)	Width (ft) associated with BRGHS(L,K,J) elevation of bridge opening; the brige opening should be closed by setting the last BRGBS(L,K,J)=0; start at invert and proceed upwards. L index goes from 1 to 8; if less than 8 values are needed to describe the bridge opening, set the remaining values to zero.

SKIP DG-47 IF INTERNAL BOUNDARY IS NOT A DAM OR A BRIDGE

47**	TFH(K,J)	Time (hr) from beginning of breach formation until it reaches its maximum size on dam/bridge K.
	DTHDB(K,J)	Computational time step (hr) to be used after failure of dam/bridge K. If DTHDB(K,J)=0, the time step size will be computed as TFH(K,J)/MDT; if multiple dams/bridges have failed, the smallest time step will be used during computations.
	HFDD(K,J)	Elevation (ft) of water when failure of dam/embankment K commences. If HFDD(K,J)<0, failure commences at time - HFDD(K,J) (hr).
	BBD(K,J)	Final (maximum) width (ft) of bottom of breach.
	ZBCH(K,J)	Side slope (1:vertical to ZBCH(K,J):horizontal) of breach.
	YBMIN(K,J)	Lowest elevation (ft msl) that bottom breach reaches.
	BREXP(K,J)	Exponent used in development of breach. Varies from 1 to 4; a good value is 1.
	CPIP(K,J)	Centerline elevation (ft msl) of piping breach. If breach is overtopping, set CPIP(K,J)=0.

REPEAT DG-26 - DG-47 FOR EACH DAM/BRIDGE ON RIVER J, K=1, NO. DAM/BRIDGE; THEN REPEAT AGAIN FOR EACH RIVER, J=1,JN

SKIP DG-48 & DG-49 IF NQL(J) \leq 0

48	LQ1(K,J)	Sequence number of upstream cross section with lateral inflow.
----	----------	--

<u>Data Group</u>	<u>Variable Name</u>	<u>Contents</u>
49	QL(L,K,J)	Lateral inflow at cross section LQ1(K,J). L index goes from 1 to NU. The time array associated with this hydrograph is the same as for the inflow hydrograph.
		REPEAT DG-48 & DG-49 FOR EACH LATERAL FLOW, K=1,NQL(J); THEN REPEAT AGAIN FOR EACH RIVER, J=1,JN
		SKIP DG-50 & DG-51 IF NGAGE(J)=0
50	NGS(K,J)	Sequence number of each observed/plotting station on river J. K index goes from 1 to NGAGE(J).
		SKIP DG-51 IF KPL = 2 OR IOBS \leq 0
51	GZ(K,J)	Gage correction to convert observed stages to mean sea level datum. K index goes from 1 to NGAGE(J).
		REPEAT DG-50 & DG-51 FOR EACH RIVER, J=1,JN.
		SKIP DG-52 IF KPL = 0 AND IOBS \leq 0
52	STNAME(K,J)	20-character name associated with gaging stations or plotting station, K.
		SKIP DG-53 & DG-54 IF IOBS \leq 0
53	STT(L,K,J)	Observed stage or discharge hydrograph at gaging station K. L index goes from 1 to NU.
		SKIP DG-54 IF NP < 0 AND KPL < 3
54	STQ(L,K,J)	Observed discharge hydrograph at gaging station K. L index goes from 1 to NU.
		REPEAT DG-52 - DG-54 FOR EACH GAGING STATION, K=1,NGAGE(J); THEN REPEAT THE GROUP FOR EACH RIVER, J=1,JN

<u>Data Group</u>	<u>Variable Name</u>	<u>Contents</u>
	SKIP DG-55 IF IOBS ≥ 0	
55	TPG(J)	Time (hr) from initial steady flow to peak of specified upstream boundary hydrograph (used in mathematical function describing the hydrograph).
	RHO(J)	Ratio of peak value of specified hydrograph to initial value of the hydrograph.
	GAMA(J)	Ratio of time TG to TPG(J), where TG is time from initial steady flow to center of gravity of the specified hydrograph. GAMA(J) must be greater than 1.
	YQI(J)	Initial steady discharge or water surface elevation at upstream boundary.
	REPEAT DG-55 FOR EACH RIVER, J=1,JN	
	SKIP DG-56 - DG-58 IF IOBS < 0	
56*	ST1(L,J)	Observed stages (ft) or discharges (cfs) at upstream boundary of river J. L index goes from 1 to NU.
	SKIP DG-57 IF DTHYD > 0	
57*	T1(L,J)	Time array associated with upstream hydrograph ST1(L,J). L index goes from 1 to NU.
	SKIP DG-58 IF KU(J) $\neq 1$	
58	GZ1(J)	Gage correction to convert observed stages at upstream boundary of river J to mean sea level datum (msl).
	REPEAT DG-56 - DG-58 FOR EACH RIVER, J=1,JN	
	SKIP DG-59 IF KD(1) > 2	

<u>Data Group</u>	<u>Variable Name</u>	<u>Contents</u>
59	STN(1)	Observed stages (KD(1)=1) or discharges (KD(1)=2) at downstream boundary of main river. K index goes from 1 to NU.
	SKIP DG-60 IF KD(1) \neq 1 and KD(1) \neq 3	
60	GZN(1)	Gage correction to convert stages at downstream boundary of main river to mean sea level datum.
	SKIP DG-61 & DG-62 IF NYQD = 0 OR KD(1) \neq 3	
61	YQD(K)	Stages used to define empirical rating curve at downstream boundary of main river. K index goes from 1 to NYQD.
62	QYQD(K)	Discharge used to define empirical rating curve at downstream boundary of main river. K index goes from 1 to NYQD.
	SKIP DG-63 IF KD(1) \neq 5	
63	SLFI(1)	Bed/initial water surface slope of the main river. This slope is used to generate the single-valued rating curve at the downstream boundary.
	SKIP DG-64 - DG-69 IF NP \neq -4	
64	IFXC(I,J)	Parameter indicating if cross section has special properties when CALXS option is used (see calibration note). If no special properties, IFXC(I,J)=0; if actual section is to be read in, IFXC(I,J)=1; I index goes from 1 to NBT(J).
65	HSC	Invert elevation (ft) at the most upstream cross section on river J.

<u>Data Group</u>	<u>Variable Name</u>	<u>Contents</u>
66	KAM	Parameter indicating the method for reading in cross sections in the calibration reach. If KAM=0, cross sections are described as topwidth vs. depth (B vs. Y) at key points in the cross section (see figure 1); if KAM=1, cross sections are described as the power function $B=kY^m$ where m is a shape factor and k is a scaling factor (see figure 2).
	CHNMN	The minimum acceptable Manning n value computed during Automatic Calibration for calibration reach I. The default value is 0.013.
	CHNMX	The maximum acceptable value of Manning n value computed during Automatic Calibration for calibration reach I. The default value is 0.25.
	SXS	Average channel bottom slope (ft/mi) along calibration reach I.
	SKIP DG-66 IF KAM = 0	
67	FKC(I,J)	Scaling parameter of in-bank channel portion of cross section in calibration reach I described in power function.
	FMC(I,J)	Shape factor for in-bank channel described in power function.
	FKF(I,J)	Scaling parameter of floodplain portion of cross section in calibration reach I described in power function.
	FMF(I,J)	Shape factor for floodplain portion of cross section described in power function.
	FKO(I,J)	Scaling parameter of dead storage (inactive) portion of cross section in calibration reach I described in power function.
	FMO(I,J)	Shape factor for dead storage (inactive) portion of cross section described in power function.
	HB	Elevation (ft msl) of cross section at top of bank.
	HF	Elevation (ft msl) of cross section at top of floodplain.

<u>Data Group</u>	<u>Variable Name</u>	<u>Contents</u>
	SKIP DG-67 & DG-68 IF KAM = 1	
68	B1	Active topwidth (ft) of typical cross section of calibration reach I at depth Y1 (half of channel depth).
	B2	Active topwidth (ft) of typical cross section of calibration reach I at depth Y2 (top of bank).
	B3	Active topwidth (ft) of typical cross section of calibration reach I at depth Y3 (midpoint of floodplain).
	B4	Active topwidth (ft) of typical cross section of calibration reach I at depth Y4 (maximum flood depth). Enter zero if no floodplain.
	B5	Dead storage (inactive) topwidth (ft) of typical cross section of calibration reach I at depth Y3. Enter zero if no inactive storage.
	B6	Dead storage (inactive) topwidth (ft) of typical cross section of calibration reach I at depth Y4. Enter zero if no inactive storage.
69	Y1	Depth (ft) of typical cross section of calibration reach I at mid-point between the invert and top of bank.
	Y2	Depth (ft) of typical cross section of calibration reach I at top of bank.
	Y3	Depth (ft) measured from invert of typical cross section of calibration reach I to midpoint between the top of bank and estimated maximum flood elevation.
	Y4	Depth (ft) of typical cross section of calibration reach I at a maximum flood elevation.
	REPEAT DG-66 - DG-69 FOR EACH CALIBRATION REACH, I=1,NGAGE(J)-1	
70*	FLST(I,J)	Elevation (ft msl) at which flooding commences. If no floodstage, enter zero.

<u>Data Group</u>	<u>Variable Name</u>	<u>Contents</u>
	YDI(I,J)	Initial water surface elevation (ft msl) at cross section I. If steady state conditions exist, the YDI value at the downstream location of the main river and pool levels behind dams must be read in (all other values are entered as zero) and the model will do backwater computations; otherwise, all values are read in.
	QDI(I,J)	Initial discharge (cfs) at cross section I. If steady state conditions exist, all QDI values are read in as zero and the QDI values are generated by summation of flows from upstream to downstream. If $KD(J) \neq 2$, the upstream discharge (QDI(I,J)) must be read in. If unsteady-state condition exists, all QDI values are read in.
	AS(1,I,J)	Active channel cross-sectional area (sq ft) below the lowest HS elevation at cross section I.
	SKIP DG-71 & DG-72 IF $NP = -4$ AND $IFXC(I,J)=0$	
71*	HS(L,I,J)	Elevation (ft msl) corresponding to each topwidth BS(L,I,J). Elevations are measured from the bottom of the cross section upward; L index goes from 1 to NCS.
72*	BS(L,I,J)	Topwidth (ft) of active flow portion of channel/valley cross section corresponding to each elevation HS(L,I,J). L index goes from 1 to NCS.
	SKIP DG-73 & DG-74 IF $KFLP = 0$	
73	BSL(L,I,J)	Topwidth (ft) of active flow portion of left floodplain corresponding to each elevation HS(L,I,J). L index goes from 1 to NCS.
74	BSR(L,I,J)	Topwidth (ft) of active flow portion of right floodplain corresponding to each elevation HS(L,I,J). L index goes from 1 to NCS.
	SKIP DG-75 & DG-76 IF $KFLP \leq 1$	

<u>Data Group</u>	<u>Variable Name</u>	<u>Contents</u>
75	HKC(L,I,J)	Elevation (ft msl) corresponding to the conveyance QKC(L,I,J). L index goes from 1 to NCS.
76	QKC(L,I,J)	Conveyance corresponding to elevation HKC(L,I,J). I index goes from 1 to NCS.
77*	BSS(L,I,J)	Topwidth (ft) of dead storage (inactive) portion of channel/valley cross section corresponding to each elevation HS(L,I,J). K index goes from 1 to NCS; if no inactive storage exists, enter zero.
REPEAT DG-70 - DG-77 FOR EACH CROSS SECTION, I=1,NBT(J)		
REPEAT DG-64 - DG-77 FOR EACH RIVER, J=1,JN		
SKIP DG-78 IF KFLP \neq 1		
78	SNM(L,I,J)	Sinuosity coefficient (channel flow-path length/floodplain flow-path length corresponding to each elevation HS(L,I,J). L index goes from 1 to NCS.
REPEAT DG-78 FOR ALL REACHES, I=1,NBT(J)-1		
79*	FKEC(I,J)	Expansion or contraction coefficients. Expansion coefficients vary from -.05 to -.75 and contraction coefficients vary from +.10 to +.40, the larger values are associated with very abrupt changes in cross section along the river; if expansion/contraction is negligible, set FKEC(I,J)=0. I index goes from 1 to NBT(J)-1.
80*	NCM(I,J)	Station number of upstream-most station in subreach that has the same Manning n. K index goes from 1 to NRCM1(J).
81*	CM(L,I,J)	Manning n corresponding to each YQCM(L,I,J) value. L index goes from 1 to NQCM(J); if NQCM(J)=0, Manning n values are treated as in the DAMBRK program where Manning n is a function of the average elevation between two cross sections and L index goes from 1 to NCS.

<u>Data Group</u>	<u>Variable Name</u>	<u>Contents</u>
	SKIP DG-82 & DG-83 IF KFLP = 0	
82	CML(L,I,J)	Manning n corresponding to each YQCM(L,I,J) value for left floodplain. L index goes from 1 to NQCM(J); the same rules apply for NQCM(J) as were previously stated in DG-81.
83	CMR(L,I,J)	Manning n corresponding to each YQCM(L,I,J) value for right floodplain. L index goes from 1 to NQCM(J); the same rules apply for NQCM(J) as were previously stated in DG-81.
	SKIP DG-84 IF NQCM(J) = 0	
84	YQCM(L,I,J)	Water surface elevation (ft msl) or discharges (cfs) associated with Manning n. L index goes from 1 to NQCM(J).
	REPEAT DG-81 - DG-84 FOR EACH MANNING REACH, I=1,NRCM1(J)	
	REPEAT DG-78 - DG-84 FOR EACH RIVER J=1,JN	
85*	MESSAGE	80-character message describing the data set for use in FLDGRF.
86*	RIVER(J)	16-character name associated with river J.
	REPEAT DG-86 FOR EACH RIVER, J=1,JN	

20.2 Alphabetical Listing of Data Variables for FLDWAV

<u>VARIABLE</u>	<u>DATA GROUP</u>	<u>DEFINITION OF THE VARIABLE</u>
AS(1,I,J)	69	Active channel area below the lowest HS elevation
ATF(J)	12	Acute angle tributary makes with main river at its confluence
B1	67	Active topwidth at depth Y1 (calibration)
B2	67	Active topwidth at depth Y2 (calibration)
B3	67	Active topwidth at depth Y3 (calibration)
B4	67	Active topwidth at depth Y4 (calibration)
B5	67	Inactive topwidth at depth Y3 (calibration)
B6	67	Inactive topwidth at depth Y4 (calibration)
BBD(K,J)	47	Final width at bottom of breach
BLVMX(L)	18	Final width of levee crevasse
BREXP(K,J)	47	Exponent used in development of breach
BRGBS(L,K,J)	46	Width associated with bridge opening
BRGHS(L,K,J)	45	Elevations associated with widths of bridge opening
BRGW(K,J)	44	Width of top of road embankment
BS(L,I,J)	71	Topwidth of active flow portion of cross section
BSL(L,I,J)	72	Topwidth of active flow portion of left floodplain
BSR(L,I,J)	73	Topwidth of active flow portion of right floodplain
BSS(L,I,J)	76	Topwidth of inactive portion of cross section
CDBRG(K,J)	44	Discharge coefficient of flow through bridge opening
CDOD(K,J)	26	Discharge coefficient for uncontrolled weir flow over the top of the dam
CGCG(L,K,J)	34	Average spillway gate width opened at time TCG(L,K,J)
CGD(K,J)	27	Discharge coefficient for gate flow
CHNMN	65	Minimum acceptable calibrated Manning n value
CHNMX	65	Maximum acceptable calibrated Manning n value
CLL(K,J)	26	Dam crest length less the length of spillway and gates
CM(L,I,J)	80	Manning n for channel
CML(L,I,J)	81	Manning n for left floodplain
CMR(L,I,J)	82	Manning n for right floodplain
COFW(J)	12	Coefficient of wind stress
CPIP(K,J)	47	Centerline elevation of piping breach
CRESL(L,K,J)	29	Variable length of dam crest for a given elevation
CSD(K,J)	27	Discharge coefficient of uncontrolled spillway
DESC	0-2	Type of output display
DHLV	10	Difference between max and min levee crest elevations
DPLV(L)	19	Diameter of flood drainage pipe
DTEXP	7	Computational time step for explicit routing
DTHDB(K,J)	47	Computational time step after dam/bridge failure
DTHII	7	Initial computational time step
DTHIN(K)	8	Variable computational time step

<u>VARIABLE</u>	<u>DATA GROUP</u>	<u>DEFINITION OF THE VARIABLE</u>
DTHLV	10	Computational time step after levee overtopping/failure
DTHPLT	7	Plotting/printing time interval
DTHYD	1	Time interval of all input hydrographs
DXM(I,J)	16	Minimum computational distance interval between sections
EMBEL1(K,J)	44	Crest elevation of lower portion (emergency overflow) road embankment
EMBEL2(K,J)	44	Crest elevation of uppermost portion of road embankment
EMBW1(K,J)	44	Crest length of lower portion of road embankment
EMBW2(K,J)	44	Crest length of uppermost portion of road embankment
EPQJ(J)	12	Discharge tolerance in tributary iteration scheme
EPSY	1	Depth tolerance in Newton-Raphson iteration scheme
F1	1	θ weighting factor in finite difference technique
FKC(I,J)	66	Scaling parameter of channel portion of synthetic section
FKEC(I,J)	78	Expansion or contraction coefficient
FKF(I,J)	66	Scaling parameter of floodplain portion of synthetic section
FKO(I,J)	66	Scaling parameter of inactive portion of synthetic section
FLST(I,J)	69	Elevation at which flooding commences
FMC(I,J)	66	Shape factor for channel portion of synthetic section
FMF(I,J)	66	Shape factor for floodplain portion of synthetic section
FMO(I,J)	66	Shape factor for inactive portion of synthetic section
FRDFR	7	Window for critical Froude number (mixed flow)
GAMA(J)	55	Ratio of time from initial steady flow to center of gravity of the specified hydrograph
GHT(I,L,M,J)	40	Dummy variable; currently not in use
GSIL(L,M,J)	38	Dummy variable; currently not in use
GZ(K,J)	51	Gage correction to convert observed stages to mean sea level datum (msl)
GZ1(J)	58	Gage correction to convert observed stages at upstream boundary to msl
GZN(1)	60	Gage correction to convert observed stages at downstream boundary to msl
HB	66	Elevation of section at top of bank (calibration)
HCRESL(L,K,J)	28	Elevation associated with variable length of dam crest
HDD(K,J)	26	Elevation of top of dam
HF	66	Elevation of section at top of floodplain (calibration)
HFDD(K,J)	47	Elevation of water when dam failure commences
HFLV(L)	18	Elevation of water surface when levee starts to fail
HGTD(K,J)	27	Elevation of center of gate openings; also elevation of bottom of still of time-dependent gate
HKC(L,I,J)	74	Elevation corresponding to the conveyance
HLVMN(L)	18	Final elevation of bottom of levee crevasse
HPLV(L)	19	Centerline elevation of flood drainage pipe (levee)
HPOND(L)	21	Initial WSEL of storage pond (levee)
HS(L,I,J)	70	Elevation corresponding to each top width

<u>VARIABLE</u>	<u>DATA GROUP</u>	<u>DEFINITION OF THE VARIABLE</u>
HSAP(K,L)	23	Elevation corresponding to SAPOND (levee)
HSAR(L,K,J)	25	Elevation at which reservoir surface area is defined
HSC	64	Invert elevation at the most upstream section
HSPD(K,J)	27	Elevation of uncontrolled spillway crest
HWLV(L)	18	Elevation of top of levee, ridge line, etc.
ICG(K,J)	27	Parameter for type of gate structure
IFXC(I,J)	63	Parameter indicating if section has special properties
IOBS	5	Parameter indicating if observed data are available
ITMAX	2	Maximum number of iterations allowed in the Newton-Raphson iteration scheme
JDBG1	6	First river with additional debug information
JDBG2	6	Last river with additional debug information
JN	2	Total number of rivers
JNK	4	Output print parameter
JNKDBG	6	Debug switch for additional information
KAM	65	Parameter for the method for reading in cross sections for calibration
KCG	3	Number of points in time-dependent spillway gate control curve
KD(J)	13	Parameter for the type of downstream boundary condition
KFLP	2	Floodplain (conveyance) parameter
KFTR(J)	13	Parameter for use of Kalman Filter option
KLPI(K)	14	Power (k) used in the LPI technique
KPL	4	Parameter for type of hydrograph to be plotted
KPRES	3	Parameter for method of computing hydraulic radius
KRCHT(I,J)	17	Parameter for routing method or internal boundary
KREVR	4	Parameter for use of the low flow filter
KTERM	5	Parameter to print terms in equation of motion
KU(J)	13	Type of upstream boundary condition parameter
KWARM	2	Number of time steps used for warm-up procedure
LAD(K,J)	26,44	Reach number corresponding to internal boundary
LDBG1	6	First reach with debug information (calibration)
LDBG2	6	Last reach with debug information (calibration)
LQ1(K,J)	48	Number of section immediately upstream of lateral flow
MCMDDBG	6	First iteration with debug information (calibration)
MDT	7	Divisor for determining the time step
MESAGE	85	80-character message describing the data set
METRIC	1	Parameter for units of input/output (English or Metric)
MIXF(J)	13	Parameter for the flow regime
MRV(J)	12	Number of river into which river J flows
MSG	0-1	Description of data set
MUD(J)	13	Dummy parameter; set MUD(J)=0
NBT(J)	12	Total number of cross sections
NCG	3	Dummy parameter; set NCG=0
NCM(I,J)	79	Section number of upstream-most station of Manning n

<u>VARIABLE</u>	<u>DATA GROUP</u>	<u>DEFINITION OF THE VARIABLE</u>
NCS	4	Number of values in table of topwidth vs. elevation
NFGRF	4	Parameter for generating FLDGRF data
NG(M,J)	37	Dummy variable
NGAGE(J)	13	Total number of observed hydrographs on river
NGS(K,J)	50	Sequence number of each observed/plotting station
NIFM(K)	11	Number of reach along the river with levee passing flow
NITO(K)	11	Number of reach along the river receiving flow (levee)
NJFM(K)	11	Number of river passing levee overtopping/failure flow
NJTO(K)	11	Number of river receiving flow from levee overtopping/ failure
NJUN(J)	12	Number of section along the main river immediately upstream of tributary confluence
NLEV	10	Total number of section reaches in the system with levees
NP	5	Parameter for use of Automatic Calibration option
NPEND	5	Last value in the computed stage hydrograph used in the statistics (calibration)
NPOND	20	Total number of storage ponds (levee)
NPST	5	First value in the computed stage hydrograph used in the statistics (calibration)
NPT(1,J)	12	Beginning cross-section number for which debug information will be printed
NPT(2,J)	12	Final cross-section number for which debug information will be printed
NQCM(J)	13	Total number of values in the Manning table. Also, denotes whether Manning n is a function of WSEL or discharge
NQL(J)	13	Total number of lateral flows on river
NRCM1(J)	13	Total number of Manning n reaches on river
NU	2	Number of values associated with observed hydrographs
NYQD	3	Number of values in rating curve at downstream boundary
QDI(I,J)	69	Initial discharges
QGH(L,K,J)	33	Distance from bottom of gate to gate sill
QGH(L,K,J)	42	Observed WSEL (pool) or discharge hydrograph at the dam
QHT(I,L,K,J)	35	Dummy variable
QKC(L,I,J)	75	Conveyance corresponding to elevation
QL(L,K,J)	49	Lateral inflow at cross section
QTD(K,J)	26	Discharge through turbines
QYQD(K)	62	Discharge defined in downstream empirical rating curve
RHI(L,K,J)	30	Head above spillway crest or gate center
RHI(L,K,J)	36	Dummy variable
RHO(J)	55	Ratio of peak flow to initial flow of inflow hydrograph
RIVER(J)	86	16-character name associated with each river
RQI(L,K,J)	31	Discharge in spillway or gate rating curve
SAPOND(K,L)	22	Surface area of storage pond corresponding to HSAP(K,L)
SAR(L,K,J)	24	Surface area of reservoir corresponding to HSA(L,K,J)
SLFI(J)	84	Bed/initial water surface slope

<u>VARIABLE</u>	<u>DATA GROUP</u>	<u>DEFINITION OF THE VARIABLE</u>
SLV(L)	18	Slope of levee 1
SNM(L,I,J)	77	Sinuosity coefficient
SPL(K,J)	27	Crest length of uncontrolled spillway
ST1(L,J)	56	Observed stages or discharges at upstream boundary
STN(1)	59	Observed hydrograph at downstream boundary
STNAME(K,J)	52	20-character name associated with each gaging station
STQ(L,K,J)	54	Observed discharge hydrograph at gaging station
STT(L,K,J)	53	Observed hydrograph at each gaging station
SXS	65	Average channel bottom slope (calibration)
T1(L,J)	57	Time array associated with upstream hydrograph
TCG(L,K,J)	32	Time associated with CGCG(L,K,J)
TCG(L,K,J)	41	Time array corresponding to QGH(L,K,J)
TDBG1	6	Time at which additional debug information begins
TDBG2	6	Time at which additional debug information ends
TDTIN(K)	9	Time at which DTIN(K) is no longer used
TEH	7	Time at which routing computations will terminate
TFH(K,J)	47	Time of failure of the structure
TFLV(L)	18	Time of levee failure (crevasse)
TGHT(I,L,M,J)	39	Dummy variable
THETA	1	Acceleration factor to solve tributary junction problem
TIBQH(K,J)	43	Time at which dam changes from discharge to pool rating
TPG(J)	55	Time from initial flow to peak flow of upstream boundary hydrograph
VWIND(J)	12	Wind velocity
WCLV(L)	18	Weir-flow discharge coefficient (levee)
WINAGL(J)	12	Acute angle that wind makes with the channel axis
XFACT	1	Units conversion factor for location of computation points
XT(I,J)	15	Location of section where computations are made
Y1	68	Depth of typical section at midpoint between the invert and top of bank (calibration)
Y2	68	Depth of typical section at top of bank (calibration)
Y3	68	Depth of typical cross section to midpoint between the top of bank and estimated maximum flood elevation
Y4	68	Depth of typical cross section at maximum flood elevation (calibration)
YBMIN(K,J)	47	Lowest elevation that bottom breach reaches
YDI(I,J)	69	Initial water surface elevations
YQCM(L,I,J)	83	WSEL or discharges associated with Manning n
YQD(K)	61	Stages corresponding to QYQD(K)
YQI(J)	55	Initial discharge or WSEL at upstream boundary
ZBCH(K,J)	47	Side slope of breach

21. FLDWAV MODEL OUTPUT

21.1 Line Printer Output

The FLDWAV model output is controlled primarily by the JNK parameter. JNK may be assigned values of 1, 4, 5, 9, 10, and 12 where the output becomes more extensive as JNK increases. It is recommended that for most runs, JNK be specified as 4; this output is considered to provide the maximum amount of information for the least number of pages of output. A JNK=1 provides the least amount of output and is intended to be used for obtaining final results to minimize permanent paper or file storage requirements. If the graphical output utility (FLDGRF) is to be used to review the output information, JNK=1 may be used. JNK values > 4 are to be used to obtain detailed hydraulic and numerical information for confronting and overcoming numerical difficulties that have caused aborted runs or suspect results. When a user first sets up the problem, it is highly recommended that $JNK \geq 5$ be used to ensure that the model is behaving in an acceptable manner for the problem being modeled. In some cases, the hydrographs and boundary information may indicate a successful run, but further inspection of the hydraulic information throughout the routing reach may reveal hidden problems in the data input setup.

Examples of the output listed in Table 21.1 are shown in Tables 21.2-21.25 and Figure 21.1. Parameters in the tables with **bold** print are defined. No examples are given for $JNK \geq 10$ since this is usually repetitive information per iteration. Generally, output variables are defined categorically with the first or first two letters; i.e., Q is discharge, Y is water surface elevation, X is cross-section distance location, FR is Froude number, T is time, V is velocity, A is wetted cross-sectional area, B is wetted cross-sectional topwidth, and CM is Manning n. Also, the J and I counters refer to the river number and cross-section number, respectively.

TABLE 21.1. Description of Debug Output

Output Description		JNK					
		0	1	4	5	9	>9
Input Echo Print and Summary of Array Sizes		X	X	X	X	X	X
Bottom Slope Profile				X	X	X	X
Initial Conditions Summary				X	X	X	X
Initial Conditions/Low Flow Filter					X	X	X
Minimum Dynamic Routing Output				X	X	X	X
Internal Boundary Information				X	X	X	X
Hydraulic Information						X	X
Levee Information					X	X	X
Subcritical/Supercritical Information				X	X	X	X
Nonconvergence Information					X	X	X
Calibration Information		X	X	X	X	X	X
Profile of Crests and Times		X	X	X	X	X	X
Computed WSEL and Discharge Hydrograph Data						X	X
Hydrograph Plot		X	X	X	X	X	X
Dynamic Routing Information at each Iteration							X

TABLE 21-2. Bottom Slope Profile

RIVER NO	SECT NO	X MILE	BED ELEV. FEET	REACH NO	LENGTH MILE	SLOPE FPM	ROUTING	STRUCT.
1	1	.00	5220.00	1	16.00	12.06	IMP(SUB)	DAM
1	2	16.00	5027.00	2	.01	.00	IMP(SUB)	
1	3	16.01	5027.00	3	5.00	12.40	IMP(SUB)	
1	4	21.01	4965.00	4	3.50	12.86	IMP(SUB)	
	.							
	.							
1	11	57.01	4736.00	11	2.00	3.50	IMP(SUB)	
1	12	59.01	4729.00	12	8.50	8.82	IMP(SUB)	
1	13	67.51	4654.00	13	8.00	6.63	IMP(SUB)	
1	14	75.51	4601.00					

WARNING: THE FOLLOWING DXMs SHOULD BE CHANGED

J	I	DXM(I,J)	RECOMMENDED	REASON
1	6	.750	.194	COURANT CONDITION
1	7	1.000	.264	COURANT CONDITION
1	8	1.000	.326	COURANT CONDITION
1	9	1.000	.202	COURANT CONDITION
1	10	1.100	.306	COURANT CONDITION
1	11	1.000	.222	EXP/CON CRITERIA
1	12	1.000	.425	COURANT CONDITION
1	13	1.400	.368	COURANT CONDITION

Definition of Variables in Bottom Slope Profile Table

River No	- River number
Sect No	- Cross section number
X	- Cross section location (mile or km)
Bed Elevation	- Invert elevation (ft or m)
Reach No	- Reach number
Length	- Reach length (mile or km)
Slope	- Slope of reach (fpm or %)
Routing	- Routing technique
Struct.	- Structure within the reach
J	- River number
I	- Cross section number
DXM	- Distance interval between cross sections (mile or km)

TABLE 21.3. Initial Conditions Summary

I	DISTANCE MILE	FLOW CFS	WSEL FT	DEPTH FT	MIN WSEL FT	BOTTOM FT
1	.000	13000.	5288.499	68.499	5231.191	5220.000
2	2.000	13000.	5288.500	92.625	5206.267	5195.875
.						
.						
.						
82	73.910	13000.	4621.069	9.469	4621.069	4611.600
83	75.510	13000.	4609.491	8.491	4609.491	4601.000

Definition of Variables in Initial Conditions Summary Table

I	- Cross section counter
DISTANCE	- Cross section location (mile or km)
FLOW	- Initial discharge (cfs or cms)
WSEL	- Initial water surface elevation (ft or m)
DEPTH	- Initial depth of flow (ft or m)
MIN WSEL	- Low flow filter (ft or m)
BOTTOM	- Invert elevation (ft or m)

TABLE 21.4. Initial Conditions/Low Flow Filter

I=	1	X=	.000	YN=	5288.55	DEPN=	261.55	YC=	5033.55	DEPC=	6.55	IFR=	0	ITN=	0	ITC=	14
I=	2	X=	.010	YN=	5036.35	DEPN=	9.35	YC=	5033.55	DEPC=	6.55	IFR=	0	ITN=	14	ITC=	14
	.																
	.																
I=	73	X=	57.910	YN=	4621.22	DEPN=	9.62	YC=	4618.02	DEPC=	6.42	IFR=	0	ITN=	12	ITC=	12
I=	74	X=	59.510	YN=	4609.64	DEPN=	8.64	YC=	4606.61	DEPC=	5.61	IFR=	0	ITN=	12	ITC=	12

	(IFR(I,J),I=1,N)					
0	0	0	0	0	0	0
0	0	0	0	0	0	0
0	0	0	0	0	0	0
0	0	0	0	0	0	0
0	0	0	0	0	0	0
0	0	0	0	0	0	0
0	0	0	0	0	0	0
0	0	0	0	0	0	0
WATER ELEVATION AT SECTION N=	74	IS	4609.49			
WATER ELEVATION AT SECTION N=	73	IS	4621.07			

BACKWATER	IN= 73	YNN= 4621.07	DEP=	9.47
I= 72	QIL= 13003.	YIL= 4632.73	DEP= 10.53	ITB= 3
I= 71	QIL= 13003.	YIL= 4644.56	DEP= 11.76	ITB= 3
.				
.				
I= 2	QIL= 13003.	YIL= 5036.36	DEP= 9.36	ITB= 3
I= 1	QIL= 13003.	YIL= 5288.55	DEP= 261.55	ITB= 3

INITIAL WATER ELEVATION:

YDI FOR RIVER NO. 1									
5288.55	5036.36	5030.18	5024.00	5017.82	5011.63	5005.45	4999.26		
4993.07	4986.87	4980.73	4974.40	4967.82	4961.25	4954.65	4948.10		
4941.41	4935.00	4927.95	4921.06	4914.17	4907.29	4900.40	4893.51		
4886.62	4879.75	4872.83	4866.01	4859.01	4852.35	4845.02	4839.00		
4830.35	4827.67	4825.95	4824.23	4822.49	4820.75	4819.01	4817.24		
4815.55	4813.39	4811.67	4809.90	4808.13	4806.37	4804.60	4802.80		
4788.19	4784.44	4780.24	4776.87	4773.79	4770.68	4767.50	4764.40		
4765.58	4760.03	4755.33	4750.90	4746.99	4742.20	4737.76	4732.34		
4709.98	4699.59	4689.36	4678.84	4668.77	4656.56	4644.56	4632.73		
4621.07	4609.49								

WATER ELEVATION FOR LOW FILTER:

YUMN FOR RIVER									
5036.36	5036.36	5030.18	5024.00	5017.82	5011.63	5005.45	4999.26		
4993.07	4986.87	4980.73	4974.40	4967.82	4961.25	4954.65	4948.10		
4941.41	4935.00	4927.95	4921.06	4914.17	4907.29	4900.40	4893.51		
4886.62	4879.75	4872.83	4866.01	4859.01	4852.35	4845.02	4839.00		
4830.35	4827.67	4825.95	4824.23	4822.49	4820.75	4819.01	4817.24		
4815.58	4813.30	4810.80	4808.91	4803.31	4799.00	4795.00	4792.50		
4785.19	4784.44	4780.24	4776.87	4774.79	4772.68	4770.56	4768.40		
4765.58	4760.03	4755.33	4750.90	4746.99	4741.20	4730.76	4720.34		
4709.98	4699.59	4689.36	4678.84	4668.77	4656.56	4644.56	4632.73		
4621.07	4609.49								

Definition of Variables in Initial Conditions / Low Flow Filter Table

I	- Cross section counter
X	- Cross section location (mile or km)
YN	- Normal flow WSEL (ft or m), for initial flow at t=0
DEPN	- Normal flow depth (ft or m) for initial flow
YC	- Critical flow WSEL (ft or m) for initial flow at t=0
DEPC	- Critical flow depth (ft or m) for initial flow
IFR	- Froude number indicator 0 indicates $Fr < 1$, 1 indicates $Fr \geq 1$
ITN	- Number of iterations to obtain YN via bi-section solution method
ITC	- Number of iterations to obtain YC via bi-section solution method
IN	- Number of cross section at downstream boundary
YNN	- WSEL (ft or m) at downstream boundary for initial flow
DEP	- Depth (ft or m) at downstream boundary for initial flow
I	- Cross section counter
J	- River number
QIL	- Discharge (cfs or cms) at t=0 for Ith cross section
YIL	- Computed backwater/downwater WSEL (ft or m) at t=0 for Ith cross section
DEP	- Backwater flow depth (ft or m)
ITB	- Number of iterations to obtain backwater elevation YIL
YDI	- Initial water surface elevation (ft or m)
YUMN	- Minimum water surface elevation (ft or m) used in routing computations (low flow filter)

TABLE 21.5. Minimum Dynamic Routing Output

TT =		.00000 HRS			DTH =		.02500 HRS			ITMX=		0							
RIVER=		1		QU(1)=		3.000		YU(1)=		2578.30		QU(N)=		3.000		YU(N)=		215.37	
J	I	X(MI)	H(MSL)	V(FPS)	A(TSQFT)	B(FT)	BT(FT)	Q(TCFS)	MANN	N	WAVHT	FROUDE	DEP(FT)	KR	QL(TCFS)	MRV			
1	1	5.000	2578.30	.01	279.904	8060.	8060.	3.0000	.0700	.00	.00	120.30	10	.0000	0				
1	2	5.010	2466.45	8.40	.357	85.	85.	3.0000	.0700	.00	.72	8.45	5	.0000	0				
1	3	5.112	2454.16	8.38	.358	85.	85.	3.0000	.0700	.00	.72	8.43	5	.0000	0				
1	4	5.214	2441.86	8.37	.359	85.	85.	3.0000	.0700	.00	.72	8.41	5	.0000	0				
1	5	5.315	2429.56	8.35	.359	86.	86.	3.0000	.0700	.00	.72	8.38	5	.0000	0				
1	6	5.417	2417.26	8.33	.360	86.	86.	3.0000	.0700	.00	.72	8.36	5	.0000	0				
1	7	5.519	2404.96	8.32	.361	87.	87.	3.0000	.0700	.00	.72	8.33	5	.0000	0				
1	8	5.621	2392.66	8.30	.361	87.	87.	3.0000	.0700	.00	.72	8.31	5	.0000	0				
1	9	5.722	2380.36	8.28	.362	87.	87.	3.0000	.0700	.00	.72	8.28	5	.0000	0				
FRMX=		.873		IFRMX=		117		FRMN=		.000		IFRMN=		1					
RESERVOIR OUTFLOW INFORMATION																			
J	I	TT	QU(I)	USH(MSL)	YB(MSL)	DSH(MSL)	SUB	BB	QU(1)	QBRCH	QOVTOP	QOTHR							
1	1	.000	3.000	2578.30	2578.30	2466.45	1.00	.00	3.000	.000	.000	3.000							

Definition of Variables in Minimum Dynamic Routing Output Table

TT	- Time at which output is given (hrs)
DTH	- Computational time step (hrs)
ITMX	- Number of iterations in Newton-Raphson Solution of Saint-Venant Equations
RIVER	- River number
QU(1)	- Discharge (cfs or cms) at upstream boundary
YU(1)	- Water surface elevation (ft or m) at upstream boundary
QU(N)	- Discharge (cfs or cms) at downstream boundary
YU(N)	- Water surface elevation (ft or m) at downstream boundary
FRMX	- Maximum Froude number in the routing reach
IFRMX	- Cross section number at which FRMX occurs
FRMN	- Minimum Froude number in the routing reach
IFRMN	- Cross section number at which FRMN occurs

TABLE 21.6. Internal Boundary Information

TT = .00000 HRS DTH = .02500 HRS ITMX= 0

RIVER= 1 QU(1)= 3.000 YU(1)= 2578.30 QU(N)= 3.000 YU(N)= 215.37

J	I	X(MI)	H(MSL)	V(FPS)	A(TSQFT)	B(FT)	BT(FT)	Q(TCFS)	MANN.	N	WAVHT	FROUDE	DEP(FT)	KR	QL(TCFS)	MRV
1	1	5.000	2578.30	.01	79.904	60.	60.	3.0000	.0700	.00	.00	120.30	10	.0000	0	
1	2	5.010	2466.45	8.40	.357	85.	85.	3.0000	.0700	.00	.72	8.45	5	.0000	0	
1	3	5.112	2454.16	8.38	.358	85.	85.	3.0000	.0700	.00	.72	8.43	5	.0000	0	
1	4	5.214	2441.86	8.37	.359	85.	85.	3.0000	.0700	.00	.72	8.41	5	.0000	0	
1	5	5.315	2429.56	8.35	.359	86.	86.	3.0000	.0700	.00	.72	8.38	5	.0000	0	
1	6	5.417	2417.26	8.33	.360	86.	86.	3.0000	.0700	.00	.72	8.36	5	.0000	0	
1	7	5.519	2404.96	8.32	.361	87.	87.	3.0000	.0700	.00	.72	8.33	5	.0000	0	
1	8	5.621	2392.66	8.30	.361	87.	87.	3.0000	.0700	.00	.72	8.31	5	.0000	0	
1	9	5.722	2380.36	8.28	.362	87.	87.	3.0000	.0700	.00	.72	8.28	5	.0000	0	

FRMX= .873 IFRMX= 117 FRMN= .000 IFRMN= 1

RESERVOIR OUTFLOW INFORMATION

J	I	TT	QU(I)	USH(MSL)	YB(MSL)	DSH(MSL)	SUB	BB	QU(1)	QBRECH	QOVTOP	QOTHR
1	1	.000	3.000	2578.30	2578.30	2466.45	1.00	.00	3.000	.00	.000	3.000

Definition of Variables in Internal Boundary Information Table

- J - River number
- I - Cross section number of internal boundary
- TT - Time at which output is given (hrs)
- QU(I) - Discharge through structure (cfs or cms)
- USH(MSL) - Water surface elevation (ft or m - msl) immediately upstream of structure (pool elevation)
- YB(MSL) - Elevation (ft or m - msl) of bottom of breach
- DSH(MSL) - Water surface elevation (ft or m - msl) immediately downstream of structure (tailwater elevation)
- SUB - Submergence correction factor for breach flow
- BB - Bottom width (ft or m) of breach
- QU(1) - Discharge (cfs or cms) at upstream end of the reach or pool upstream of the structure
- QBRECH - Discharge (cfs or cms) through breach
- QOVTOP - Discharge (cfs or cms) over the top of dam or over crest of bridge embankment
- QOTHR - Discharge (cfs or cms) of all other flows (Dams: spillways, gates, turbines; Bridge: bridge opening)

TABLE 21.7. Hydraulic Information

```

TT = .00000 HRS      DTH = .02500 HRS      ITMX= 0
RIVER= 1      QU(1)= 3.000      YU(1)= 2578.30      QU(N)= 3.000      YU(N)= 215.37

J I X(MI) H(MSL) V(FPS) A(TSQFT) B(FT) BT(FT) Q(TCFS) MANN. N WAVHT FROUDE DEP(FT) KR QL(TCFS) MRV
1 1 5.000 2578.30 .01 79.904 60. 60. 3.0000 .0700 .00 .00 120.30 10 .0000 0
1 2 5.010 2466.45 8.40 .357 85. 85. 3.0000 .0700 .00 .72 8.45 5 .0000 0
1 3 5.112 2454.16 8.38 .358 85. 85. 3.0000 .0700 .00 .72 8.43 5 .0000 0
1 4 5.214 2441.86 8.37 .359 85. 85. 3.0000 .0700 .00 .72 8.41 5 .0000 0
1 5 5.315 2429.56 8.35 .359 86. 86. 3.0000 .0700 .00 .72 8.38 5 .0000 0
1 6 5.417 2417.26 8.33 .360 86. 86. 3.0000 .0700 .00 .72 8.36 5 .0000 0
1 7 5.519 2404.96 8.32 .361 87. 87. 3.0000 .0700 .00 .72 8.33 5 .0000 0
1 8 5.621 2392.66 8.30 .361 87. 87. 3.0000 .0700 .00 .72 8.31 5 .0000 0
1 9 5.722 2380.36 8.28 .362 87. 87. 3.0000 .0700 .00 .72 8.28 5 .0000 0

FRMX= .873 IFRMX= 117 FRMN= .000 IFRMN= 1

RESERVOIR OUTFLOW INFORMATION
J I TT QU(I) USH(MSL) YB(MSL) DSH(MSL) SUB BB QU(1) QBRECH QOVTOP QOTHR
1 1 .000 3.000 2578.30 2578.30 2466.45 1.00 .00 3.000 .00 .000 3.000

```

Definition of Variables in Hydraulic Information Table

J	- River number
I	- Cross section number
X(MI)	- Cross section location (miles or km)
H(MSL)	- Water surface elevation (ft or m - msl)
V(FPS)	- Velocity (ft/sec or m/sec)
A(TSQFT)	- Active cross sectional area (1000 sq ft or 1000 sq m)
B(FT)	- Active topwidth (ft or m)
BT(FT)	- Total topwidth (ft or m)
Q(TCFS)	- Discharge (1000 cfs or 1000 cms)
MANN. N	- Roughness coefficient
WAVHT	- Wave height (ft or cms) -- H minus initial WSEL
FROUDE	- Froude number
DEP(FT)	- Water depth (ft or cms) -- H minus invert elevation
KR	- KRCH routing/internal boundary type parameter
QL(TCFS)	- Lateral flow (1000 cfs or 1000 cms)
MRV	- River into which tributary flows

TABLE 21.8. Levee Information

TT = .50000 HRS DTH = .50000 HRS ITMX= 1 1

RIVER= 1 QU(1)= 3.354 YU(1)= 109.37 QU(N)= 5.994 YU(N)= 71.83

J	I	X(MI)	H(MSL)	V(FPS)	A(TSQFT)	B(FT)	BT(FT)	Q(TCFS)	MANN. N	WAVHT	FROUDE	DEP(FT)	KR	QL(TCFS)	MRV
1	1	.000	109.37	1.53	2.193	468.	468.	3.3542	.0400	.16	.12	9.37	0	.0000	0
1	2	5.000	104.14	11.36	2.088	457.	457.	2.8485	.4000	-.07	.11	9.14	0	.0000	0
1	3	10.000	99.25	1.43	2.140	463.	463.	3.0649	.0400	.03	.12	9.25	9	.0000	0
1	4	11.250	98.00	1.41	2.137	462.	462.	3.0151	.0400	.01	.12	9.25	9	.0000	0
1	5	12.500	96.77	1.40	2.150	464.	464.	3.0035	.0400	.00	.11	9.27	9	.0000	0
1	6	13.750	95.59	1.38	2.181	467.	467.	3.0008	.0400	.00	.11	9.34	9	.0000	0
1	7	15.000	94.48	1.34	2.246	474.	474.	3.0002	.0400	.00	.11	9.48	9	.0000	0
1	8	17.500	92.80	1.13	2.649	510.	510.	3.0000	.0400	.00	.09	10.30	9	.0000	0
1	9	20.000	91.93	.85	3.526	564.	564.	3.0000	.0400	.00	.06	11.93	0	.0000	0
1	0	20.100	91.80	1.74	3.452	560.	560.	6.0000	.0400	.00	.12	11.80	0	.0000	0
1	11	25.000	86.84	1.72	3.479	561.	561.	6.0000	.0400	.00	.12	11.84	9	.0000	0
1	12	26.000	85.84	1.72	3.479	561.	561.	6.0000	.0400	.00	.12	11.84	9	.0000	0
1	13	27.000	84.84	1.72	3.479	561.	561.	6.0000	.0400	.00	.12	11.84	9	.0000	0
1	14	28.000	83.84	1.72	3.479	561.	561.	5.9999	.0400	.00	.12	11.84	9	.0000	0
1	15	29.000	82.84	1.72	3.479	561.	561.	5.9996	.0400	.00	.12	11.84	9	.0000	0
1	16	30.000	81.85	1.72	3.479	562.	562.	5.9982	.0400	.00	.12	11.85	0	.0000	0
1	17	35.000	76.84	1.73	3.479	561.	561.	6.0034	.0400	.00	.12	11.84	0	.0000	0
1	18	40.000	71.83	1.73	3.473	561.	561.	5.9937	.0400	.00	.12	11.83	0	.0000	0

FRMX= .125 IFRMX= 1 FRMN= .060

RIVER= 2 QU(2)= 3.063 YU(1)= 109.24 QU(N)= 3.000 YU(N)= 91.86

J	I	X(MI)	H(MSL)	V(FPS)	A(TSQFT)	B(FT)	BT(FT)	Q(TCFS)	MANN. N	WAVHT	FROUDE	DEP(FT)	KR	QL(TCFS)	MRV
2	1	.000	109.24	1.44	2.133	462.	462.	3.0625	.0400	.03	.12	9.24	0	.0000	1
2	2	5.000	104.20	1.41	2.115	460.	460.	2.9732	.0400	.01	.12	9.20	9	.0000	1
2	3	7.500	101.71	1.42	2.121	460.	460.	3.0030	.0400	.00	.12	9.21	9	.0000	1
2	4	10.000	99.21	1.42	2.119	460.	460.	2.9997	.0400	.00	.12	9.21	9	.0000	1
2	5	11.250	97.95	1.42	2.117	460.	460.	2.9999	.0400	.00	.12	9.20	9	.0000	1
2	6	12.500	96.69	1.42	2.113	460.	460.	3.0000	.0400	.00	.12	9.19	9	.0000	1
2	7	13.750	95.43	1.42	2.105	459.	459.	3.0000	.0400	.00	.12	9.18	9	.0000	1
2	8	15.000	94.14	1.44	2.088	457.	457.	3.0000	.0400	.00	.12	9.14	0	.0000	1
2	9	20.000	91.86	.86	3.489	562.	562.	3.0000	.0400	.00	.06	11.86	0	.0000	1

FRMX= 118 IFRMX= 8 FRMN= .061 IFRMN= 9

TT	LV	JM	IM	JT	IT	QLOVTP	QLPOND	QLBRCH	BR-WDTH	WSEL-M	WSEL-T	SUB-M	SUB-T
0.500	9	1	7	1	0	0.000	75.708	0.000	0.000	93.637	94.000	1.00	1.00
0.500	10	1	8	1	0	0.000	160.862	0.000	0.000	92.361	94.000	1.00	1.00

QPOND(L)= -237. 0. 0.
HPOND(L)= 93.99 85.00 70.00

Definition of Variables in Levee Information Table

L - Pond counter
 QPOND(L) - Discharge into (+) or leaving (-) pond
 HPOND(L) - WSEL in pond (ft or m)
 LV - Levee reach number
 JM - Number of river passing flow over levee reach LV
 IM - Cross section reach number on river JM passing flow over levee reach LV
 JT - Number of river receiving flow from levee reach LV
 IT - Cross section reach number on river JT receiving flow from levee reach LV
 QLOVTP - Flow over the levee (cfs or cms)
 QLBRCH - Flow through the levee breach (cfs or cms)
 QLPOND - Flow from the pond (cfs or cms)
 BR-WDTH - Width of levee breach (ft or m)
 WSEL-M - Average WSEL in reach IM (pool)
 WSEL-T - Average WSEL in reach IT (tailwater)
 SUB-M - Submergence correction factor for the main river
 SUB-T - Submergence correction factor for the tributary

TABLE 21.9. Subcritical/Supercritical Flow Information

L= 1 KSP= 0 KS1= 1 KSN= 12
L= 2 KSP= 1 KS1= 12 KSN= 13
L= 3 KSP= 0 KS1= 14 KSN= 24

TT = .00000 HRS DTH = .01250 HRS ITMX= 0

RIVER= 1 QU(1)= .804 YU(1)= 549.98 QU(N)= 1.204 YU(N)= 466.81

J	I	X(MI)	H(MSL)	V(FPS)	A(TSQFT)	B(FT)	BT(FT)	Q(TCFS)	MANN. N	WAVHT	FROUDE	DEP(FT)	KR	QL(TCFS)	MRV
1	10	2.001	506.49	5.71	.211	65.	65.	1.2040	.0400	.00	.56	6.49	0	.0000	0
1	11	2.250	502.56	4.22	.285	76.	76.	1.2040	.0400	.00	.38	7.56	0	.0000	0
1	12	2.500	495.14	9.11	.132	51.	51.	1.2040	.0400	.00	1.00	5.14	0	.0000	0
1	13	2.600	477.02	1.09	.109	43.	43.	1.2040	.0400	.00	1.23	5.02	0	.0000	0
1	14	2.700	477.02	.60	.007	74.	74.	1.2040	.0400	.00	.03	23.02	0	.0000	0
1	15	2.800	477.02	.21	.684	77.	77.	1.2040	.0400	.00	.01	41.02	0	.0000	0
1	16	2.900	477.02	.11	.620	60.	60.	1.2040	.0400	.00	.00	59.02	0	.0000	0
1	17	3.000	477.02	.07	.478	28.	28.	1.2040	.0400	.00	.00	77.02	0	.0000	0
1	18	3.100	477.02	.10	.108	84.	84.	1.2040	.0400	.00	.00	63.02	0	.0000	0
1	19	3.200	477.02	.15	.118	31.	31.	1.2040	.0400	.00	.01	49.02	0	.0000	0

FRMX= 1.234 IFRMX= 1 FRMN= .002 IFRMN= 17

RESERVOIR OUTFLOW INFORMATION												
J	I	TT	QU(I)	USH(MSL)	YB(MSL)	DSH(MSL)	SUB	BB	QU(1)	QBRECH	QOVTOP	QOTHR
1	9	.000	1.204	549.90	550.00	506.49	1.00	.00	.804	.000	.000	1.204

Definition of Variables in Subcritical/Supercritical Flow Information Table

L - Flow regime reach counter
KSP - Flow regime indicator: 0 for subcritical flow, 1 for supercritical flow
KS1 - Beginning cross section in flow regime
KSN - Ending cross section in flow regime

TABLE 21.10. Nonconvergence Information

L=	1	KSP=	0	KS1=	1	KSN=	2
L=	2	KSP=	1	KS1=	2	KSN=	16
L=	3	KSP=	0	KS1=	17	KSN=	36
L=	4	KSP=	1	KS1=	36	KSN=	42
L=	5	KSP=	0	KS1=	43	KSN=	112

NONCONVERGENCE FOR TT= .08300 USING DTH= .00415
 AT RIVER= 1 SECT NO.= 17 18 19 20
 PREVIOUS TT= .07885 NEW DTH= .00207 NEW F1= 1.00 NEW TT= .08093

L=	1	KSP=	0	KS1=	1	KSN=	2
L=	2	KSP=	1	KS1=	2	KSN=	17
L=	3	KSP=	0	KS1=	18	KSN=	36
L=	4	KSP=	1	KS1=	36	KSN=	42
L=	5	KSP=	0	KS1=	43	KSN=	112

TT = .08093 HRS DTH = .00207 HRS ITMX= 4

RIVER= 1 QU(1)= 77.897 YU(1)= 1527.29 QU(N)= 1.002 YU(N)= 720.18

J	I	X(MI)	H(MSL)	V(FPS)	A(TSQFT)	B(FT)	BT(FT)	Q(TCFS)	MANN.	N	WAVHT	FROUDE	DEP(FT)	KR	QL(TCFS)	MRV
1	1	.000	1527.29	22.15	3.517	215.	215.	77.8972	.0350	-21.71	.97	22.29	10	.0000	0	
1	2	.010	1523.53	27.32	2.852	243.	243.	77.8972	.0350	14.97	1.40	18.53	0	.0000	0	
1	3	.064	1568.06	28.80	2.819	241.	251.	81.1905	.0350	15.20	1.48	17.42	0	.0000	0	
1	4	.117	1512.68	29.67	2.797	240.	261.	82.9958	.0350	14.43	1.53	16.40	0	.0000	0	
1	5	.171	1507.33	30.04	2.774	241.	271.	83.3153	.0350	13.91	1.56	15.42	0	.0000	0	
1	6	.225	1502.02	30.01	2.749	243.	283.	82.4936	.0350	13.00	1.57	14.48	0	.0000	0	
1	7	.278	1496.71	29.76	2.710	245.	295.	80.6580	.0350	12.40	1.58	13.53	0	.0000	0	
1	8	.332	1491.41	29.32	2.660	249.	307.	77.9996	.0350	11.40	1.58	12.59	0	.0000	0	
1	9	.385	1486.11	28.75	2.595	253.	320.	74.5900	.0350	10.70	1.58	11.66	0	.0000	0	
		FRMX=	1.582	IFRMX=	9	FRMN=	.282	IFRMN=	101							

RESERVOIR OUTFLOW INFORMATION

J	I	TT	QU(I)	USH(MSL)	YB(MSL)	DSH(MSL)	SUB	BB	QU(1)	QBRECH	QOVTOP	QOTHR
1	1	.081	77.897	1527.29	1506.10	1523.53	.86	165.75	77.897	77.877	.000	.000

Definition of Variables in Nonconvergence Information Table

SECT NO. - Cross locations (interpolated) where nonconvergence occurred.
 TT - Last computational time (hr) prior to nonconvergence
 NEW DTH - New computation time step (hr) to be used (Usually half of the previous time step)
 NEW F1 - New theta weighting factor to be used.
 NEW TT - New time (hr) for which computations are made

TABLE 21.11. Calibration Information

RIVER NO. 1	REACH NO. 5	METROPOLIS	STA NO. 13	RIVER MILE=	991.200				
RIVER NO. 1	MANNING N	REACH NO. 5							
FKC= 1000.0000	FMC=	0.5000	FKF= 400.0000	FMF=	1.0000	FKO=	0.0000	FMO=	0.0000
X(I,J)	991.20	981.70	972.20						
IFXC=	0	0	0						
HS=	271.56	281.56	321.56	325.56	341.56	441.56			
BS=	0.00	3162.28	7071.07	8671.07	15071.07	15071.07			
AS=	0.	15811.	220478.	251963.	441900.	1949007.			
MCM= 1	TOTAL RMS (SEA)=	1.91	TOTAL MEAN DEVIATION (AVD)=	0.99					
M	IIM	RMSL	AVDL	CM	YQR				
1	0	0.0000	0.0000	0.0210	150000.				
2	5	0.7607	0.7569	0.0210	250000.				
3	18	1.4101	0.8834	0.0210	350000.				
4	29	2.9710	2.7012	0.0210	450000.				
5	6	0.2570	-0.0209	0.0210	550000.				
6	6	0.5158	-0.3314	0.0210	650000.				
7	20	0.7275	-0.6556	0.0210	750000.				
8	0	0.0000	0.0000	0.0210	10000000000.				
NEW CM=	0.0210	0.0194	0.0191	0.0168	0.0210	0.0217	0.0224	0.0210	

Definition of Variables in Calibration Information Table

FKC	- Scaling parameter of in-bank channel portion of cross section
FMC	- Shape factor for in-bank channel portion of cross section
FKF	- Scaling parameter of floodplain portion of cross section
FMF	- Shape factor for floodplain portion of cross section
FKO	- Scaling parameter of inactive portion of cross section
FMO	- Shape factor for inactive portion of cross section
X(I,J)	- Cross section location (mile or km)
IFXC	- Parameter indicating if cross sections have special properties
HS	- Elevation (ft or m) corresponding to each topwidth
BS	- Topwidth (ft or m) of active flow portion of cross section
AS	- Cross-sectional area (sq-ft or sq-m) below the corresponding HS value
MCM	- Iteration counter of each new calibration trial in the reach
M	- Level in Manning n table
IIM	- No. of hydrograph points in this level
RMSL	- Root-mean-squared (RMS) error for points in the level
AVDL	- Mean deviation of points in this level
CM	- Manning n value used in this range
YQR	- Average discharge/water surface elevation is this range

TABLE 21.12. Profile of Crests and Times

RVR NO.	SEC NO.	LOCATION MILE	BOTTOM FEET	TIME MAX WSEL (HR)	MAX WSEL FEET	TIME MAX FLOW (CFS)	MAX FLOW CFS	MAX VL (FPS)	MAX VC (FPS)	MAX VR (FPS)
1	1*#	0.000	500.10	7.20002	551.04	7.57502	100976.	3.18	3.66	3.17
1	2*	0.010	500.00	7.85002	533.03	7.57502	100976.	7.73	14.07	7.73
1	3	0.111	499.50	7.90002	532.42	7.60002	98258.	7.57	13.46	7.57
1	4	0.212	498.99	7.92502	531.81	7.60002	95726.	7.37	12.98	7.37
1	5	0.313	498.49	7.95002	531.20	7.67502	93227.	7.17	12.54	7.17
1	6	0.413	497.98	7.97502	530.62	7.70002	91650.	7.01	12.25	7.01
1	7	0.514	497.48	8.00002	530.04	7.72502	90403.	6.92	11.88	6.92
1	8	0.615	496.97	8.05002	529.48	7.75002	89353.	6.84	11.53	6.84
1	9	0.716	496.47	8.25002	528.94	7.77502	88337.	6.75	11.19	6.75
1	10	0.817	495.97	8.27502	528.48	7.80002	87360.	6.74	10.57	6.74
1	11	0.918	495.46	8.30002	528.02	7.82502	86456.	6.64	10.16	6.64
	.									
	.									
	.									
1	77	7.600	469.80	9.87499	498.98	9.50000	59009.	4.72	9.21	4.72
1	78	7.800	469.40	9.89999	498.39	9.52500	58782.	4.74	9.23	4.74
1	79	8.000	469.00	9.92499	497.79	9.57500	58553.	4.73	9.23	4.73
1	80	8.200	468.60	9.94999	497.21	9.60000	58314.	4.72	9.20	4.72
1	81	8.400	468.20	9.97499	496.59	9.65000	58072.	4.66	9.18	4.66
1	82	8.600	467.80	9.97499	495.88	9.67500	57846.	4.23	9.29	4.23
1	83	8.800	467.40	9.99999	495.11	9.72499	57622.	4.05	9.32	4.05
1	84	9.000	467.00	10.02499	494.22	9.77499	57394.	4.03	9.28	4.03
1	85	9.200	466.60	10.07499	493.27	9.79999	57160.	4.05	9.21	4.05
1	86	9.400	466.20	10.09999	492.25	9.87499	56931.	4.10	9.10	4.10
1	87	9.600	465.80	10.12499	491.15	9.92499	56728.	4.21	8.93	4.21
1	88	9.800	465.40	10.17499	490.01	9.99999	56539.	4.26	8.79	4.26
1	89*	10.000	465.00	10.22499	488.84	10.04999	56366.	4.38	8.51	4.38

Definition of Variables in Profile of Crests and Times Table

RVR NO.	- River number
SEC NO.	- Cross section number
LOCATION	- Cross section location (mile or km)
BOTTOM	- Invert elevation (ft or m)
TIME MAX WSEL	- Time to maximum water surface elevation (hr)
MAX WSEL	- Maximum water surface elevation (ft or m)
TIME MAX FLOW	- Time to maximum flow (hr)
MAX FLOW	- Maximum flow (cfs or cms)
MAX VL	- Maximum flow velocity in the left floodplain (fps or m/s) (floodplain option only)
MAX VC	- Maximum flow velocity in the channel (fps or m/s) (floodplain option only)
MAX VR	- Maximum flow velocity in the right floodplain (fps or m/s) (floodplain option only)
MAX VEL	- Maximum flow velocity in the composite channel (fps or m/s) (composite channel option only)

TABLE 21.13. Computed Water Surface Elevation and Discharges

KTIME	TII(KTIME)	COMPUTED STAGES FOR RIVER= 1 SECTION= 1 2 43 112				
1	.000	1549.00	1508.55	1202.32	720.18	
2	.008	1548.99	1509.50	1202.33	720.18	
3	.017	1548.88	1511.81	1202.35	720.18	
4	.025	1548.53	1514.23	1202.36	720.18	
5	.033	1547.77	1516.33	1202.36	720.18	
6	.041	1546.44	1518.31	1202.36	720.18	
7	.050	1544.36	1520.23	1202.36	720.18	
8	.058	1541.37	1521.92	1202.36	720.18	
9	.066	1537.29	1523.36	1202.36	720.18	
10	.075	1531.79	1524.90	1202.36	720.18	
11	.083	1525.96	1522.33	1202.36	720.18	
12	.091	1522.53	1518.49	1202.36	720.18	
13	.100	1520.06	1517.47	1202.36	720.18	

KTIME	TII(KTIME)	COMPUTED DISCHARGE FOR RIVER= 1 SECTION= 1 2 43 112				
1	.000	1000.	1000.	1001.	1000.	
2	.008	1741.	1741.	1021.	1000.	
3	.017	5114.	5114.	1041.	1001.	
4	.025	11700.	11700.	1053.	1001.	
5	.033	21477.	21477.	1058.	1001.	
6	.041	33930.	33930.	1060.	1001.	
7	.050	48255.	48255.	1061.	1001.	
8	.058	62646.	62646.	1061.	1001.	
9	.066	76294.	76294.	1062.	1002.	
10	.075	92148.	92148.	1062.	1002.	
11	.083	66385.	66385.	1062.	1002.	
12	.091	35124.	35124.	1061.	1002.	
13	.100	28365.	28365.	1061.	1002.	

Definition of Variables in Computed Water Surface Elevation and Discharges Table

- KTIME - Time step counter
- TII(KTIME) - Time (hrs) at which computed stages and computed discharges for each river occur.
- SECTION - Number of cross sections
- YC(KTIME,I) - Water surface elevation (ft or m) for each time at each station where hydrograph plot is made
- QC(KTIME,I) - Discharge (cfs or cms) for each time at each station where hydrograph plot is made

TABLE 21.14. Initial Conditions/Low Flow Filter:
Normal Depth Computations

I= 1	X= .000	YN= 5288.55	DEPN= 261.55	YC= 5033.55	DEPC= 6.55	IFR= 0	ITN= 0	ITC= 14
I= 2	Y= 5076.00	F= 684119.8	FK= .0722	A= 35049.91	R= 36.57	CMU= .0400	Q1= 13003.33	
I= 2	Y= 5051.50	F= 139161.1	FK= .0722	A= 13230.69	R= 16.08	CMU= .0400	Q1= 13003.33	
I= 2	Y= 5039.25	F= 15225.0	FK= .0722	A= 4319.08	R= 6.89	CMU= .0400	Q1= 13003.33	
I= 2	Y= 5033.13	F= -8790.1	FK= .0722	A= 1106.71	R= 3.06	CMU= .0400	Q1= 13003.33	
I= 2	Y= 5036.19	F= -581.4	FK= .0722	A= 2490.10	R= 4.59	CMU= .0400	Q1= 13003.33	
I= 2	Y= 5037.72	F= 6259.5	FK= .0722	A= 3378.31	R= 5.61	CMU= .0400	Q1= 13003.33	
I= 2	Y= 5036.95	F= 2374.2	FK= .0722	A= 2922.41	R= 4.98	CMU= .0400	Q1= 13003.33	
I= 2	Y= 5036.57	F= 847.2	FK= .0722	A= 2701.93	R= 4.79	CMU= .0400	Q1= 13003.33	
I= 2	Y= 5036.38	F= 120.7	FK= .0722	A= 2594.93	R= 4.69	CMU= .0400	Q1= 13003.33	
I= 2	Y= 5036.28	F= -233.4	FK= .0722	A= 2542.25	R= 4.64	CMU= .0400	Q1= 13003.33	
I= 2	Y= 5036.33	F= -57.1	FK= .0722	A= 2568.52	R= 4.67	CMU= .0400	Q1= 13003.33	
I= 2	Y= 5036.35	F= 31.6	FK= .0722	A= 2581.71	R= 4.68	CMU= .0400	Q1= 13003.33	
I= 2	Y= 5036.34	F= -13.7	FK= .0722	A= 2574.98	R= 4.67	CMU= .0400	Q1= 13003.33	
I= 2	Y= 5036.35	F= 8.1	FK= .0722	A= 2578.21	R= 4.67	CMU= .0400	Q1= 13003.33	
I= 2	Y= 5036.35	F= -2.8	FK= .0722	A= 2576.59	R= 4.67	CMU= .0400	Q1= 13003.33	
.								
I= 74	Y= 4610.50	F= 3243.9	FK= .0528	A= 3143.75	R= 6.62	CMU= .0360	Q1= 13003.33	
I= 74	Y= 4605.75	F= -10606.5	FK= .0528	A= 953.20	R= 2.25	CMU= .0360	Q1= 13003.33	
I= 74	Y= 4608.13	F= -5008.5	FK= .0528	A= 2031.29	R= 4.40	CMU= .0360	Q1= 13003.33	
I= 74	Y= 4609.31	F= -1178.6	FK= .0528	A= 2583.60	R= 5.52	CMU= .0360	Q1= 13003.33	
I= 74	Y= 4609.91	F= 960.6	FK= .0528	A= 2862.70	R= 6.07	CMU= .0360	Q1= 13003.33	
I= 74	Y= 4609.61	F= -127.2	FK= .0528	A= 2722.91	R= 5.79	CMU= .0360	Q1= 13003.33	
I= 74	Y= 4609.76	F= 412.2	FK= .0528	A= 2792.74	R= 5.93	CMU= .0360	Q1= 13003.33	
I= 74	Y= 4609.68	F= 141.3	FK= .0528	A= 2757.81	R= 5.86	CMU= .0360	Q1= 13003.33	
I= 74	Y= 4609.65	F= 6.8	FK= .0528	A= 2740.35	R= 5.83	CMU= .0360	Q1= 13003.33	
I= 74	Y= 4609.63	F= -60.3	FK= .0528	A= 2731.63	R= 5.81	CMU= .0360	Q1= 13003.33	
I= 74	Y= 4609.64	F= -26.8	FK= .0528	A= 2735.99	R= 5.82	CMU= .0360	Q1= 13003.33	
I= 74	Y= 4609.64	F= -10.9	FK= .0528	A= 2738.06	R= 5.82	CMU= .0360	Q1= 13003.33	
I= 74	Y= 4609.64	F= -2.1	FK= .0528	A= 2739.21	R= 5.83	CMU= .0360	Q1= 13003.33	
I= 74	X= 59.510	YN= 4609.64	DEPN= 8.64	YC= 4606.61	DEPC= 5.61	IFR= 0	ITN= 12	ITC= 12

Definition of Variables in Initial Conditions / Low Flow Filter:
Normal Depth Computations Table

I	- Cross section counter
X	- Cross section location (mile or km)
YN	- Normal flow WSEL (ft or m), for initial flow at t=0
DEPN	- Normal flow depth (ft or m) for initial flow
YC	- Critical flow WSEL (ft or m) for initial flow at t=0
DEPC	- Critical flow depth (ft or m) for initial flow
IFR	- Froude number indicator 0 indicates $Fr < 1$, 1 indicates $Fr \geq 1$
ITN	- Number of iterations to obtain YN via bi-section solution method
ITC	- Number of iterations to obtain YC via bi-section solution method
J	- River number
N	- Total number of cross sections
Y	- Water surface elevation (ft or m)
F	- Difference between the computed discharge and the actual discharge
FK	- $1.49 * \text{SQRT}(S)$
A	- Active cross sectional area (sq-ft or sq-m)
R	- Hydraulic Radius (ft or m)
CMU	- Manning Roughness Coefficient
Q1	- Discharge (cfs or cms)

**TABLE 21.15. Initial Conditions/Low Flow Filter:
Downwater Computations**

```

I= 1  X= .000  YN= 5288.55  DEPN= 261.55  YC= 5033.55  DEPC= 6.55  IFR= 0  ITN= 0  ITC= 14
I= 2  Y= 5076.00  F= 684119.8  FK= .0722  A= 35049.91  R= 36.57  CMU= .0400  Q1= 13003.33
I= 2  Y= 5051.50  F= 139161.1  FK= .0722  A= 13230.69  R= 16.08  CMU= .0400  Q1= 13003.33
I= 2  Y= 5039.25  F= 15225.0  FK= .0722  A= 4319.08  R= 6.89  CMU= .0400  Q1= 13003.33
.
I= 74  Y= 4609.64  F= -26.8  FK= .0528  A= 2735.99  R= 5.82  CMU= .0360  Q1= 13003.33
I= 74  Y= 4609.64  F= -10.9  FK= .0528  A= 2738.06  R= 5.82  CMU= .0360  Q1= 13003.33
I= 74  Y= 4609.64  F= -2.1  FK= .0528  A= 2739.21  R= 5.83  CMU= .0360  Q1= 13003.33
I= 74  X= 59.510  YN= 4609.64  DEPN= 8.64  YC= 4606.61  DEPC= 5.61  IFR= 0  ITN= 12  ITC= 12

      (IFR(I,J),I=1,N)
0  0  0  0  0  0  0  0  0  0
0  0  0  0  0  0  0  0  0  0
0  0  0  0  0  0  0  0  0  0
0  0  0  0  0  0  0  0  0  0
0  0  0  0  0  0  0  0  0  0
0  0  0  0  0  0  0  0  0  0
0  0  0  0  0  0  0  0  0  0
0  0  0  0  0  0  0  0  0  0
0  0  0  0  0  0  0  0  0  0
ITB= 0  I= 73  YIR= 4609.64  QII= 13003.  YA= 4630.56  F= -3015074.000
ITB= 1  I= 73  YIR= 4609.64  QII= 13003.  YA= 4624.29  F= -1026617.000
ITB= 2  I= 73  YIR= 4609.64  QII= 13003.  YA= 4621.16  F= -59822.660
.
ITB= 11  I= 73  YIR= 4609.64  QII= 13003.  YA= 4620.98  F= -549.270
ITB= 12  I= 73  YIR= 4609.64  QII= 13003.  YA= 4620.98  F= 602.136

WATER ELEVATION AT SECTION N= 74 IS 4609.49
WATER ELEVATION AT SECTION N= 73 IS 4621.07

BACKWATER      IN= 73      YNN= 4621.07      DEP= 9.47
ITB= 1  I= 72  YBWO= 4631.41  YBWN= 4632.64  F= 460831.400
ITB= 2  I= 72  YBWO= 4632.64  YBWN= 4632.73  F= 31074.660
ITB= 3  I= 72  YBWO= 4632.73  YBWN= 4632.73  F= 106.291
I= 72  QIL= 13003.  YIL= 4632.73  DEP= 10.53  ITB= 3
ITB= 1  I= 71  YBWO= 4642.95  YBWN= 4644.80  F= 528940.500
ITB= 2  I= 71  YBWO= 4644.80  YBWN= 4644.56  F= -73286.410
ITB= 3  I= 71  YBWO= 4644.56  YBWN= 4644.56  F= 687.131
I= 71  QIL= 13003.  YIL= 4644.56  DEP= 11.76  ITB= 3
ITB= 1  I= 70  YBWO= 4654.70  YBWN= 4656.77  F= 538055.800
ITB= 2  I= 70  YBWO= 4656.77  YBWN= 4656.56  F= -64059.640
ITB= 3  I= 70  YBWO= 4656.56  YBWN= 4656.56  F= 411.615
.
I= 3  QIL= 13003.  YIL= 5030.18  DEP= 9.38  ITB= 3
ITB= 1  I= 2  YBWO= 5035.55  YBWN= 5036.38  F= 169358.600
ITB= 2  I= 2  YBWO= 5036.38  YBWN= 5036.36  F= -4883.037
ITB= 3  I= 2  YBWO= 5036.36  YBWN= 5036.36  F= -52.562
I= 2  QIL= 13003.  YIL= 5036.36  DEP= 9.36  ITB= 3
I= 1  QIL= 13003.  YIL= 5288.55  DEP= 261.55  ITB= 3

```

Definition of Variables in Initial Conditions / Low Flow Filter:
Downwater Computations Table

I	- Cross section counter
F	- Difference between the computed discharge and the actual discharge
YIR	- Final water surface elevation (ft or m)
QII	- Discharge (same as Q1) (cfs or cms)
YA	- Water surface elevation within the reach (ft or m)

**TABLE 21.16. Initial Conditions/Low Flow Filter:
Backwater Computations**

```

ITB= 0   I= 73   YIR= 4609.64   QII= 13003.   YA= 4630.56   F= -3015074.000
ITB= 1   I= 73   YIR= 4609.64   QII= 13003.   YA= 4624.29   F= -1026617.000
ITB= 2   I= 73   YIR= 4609.64   QII= 13003.   YA= 4621.16   F= -59822.660
.
.

```

```

ITB= 11  I= 73   YIR= 4609.64   QII= 13003.   YA= 4620.98   F= -549.270
ITB= 12  I= 73   YIR= 4609.64   QII= 13003.   YA= 4620.98   F= 602.136

```

WATER ELEVATION AT SECTION N= 74 IS 4609.49

WATER ELEVATION AT SECTION N= 73 IS 4621.07

```

BACKWATER      IN= 73      YNN= 4621.07      DEP= 9.47
ITB= 1   I= 72   YBWO= 4631.41   YBWN= 4632.64   F= 460831.400
ITB= 2   I= 72   YBWO= 4632.64   YBWN= 4632.73   F= 31074.660
ITB= 3   I= 72   YBWO= 4632.73   YBWN= 4632.73   F= 106.291
I= 72   QIL= 13003.   YIL= 4632.73   DEP= 10.53   ITB= 3
ITB= 1   I= 71   YBWO= 4642.95   YBWN= 4644.80   F= 528940.500
ITB= 2   I= 71   YBWO= 4644.80   YBWN= 4644.56   F= -73286.410
ITB= 3   I= 71   YBWO= 4644.56   YBWN= 4644.56   F= 687.131
I= 71   QIL= 13003.   YIL= 4644.56   DEP= 11.76   ITB= 3
ITB= 1   I= 70   YBWO= 4654.70   YBWN= 4656.77   F= 538055.800
ITB= 2   I= 70   YBWO= 4656.77   YBWN= 4656.56   F= -64059.640
ITB= 3   I= 70   YBWO= 4656.56   YBWN= 4656.56   F= 411.615
.
.
I= 3   QIL= 13003.   YIL= 5030.18   DEP= 9.38   ITB= 3
ITB= 1   I= 2   YBWO= 5035.55   YBWN= 5036.38   F= 169358.600
ITB= 2   I= 2   YBWO= 5036.38   YBWN= 5036.36   F= -4883.037
ITB= 3   I= 2   YBWO= 5036.36   YBWN= 5036.36   F= -52.562
I= 2   QIL= 13003.   YIL= 5036.36   DEP= 9.36   ITB= 3
I= 1   QIL= 13003.   YIL= 5288.55   DEP= 261.55   ITB= 3

```

INITIAL WATER ELEVATION:

YDI	FOR RIVER NO. 1						
5288.55	5036.36	5030.18	5024.00	5017.82	5011.63	5005.45	4999.26
5993.07	4986.87	4980.73	4974.40	4967.82	4961.25	4954.65	4948.10
5941.41	4935.00	4927.95	4921.06	4914.17	4907.29	4900.40	4893.51
5886.62	4879.75	4872.83	4866.01	4859.01	4852.35	4845.02	4839.00
5830.35	4827.67	4825.95	4824.23	4822.49	4820.75	4819.01	4817.24
5815.44	4813.59	4810.39	4806.91	4803.31	4799.70	4795.90	4792.09
5788.19	4784.44	4780.24	4776.87	4774.79	4772.68	4770.56	4768.40
5765.58	4760.03	4755.33	4750.90	4746.99	4741.20	4730.76	4720.34
5709.98	4699.59	4689.36	4678.84	4668.77	4656.56	4644.56	4632.73
5621.07	4609.49						

**Definition of Variables in Initial Conditions / Low Flow Filter:
Backwater Computations Table**

I	- Cross section counter
F	- Difference between the computed discharge and the actual discharge
IN	- Number of cross section at downstream boundary
YNN	- WSEL (ft or m) at downstream boundary for initial flow
DEP	- Depth (ft or m) at downstream boundary for initial flow
QIL	- Discharge (cfs or cms) at t=0 for Ith cross section
YIL	- Computed backwater/downwater WSEL (ft or m) at t=0 for Ith cross section
DEP	- Backwater flow depth (ft or m)
ITB	- Number of iterations to obtain backwater elevation YIL
YDI	- Initial water surface elevation (ft or m)
YUMN	- Minimum water surface elevation (ft or m) used in routing computations (low flow filter)
YBWN	- New guess for the water surface elevation (ft or m)
YBWO	- Old guess for the water surface elevation (ft or m)

TABLE 21.17. Outflow Summary

TT = 48.00000 HRS				DTH = 24.00000 HRS				ITMX= 2 1 1 1									
RIVER= 1		QU(1)= 330.000		YU(1)= 337.15		QU(N)= 619.472		YU(N)= 257.99									
J	I	X(MI)	H(MSL)	V(FPS)	A(TSQFT)	B(FT)	BT(FT)	Q(TCFS)	MANN.	N	WAVHT	FROUDE	DEP(FT)	KR	QL(TCFS)	MRV	
1	1	1076.500	337.15	3.65	90.463	3182.	3182.	330.0000	.0294	1.58	.12	37.15	0	.0000	0		
1	2	1067.300	334.30	3.07	07.291	4775.	4775.	328.9608	.0294	2.15	.11	34.30	0	.0160	0		
1	3	1058.000	330.88	3.71	89.024	3845.	3845.	330.2678	.0229	2.18	.14	30.88	0	.0000	0		
1	4	1049.900	328.98	3.57	91.995	3587.	3587.	328.6409	.0229	2.77	.12	33.98	0	.0000	0		
1	5	1031.700	322.86	4.54	71.678	3924.	3924.	325.5422	.0199	2.26	.19	22.86	0	.0000	0		
.																	
.																	
1	19	937.400	298.45	4.25	48.958	5770.	5770.	632.6872	.0237	4.45	.15	38.45	0	.0000	0		
1	20	920.000	291.49	5.04	25.068	5280.	5280.	630.1964	.0237	4.07	.18	31.49	0	.0000	0		
1	21	904.500	283.91	4.92	27.549	5411.	5411.	627.2339	.0237	2.36	.18	33.91	0	.0000	0		
1	22	889.000	278.75	4.15	50.285	4943.	4943.	623.9164	.0258	2.07	.13	38.75	0	.0000	0		
1	23	867.700	270.83	4.11	51.008	7100.	7100.	621.2112	.0258	5.09	.16	30.83	0	.0000	0		
1	24	846.400	257.99	5.40	14.722	5492.	5492.	619.4720	.0258	2.20	.21	17.99	0	.0000	0		
FRMX= .263		IFRMX= 7		FRMN= .112		IFRMN= 15											
RIVER= 2		QU(1)= 53.800		YU(1)= 320.50		QU(N)= 53.270		YU(N)= 315.36									
J	I	X(MI)	H(MSL)	V(FPS)	A(TSQFT)	B(FT)	BT(FT)	Q(TCFS)	MANN.	N	WAVHT	FROUDE	DEP(FT)	KR	QL(TCFS)	MRV	
2	1	30.600	320.50	3.14	17.129	728.	728.	53.8000	.0213	1.36	.11	20.50	0	.0000	1		
2	2	23.000	319.30	3.01	17.831	819.	819.	53.7196	.0213	1.33	.11	19.30	0	.0000	1		
2	3	15.300	317.88	3.23	16.587	823.	823.	53.6077	.0213	1.09	.13	17.88	0	.0000	1		
2	4	7.700	316.47	3.15	16.956	759.	759.	53.4608	.0213	.85	.12	16.47	0	.0000	1		
2	5	.000	315.36	2.80	19.053	830.	830.	53.2705	.0213	.92	.10	15.36	0	.0000	1		
FRMX= .127		IFRMX= 3		FRMN= .103		IFRMN= 5											
RIVER= 3		QU(1)= 53.000		YU(1)= 312.54		QU(N)= 53.644		YU(N)= 311.8									
J	I	X(MI)	H(MSL)	V(FPS)	A(TSQFT)	B(FT)	BT(FT)	Q(TCFS)	MANN.	N	WAVHT	FROUDE	DEP(FT)	KR	QL(TCFS)	MRV	
3	1	22.400	312.54	1.48	35.886	1638.	1638.	53.0000	.0184	2.51	.06	22.54	0	.0000	1		
3	2	16.800	312.35	1.63	32.474	1453.	1453.	53.0368	.0184	2.49	.06	22.35	0	.0000	1		
3	3	11.200	312.17	1.62	32.790	1392.	1392.	53.0819	.0184	2.49	.06	22.17	0	.0000	1		
3	4	5.600	312.00	1.53	34.785	1430.	1430.	53.1536	.0183	2.49	.05	22.00	0	.0000	1		
3	5	.000	311.80	1.80	29.770	1304.	1304.	53.6442	.0182	2.47	.07	21.80	0	.0000	1		
FRMX= .066		IFRMX= 5		FRMN= .055		IFRMN= 4											
RIVER= 4		QU(1)= 209.000		YU(1)= 354.86		QU(N)= 208.413		YU(N)= 303.7									
J	I	X(MI)	H(MSL)	V(FPS)	A(TSQFT)	B(FT)	BT(FT)	Q(TCFS)	MANN.	N	WAVHT	FROUDE	DEP(FT)	KR	QL(TCFS)	MRV	
4	1	109.900	354.86	4.63	45.134	2108.	2108.	209.0000	.0336	.21	.18	24.86	0	.0000	1		
4	2	106.800	352.57	3.73	55.929	2617.	2617.	208.8759	.0336	.68	.14	22.57	0	.0000	1		
4	3	94.100	345.92	3.59	58.038	2154.	2154.	208.3894	.0262	.90	.12	20.92	0	.0000	1		
4	4	88.000	343.70	4.17	49.982	2350.	2350.	208.1935	.0262	1.32	.16	18.70	0	.0000	1		
.																	
.																	
4	9	30.000	312.55	4.25	50.104	2563.	2563.	212.9984	.0317	.80	.17	12.55	0	.0000	1		
4	10	15.000	307.51	2.39	88.544	3515.	3888.	211.3783	.0317	1.41	.08	27.51	0	.0000	1		
4	11	.000	303.73	3.25	64.068	2557.	2605.	208.4129	.0317	3.29	.11	23.73	0	.0000	1		
FRMX= .187		IFRMX= 6		FRMN= .084		IFRMN= 10											
TOTAL INFLOW (1000 CF)				TOTAL OUTFLOW (1000 CF)				TOTAL VOLUME				CONTINUITY ERROR					
RIVER				RIVER				CHANGE(1000 CUFT)				(PERCENT)					
81590020.00				85050680.00				158817100.00				4884262.00				1.76	
TOTAL VOLUME/ACTIVE VOLUME CHANGE (%) OF RIVER 1 =												94.65		242.67			
TRIBUTARY ITERATIONS = 5																	
TOTAL ITERATIONS FOR EACH OF 4 RIVERS.																	
37				8				17				11					
TOTAL TIME= 48.00				TOTAL NO. OF TIME STEPS: KTIME= 3				NUMTIM= 3									

Definition of Variables in Outflow Summary Table

- KTIME - Total number of time steps used in the computations
- NUMTIM - Total number of time steps stored for use in FLDGRF model

TABLE 21.18. Counters after Interpolation Information

NEW INPUT CROSS SECTION NO. AFTER INTERPOLATION

```

RIVER NO. 1
NN= 1 2 3 4 5 6 7 8 9 10 11 12 13 14 15 16 17 18 19 20

RIVER NO. 1
NGS= 1 3 5 7 12 14 16 20
LQ1= 9
LQN= 10

L= 1 KRTYP= 0 KRT1= 1 KRTN= 3
L= 2 KRTYP= 0 KRT1= 3 KRTN= 5
L= 3 KRTYP= 0 KRT1= 5 KRTN= 7
L= 4 KRTYP= 0 KRT1= 7 KRTN= 12
L= 5 KRTYP= 0 KRT1= 12 KRTN= 14
L= 6 KRTYP= 0 KRT1= 14 KRTN= 16
L= 7 KRTYP= 0 KRT1= 16 KRTN= 20

(SLOP(I,J),I=1,N) FOR RIVER NO. 1
.000001 .000168 .000001 .000042 .000001 .000046 .000001 .000001
.000001 .000001 .000022 .000001 .000021 .000001 .000031 .000001
.000001 .000001 .000001 .000001

QDI(I, 1)
150600. 0. 0. 0. 0. 0. 0. 0.
0. 0. 0. 0. 0. 0. 0. 0.
0. 0. 0. 0.

YDI(I, 1)
.00 .00 .00 .00 .00 .00 .00 .00
.00 .00 .00 .00 .00 .00 .00 .00
.00 .00 .00 -.26

```

Definition of Variables in Counters after Interpolation Information Table

RIVER NO. - River number
 NGS - Gage locations
 LQ1 - Beginning location for lateral flow
 LQN - Ending location for lateral flow
 L - Counter for different routing techniques (simulation mode) or for calibration reaches (calibration mode)
 KRTYP - Routing type
 KRT1 - Beginning location of the routing/calibration reach
 KRTN - Ending location of the routing/calibration reach
 SLOP - Slope of channel
 I - Cross section counter
 J - River number
 QDI - Initial discharges (cfs or cms)
 YDI - Initial water surface elevation (ft or m)

TABLE 21.19. Levee Information after Interpolation

L	NJFM	NIFM	NJTO	NITO	X	HWLV	TFLV	WCLV	BLVMX	HFLV	HLVMN	SLV	HPLV	DPLV
1	1	3	1	0	10.00	107.00	3.00	2.50	125.00	1000.00	105.00	.00010	.00	.00
2	1	4	1	0	11.25	106.34	3.00	2.50	125.00	999.34	104.34	.00010	.00	.00
3	1	5	1	0	12.50	105.68	3.00	2.50	125.00	998.68	103.68	.00010	.00	.00
4	1	6	1	0	13.75	105.02	3.00	2.50	125.00	998.02	103.02	.00010	.00	.00
5	1	3	2	2	10.00	107.00	3.00	2.50	125.00	1000.00	105.00	.00010	.00	.00
.														
.														
22	1	11	3	0	25.00	91.00	3.00	2.50	1000.00	91.00	89.00	.00010	.00	.00
23	1	12	3	0	26.00	90.47	3.00	2.50	1000.00	90.47	88.47	.00010	.00	.00
24	1	13	3	0	27.00	89.94	3.00	2.50	1000.00	89.94	87.94	.00010	.00	.00
25	1	14	3	0	28.00	89.42	3.00	2.50	1000.00	89.42	87.42	.00010	.00	.00
26	1	15	3	0	29.00	88.89	3.00	2.50	1000.00	88.89	86.89	.00010	.00	.00

Definition of Variables in Levee Information after Interpolation Table

L	- Levee counter
NJFM	- Number of river passing levee overtopping/failure flow
NIFM	- Number of reach along the river with levee passing flow
NJTO	- Number of river receiving flow from levee overtopping/failure
X	- Cross section location (mile or km)
HWLV	- Elevation (ft or m) of top of levee, ridge line, etc.
TFLV	- Time of levee failure (crevasse)
WCLV	- Weir-flow discharge coefficient (levee)
BLVMX	- Final width of levee crevasse
HFLV	- Elevation of water surface (ft or m) when levee starts to fail (ft or m)
HLVMN	- Final elevation of bottom of levee crevasse (ft or m)
SLV	- Slope of the levee
HPLV	- Centerline elevation (ft or m) of flood drainage pipe (levee)
DPLV	- Diameter of flood drainage pipe

TABLE 21.20. Mixed Flow Debug Output

[illegible]

Definition of Variables in Debug Output Table

TERM1	- First term in momentum equation
TERM2	- Second term in momentum equation
TERM3	- Third term in momentum equation
SF	- Friction slope
SMIN	- Minimum allowable friction slope
MAX DQ	- Maximum flow error using Newton Raphson technique
MAX DY	- Maximum elevation error using Newton Raphson technique
ITER	- Iteration counter for Newton Raphson technique
CFACT	- Multiplier used to update the next guess for flow/water elevation in the Newton Raphson technique
RIVER	- River number
DYN/CUN REACH	- Routing type
SUP/SUB FLOW	
REACH	- Reach number contained in the routing type
KIT	- Iteration counter
K	- Iteration counter
I	- Cross section number
YNO	- Old guess for the normal water surface elevation (ft or m)
YNN	- New guess for the normal water surface elevation (ft or m)
IFR	- Flow regime
0	- Subcritical flow
1	- Supercritical flow
2	- Critical flow

TABLE 21.21. Tributary Debug Information

```

INITIAL CONDITIONS IMPROVED BY SOLVING UNSTEADY FLOW EQUATIONS WITH BOUNDARIES HELD CONSTANT
RIVER= 1 DYN/CUN REACH= 1 SUP/SUB FLOW REACH= 1 KIT = 2
MAX DQ AND MAX DY ARE FINAL MAXIMUM ERROR IN NEWTON RAPHSON ITERATION METHOD WHILE SOLVING ST. VENANT EQUATION
MAX DQ=***** AT I= 24 MAX DY= 4.492 AT I= 23 ITER= 0 CFACT= 1.000
MAX DQ=***** AT I= 24 MAX DY= .906 AT I= 17 ITER= 1 CFACT= 1.000
MAX DQ= .0 AT I= 24 MAX DY= .147 AT I= 13 ITER= 2 CFACT= 1.000
MAX DQ= .0 AT I= 24 MAX DY= .000 AT I= 13 ITER= 3 CFACT= 1.000
RIVER= 2 DYN/CUN REACH= 1 SUP/SUB FLOW REACH= 1 KIT = 2
MAX DQ= .0 AT I= 0 MAX DY= 1.250 AT I= 1 ITER= 0 CFACT= 1.000
MAX DQ= .0 AT I= 0 MAX DY= .000 AT I= 1 ITER= 1 CFACT= 1.000
RIVER= 3 DYN/CUN REACH= 1 SUP/SUB FLOW REACH= 1 KIT = 2
MAX DQ= .0 AT I= 0 MAX DY= 2.031 AT I= 1 ITER= 0 CFACT= 1.000
MAX DQ= .0 AT I= 0 MAX DY= .000 AT I= 1 ITER= 1 CFACT= 1.000
RIVER= 4 DYN/CUN REACH= 1 SUP/SUB FLOW REACH= 1 KIT = 2
MAX DQ= .0 AT I= 0 MAX DY= 1.080 AT I= 4 ITER= 0 CFACT= 1.000
MAX DQ= .0 AT I= 0 MAX DY= .000 AT I= 4 ITER= 1 CFACT= 1.000
RELX ITR JRIVER ERQ QOLD QNEW NEWTON ITRMX
0 2 619. 54181. 54800. 1
0 3 6205. 47573. 53778. 1
0 4 1209. 206791. 208000. 1

TT = .00000 HRS DTH = 24.00000 HRS ITMX= 3 1 1 1
RIVER= 1 QU(1)= 288.000 YU(1)= 335.12 QU(N)= 446.638 YU(N)= 255.79
J I X(MI) H(MSL) V(FPS) A(TSQFT) B(FT) BT(FT) Q(TCFS) MANN. N WAVHT FROUDE DEP(FT) KR QL(TCFS) MRV
1 1 1076.500 335.12 3.42 84.139 3064. 3064. 288.0000 .0309 -.45 .12 35.12 0 .0000 0
1 2 1067.300 332.66 2.88 99.700 4442. 4442. 287.5988 .0308 .51 .11 32.66 0 .3720 0
1 3 1058.000 328.77 3.64 80.934 3787. 3787. 294.7946 .0225 .07 .14 28.77 0 .0000 0
1 4 1049.900 327.33 3.40 86.226 3387. 3387. 293.1569 .0225 1.12 .12 32.33 0 .0000 0
1 5 1031.700 321.61 4.28 66.893 3694. 3694. 286.3499 .0195 1.01 .18 21.61 0 .0000 0
.
.
1 20 920.000 290.04 4.37 117.613 5011. 5011. 514.2587 .0248 2.62 .16 30.04 0 .0000 0
1 21 904.500 281.31 4.42 114.388 4689. 4689. 505.1895 .0248 -.24 .16 31.31 0 .0000 0
1 22 889.000 276.18 3.68 137.917 4698. 4698. 507.9590 .0262 -.50 .12 36.18 0 .0000 0
1 23 867.700 270.33 3.24 147.489 6912. 6912. 478.5753 .0262 4.59 .12 30.33 0 .0000 0
1 24 846.400 255.79 4.34 102.819 5328. 5328. 446.6384 .0262 .00 .17 15.79 0 .0000 0
FRMX= .270 IFRMX= 7 FRMN= .107 IFRMN= 2
RIVER= 2 QU(1)= 54.800 YU(1)= 320.39 QU(N)= 54.181 YU(N)= 313.67
J I X(MI) H(MSL) V(FPS) A(TSQFT) B(FT) BT(FT) Q(TCFS) MANN. N WAVHT FROUDE DEP(FT) KR QL(TCFS) MRV
2 1 30.600 320.39 3.22 17.045 720. 720. 54.8000 .0212 1.25 .12 20.39 0 .0000 1
2 2 23.000 318.97 3.08 17.565 811. 811. 54.1544 .0213 1.00 .12 18.97 0 .0000 1
2 3 15.300 317.10 3.37 15.948 803. 803. 53.7437 .0213 .31 .13 17.10 0 .0000 1
2 4 7.700 315.12 3.37 15.951 738. 738. 53.7915 .0213 -.50 .13 15.12 0 .0000 1
2 5 .000 313.67 3.07 17.669 802. 802. 54.1815 .0212 -.77 .12 13.67 0 .0000 1
FRMX= .133 IFRMX= 3 FRMN= .115 IFRMN= 5

```

Definition of Variables in Tributary Debug Information Table

RELX ITR - Iteration counter
JRIVER - River number
ERQ - Flow error
QOLD - Flow at previous time step (cfs or cms)
QNEW - Flow at current time step (cfs or cms)

TABLE 21.22. Downwater Debug Information

DOWNWATER	IN= 9	YNN= 506.91	DEP= 5.71			
	ITD= 1	I= 10	YDWO= 498.12	YDWN= 498.48	F= 13278.2	
	ITD= 2	I= 10	YDWO= 498.48	YDWN= 498.50	F= 806.1	
	ITD= 3	I= 10	YDWO= 498.50	YDWN= 498.50	F= 3.2	
	ITD= 1	I= 10	YIL= 506.91	QII= 6000.	YA= 494.98	F= 234737.9
	ITD= 2	I= 10	YIL= 506.91	QII= 6000.	YA= 496.57	F= 94487.3
	ITD= 3	I= 10	YIL= 506.91	QII= 6000.	YA= 497.36	F= 50248.1
	ITD= 4	I= 10	YIL= 506.91	QII= 6000.	YA= 497.76	F= 32323.5
	ITD= 5	I= 10	YIL= 506.91	QII= 6000.	YA= 497.96	F= 24246.5
	ITD= 6	I= 10	YIL= 506.91	QII= 6000.	YA= 498.06	F= 20412.3
	ITD= 7	I= 10	YIL= 506.91	QII= 6000.	YA= 498.11	F= 18544.5
	ITD= 8	I= 10	YIL= 506.91	QII= 6000.	YA= 498.13	F= 17623.3
	ITD= 9	I= 10	YIL= 506.91	QII= 6000.	YA= 498.14	F= 17165.2
	ITD= 10	I= 10	YIL= 506.91	QII= 6000.	YA= 498.15	F= 16937.4
	ITD= 11	I= 10	YIL= 506.91	QII= 6000.	YA= 498.15	F= 16823.2
.						
.						
.	I= 12	QIR= 6000.	YIR= 481.35	DEP= 8.35	ITD= 12	
BACKWATER	IN= 9	YNN= 506.91	DEP= 5.71			
	ITB= 1	I= 8	YBWO= 517.84	YBWN= 515.79	F= -73417.240	
	ITB= 2	I= 8	YBWO= 515.79	YBWN= 516.08	F= 13213.320	
	ITB= 3	I= 8	YBWO= 516.08	YBWN= 516.08	F= 30.392	
I= 8	QIL= 6000.	YIL= 516.08	DEP= 5.48	ITB= 3		
	ITB= 1	I= 7	YBWO= 526.82	YBWN= 525.19	F= -79298.310	
	ITB= 2	I= 7	YBWO= 525.19	YBWN= 524.73	F= -14139.490	
	ITB= 3	I= 7	YBWO= 524.73	YBWN= 524.82	F= 4193.991	
	ITB= 4	I= 7	YBWO= 524.82	YBWN= 524.82	F= 6.298	
.						
.						
.	I= 3	QIL= 6000.	YIL= 589.18	DEP= 5.85	ITB= 3	
	ITB= 1	I= 2	YBWO= 607.14	YBWN= 605.69	F= -207120.900	
	ITB= 2	I= 2	YBWO= 605.69	YBWN= 605.67	F= -1737.361	
	ITB= 3	I= 2	YBWO= 605.67	YBWN= 605.67	F= 1.942	
I= 2	QIL= 6000.	YIL= 605.67	DEP= 6.51	ITB= 3		
	ITB= 1	I= 1	YBWO= 623.30	YBWN= 621.57	F= -249028.800	
	ITB= 2	I= 1	YBWO= 621.57	YBWN= 621.52	F= -7117.417	
	ITB= 3	I= 1	YBWO= 621.52	YBWN= 621.52	F= -10.743	
I= 1	QIL= 6000.	YIL= 621.52	DEP= 6.52	ITB= 3		

Definition of Variables in Downwater Debug Information Table

IN	- Beginning cross section number for downwater computations
YNN	- Water surface elevation at initial boundary
DEP	- Water depth
ITD	- Iteration counter
I	- Cross section number
YDWO	- Old guess for the water surface elevation (ft or m)
YDWN	- New guess for the water surface elevation (ft or m)
F	- Difference between the computed discharge and the actual discharge
YIL	- Initial water surface elevation (ft or m)
QII	- Initial discharge (cfs or cms)
YA	- Average water surface elevation within the reach (ft or m)

TABLE 21.23. Conveyance Debug Information

GENERATING CONVEYANCE CURVE

QKT(K)=	0.	4.	23.	67.	144.	261.	425.	641.
QKT(K)=	915.	1253.	1659.	2139.	2698.	3340.	4070.	4892.
QKT(K)=	5811.	6830.	7955.	9189.	10535.	11999.	13584.	15294.

.

.

QKT(K)=	6281732.	6348753.	6279316.	6180960.	6090048.	6005922.	5927997.	5855756.
QKT(K)=	5788739.	5743179.	5729040.	5716623.	5705842.	5696618.	5688877.	5682550.
QKT(K)=	5677571.	5673881.	5671424.					

QKT(K)=	0.	4.	23.	67.	144.	261.	425.	641.
QKT(K)=	915.	1253.	1659.	2139.	2698.	3340.	4070.	4892.
QKT(K)=	5811.	6830.	7955.	9189.	10535.	11999.	13584.	15294.

.

.

QKT(K)=	6281732.	6348753.	6308910.	6269067.	6229224.	6189381.	6149538.	6109695.
QKT(K)=	6069852.	6030009.	5990166.	5950323.	5910480.	5870637.	5830794.	5790951.
QKT(K)=	5751108.	5711265.	5671424.					

BKT(K)=	1.060	1.124	1.076	1.067	1.064	1.063	1.062	1.061
BKT(K)=	1.061	1.061	1.061	1.061	1.060	1.060	1.060	1.060
BKT(K)=	1.060	1.060	1.060	1.060	1.060	1.060	1.060	1.060

.

.

BKT(K)=	1.140	1.140	1.140	1.140	1.140	1.140	1.140	1.140
BKT(K)=	1.140	1.139	1.139	1.139	1.139	1.139	1.139	1.138
BKT(K)=	1.138	1.138	1.138					

J= 1 I= 1 L= 30 ERQK= 2.15 NKC(I,J)= 30

HKC(L,I,J)=	500.10	500.36	500.61	500.87	501.12	501.38	501.64	501.89
HKC(L,I,J)=	502.15	502.40	502.66	503.17	503.68	504.45	505.22	506.24
HKC(L,I,J)=	507.52	509.06	510.08	511.87	513.66	515.71	518.27	521.08
HKC(L,I,J)=	524.67	528.76	533.88	541.04	545.65	549.74		

QKC(L,I,J)=	0.	4.	23.	67.	144.	261.	425.	641.
QKC(L,I,J)=	915.	1253.	1659.	2698.	4070.	6830.	10535.	17132.
QKC(L,I,J)=	28377.	46855.	62858.	106576.	166867.	261695.	427088.	679722.
QKC(L,I,J)=	1125954.	1832946.	3056293.	5309196.	6308910.	5671424.		

BEV(L,I,J)=	1.060	1.124	1.076	1.067	1.064	1.063	1.062	1.061
BEV(L,I,J)=	1.061	1.061	1.061	1.060	1.060	1.060	1.060	1.060
BEV(L,I,J)=	1.060	1.060	1.060	1.102	1.147	1.177	1.190	1.188
BEV(L,I,J)=	1.177	1.164	1.149	1.137	1.140	1.138		

SNM(K, 1, 1)=	1.00	1.00	1.00	1.00	1.00	1.00	1.00	1.00
SNM(K, 2, 1)=	1.00	1.00	1.00	1.00	1.00	1.00	1.00	1.00
SNM(K, 3, 1)=	1.00	1.00	1.00	1.00	1.00	1.00	1.00	1.00

.

.

SNM(K, 88, 1)=	1.00	1.00	1.00	1.00	1.00	1.00	1.00	1.00
SNM(K, 89, 1)=	1.00	1.00	1.00	1.00	1.00	1.00	1.00	1.00

ERQMX= 2.14 2.13 2.15 2.13 2.15 2.14 2.15 2.15 2.14 1.79* 1.79 1.79 1.79 1.79 1.79 1.78 1.79 1.78 1.78 1.79
ERQMX= 1.78 1.79 1.79 1.78 1.49 1.49 1.48 1.48 1.49 1.49* 1.49 1.49 1.49 1.49 1.24 1.24 1.24 1.49 1.24 1.48
ERQMX= 1.24 1.49 1.46 1.49 1.49 1.24 1.24 1.49 1.24 1.24* 1.24 1.03 1.24 1.24 1.24 1.24 1.24 1.24 1.03 1.03
ERQMX= .86 1.03 .86 .86 .86 .86 .72 .72 .72 .72* .72 .72 .72 .72 .72 .71 .72 .71 1.79 .86
ERQMX= .86 .86 .86 .86 .86 .85 .86 .86 .86

SNC(K, 1, 1)=	1.00	1.00	1.00	1.00	1.00	1.00	1.00	1.00
SNC(K, 2, 1)=	1.00	1.00	1.00	1.00	1.00	1.00	1.00	1.00
SNC(K, 3, 1)=	1.00	1.00	1.00	1.00	1.00	1.00	1.00	1.00

.

.

SNC(K, 87, 1)=	1.00	1.00	1.00	1.00	1.00	1.00	1.00	1.00
SNC(K, 88, 1)=	1.00	1.00	1.00	1.00	1.00	1.00	1.00	1.00
SNC(K, 89, 1)=	1.00	1.00	1.00	1.00	1.00	1.00	1.00	1.00

Definition of Variables in Conveyance Debug Information Table

QKT(K)	- Discharges in the initial conveyance curve (cfs or cms)
BKT(K)	- Initial beta correction coefficient used in the momentum equation
J	- River number
I	- Cross section number
L	- Final number of points in the conveyance table
ERQK	- Flow difference between two points on the conveyance curve
NKC(L,J)	- Number of points in the conveyance curve for cross section I on river J
HKC(L,I,J)	- Elevations in the final conveyance table (ft or m)
QKC(L,I,J)	- Discharges in the final conveyance curve (cfs or cms)
BEV(L,I,J)	- Final beta correction coefficient used in the momentum equation
SNM	- Sinuosity coefficient used in the momentum equation
ERQMX	- Error in maximum flow
SNC	- Sinuosity coefficient used in the continuity equation

TABLE 21.24. Cross Section Debug Information

** COMPUTE INITIAL FLOW, NORMAL AND INITIAL DEPTH FOR RIVER NO 1 **

```
(QDI(I,1),I=1,N)
288000. 288000. 296372. 296372. 296372. 296372. 296372. 351172.
351172. 351172. 404950. 404950. 404950. 404950. 404950. 404950.
405724. 613724. 613724. 613724. 613724. 613724. 613724. 613724.

(QDI(I,2),I=1,N)
54800. 54800. 54800. 54800. 54800.

(QDI(I,3),I=1,N)
53200. 53200. 53200. 53200. 53778.

(QDI(I,4),I=1,N)
200000. 200000. 200000. 200000. 200000. 208000. 208000. 208000.
208000. 208000. 208000.
```

INITIAL DISCHARGES:

```
(QDI FOR RIVER NO. 1
288000. 288000. 296372. 296372. 296372. 296372. 296372. 351172.
351172. 351172. 404950. 404950. 404950. 404950. 404950. 404950.
405724. 613724. 613724. 613724. 613724. 613724. 613724. 613724.
```

** COMPUTE NORMAL/CRITICAL DEPTH **

```
AS(1, 1 1)= 13820. > 0.0; SUB-CRITICAL FLOW ASSUMED!
AS(1, 2 1)= 11627. > 0.0; SUB-CRITICAL FLOW ASSUMED!
AS(1, 3 1)= 9750. > 0.0; SUB-CRITICAL FLOW ASSUMED!
AS(1, 4 1)= 5727. > 0.0; SUB-CRITICAL FLOW ASSUMED!
AS(1, 5 1)= 10243. > 0.0; SUB-CRITICAL FLOW ASSUMED!
AS(1, 6 1)= 15683. > 0.0; SUB-CRITICAL FLOW ASSUMED!
AS(1, 7 1)= 6085. > 0.0; SUB-CRITICAL FLOW ASSUMED!
I= 8 X= 1014.500 YN= 314.37 DEPN= 24.37 YC= 297.72 DEPC= 7.72 IFR= 0 ITN= 0
ITC= 14
AS(1, 9 1)= 16740. > 0.0; SUB-CRITICAL FLOW ASSUMED!
AS(1, 10 1)= 20344. > 0.0; SUB-CRITICAL FLOW ASSUMED!
AS(1, 11 1)= 5440. > 0.0; SUB-CRITICAL FLOW ASSUMED!
AS(1, 12 1)= 8234. > 0.0; SUB-CRITICAL FLOW ASSUMED!
AS(1, 13 1)= 12807. > 0.0; SUB-CRITICAL FLOW ASSUMED!
AS(1, 14 1)= 12983. > 0.0; SUB-CRITICAL FLOW ASSUMED!
AS(1, 15 1)= 15838. > 0.0; SUB-CRITICAL FLOW ASSUMED!
AS(1, 16 1)= 7059. > 0.0; SUB-CRITICAL FLOW ASSUMED!
AS(1, 17 1)= 22460. > 0.0; SUB-CRITICAL FLOW ASSUMED!
AS(1, 18 1)= 23569. > 0.0; SUB-CRITICAL FLOW ASSUMED!
AS(1, 19 1)= 14143. > 0.0; SUB-CRITICAL FLOW ASSUMED!
AS(1, 20 1)= 20793. > 0.0; SUB-CRITICAL FLOW ASSUMED!
AS(1, 21 1)= 18379. > 0.0; SUB-CRITICAL FLOW ASSUMED!
AS(1, 22 1)= 22182. > 0.0; SUB-CRITICAL FLOW ASSUMED!
AS(1, 23 1)= 21317. > 0.0; SUB-CRITICAL FLOW ASSUMED!
AS(1, 24 1)= 28453. > 0.0; SUB-CRITICAL FLOW ASSUMED!
```

Definition of Variables in Cross Section Debug Information Table

AS	- Area of cross section (sq-ft or sq-m)
I	- Cross section number
X	- Cross section location (mile or km)
YN	- Normal flow water surface elevation (ft or m) for initial flow at t=0
DEPN	- Normal flow depth (ft or m) for initial flow
YC	- Critical flow water surface elevation (ft or m) for initial flow at t=0
DEPC	- Critical flow depth (ft or m)
IFR	- Froude number indicator: 0 indicates $Fr < 1$, 1 indicates $Fr > 1$
ITN	- Number of iterations to obtain YN via bi-section solution method
ITC	- Number of iterations to obtain YC via bi-section solution method

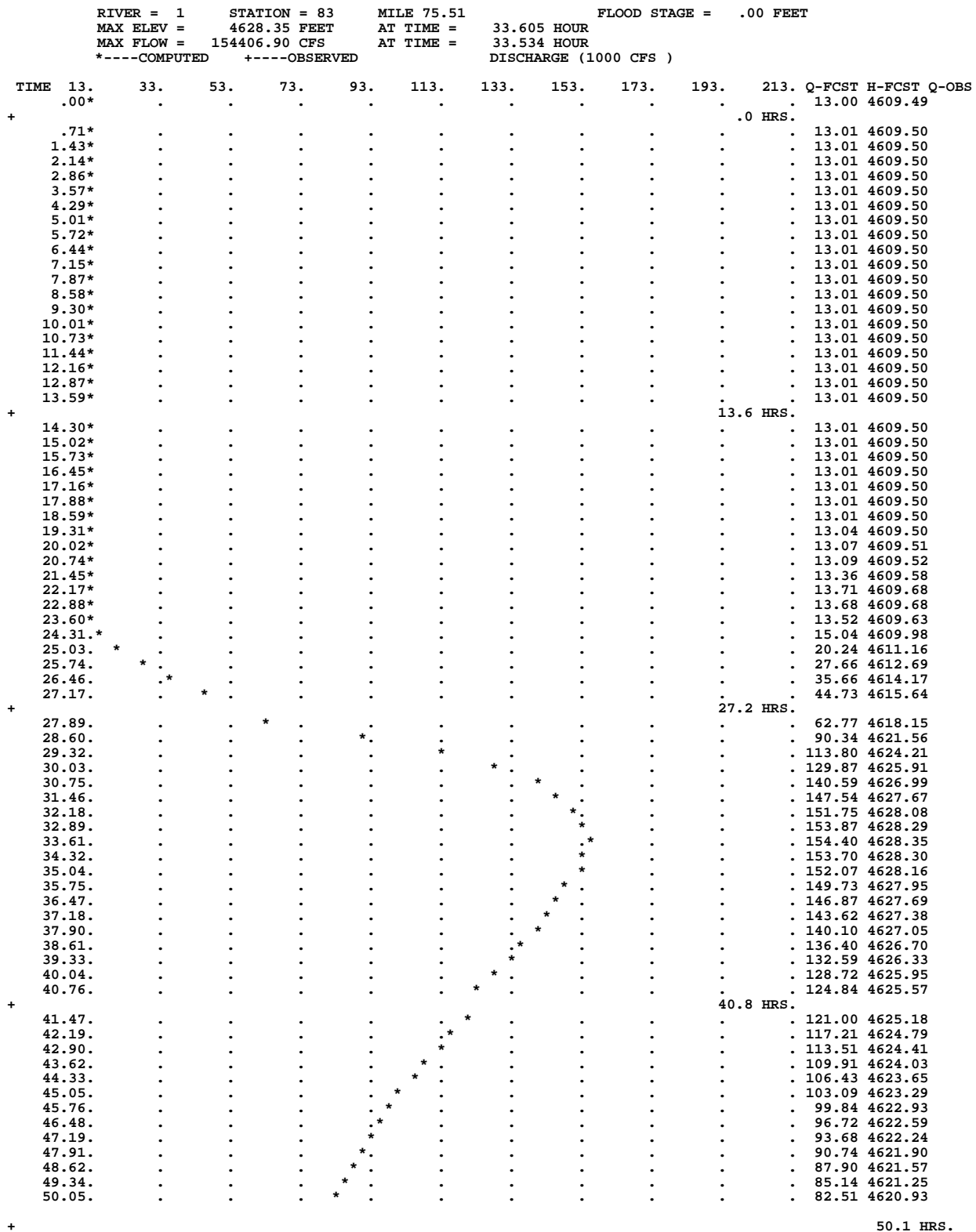
TABLE 21.25. Cross Section Calibration Debug Information

DOUBLE MAX ITERATION FOR CALIBRATION, ITMAX=										20
RIVER NO. 1	REACH NO. 1	JACKSON MI 216				STA NO. 1	RIVER MILE=			216.000
RIVER NO. 1	MANNING N REACH NO. 1									
FKC= 61.8575		FMC= .2500		FKF= 57.3247		FMF= .4000		FKO= .0000		FMO= .0000
X(I,J)	216.00	210.00	205.00	200.00	199.99	194.99	190.00	185.00		
X(I,J)	184.00	183.00	182.00	181.00	180.00	179.99	179.00	178.00		
IFXC=	0	0	0	0	0	0	0	0		
IFXC=	0	0	0	0	0	0	1	1	1	
HS=	906.30	908.30	916.30	920.30	936.30	1036.30				
BS=	.00	73.56	110.00	209.81	300.00	300.00				
AS=	0.	74.	808.	1447.	5526.	35526.				
TT = .00000 DTH = 6.00000 HRS ITMX= 0										
RIVER= 1	MANNING	REACH= 1	QU(1)= .094	YU(1)= 908.54	QU(N)= .300	YU(N)= 854.68				
J	I	X	Y	V	A	B	BT	Q	CMM	
1	1	216.00	908.54	1.03	92.	75.	75.	.09	.0400	
1	2	210.00	903.39	.52	180.	80.	80.	.09	.0400	
1	3	205.00	896.26	2.25	42.	55.	55.	.09	.0400	
1	4	200.00	894.06	.34	277.	85.	85.	.09	.0400	
.										
1	11	182.00	883.23	.25	1183.	176.	176.	.30	.0400	
1	12	181.00	883.21	.22	1378.	201.	201.	.30	.0400	
1	13	180.00	883.20	.19	1596.	214.	214.	.30	.0400	
1	14	179.99	858.97	1.13	266.	110.	110.	.30	.0400	
1	15	179.00	856.11	1.74	172.	110.	110.	.30	.0400	
1	16	178.00	854.68	.73	409.	160.	160.	.30	.0400	

Definition of Variables in Cross Section Calibration Debug Information Table

FKC	- Scaling parameter of in-bank channel portion of cross section
FMC	- Shape factor for in-bank channel portion of cross section
FKF	- Scaling parameter of flood plain portion of cross section
FKO	- Scaling parameter of inactive portion of cross section
FMO	- Shape factor for inactive portion of cross section
X	- Cross section location (mile or km)
I	- Cross section number
J	- River number
IFXC	- Parameter indicating if cross sections have special properties
HS	- Height of section (ft or m)
BS	- Topwidth of section (ft or m)
AS	- Area of cross section (sq-ft or sq-m)
TT	- Time at which output is given (hrs)
DTH	- Computational time step
ITMX	- Number of iterations in Newton Raphson solution of Saint-Venant equations
RIVER	- River number
QU(1)	- Discharge (cfs or cms) at upstream boundary
YU(1)	- Water surface elevation (ft or m) at upstream boundary
QU(N)	- Discharge (cfs or cms) at downstream boundary
YU(N)	- Water surface elevation (ft or m) at downstream boundary
Y	- Water surface elevation (ft or m) in cross section I
V	- Velocity (fps or mps) in cross section I
A	- Active area in cross section I (sq-ft or sq-m)
B	- Active topwidth in cross section I (ft or m)
BT	- Total topwidth in cross section I (ft or m)
Q	- Discharge (cfs or cms)

Figure 21.1. Hydrograph Plot



21.2 Graphical Output Utility - FLDGRF

The NWS FLDGRF program is a user friendly, menu-driven, DOS application which was developed to display the output data generated by the NWS FLDWAV model. The FLDWAV model generates 17 files which contain the hydraulic information for the dataset being run. The name of the output file is merged with each extension described in Table 21.26. All of these files are binary files except the .TTL file which is an ASCII file. The .TTL file contains a description of the problem, the names of rivers, and information needed by FLDGRF to access the other files. This file may be edited to change the descriptive lines only (i.e., river names and problem description).

When executed, the FLDGRF program will prompt the user for a dataset name (Figure 21.2). The user should enter the name of the file to be displayed without an extension. The program will read the information in the .TTL file. The Menu Options shown in Figure 21.3 will be displayed. There are 11 displays (Option 9 has 3 possible displays) available for each river in the dataset. An example of each display is shown in Figures 21.4-21.14. The boxes ahead of each display indicate the information needed prior to displaying the graph. The **bold** printing represents the option selected and/or the information supplied by the user. For river systems with multiple rivers, the user may select **R** which will display a list of names of all the rivers in the system (Figure 21.15). To view data from another dataset, the user may select the **A** option.

Except for Menu Options 7 and 8, the user will be prompted for cross-section locations and/or times. Exact values are not required. FLDGRF will use the value closest to the one specified. When entering cross-section locations, the river orientation is important. Although FLDGRF will display the graph in either direction, the user must specify the locations in the correct order. For example, Figure 21.3 displays the peak discharge profile of a river in which the mouth of the river is the zero location (as opposed to DAMBRK type datasets where the zero location is at the upstream end of the river). In this example the beginning location must be larger than the ending location.

Discharge and/or water-surface elevation hydrographs (Options 3 and 4) may be displayed at any interpolated cross section with the peak condition noted. The peak condition and its time of

occurrence will be shown. If observed data are available, computed vs. observed hydrographs will be displayed along with statistical information (root-mean-square (RMS) error and standard deviation (BIAS)). Multiple discharge hydrographs at several locations along the river (Option 9-3) may be displayed on the same graph. The user may select specific points along the river to be displayed or select a distance interval at which the hydrographs will be displayed.

Using Menu Options 1 and 2, profiles at the peak conditions (water-surface elevation and discharge) may be displayed for a specified reach of the river. The user must enter the range of data, and FLDGRF will display the peak condition for all interpolated cross sections in the specified range. Multiple "snapshots" in time of the river profile (Menu Options 9-1 and 9-2) may also be displayed. The user may select specific times for display or select a time interval at which the profiles will be displayed.

Cross sections (Menu Option 5) may be displayed at the actual locations only (not interpolated sections). The maximum water-surface elevation along with its corresponding topwidth, and the flood stage will be shown. In cases where the cross section has not been defined adequately in the vertical to accommodate the maximum condition, the display will not show the channel/valley bank above the maximum cross-section elevation.

Rating curves (Menu Option 6) may be displayed at any interpolated cross section. The maximum water-surface elevation and discharge will be shown.

The inflow hydrograph (Menu Option 7) may be displayed. In most cases, this display will be the same as shown when selecting the upstream location for Menu Options 3 or 4; however, if a dam is located at the upstream section, Menu Option 3 will display the outflow from the dam, not the inflow hydrograph.

The downstream boundary (Menu Option 8) may display either a hydrograph or rating curve as specified by FLDWAV. On tributaries, the downstream boundary will always be displayed as a water-surface elevation hydrograph.

TABLE 21.26. FLDGRF Files Generated by FLDWAV

EXTension	Description
.BS	Active topwidths (channel) for each actual cross section.
.BSL	Active topwidths (left floodplain) for each actual cross section.
.BSR	Active topwidths (right floodplain) for each actual cross section.
.BSS	Inactive topwidths for each actual cross section.
.DS	Downstream boundary information for the main river.
.FLD	Flood stages at each actual cross section.
.GZ	Gage information at each gaging station.
.H	WSELs at each interpolated cross section at each computational time step.
.HS	Elevation corresponding to eat topwidth (BS).
.LOC	Location of each actual cross section.
.OBS	Observed hydrographs at each gaging station.
.PK	Peak WSELs and discharges and their times at each cross section.
.Q	Discharges at each interpolated cross section at each computational time step.
.TIM	Computation time array.
.TTL	Description of data set and size of all necessary arrays
.US	Upstream boundary information for each river.
.X	Location of each interpolated cross section.

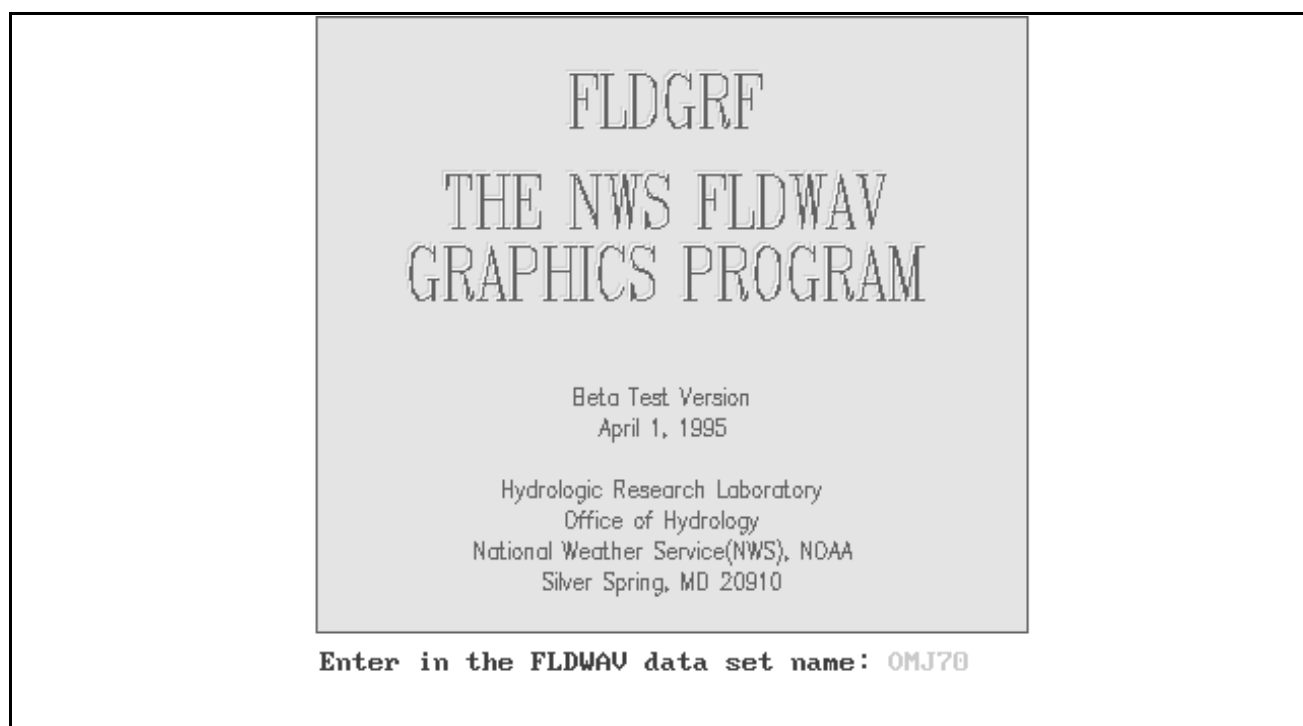


Figure 21.2 - Title Page

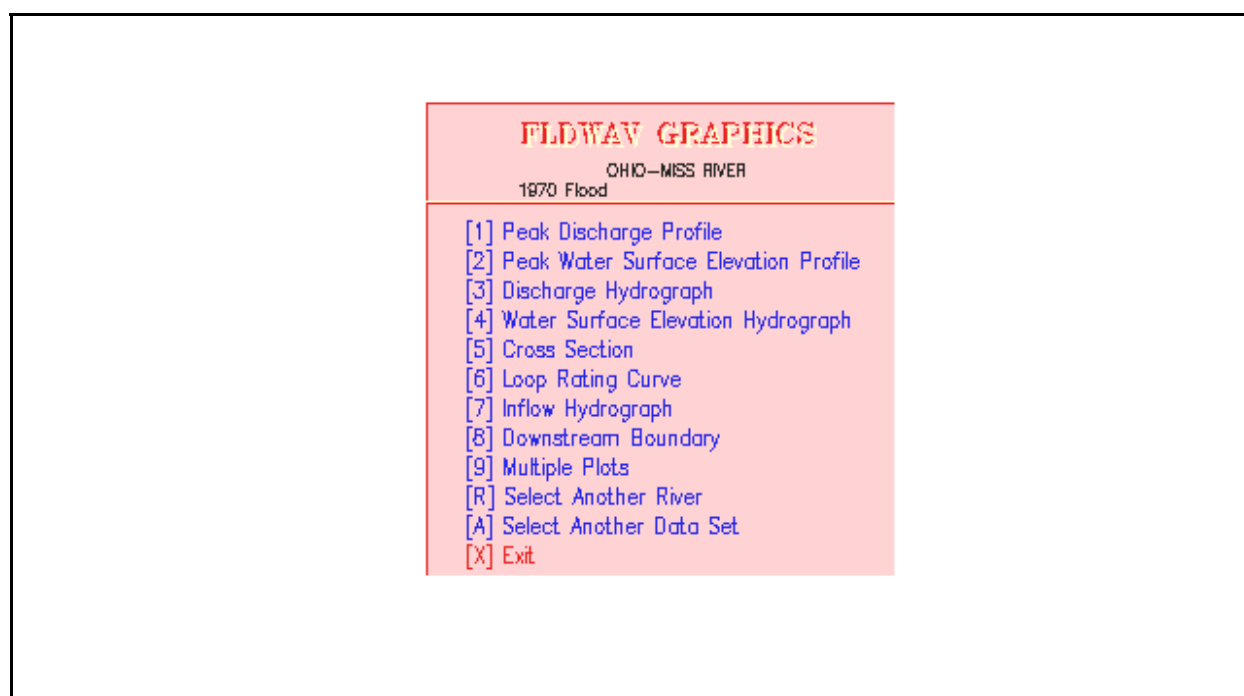


Figure 21.3 - FLDGRF Menu

Cross sections range from 1076.50 to 846.40 miles.

Beginning cross section location? 9999

Ending cross section location? 0

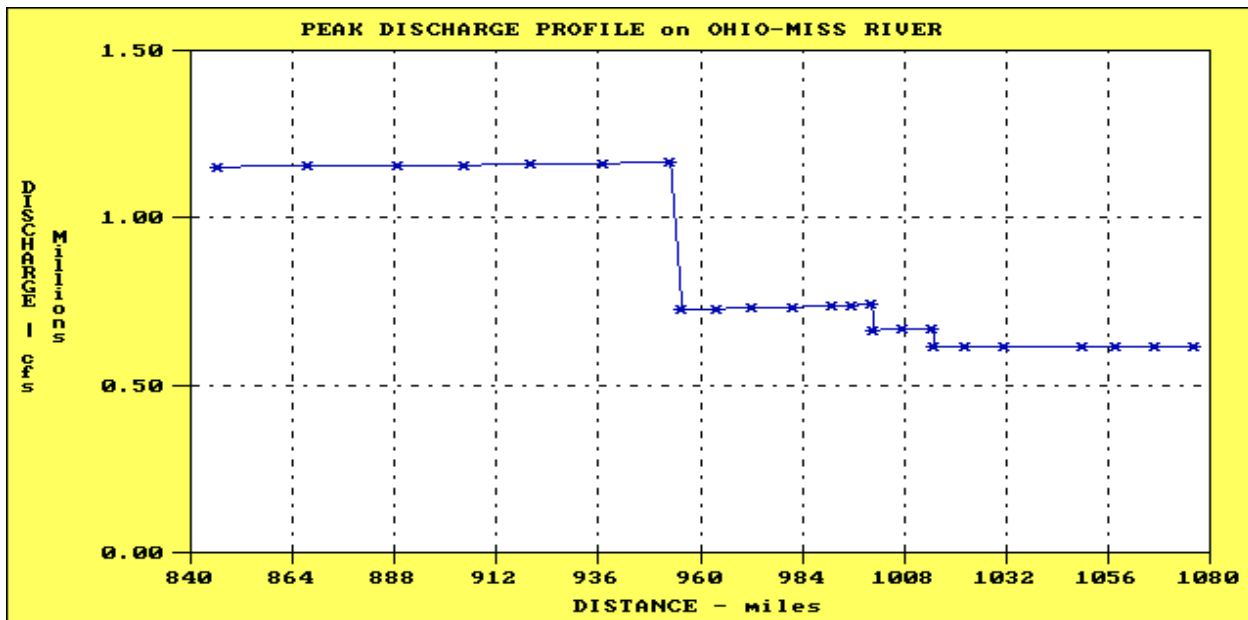


Figure 21.4 - Menu Option 1: Peak Discharge Profile

Cross sections range from 1076.50 to 846.40 miles.

Beginning cross section location? 9999

Ending cross section location? 0

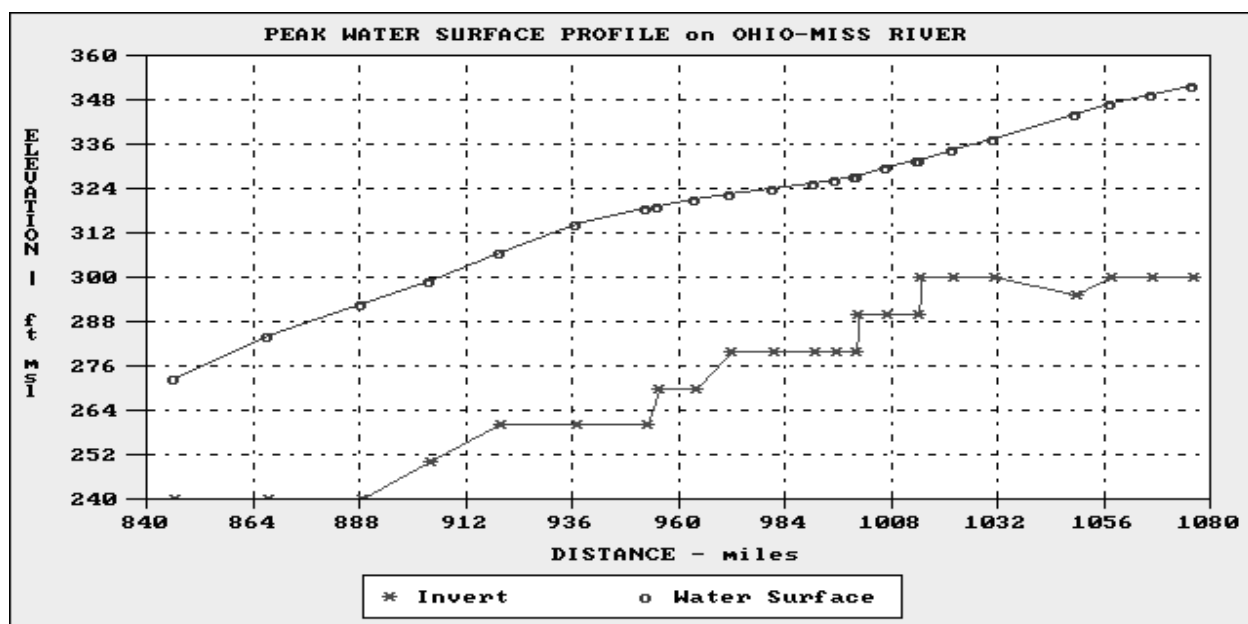


Figure 21.5 - Menu Option 2 : Peak Water Surface Elevation Profile

Cross section location? 0

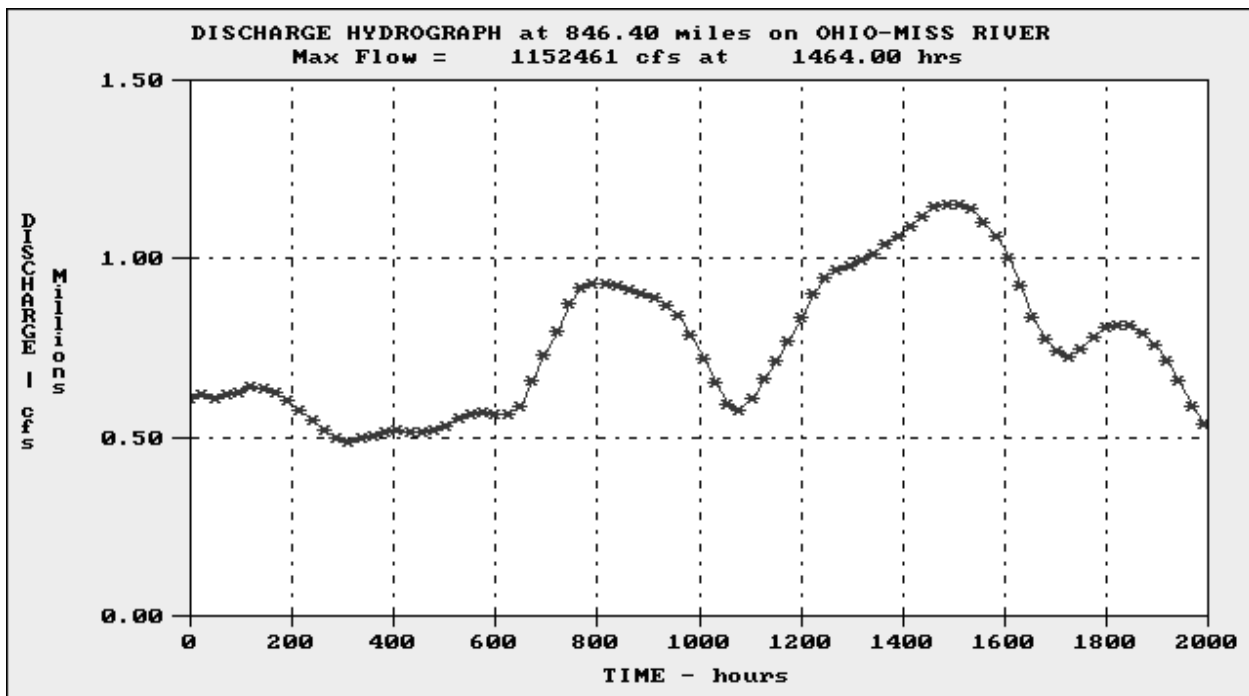


Figure 21.6 - Menu Option 3: Discharge Hydrographs

Cross section location? 0

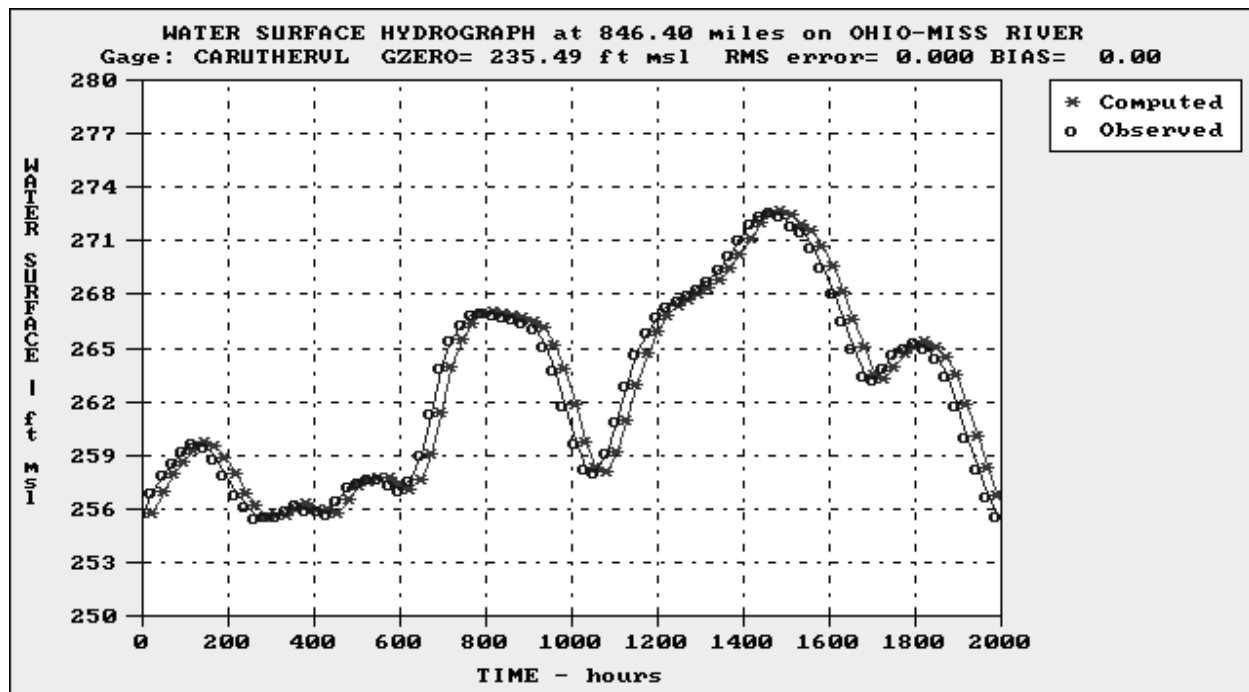


Figure 21.7 - Menu Option 4: Water Surface Elevation Hydrograph

Cross section location? 0

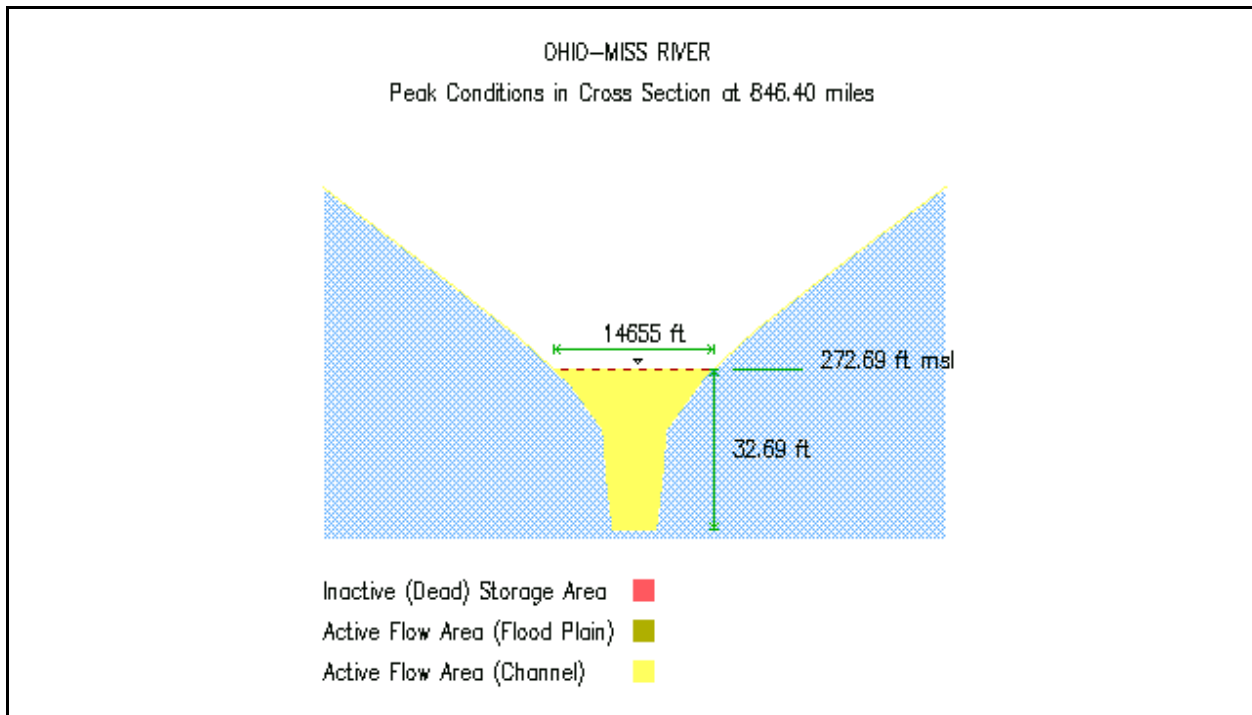


Figure 21.8 -Menu Option 5: Cross Section

Cross section location? 0

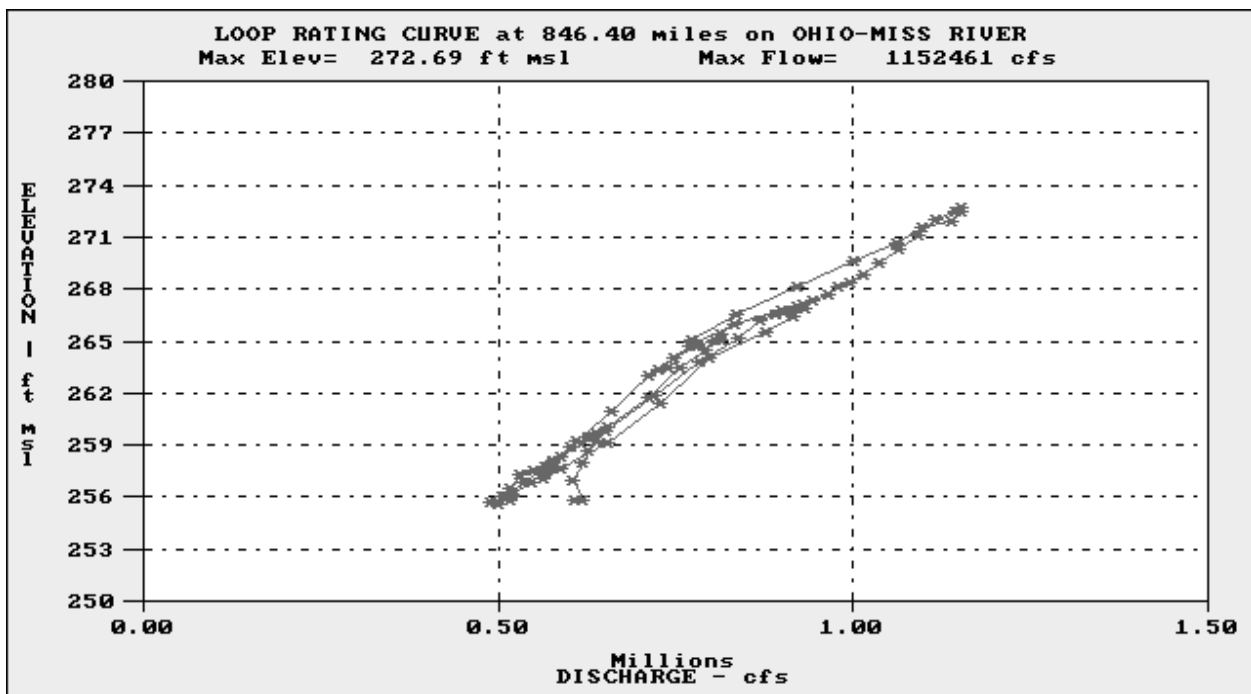


Figure 21.9 - Menu Option 6: Loop Rating Curve

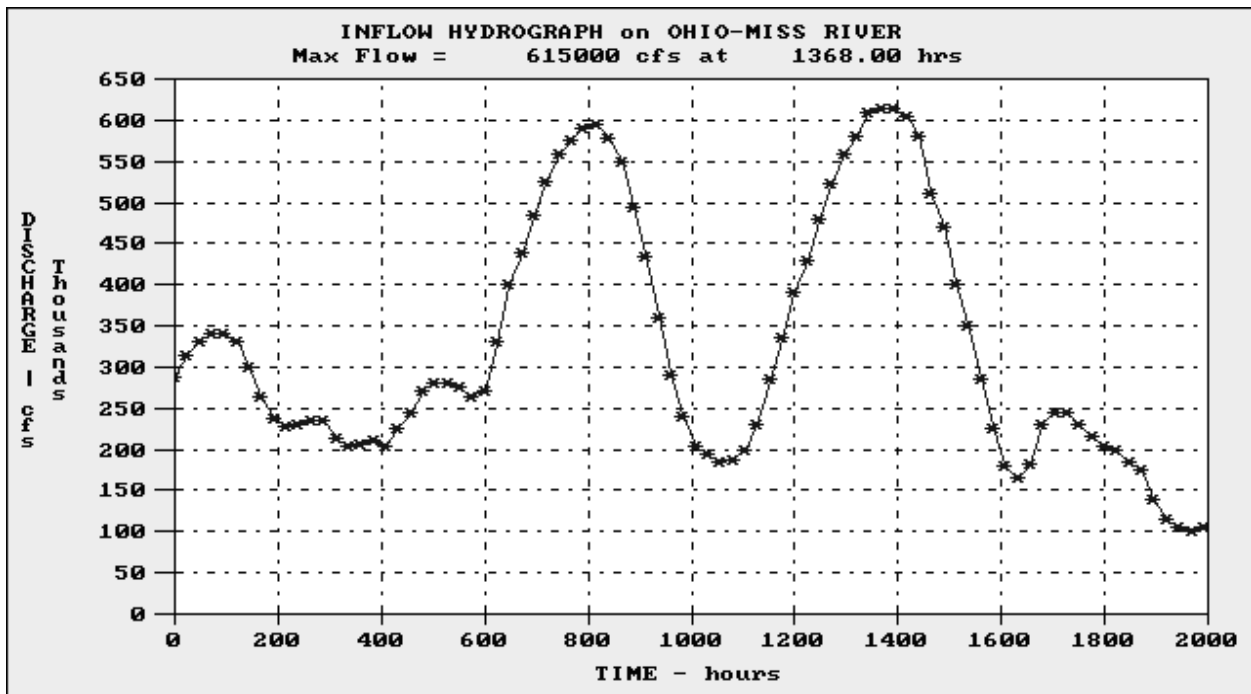


Figure 21.10 - Menu Option 7: Inflow Hydrograph

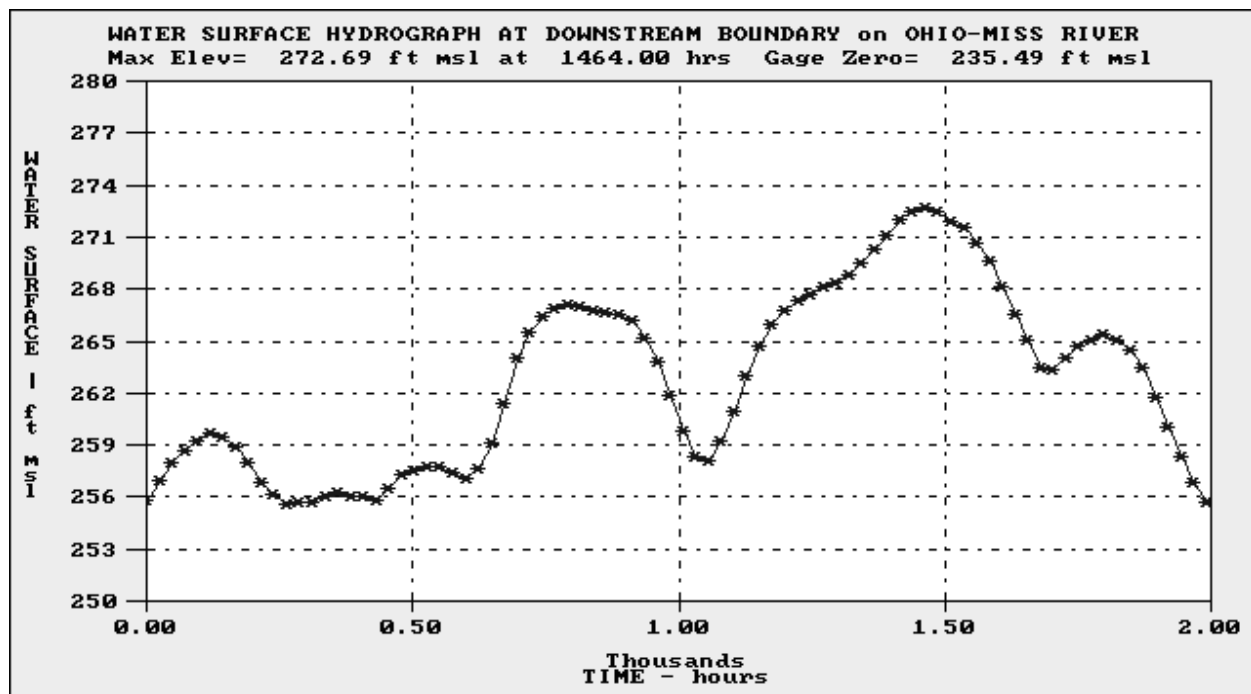


Figure 21.11 - Menu Option 8: Downstream Boundary

1) Multiple Water Surface Profiles

2) Multiple Discharge Profiles

3) Multiple Discharge Hydrographs

Enter **1**

1) Specify a Time Increment

2) List Profile Times

Enter **1**

Time of first profile? **0**

Step Increment: **600**

Cross sections range from 1076.50 to 846.40 miles.

Beginning cross section location? **9999**

Ending cross section location? **0**

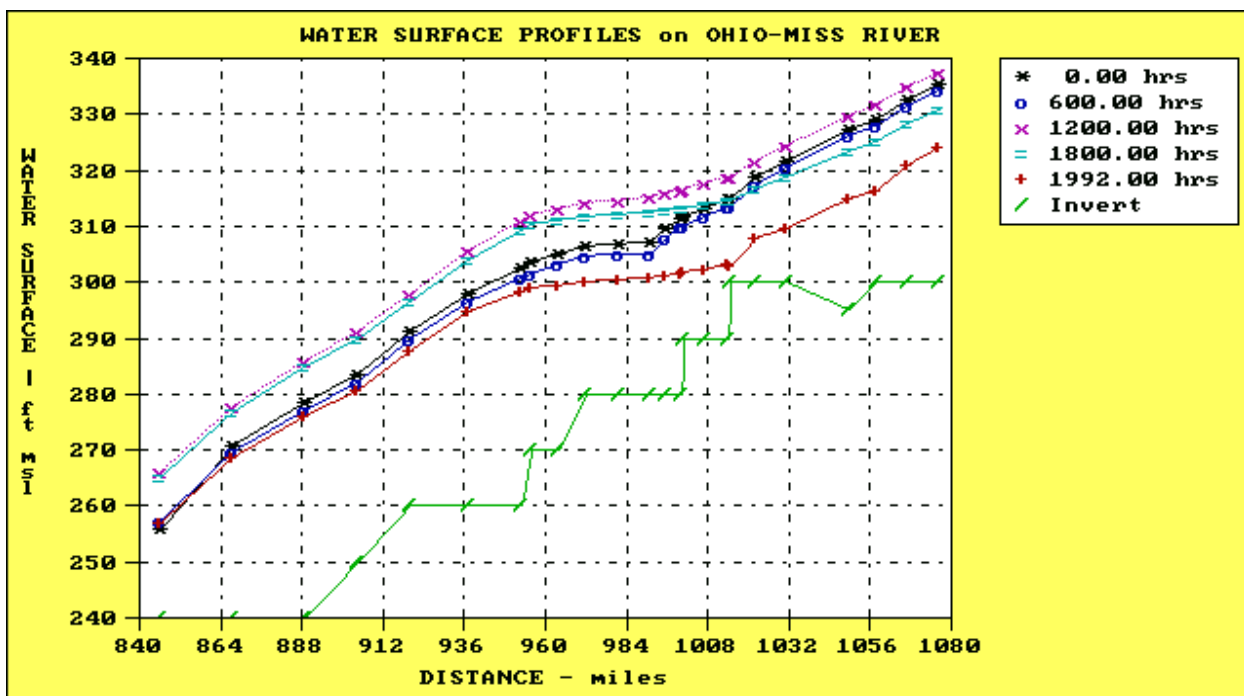


Figure 21.12 - Menu Option 9: Multiple Plots (Water Surface Profiles)

1) Multiple Water Surface Profiles
2) **Multiple Discharge Profiles**
3) Multiple Discharge Hydrographs
Enter **1**

1) **Specify a Time Increment**
2) List Profile Times
Enter **1**

Time of first profile? **0**
Step Increment: **600**

Cross sections range from 1076.50 to 846.40 miles.
Beginning cross section location? **9999**
Ending cross section location? **0**

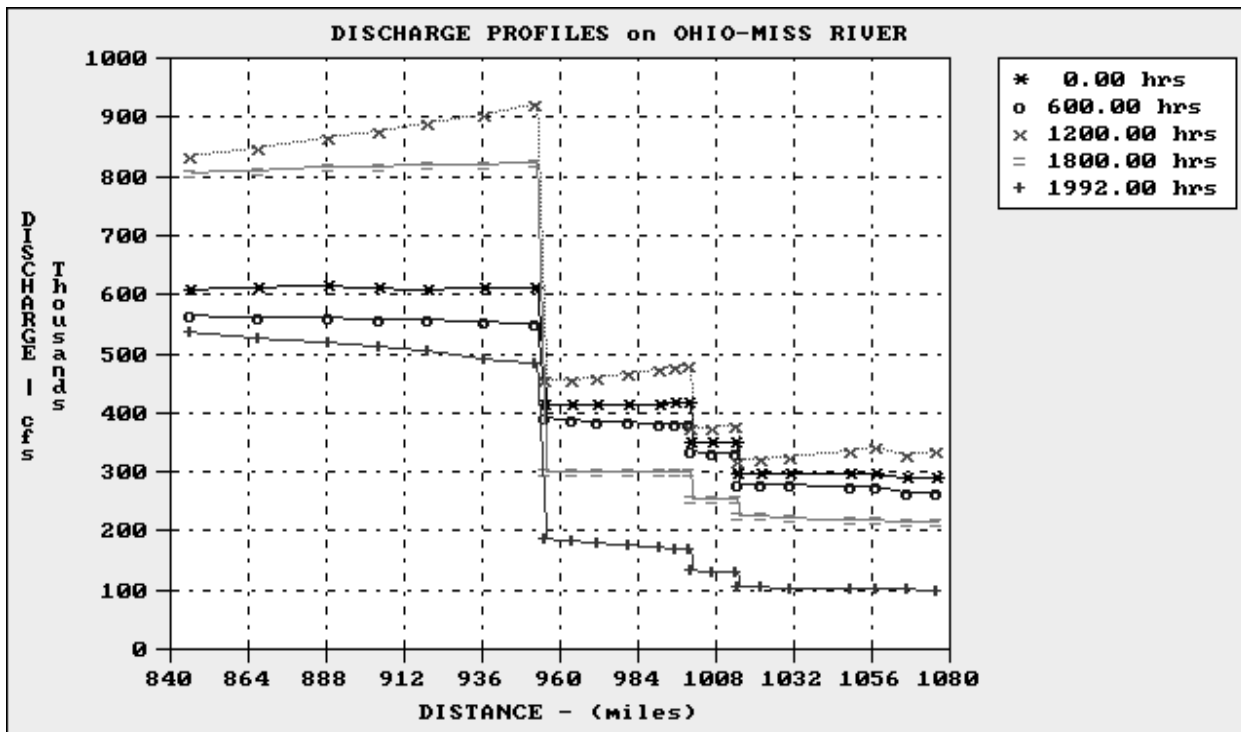


Figure 21.13 - Option 9: Multiple Plots (Discharge Profiles)

1) Multiple Water Surface Profiles
 2) Multiple Discharge Profiles
3) Multiple Discharge Hydrographs
 Enter 3

1) Specify a Time Increment
2) List Hydrograph Locations
 Enter 2

Number of Values (MAX:15)? 5
9999 1015 1000.8 955 0

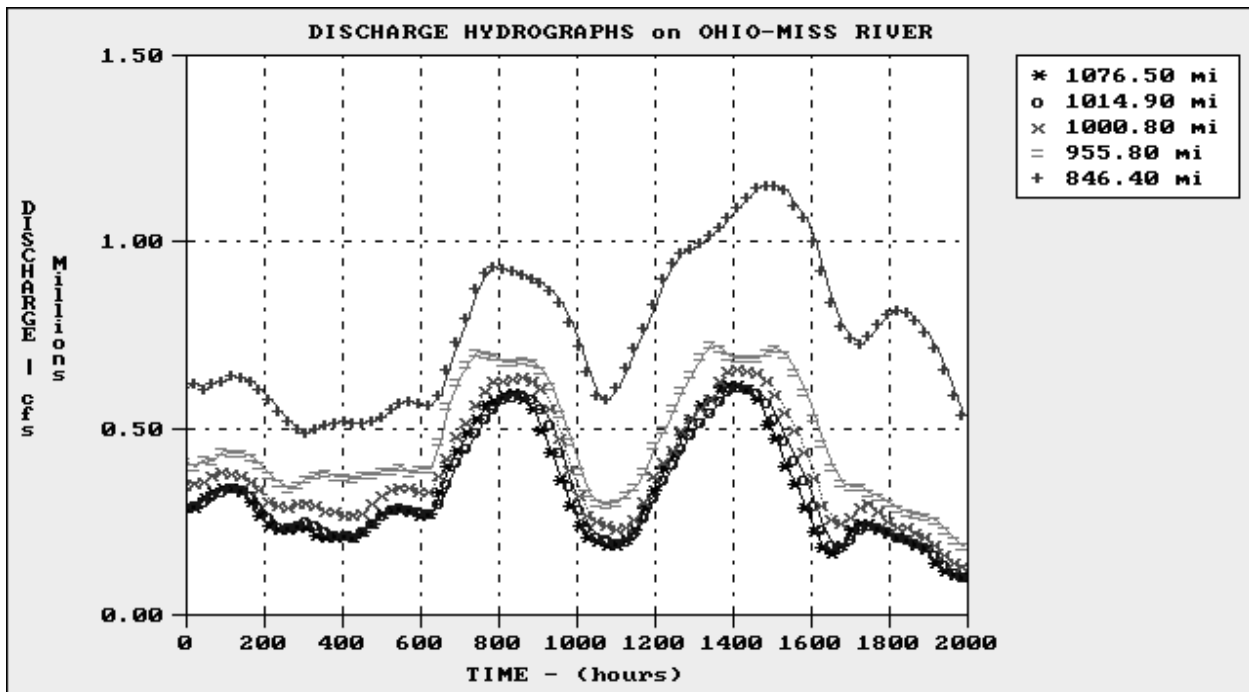


Figure 21.14- Option 9: Multiple Plots (Discharge Hydrographs)

River No.	River Name
1	OHIO-MISS RIVER
2	CUMBERLAND RVR
3	TENNESSEE RVR
4	UPPER MISS RVR

Enter River No. 4

Figure 21.15 - Menu Option R: Select Another River

21.21.2.1 Computer Requirements for FLDGRF

The minimum computer requirements to run FLDGRF are a 386-based IBM-compatible machine with 4mb of extended memory (RAM) and 10mb of computer storage space (a 200 mhz Pentiummachine is recommended), and a VGA color monitor. Although the executable file requires less than 150Kb of space, the files generated by FLDWAV could utilize space in excess of 10mb. FLDGRF is a DOS application and may be run in DOS 3.1 and higher, Windows 3.1 and higher, and Windows 95.

Currently, FLDGRF has no printing capabilities. To obtain a hard copy of the graphs, the users must capture the screen and print using a program with a screen capturing capability.

22. ILLUSTRATIVE EXAMPLES OF DATA INPUT

The following examples of data input illustrate some of the more frequently used options as well as some of the special features available within the FLDWAV model, e.g., time-dependent movable-gated spillway, level-pool routing with conveyance treatment of floodplains, channel sinuosity, lateral inflows, levees, metric input/output option, mixed subcritical/supercritical routing option, and the closed conduit (pressurized flow) option. Although the example numbers (except Example 7) correspond to the examples described in the DAMBRK documentation, some options have been changed. The examples include a brief physical description of the problem. A graphic display of the problem, a formatted input data set, and a listing (echo-print) of the input data set as printed-out by the FLDWAV model for each example are shown in this section.

22.1 FLDWAV Example 1.0 – Single Dam with Dynamic Routing

This example illustrates the use of FLDWAV to compute the outflow hydrograph from a breached dam and route it through a 59.5 mile-long downstream river/valley. The routing within the reservoir and through the valley is via the dynamic (Saint-Venant) method. The dam breaches when the dam crest (5288.0 ft.) is overtopped by 0.5 ft. The initial reservoir elevation is 5288.0 ft. The flow is entirely subcritical. There are 11 input cross sections downstream of the dam, 2 sections at the dam, and 1 section at the upstream end of the reservoir as shown in the schematic plan for Example 1 (Figure 22.1). The longitudinal profile giving the bottom slope of each reach is also shown along with the cross section at the dam depicting critical information about the dam and the breach. The input and output for this example are shown in Tables 22.1 and 22.2, respectively. This example is similar to DAMBRK Option 11.

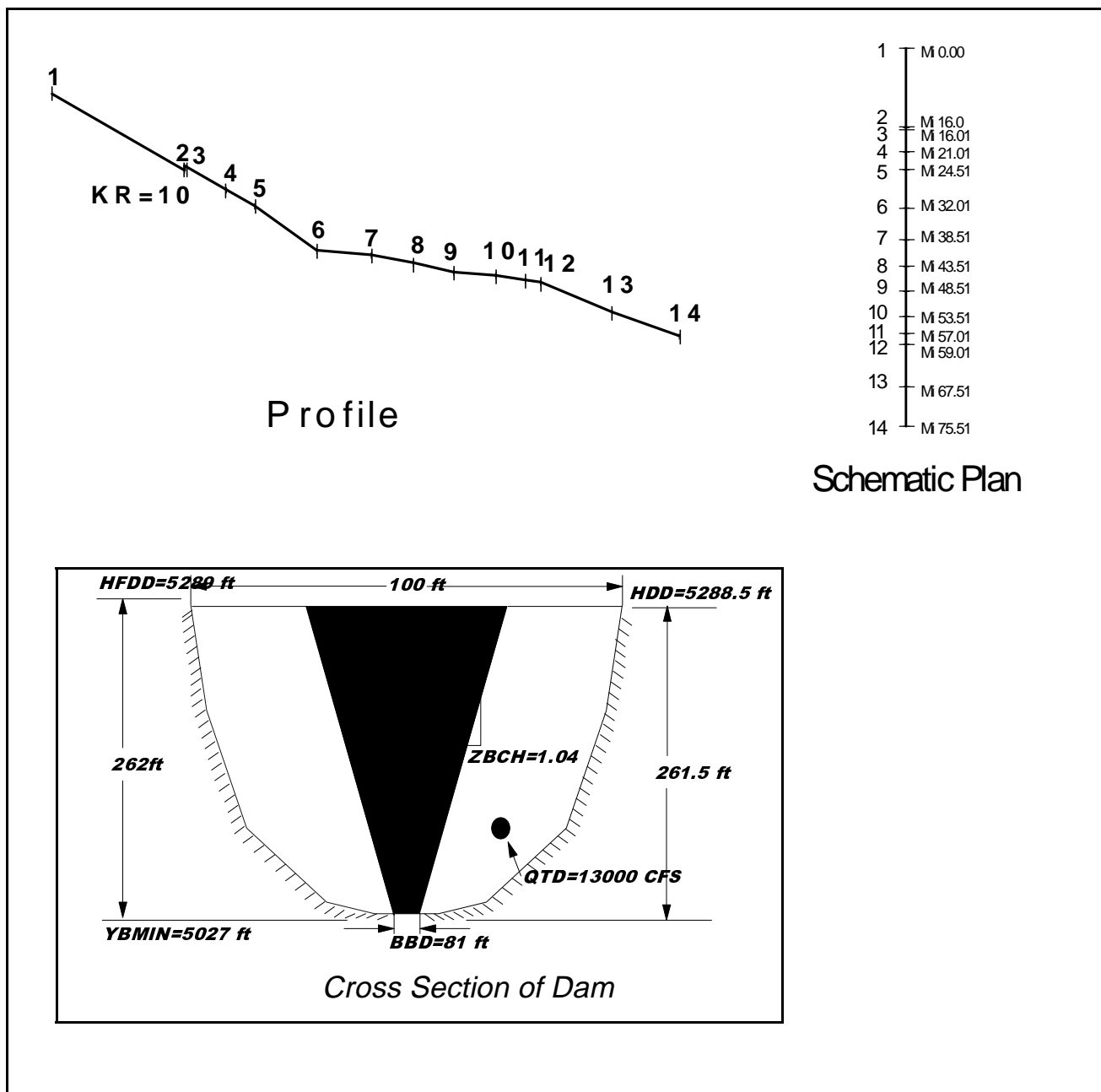


Figure 22.1 - Example 1.0 – Single Dam with Dynamic Routing.

Table 22.1 Input Data Set for Example 1

```

PROBLEM E-1
EOM
NO DESC

.01          1          0.6          5280.00  0          0
1           3           10           2           0           0           0 0 0 0
0           0           0           0
5           2           005           0           0
0           0           0           0           0
55.00       .0715       .715       0           0.       0
0           0           0
14          1           14  100.  0.  0.  0.
2   4   0   6   10   0   0 0 0 0
0   0   0   0 0 0 0 0 0 0
0.0         16         16.01      21.01      24.51      32.01      38.51      43.51
48.51       53.51      57.01      59.01      67.51      75.51      0
2.0         2.0        .5         .5         .5         .75        1.0        1.0
1.0         1.1        1.0        1.0        1.4        0
0           10         0         0         0         0         0         0
0           0         0         0         0         0         0
2           5288.5     100       3         13000.     0
0           0         0         0         0         0
1.43        0         5289.     81         1.04       5027.     1.         0.
1           2         3         5         12         14
MILE 0
MILE 16.
MILE 16.01
MILE 24.51
MILE 59.01
MILE 75.51
13000.       50000.0       13000.
0.0         1.0         55.0
5230.       0         0         0
5220.       5230.      5240.      5250.      5290.
200.        200.        200.        200.        200.
0           0         0         0         0
5037.       5288.5     0         0
5027.       5037.      5100.      5200.      5290.

```

200.	500.	1000.	1250.	1350.
0	0	0	0	0
5047.	0	0	0	
5027.	5037.	5051.	5107.	5125.
0.	590.	820.	1130.	1200.
0	0	0	0	0
4985.	0	0	0	0
4965.	4980.	5015.	5020.	5030.
0.	850.	1100.	1200.	1300.
0.	0.	3500.	4300.	5300.
4946.	0	0	0	
4920.	4930.	4942.	4953.	4958.
0.	800.	4000.	11000.	15000.
0.	0.	0.	7000.	10000.
4830.	0	0	0	
4817.	4827.	4845.	4847.	4852.
0.	884.	4000.	11000.	22000.
0.	0.	30000.	27000.	25000.
4820.	0	0	0	
4805.	4812.	4814.	4825.	4830.
0.	1000.	1200.	11000.	16000.
0.	0.	0.	6000.	8000.
4800.	0	0	0	
4788.	4792.	4802.	4808.	4810.
0.	286.	7000.	10000.	11000.
0.	0.	0.	3500.	5000.
4777.	0	0	0	
4762.	4774.	4777.	4780.	4785.
0.	352.	5000.	10000.	18000.
0.	0.	9000.	16000.	24000.
4767.	0	0	0	
4752.	4763.	4768.	4773.	4778.
0.	450.	3500.	6000.	9000.
0.	0.	4000.	8500.	12000.
4756.	0	0	0	
4736.	4756.	4761.	4763.	4768.
0.	540.	2000.	4000.	6000.
0.	0.	3700.	3700.	5500.

4749.	0	0	0						
4729.	4737.	4749.	4757.	4759.					
0.	250.	587.	1750.	2000.					
0.	0.	0.	1500.	2000.					
4674.	0	0	0						
4654.	4659.	4668.	4678.	4683.					
0.	70.	352.	400.	420.					
0.	0	0	0	0					
4612.	0	0	0						
4601.	4604.	4606.	4615.	4620.					
0.	245.	450.	500.	520.					
0.	0	0	0	0					
0	0	0	-0.9	0	0	0.1	-0.5		
0	0	0	0	0					
1	2	3	4	5	6	7	8	9	12
.06	.06	.05	.04	.04					
.03	.03	.03	.03	.03					
.08	.08	.08	.08	.08					
.05	.05	.05	.05	.05					
.031	.031	.031	.031	.031					
.034	.034	.034	.034	.034					
.038	.038	.038	.038	.038					
.037	.037	.037	.037	.037					
.034	.034	.034	.034	.034					
.036	.036	.036	.036	.036					

TETON DAM FAILURE -- E-1

SNAKE RIVER

Table 22.2 Echo Print of Example 1

PROGRAM FLDWAV - BETA VERSION 1.0 2/1/95

HYDROLOGIC RESEACH LABORATORY
W/OH3 OFFICE OF HYDROLOGY
NOAA, NATIONAL WEATHER SERVICE
SILVER SPRING, MARYLAND 20910

*** SUMMARY OF INPUT DATA ***

PROBLEM E-1

EPSY	THETA	F1	XFACT	DTHYD	DTOUT	METRIC		
0.010	1.000	0.600	5280.000	0.000	0.000	0		
JN	NU	ITMAX	KWARM	KFLP	NET	ICOND	FUTURE DATA	
1	3	10	2	0	0	0	0 0 0	
NYQD	KCG	NCG	KPRES					
0	0	0	0					
NCS	KPL	JNK	KREVR5	NFGRF				
5	2	5	0	0				
IOBS	KTERM	NP	NPST	NPEND				
0	0	0	0	0				
TEH	DTHII	DTHPLT	FRDFR	DTEXP	MDT			
55.000	0.07150	0.71500	0.00	0.00000	0			
NLEV	DHLV	DTHLV						
0	0.00000	0.00000						
RIVER NO.	NBT	NPT1	NPT2	EPQJ	COFW	VWIND	WINAGL	
1	14	1	14	100.00	0.00	0.00	0.00	
RIVER NO.	KU	KD	NQL	NGAGE	NRCM1	NQCM	NSTR	FUTURE DATA
1	2	4	0	6	10	0	0	0 0 0
RIVER NO.	MIXF	MUD	KFTR	KLOS	FUTURE DATA			
1	0	0	0	0	0 0 0 0 0 0			
XT(I, 1) I=1,NB(1)								
0.000	16.000	16.010	21.010	24.510	32.010	38.510	43.510	
48.510	53.510	57.010	59.010	67.510	75.510			
DXM(I, 1) I=1,NB(1)								
2.000	2.000	0.500	0.500	0.500	0.750	1.000	1.000	
1.000	1.100	1.000	1.000	1.400				
KRCH(I, 1) I=1,NRCH								
0	10	0	0	0	0	0		
0	0	0	0	0				
RIVER NO.	1,	DAM NO.	1					
LAD	HDD	CLL	CDOD	QTD	ICHAN			
2	5288.50	100.00	3.00	13000.00	0			
ICG	HSPD	SPL	CSD	HGTD	CGD			
0	0.00	0.00	0.00	0.00	0.00			

TFH	DTHDB	HFDD	BBD	ZBCH	YBMIN	BREXP	CPIP
1.430	0.00000	5289.00	81.00	1.04	5027.00	1.00	0.00

PLOTTING/OBSERVED TIME SERIES FOR RIVER J= 1

I	NGS	ID
1	1	MILE 0
2	2	MILE 16.
3	3	MILE 16.01
4	5	MILE 24.51
5	12	MILE 59.01
6	14	MILE 75.51

ST1(K,1), K = 1, NU
13000.00 50000.00 13000.00

T1(K,1), K = 1, NU
0.00 1.00 55.00

RIVER NO. 1

I=	1	FLDSTG= 5230.00	YDI= 0.00	QDI= 0.	AS1= 0.
		HS= 5220.00 5230.00 5240.00 5250.00 5290.00			
		BS= 200.0 200.0 200.0 200.0 200.0			
		BSS= 0.0 0.0 0.0 0.0 0.0			
I=	2	FLDSTG= 5037.00	YDI= 5288.50	QDI= 0.	AS1= 0.
		HS= 5027.00 5037.00 5100.00 5200.00 5290.00			
		BS= 200.0 500.0 1000.0 1250.0 1350.0			
		BSS= 0.0 0.0 0.0 0.0 0.0			
I=	3	FLDSTG= 5047.00	YDI= 0.00	QDI= 0.	AS1= 0.
		HS= 5027.00 5037.00 5051.00 5107.00 5125.00			
		BS= 0.0 590.0 820.0 1130.0 1200.0			
		BSS= 0.0 0.0 0.0 0.0 0.0			
I=	4	FLDSTG= 4985.00	YDI= 0.00	QDI= 0.	AS1= 0.
		HS= 4965.00 4980.00 5015.00 5020.00 5030.00			
		BS= 0.0 850.0 1100.0 1200.0 1300.0			
		BSS= 0.0 0.0 3500.0 4300.0 5300.0			
I=	5	FLDSTG= 4946.00	YDI= 0.00	QDI= 0.	AS1= 0.
		HS= 4920.00 4930.00 4942.00 4953.00 4958.00			
		BS= 0.0 800.0 4000.0 11000.0 15000.0			
		BSS= 0.0 0.0 0.0 7000.0 10000.0			
I=	6	FLDSTG= 4830.00	YDI= 0.00	QDI= 0.	AS1= 0.
		HS= 4817.00 4827.00 4845.00 4847.00 4852.00			
		BS= 0.0 884.0 4000.0 11000.0 22000.0			
		BSS= 0.0 0.0 30000.0 27000.0 25000.0			
I=	7	FLDSTG= 4820.00	YDI= 0.00	QDI= 0.	AS1= 0.
		HS= 4805.00 4812.00 4814.00 4825.00 4830.00			
		BS= 0.0 1000.0 1200.0 11000.0 16000.0			
		BSS= 0.0 0.0 0.0 6000.0 8000.0			
I=	8	FLDSTG= 4800.00	YDI= 0.00	QDI= 0.	AS1= 0.
		HS= 4788.00 4792.00 4802.00 4808.00 4810.00			
		BS= 0.0 286.0 7000.0 10000.0 11000.0			
		BSS= 0.0 0.0 0.0 3500.0 5000.0			
I=	9	FLDSTG= 4777.00	YDI= 0.00	QDI= 0.	AS1= 0.
		HS= 4762.00 4774.00 4777.00 4780.00 4785.00			
		BS= 0.0 352.0 5000.0 10000.0 18000.0			
		BSS= 0.0 0.0 9000.0 16000.0 24000.0			
I=	10	FLDSTG= 4767.00	YDI= 0.00	QDI= 0.	AS1= 0.
		HS= 4752.00 4763.00 4768.00 4773.00 4778.00			
		BS= 0.0 450.0 3500.0 6000.0 9000.0			
		BSS= 0.0 0.0 4000.0 8500.0 12000.0			
I=	11	FLDSTG= 4756.00	YDI= 0.00	QDI= 0.	AS1= 0.
		HS= 4736.00 4756.00 4761.00 4763.00 4768.00			

	BS=	0.0	540.0	2000.0	4000.0	6000.0	
	BSS=	0.0	0.0	3700.0	3700.0	5500.0	
I=	12	FLDSTG= 4749.00	YDI= 0.00	QDI= 0.	AS1= 0.		
	HS=	4729.00	4737.00	4749.00	4757.00	4759.00	
	BS=	0.0	250.0	587.0	1750.0	2000.0	
	BSS=	0.0	0.0	0.0	1500.0	2000.0	
I=	13	FLDSTG= 4674.00	YDI= 0.00	QDI= 0.	AS1= 0.		
	HS=	4654.00	4659.00	4668.00	4678.00	4683.00	
	BS=	0.0	70.0	352.0	400.0	420.0	
	BSS=	0.0	0.0	0.0	0.0	0.0	
I=	14	FLDSTG= 4612.00	YDI= 0.00	QDI= 0.	AS1= 0.		
	HS=	4601.00	4604.00	4606.00	4615.00	4620.00	
	BS=	0.0	245.0	450.0	500.0	520.0	
	BSS=	0.0	0.0	0.0	0.0	0.0	

REACH INFO RIVER NO. 1

FKEC(I,1), I = 1, NM(1)							
0.00	0.00	0.00	-0.90	0.00	0.00	0.10	-0.50
0.00	0.00	0.00	0.00	0.00			

NCM(K, 1), K=1,NRCM1(1)	1	2	3	4	5	6	7	8	9	12
CM(K, 1, 1)=				0.0600		0.0600		0.0500	0.0400	0.0400
CM(K, 2, 1)=				0.0300		0.0300		0.0300	0.0300	0.0300
CM(K, 3, 1)=				0.0800		0.0800		0.0800	0.0800	0.0800
CM(K, 4, 1)=				0.0500		0.0500		0.0500	0.0500	0.0500
CM(K, 5, 1)=				0.0310		0.0310		0.0310	0.0310	0.0310
CM(K, 6, 1)=				0.0340		0.0340		0.0340	0.0340	0.0340
CM(K, 7, 1)=				0.0380		0.0380		0.0380	0.0380	0.0380
CM(K, 8, 1)=				0.0370		0.0370		0.0370	0.0370	0.0370
CM(K, 9, 1)=				0.0340		0.0340		0.0340	0.0340	0.0340
CM(K,10, 1)=				0.0360		0.0360		0.0360	0.0360	0.0360

TETON DAM FAILURE -- E-1

22.2 FLDWAV Example 2.0 – Single Dam with Level-Pool Routing

This example illustrates the use of FLDWAV to simulate the breach of a dam and route it through a 59.5-mile-long downstream river/valley. Storage (level-pool) routing is used within the reservoir with the tailwater elevations computed via the Saint-Venant equations, and dynamic routing used through the 59.5 mile routing reach downstream of the dam. The flow is subcritical. There are 11 input cross sections downstream of the dam, and two sections at the dam with the one just upstream of the dam being the first cross section. This example is similar to DAMBRK option 11: Level Pool.

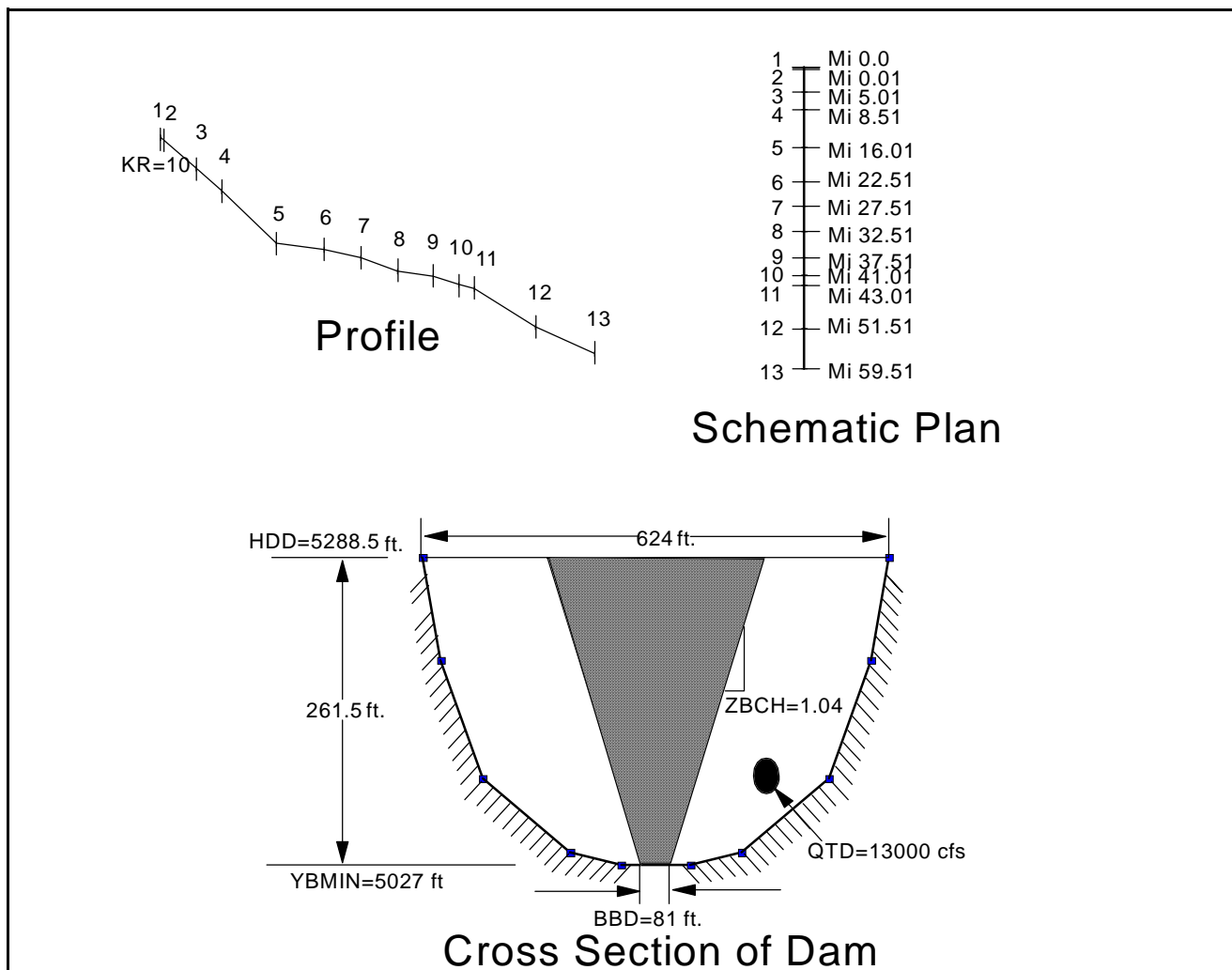


Figure 22.2 - Example 2.0 – Single Dam with Level-Pool Routing

PROBLEM E-2
EOM
NO DESC

22.10

5047.	0.	0.	0.	
5027.0	5037.0	5051.0	5107.0	5125.0
.0	590.0	820.0	1130.0	1200.0
.0	.0	.0	.0	.0
4985.	0.	0.	0.	
4965.0	4980.0	5015.0	5020.0	5030.0
.0	850.0	1100.0	1200.0	1300.0
.0	.0	3500.0	4300.0	5300.0
4946.	0.	0.	0.	
4920.0	4930.0	4942.0	4953.0	4958.0
.0	800.0	4000.0	11000.0	15000.0
.0	.0	.0	7000.0	10000.0
4830.	0.	0.	0.	
4817.0	4827.0	4845.0	4847.0	4852.0
.0	884.0	4000.0	11000.0	22000.0
.0	.0	30000.0	27000.0	25000.0
4820.	0.	0.	0.	
4805.0	4812.0	4814.0	4825.0	4830.0
.0	1000.0	1200.0	11000.0	16000.0
.0	.0	.0	6000.0	8000.0
4800.	0.	0.	0.	
4788.0	4792.0	4802.0	4808.0	4810.0
.0	286.0	7000.0	10000.0	11000.0
.0	.0	.0	3500.0	5000.0
4777.	0.	0.	0.	
4762.0	4774.0	4777.0	4780.0	4785.0
.0	352.0	5000.0	10000.0	18000.0
.0	.0	9000.0	16000.0	24000.0
4767.	0.	0.	0.	
4752.0	4763.0	4768.0	4773.0	4778.0
.0	450.0	3500.0	6000.0	9000.0
.0	.0	4000.0	8500.0	12000.0
4756.	0.	0.	0.	
4736.0	4756.0	4761.0	4763.0	4768.0
.0	540.0	2000.0	4000.0	6000.0
.0	.0	3700.0	3700.0	5500.0
4749.	0.	0.	0.	
4729.0	4737.0	4749.0	4757.0	4759.0

.0	250.0	587.0	1750.0	2000.0					
.0	.0	.0	1500.0	2000.0					
4674.	0.	0.	0.						
4654.0	4659.0	4668.0	4678.0	4683.0					
.0	70.0	352.0	400.0	420.0					
.0	.0	.0	.0	.0					
4612.	0.	0.	0.						
4601.0	4604.0	4606.0	4615.0	4620.0					
.0	245.0	450.0	500.0	520.0					
.0	.0	.0	.0	.0					
0.0	-0.9	0.0	0.0	0.1	-0.5	0.0	0.0	0.0	
0.0	0.0	0.0							
1	3	4	5	6	7	8	11		
.080	.080	.080	.080	.080	.080				
.060	.060	.060	.060	.060	.060				
.031	.031	.031	.031	.031	.031				
.034	.034	.034	.034	.034	.034				
.038	.038	.038	.038	.038	.038				
.037	.037	.037	.037	.037	.037				
.034	.034	.034	.034	.034	.034				
.036	.036	.036	.036	.036	.036				

END OF THE DATA -- E-2

E-2 RIVER

Table 22.4 Echo Print of Example 2

PROGRAM FLDWAV - BETA VERSION 1.0 2/1/95

HYDROLOGIC RESEACH LABORATORY
W/OH3 OFFICE OF HYDROLOGY
NOAA, NATIONAL WEATHER SERVICE
SILVER SPRING, MARYLAND 20910

*** SUMMARY OF INPUT DATA ***

PROBLEM E-2

EPSY	THETA	F1	XFACT	DTHYD	DTOUT	METRIC		
0.010	1.000	0.600	5280.000	0.000	0.000	0		
JN	NU	ITMAX	KWARM	KFLP	NET	ICOND	FUTURE DATA	
1	3	10	2	0	0	0	0 0 0	
NYQD	KCG	NCG	KPRES					
0	0	0	0					
NCS	KPL	JNK	KREVR5	NFGRF				
5	2	5	0	0				
IOBS	KTERM	NP	NPST	NPEND				
0	0	0	0	0				
TEH	DTHII	DTHPLT	FRDFR	DTEXP	MDT			
55.000	0.07150	0.07150	0.00	0.00000	0			
NLEV	DHLV	DTHLV						
0	0.00000	0.00000						
RIVER NO.	NBT	NPT1	NPT2	EPQJ	COFW	VWIND	WINAGL	
1	13	1	13	100.00	0.00	0.00	0.00	
RIVER NO.	KU	KD	NQL	NGAGE	NRCM1	NQCM	NSTR	FUTURE DATA
1	2	4	0	6	8	0	0	0 0 0
RIVER NO.	MIXF	MUD	KFTR	KLOS	FUTURE DATA			
1	0	0	0	0	0 0 0 0 0 0			
XT(I, 1) I=1,NB(1)								
0.000	0.010	5.010	8.510	16.010	22.510	27.510	32.510	
37.510	41.010	43.010	51.510	59.510				
DXM(I, 1) I=1,NB(1)								
100.000	0.500	0.500	0.500	0.750	1.000	1.000	1.000	
1.000	1.000	1.100	1.400					
KRCH(I, 1) I=1,NRCH								
10	0	0	0	0	0	0		
0	0	0	0					
RIVER NO.	1,	DAM NO.	1					
SAR(L, 1, 1) L=1,8								
1937.00	1156.00	577.00	216.00	0.00	0.00	0.00	0.00	
HSAR(L, 1, 1) L=1,8								
5288.50	5228.50	5098.50	5038.50	5027.00	0.00	0.00	0.00	

LAD	HDD	CLL	CDOD	QTD	ICHAN		
1	5288.50	100.00	3.00	13000.00	0		
ICG	HSPD	SPL	CSD	HGTD	CGD		
0	0.00	0.00	0.00	0.00	0.00		
TFH	DTHDB	HFDD	BBD	ZBCH	YBMIN	BREXP	CPIP
1.430	0.00000	5288.50	81.00	1.04	5027.00	1.00	0.00

PLOTTING/OBSERVED TIME SERIES FOR RIVER J= 1

I	NGS	ID	
1	2	MI	.01
2	3	MI	5.01
3	4	MI	8.51
4	5	MI	16.01
5	11	MI	43.01
6	13	MI	59.51

ST1(K,1), K = 1, NU
13000.00 13000.00 13000.00

T1(K,1), K = 1, NU
0.00 1.00 55.00

RIVER NO. 1

I=	1	FLDSTG=	5047.00	YDI=	5288.55	QDI=	0.	AS1=	0.
		HS=	5027.00	5037.00	5051.00	5107.00	5125.00		
		BS=	0.0	590.0	820.0	1130.0	1200.0		
		BSS=	0.0	0.0	0.0	0.0	0.0		
I=	2	FLDSTG=	5047.00	YDI=	0.00	QDI=	0.	AS1=	0.
		HS=	5027.00	5037.00	5051.00	5107.00	5125.00		
		BS=	0.0	590.0	820.0	1130.0	1200.0		
		BSS=	0.0	0.0	0.0	0.0	0.0		
I=	3	FLDSTG=	4985.00	YDI=	0.00	QDI=	0.	AS1=	0.
		HS=	4965.00	4980.00	5015.00	5020.00	5030.00		
		BS=	0.0	850.0	1100.0	1200.0	1300.0		
		BSS=	0.0	0.0	3500.0	4300.0	5300.0		
I=	4	FLDSTG=	4946.00	YDI=	0.00	QDI=	0.	AS1=	0.
		HS=	4920.00	4930.00	4942.00	4953.00	4958.00		
		BS=	0.0	800.0	4000.0	11000.0	15000.0		
		BSS=	0.0	0.0	0.0	7000.0	10000.0		
I=	5	FLDSTG=	4830.00	YDI=	0.00	QDI=	0.	AS1=	0.
		HS=	4817.00	4827.00	4845.00	4847.00	4852.00		
		BS=	0.0	884.0	4000.0	11000.0	22000.0		
		BSS=	0.0	0.0	30000.0	27000.0	25000.0		
I=	6	FLDSTG=	4820.00	YDI=	0.00	QDI=	0.	AS1=	0.
		HS=	4805.00	4812.00	4814.00	4825.00	4830.00		
		BS=	0.0	1000.0	1200.0	11000.0	16000.0		
		BSS=	0.0	0.0	0.0	6000.0	8000.0		
I=	7	FLDSTG=	4800.00	YDI=	0.00	QDI=	0.	AS1=	0.
		HS=	4788.00	4792.00	4802.00	4808.00	4810.00		
		BS=	0.0	286.0	7000.0	10000.0	11000.0		
		BSS=	0.0	0.0	0.0	3500.0	5000.0		
I=	8	FLDSTG=	4777.00	YDI=	0.00	QDI=	0.	AS1=	0.
		HS=	4762.00	4774.00	4777.00	4780.00	4785.00		
		BS=	0.0	352.0	5000.0	10000.0	18000.0		
		BSS=	0.0	0.0	9000.0	16000.0	24000.0		
I=	9	FLDSTG=	4767.00	YDI=	0.00	QDI=	0.	AS1=	0.
		HS=	4752.00	4763.00	4768.00	4773.00	4778.00		
		BS=	0.0	450.0	3500.0	6000.0	9000.0		
		BSS=	0.0	0.0	4000.0	8500.0	12000.0		
I=	10	FLDSTG=	4756.00	YDI=	0.00	QDI=	0.	AS1=	0.

	HS=	4736.00	4756.00	4761.00	4763.00	4768.00		
	BS=	0.0	540.0	2000.0	4000.0	6000.0		
	BSS=	0.0	0.0	3700.0	3700.0	5500.0		
I=	11	FLDSTG= 4749.00	YDI= 0.00	QDI= 0.	AS1= 0.			
		HS= 4729.00	4737.00	4749.00	4757.00	4759.00		
		BS= 0.0	250.0	587.0	1750.0	2000.0		
		BSS= 0.0	0.0	0.0	1500.0	2000.0		
I=	12	FLDSTG= 4674.00	YDI= 0.00	QDI= 0.	AS1= 0.			
		HS= 4654.00	4659.00	4668.00	4678.00	4683.00		
		BS= 0.0	70.0	352.0	400.0	420.0		
		BSS= 0.0	0.0	0.0	0.0	0.0		
I=	13	FLDSTG= 4612.00	YDI= 0.00	QDI= 0.	AS1= 0.			
		HS= 4601.00	4604.00	4606.00	4615.00	4620.00		
		BS= 0.0	245.0	450.0	500.0	520.0		
		BSS= 0.0	0.0	0.0	0.0	0.0		

REACH INFO RIVER NO. 1

FKEC(I,1), I = 1, NM(1)							
0.00	-0.90	0.00	0.00	0.10	-0.50	0.00	0.00
0.00	0.00	0.00	0.00				

NCM(K, 1), K=1, NRCM1(1)							
1	3	4	5	6	7	8	11
CM(K, 1, 1)=	0.0800	0.0800	0.0800	0.0800	0.0800	0.0800	
CM(K, 2, 1)=	0.0600	0.0600	0.0600	0.0600	0.0600	0.0600	
CM(K, 3, 1)=	0.0310	0.0310	0.0310	0.0310	0.0310	0.0310	
CM(K, 4, 1)=	0.0340	0.0340	0.0340	0.0340	0.0340	0.0340	
CM(K, 5, 1)=	0.0380	0.0380	0.0380	0.0380	0.0380	0.0380	
CM(K, 6, 1)=	0.0370	0.0370	0.0370	0.0370	0.0370	0.0370	
CM(K, 7, 1)=	0.0340	0.0340	0.0340	0.0340	0.0340	0.0340	
CM(K, 8, 1)=	0.0360	0.0360	0.0360	0.0360	0.0360	0.0360	

END OF THE DATA -- E-2

22.3 FLDWAV Example 3.0

This example illustrates the use of FLDWAV to simulate unsteady flow through a reach of river having two structures; the first is a dam which is breached, and the second is a bridge located 10 miles downstream of the dam. Level-pool routing is used for the reservoir with the tailwater elevations computed via the Saint-Venant equations. The dam and the bridge are each treated as an internal boundaries. A short Δx reach bounded by cross sections at miles 0.00 and 0.01 serves as the internal boundary for the dam, and a short Δx reach bounded by cross sections at miles 10.0 and 10.01 defines the second internal boundary for the bridge. The dam breaches immediately since the initial water surface elevation of the reservoir (1050.00 ft) is the same as the elevation (HFDD) at which breaching commences.

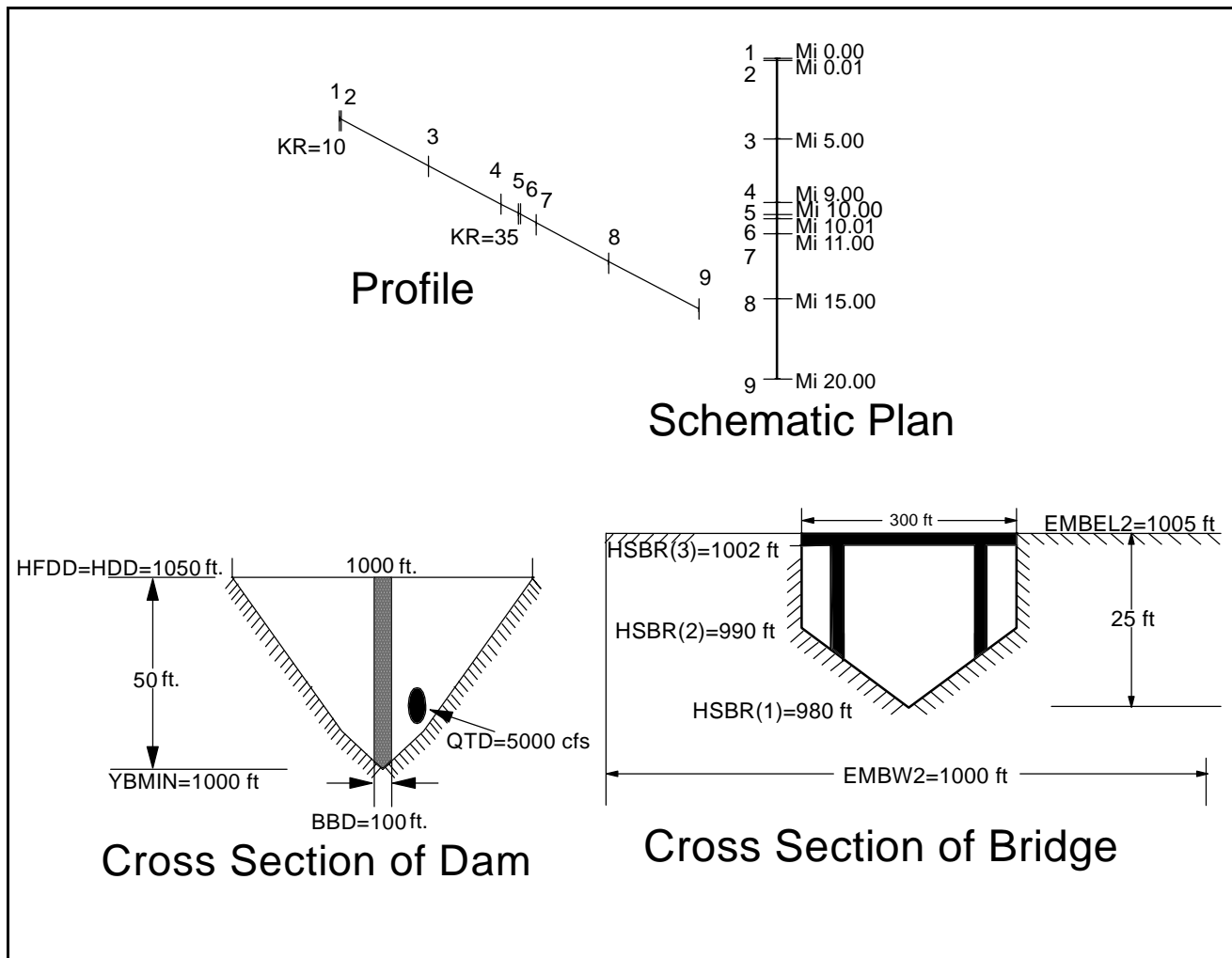


Figure 22.3 - Example 3.0 – Dam and Bridge.

PROBLEM E-3
EOM
NO DESC

22.17

0	0	0	0				
1000	1010	1025					
0	500	1000					
0	0	0					
0	0	0	0				
990	1000	1015					
0	500	1000					
0	0	0					
0	0	0	0				
982	992	1007					
0	500	1000					
0	0	0	0				
0	0	0	0				
980	990	1005					
0	300	300					
0	200	700					
0	0	0	0				
980	990	1005					
0	300	300					
0	200	300					
0	0	0	0				
978	988	1003					
0	500	1000					
0	0	0					
0	0	0	0				
970	980	995					
0	500	1000					
0	0	0					
0	0	0	0				
960	970	985					
0	500	1000					
0	0	0					
0	0	0	.200	0	-1.00	0	0
1							
.060	.060	.060					
0.							
END OF DATA							
E-3 RIVER							

Table 22.6 Echo Print of Example 3

PROGRAM FLDWAV - BETA VERSION 1.0 2/1/95

HYDROLOGIC RESEACH LABORATORY
W/OH3 OFFICE OF HYDROLOGY
NOAA, NATIONAL WEATHER SERVICE
SILVER SPRING, MARYLAND 20910

*** SUMMARY OF INPUT DATA ***

PROBLEM E-3

EPSY	THETA	F1	XFACT	DTHYD	DTOUT	METRIC		
0.010	1.000	0.600	5280.000	0.000	0.000	0		
JN	NU	ITMAX	KWARM	KFLP	NET	ICOND	FUTURE DATA	
1	4	10	2	0	0	0	0 0 0	
NYQD	KCG	NCG	KPRES					
0	0	0	0					
NCS	KPL	JNK	KREVRS	NFGRF				
3	2	5	0	0				
IOBS	KTERM	NP	NPST	NPEND				
0	0	0	0	0				
TEH	DTHII	DTHPLT	FRDFR	DTEXP	MDT			
15.000	0.20000	0.20000	0.00	0.00000	0			
NLEV	DHLV	DTHLV						
0	0.00000	0.00000						
RIVER NO.	NBT	NPT1	NPT2	EPQJ	COFW	VWIND	WINAGL	
1	9	1	9	100.00	0.00	0.00	0.00	
RIVER NO.	KU	KD	NQL	NGAGE	NRCM1	NQCM	NSTR	FUTURE DATA
1	2	4	0	5	1	0	0	0 0 0
RIVER NO.	MIXF	MUD	KFTR	KLOS	FUTURE DATA			
1	0	0	0	0	0 0 0 0 0 0			
XT(I, 1) I=1,NB(1)								
0.000	0.010	5.000	9.000	10.000	10.010	11.000	15.000	
20.000								
DXM(I, 1) I=1,NB(1)								
100.000	0.500	0.500	0.200	0.500	0.200	0.500	0.500	
KRCH(I, 1) I=1,NRCH								
10	0	0	0	35	0	0	0	
RIVER NO.	1,	DAM NO.	1					
SAR(L, 1, 1) L=1,8								
1500.00	0.00	0.00	0.00	0.00	0.00	0.00	0.00	
HSAR(L, 1, 1) L=1,8								
1050.00	1000.00	0.00	0.00	0.00	0.00	0.00	0.00	
LAD	HDD	CLL	CDOD	QTD	ICHAN			
1	1050.00	1.00	3.00	5000.00	0			

ICG	HSPD	SPL	CSD	HGTD	CGD		
0	0.00	0.00	0.00	0.00	0.00		
TFH	DTHDB	HFDD	BBD	ZBCH	YBMIN	BREXP	CPIP
4.000	0.00000	1050.00	100.00	0.00	1000.00	1.00	0.00

RIVER NO. 1, BRIDGE NO. 1

LAD	EMBEL2	EMBW2	EMBEL1	EMBW1	BRGW	CDBRG	
5	1005.00	1000.00	0.00	0.00	50.00	0.80	
BRGHS(L, 2, 1), L=1,8)							
980.00	990.00	1002.00	1002.10	0.00	0.00	0.00	0.00
BRGBS(L, 2, 1), L=1,8)							
0.00	300.00	300.00	0.00	0.00	0.00	0.00	0.00
TFH	DTHDB	HFDD	BBD	ZBCH	YBMIN	BREXP	CPIP
1.00	0.00	1100.00	0.00	0.00	0.00	1.00	0.00

PLOTTING/OBSERVED TIME SERIES FOR RIVER J= 1

I	NGS	ID
1	1	MI 0
2	2	MI .01
3	5	MI 10.
4	6	MI 10.01
5	9	MI 20.

ST1(K,1), K = 1, NU
3000.00 3000.00 3000.00 3000.00

T1(K,1), K = 1, NU
0.00 24.00 48.00 72.00

RIVER NO. 1

I=	1	FLDSTG=	0.00	YDI=	1050.00	QDI=	0.	AS1=	0.
		HS=	1000.00	1010.00	1025.00				
		BS=	0.0	500.0	1000.0				
		BSS=	0.0	0.0	0.0				
I=	2	FLDSTG=	0.00	YDI=	0.00	QDI=	0.	AS1=	0.
		HS=	1000.00	1010.00	1025.00				
		BS=	0.0	500.0	1000.0				
		BSS=	0.0	0.0	0.0				
I=	3	FLDSTG=	0.00	YDI=	0.00	QDI=	0.	AS1=	0.
		HS=	990.00	1000.00	1015.00				
		BS=	0.0	500.0	1000.0				
		BSS=	0.0	0.0	0.0				
I=	4	FLDSTG=	0.00	YDI=	0.00	QDI=	0.	AS1=	0.
		HS=	982.00	992.00	1007.00				
		BS=	0.0	500.0	1000.0				
		BSS=	0.0	0.0	0.0				
I=	5	FLDSTG=	0.00	YDI=	0.00	QDI=	0.	AS1=	0.
		HS=	980.00	990.00	1005.00				
		BS=	0.0	300.0	300.0				
		BSS=	0.0	200.0	700.0				
I=	6	FLDSTG=	0.00	YDI=	0.00	QDI=	0.	AS1=	0.
		HS=	980.00	990.00	1005.00				
		BS=	0.0	300.0	300.0				
		BSS=	0.0	200.0	300.0				
I=	7	FLDSTG=	0.00	YDI=	0.00	QDI=	0.	AS1=	0.
		HS=	978.00	988.00	1003.00				
		BS=	0.0	500.0	1000.0				
		BSS=	0.0	0.0	0.0				

I=	8	FLDSTG=	0.00	YDI=	0.00	QDI=	0.	AS1=	0.
		HS=	970.00	980.00	995.00				
		BS=	0.0	500.0	1000.0				
		BSS=	0.0	0.0	0.0				

I=	9	FLDSTG=	0.00	YDI=	0.00	QDI=	0.	AS1=	0.
		HS=	960.00	970.00	985.00				
		BS=	0.0	500.0	1000.0				
		BSS=	0.0	0.0	0.0				

REACH INFO RIVER NO. 1

FKEC(I,1), I = 1, NM(1)								
0.00	0.00	0.00	0.20	0.00	-1.00	0.00	0.00	

NCM(K, 1), K=1,NRCM1(1)

CM(K, 1, 1)=	0.0600	0.0600	0.0600
--------------	--------	--------	--------

END OF DATA

22.4 FLDWAV Example 4.0 -- Level-Pool Routing, Average Movable Gate, Conveyance.

This example illustrates the use of FLDWAV to simulate the development of a dam-break wave due to the failure of a single dam and then dynamically route the wave through 20 miles of the downstream channel/valley. The reservoir hydraulics are treated via level-pool routing. The use of time-dependent movable gates is also illustrated in this example. This requires the parameter (KCG) to be nonzero (in this case it was set to a value of 6 indicating the number of points in the time series for the gate width and height of opening). Another special feature, the conveyance option, for treating the channel/floodplain is illustrated in this example.

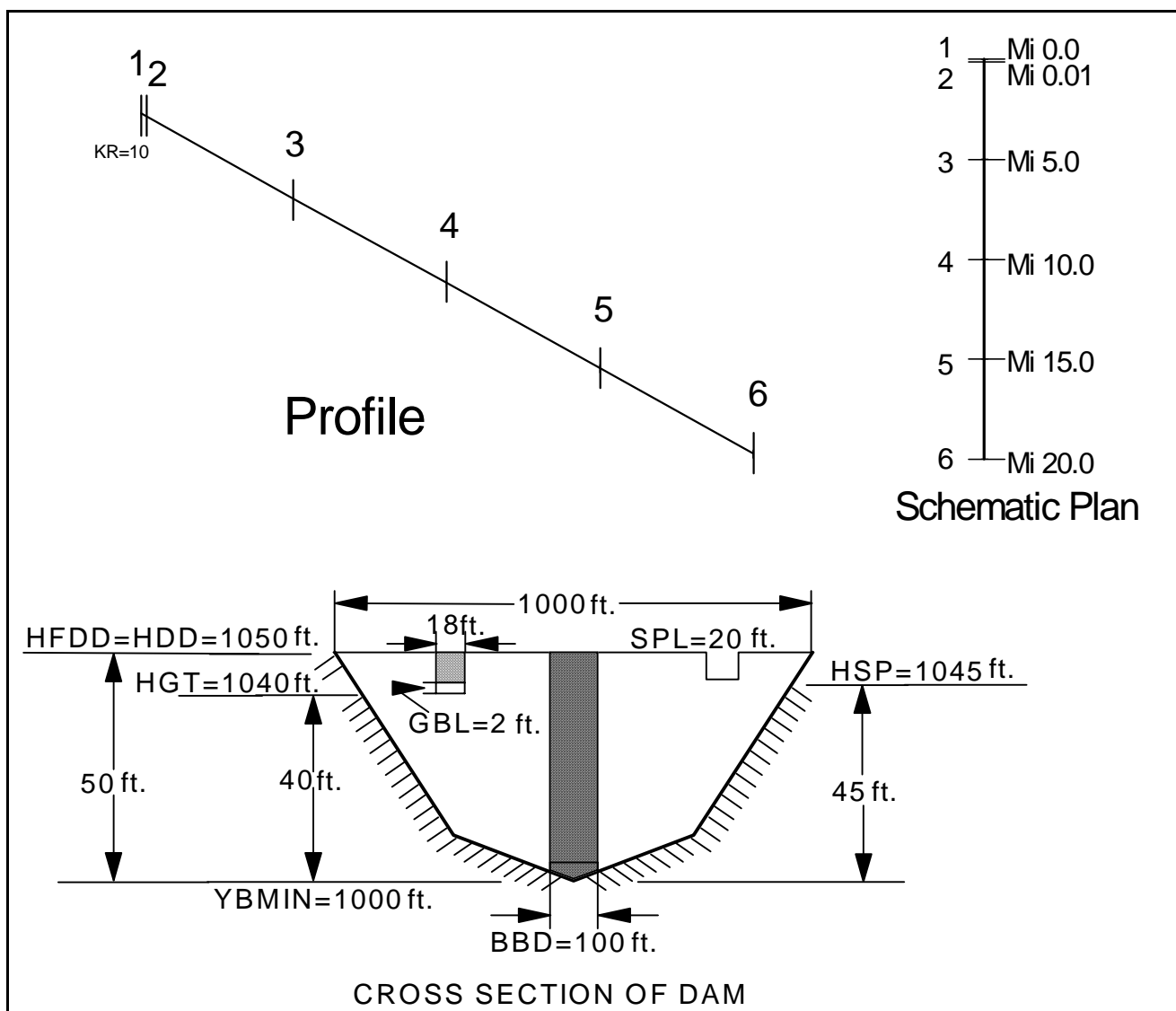


Figure 22.4 - Example 4.0 – Level-Pool Routing, Average Movable Gate, Conveyance

Table 22.7 Input Data Set for Example 4

PROBLEM E-4
EOM
NO DESC

.01				1		.6		5280		0.		0
1	4	10		2	1	0		0		0 0 0 0		
0		6		0		0						
3		2		005		0		0				
0		0		0		0		0				
15.00		.025		0		0		0.		0		
0		0	0									
6	1	6	100.	0.	0.	0.						
2	4	0	6	5		0 0 0 0 0						
0	0	0	0 0 0 0 0 0 0									
0.0		.010		5.0		10.		15.		20.		
2.0		.130		.130		.130		.130				
15		0		0		0		0				
1500.	0	0		0	0	0		0		0		
1050.	1000.			0	0	0	0	0	0			
1		1050.0		1000.	3.0		0.0		0			
0		1045.0		20.0	3.0		1040.0		28.80			
0		.5		1.	1.5		10		20			
2		2		3	4		2		2			
28.8	28.8			43.2	57.6		28.8		28.8			
.50	0.			1050.0	100.00		0.0		1000.0	1.0		0.0
1	2			3	4		5		6			
MI 000.												
MI .010												
MI 5.0												
MI 10.												
MI 15.80												
MI 20.												
3000.	13000.			3000.		3000.						
0.0	1.000			20.000		50.00000						
.0	1049.9			0		0						
1000.	1010.			1050.								
.0	50.			100.								
.0	225.			450.								

.0	225.	450.				
0	0	0				
.0	0	0	0			
1000.	1010.	1025.				
.0	50.	100.				
.0	225.	450.				
.0	225.	450.				
0	0	0				
.0	0	0	0			
975.	985.	1000.				
.0	75.	100.				
.0	175.	500.				
.0	100.	200.				
0.	0.	0.				
0	0	0	0			
950.	960.	975.				
0.	200.	200.				
0.	500.	1000.				
0.	150.	250.				
0	0	0				
0	0	0	0			
925.	935.	950.				
0.	50.	100.				
0.	100.	150.				
0	450.	800.				
0	0	0				
0	0	0	0			
900.	910.	925.0				
0.	50.	150.				
0	75.	400.				
0	500.	600.				
0.	0.	0.				
1.00	1.00	1.00				
1.50	1.50	1.10				
1.50	1.50	1.10				
1.40	1.40	1.00				
1.30	1.30	1.00				
0	0	0	0	0	0	

1	2	3	4	5
.040		.040	.040	
.060		.060	.060	
.060		.060	.060	
.040		.050	.040	
.060		.060	.070	
.060		.080	.090	
.040		.050	.040	
.060		.060	.050	
.050		.060	.070	
.040		.035	.040	
.060		.060	.060	
.050		.060	.050	
.040		.040	.030	
.060		.070	.090	
.060		.070	.070	
0				
END OF DATA -- E-4				
E-4 RIVER				

Table 22.8 Echo Print of Example 4

PROGRAM FLDWAV - BETA VERSION 1.0 2/1/95

HYDROLOGIC RESEACH LABORATORY
W/OH3 OFFICE OF HYDROLOGY
NOAA, NATIONAL WEATHER SERVICE
SILVER SPRING, MARYLAND 20910

*** SUMMARY OF INPUT DATA ***

PROBLEM E-4

EPSY	THETA	F1	XFACT	DTHYD	DTOUT	METRIC	
0.010	1.000	0.600	5280.000	0.000	0.000	0	
JN	NU	ITMAX	KWARM	KFLP	NET	ICOND	FUTURE DATA
1	4	10	2	1	0	0	0 0 0
NYQD	KCG	NCG	KPRES				
0	6	0	0				
NCS	KPL	JNK	KREVRS	NFGRF			
3	2	5	0	0			
IOBS	KTERM	NP	NPST	NPEND			
0	0	0	0	0			
TEH	DTHII	DTHPLT	FRDFR	DTEXP	MDT		
15.000	0.02500	0.02500	0.00	0.00000	0		
NLEV	DHLV	DTHLV					
0	0.00000	0.00000					
RIVER NO.	NBT	NPT1	NPT2	EPQJ	COFW	VWIND	WINAGL
1	6	1	6	100.00	0.00	0.00	0.00
RIVER NO.	KU	KD	NQL	NGAGE	NRCM1	NQCM	NSTR
1	2	4	0	6	5	0	0
							0 0 0
RIVER NO.	MIXF	MUD	KFTR	KLOS	FUTURE DATA		
1	0	0	0	0	0 0 0 0 0 0		
XT(I, 1) I=1,NB(1)							
0.000	0.010	5.000	10.000	15.000	20.000		
DXM(I, 1) I=1,NB(1)							
2.000	0.130	0.130	0.130	0.130			
KRCH(I, 1) I=1,NRCH							
15	0	0	0	0			
RIVER NO. 1, DAM NO. 1							
SAR(L, 1, 1) L=1,8							
1500.00	0.00	0.00	0.00	0.00	0.00	0.00	0.00
HSAR(L, 1, 1) L=1,8							
1050.00	1000.00	0.00	0.00	0.00	0.00	0.00	0.00
LAD	HDD	CLL	CDOD	QTD	ICHAN		
1	1050.00	1000.00	3.00	0.00	0		
ICG	HSPD	SPL	CSD	HGTD	CGD		

0	1045.00	20.00	3.00	1040.00	28.80		
(TCG(L, 1,1), L=1,KCG)							
0.00	0.50	1.00	1.50	10.00	20.00		
(QGH(L, 1,1), L=1,KCG)							
2.00	2.00	3.00	4.00	2.00	2.00		
(CGCG(L, 1,1), L=1,KCG)							
28.80	28.80	43.20	57.60	28.80	28.80		
TFH	DTHDB	HFDD	BBD	ZBCH	YBMIN	BREXP	CPIP
0.500	0.00000	1050.00	100.00	0.00	1000.00	1.00	0.00

PLOTTING/OBSERVED TIME SERIES FOR RIVER J= 1

I	NGS	ID
1	1	MI 000.
2	2	MI .010
3	3	MI 5.0
4	4	MI 10.
5	5	MI 15.80
6	6	MI 20.

ST1(K,1), K = 1, NU
3000.00 13000.00 3000.00 3000.00

T1(K,1), K = 1, NU
0.00 1.00 20.00 50.00

RIVER NO. 1

I=	1	FLDSTG=	0.00	YDI=	1049.90	QDI=	0.	AS1=	0.
		HS=	1000.00		1010.00				
		BS=	0.0		50.0				
		BSL=	0.0		225.0				
		BSR=	0.0		225.0				
		BSS=	0.0		0.0				
I=	2	FLDSTG=	0.00	YDI=	0.00	QDI=	0.	AS1=	0.
		HS=	1000.00		1010.00				
		BS=	0.0		50.0				
		BSL=	0.0		225.0				
		BSR=	0.0		225.0				
		BSS=	0.0		0.0				
I=	3	FLDSTG=	0.00	YDI=	0.00	QDI=	0.	AS1=	0.
		HS=	975.00		985.00				
		BS=	0.0		75.0				
		BSL=	0.0		175.0				
		BSR=	0.0		100.0				
		BSS=	0.0		0.0				
I=	4	FLDSTG=	0.00	YDI=	0.00	QDI=	0.	AS1=	0.
		HS=	950.00		960.00				
		BS=	0.0		200.0				
		BSL=	0.0		500.0				
		BSR=	0.0		150.0				
		BSS=	0.0		0.0				
I=	5	FLDSTG=	0.00	YDI=	0.00	QDI=	0.	AS1=	0.
		HS=	925.00		935.00				
		BS=	0.0		50.0				
		BSL=	0.0		100.0				
		BSR=	0.0		450.0				
		BSS=	0.0		0.0				
I=	6	FLDSTG=	0.00	YDI=	0.00	QDI=	0.	AS1=	0.
		HS=	900.00		910.00				
		BS=	0.0		50.0				
		BSL=	0.0		75.0				
		BSR=	0.0		500.0				
		BSS=	0.0		0.0				

REACH INFO RIVER NO. 1

SNM=	1.000	1.000	1.000
SNC=	1.000	1.000	1.000
SNM=	1.500	1.500	1.100
SNC=	1.500	1.000	1.000
SNM=	1.500	1.500	1.100
SNC=	1.500	1.000	1.000
SNM=	1.400	1.400	1.000
SNC=	1.400	1.000	1.000
SNM=	1.300	1.300	1.000
SNC=	1.300	1.000	1.000

FKEC(I,1), I = 1, NM(1)
0.00 0.00 0.00 0.00 0.00

NCM(K, 1), K=1,NRCM1(1)
1 2 3 4 5

CM(K, 1, 1)=	0.0400	0.0400	0.0400
CML(K, 1, 1)=	0.0600	0.0600	0.0600
CMR(K, 1, 1)=	0.0600	0.0600	0.0600
CM(K, 2, 1)=	0.0400	0.0500	0.0400
CML(K, 2, 1)=	0.0600	0.0600	0.0700
CMR(K, 2, 1)=	0.0600	0.0800	0.0900
CM(K, 3, 1)=	0.0400	0.0500	0.0400
CML(K, 3, 1)=	0.0600	0.0600	0.0500
CMR(K, 3, 1)=	0.0500	0.0600	0.0700
CM(K, 4, 1)=	0.0400	0.0350	0.0400
CML(K, 4, 1)=	0.0600	0.0600	0.0600
CMR(K, 4, 1)=	0.0500	0.0600	0.0500
CM(K, 5, 1)=	0.0400	0.0400	0.0300
CML(K, 5, 1)=	0.0600	0.0700	0.0900
CMR(K, 5, 1)=	0.0600	0.0700	0.0700

END OF DATA - E-4

22.5 FLDWAV Example 5.0 -- Subcritical/Supercritical

This example illustrates the use of the subcritical/supercritical mixed flow algorithm for dynamic routing of a specified hydrograph through a channel reach. Some reaches are mild sloping and tend to be subcritical ($-5 \text{ ft/mi} \leq S_o \leq 5 \text{ ft/mi}$) while others are supercritical reaches ($S_o = 20 \text{ ft/mi}$). The parameter MIXF(1) is set to a value of 2 which activates the mixed-flow algorithm and allows the hydraulic jump to move. The printed-output control parameter (JNK) is set to a value of 5 which provides more information than JNK=4.

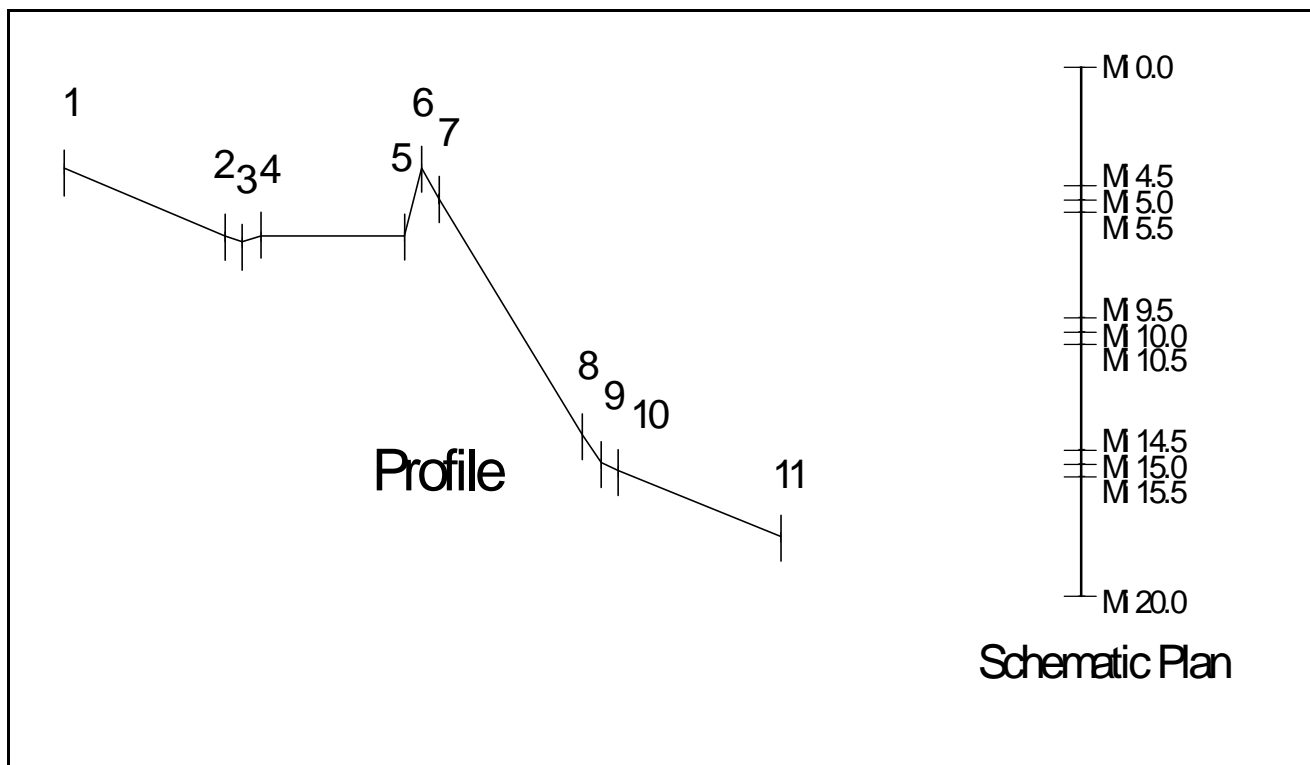


Figure 22.5 - Example 5.0 – Subcritical/Supercritical.

PROBLEM E-5
EOM
NO DESC

22.30

0.	100.	1000.						
0.	0	0						
0	0	0	0					
977.5	987.5	1077.5						
0.	100.	1000.						
0.	0	0						
0	0	0	0					
997.5	1007.5	1097.5						
0.	100.	1000.						
0.	0	0						
0	0	0	0					
1000.	1010.	1100.						
0.	100.	1000.						
0.	0	0						
0	0	0	0					
990.	1000.	1090.						
0.	100.	1000.						
0.	0	0						
0	0	0	0					
910.	920.	1010.						
0.	100.	1000.						
0.	0	0						
0	0	0	0					
900.	910.	1000.						
0.	100.	1000.						
0.	0	0						
0	0	0	0					
897.5	907.5	997.5						
0.	100.	1000.						
0.	0	0						
0	0	0	0					
875.0	885.	975.						
0.	100.	1000.						
0.	0	0						
0.	0.	0.	0.	0.	0.	0.	0.	
0.	0.							
	1	5	9					
.060	.060	.060						

.010	.010	.010
.060	.060	.060

0

SUB/SUP/SUB TEST RUN (E-5)

E-5 RIVER

Table 22.10 Echo Print of Example 5

```

PROGRAM FLDWAV - BETA VERSION 1.0  2/1/95

HYDROLOGIC RESEACH LABORATORY
W/OH3 OFFICE OF HYDROLOGY
NOAA, NATIONAL WEATHER SERVICE
SILVER SPRING, MARYLAND  20910

*****
*****
***                               ***
*** SUMMARY OF INPUT DATA      ***
***                               ***
*****
*****

PROBLEM E-5

      EPSY      THETA      F1      XFACT      DTHYD      DTOUT      METRIC
0.010      0.500      0.600  5280.000      0.000      0.000      0

      JN      NU      ITMAX      KWARM      KFLP      NET      ICOND      FUTURE DATA
      1      5      10      3      0      0      0      0 0 0

      NYQD      KCG      NCG      KPRES
      0      0      0      0

      NCS      KPL      JNK      KREVRS      NFGRF
      3      2      5      0      0

      IOBS      KTERM      NP      NPST      NPEND
      0      0      0      0      0

      TEH      DTHII      DTHPLT      FRDFR      DTEXP      MDT
10.000      0.05000      0.20000      0.05      0.00000      0

      NLEV      DHLV      DTHLV
      0      0.00000      0.00000

RIVER NO.      NBT NPT1 NPT2      EPQJ      COFW      VWIND      WINAGL
      1      11      1      47      10.00      0.00      0.00      0.00

RIVER NO.      KU      KD      NQL NGAGE NRCM1      NQCM      NSTR      FUTURE DATA
      1      2      4      0      5      3      0      0      0 0 0

RIVER NO.      MIXF      MUD      KFTR      KLOS      FUTURE DATA
      1      2      0      0      0      0 0 0 0 0 0

XT(I, 1) I=1,NB( 1)
      0.000      4.500      5.000      5.500      9.500      10.000      10.500      14.500
      15.000      15.500      20.000

DXM(I, 1) I=1,NB( 1)
      0.500      0.200      0.200      0.500      0.200      0.200      0.500      0.200
      0.200      0.500

KRCH(I, 1) I=1,NRCH
      0      0      0      0      0      0      0
      0      0

PLOTING/OBSERVED TIME SERIES FOR RIVER J= 1

      I      NGS      ID
      1      1      MI 0
      2      3      MI 5
      3      6      MI 10
      4      9      MI 15
      5      11      MI 20

ST1(K,1), K = 1, NU
      100.00      100.00      12000.00      100.00      100.00

T1(K,1), K = 1, NU

```


	0.00	1.00	2.00	3.00	15.00			
RIVER NO. 1								
I= 1	FLDSTG=	0.00	YDI=	0.00	QDI=	100.	AS1=	0.
	HS=	1000.00		1010.00				
	BS=	0.0		100.0				
	BSS=	0.0		0.0				
I= 2	FLDSTG=	0.00	YDI=	0.00	QDI=	0.	AS1=	0.
	HS=	977.50		987.50				
	BS=	0.0		100.0				
	BSS=	0.0		0.0				
I= 3	FLDSTG=	0.00	YDI=	0.00	QDI=	0.	AS1=	0.
	HS=	975.00		985.00				
	BS=	0.0		100.0				
	BSS=	0.0		0.0				
I= 4	FLDSTG=	0.00	YDI=	0.00	QDI=	0.	AS1=	0.
	HS=	977.50		987.50				
	BS=	0.0		100.0				
	BSS=	0.0		0.0				
I= 5	FLDSTG=	0.00	YDI=	0.00	QDI=	0.	AS1=	0.
	HS=	997.50		1007.50				
	BS=	0.0		100.0				
	BSS=	0.0		0.0				
I= 6	FLDSTG=	0.00	YDI=	0.00	QDI=	0.	AS1=	0.
	HS=	1000.00		1010.00				
	BS=	0.0		100.0				
	BSS=	0.0		0.0				
I= 7	FLDSTG=	0.00	YDI=	0.00	QDI=	0.	AS1=	0.
	HS=	990.00		1000.00				
	BS=	0.0		100.0				
	BSS=	0.0		0.0				
I= 8	FLDSTG=	0.00	YDI=	0.00	QDI=	0.	AS1=	0.
	HS=	910.00		920.00				
	BS=	0.0		100.0				
	BSS=	0.0		0.0				
I= 9	FLDSTG=	0.00	YDI=	0.00	QDI=	0.	AS1=	0.
	HS=	900.00		910.00				
	BS=	0.0		100.0				
	BSS=	0.0		0.0				
I= 10	FLDSTG=	0.00	YDI=	0.00	QDI=	0.	AS1=	0.
	HS=	897.50		907.50				
	BS=	0.0		100.0				
	BSS=	0.0		0.0				
I= 11	FLDSTG=	0.00	YDI=	0.00	QDI=	0.	AS1=	0.
	HS=	875.00		885.00				
	BS=	0.0		100.0				
	BSS=	0.0		0.0				
REACH INFO RIVER NO. 1								
FKEC(I,1), I = 1, NM(1)								
	0.00	0.00	0.00	0.00	0.00	0.00	0.00	0.00
	0.00	0.00						
NCM(K, 1), K=1,NRCM1(1)								
1	5	9						
CM(K, 1, 1)=		0.0600	0.0600	0.0600				
CM(K, 2, 1)=		0.0100	0.0100	0.0100				
CM(K, 3, 1)=		0.0600	0.0600	0.0600				
0								

22.6 FLDWAV Example 6.0 -- Free-Surface/Pressurized Flow

This example illustrates the use of free surface/pressurized flow option. The reach of channel between mile 10.1 and mile 14.9 is a closed conduit 200 ft wide and 10 ft high. The closed conduit sections have topwidths (fictitious chimney width 0.01 ft.) at elevations 960.1 and 990.00. This value for the fictitious chimney width (b^*) is computed from the following: $b^* = gA/\hat{c}^2$ in which the area, $A = 2000 \text{ ft}^2$; the wave speed celerity, $\hat{c} = 2538 \text{ ft/sec}$; and the gravity acceleration factor, $g = 32.2 \text{ ft/sec}^2$.

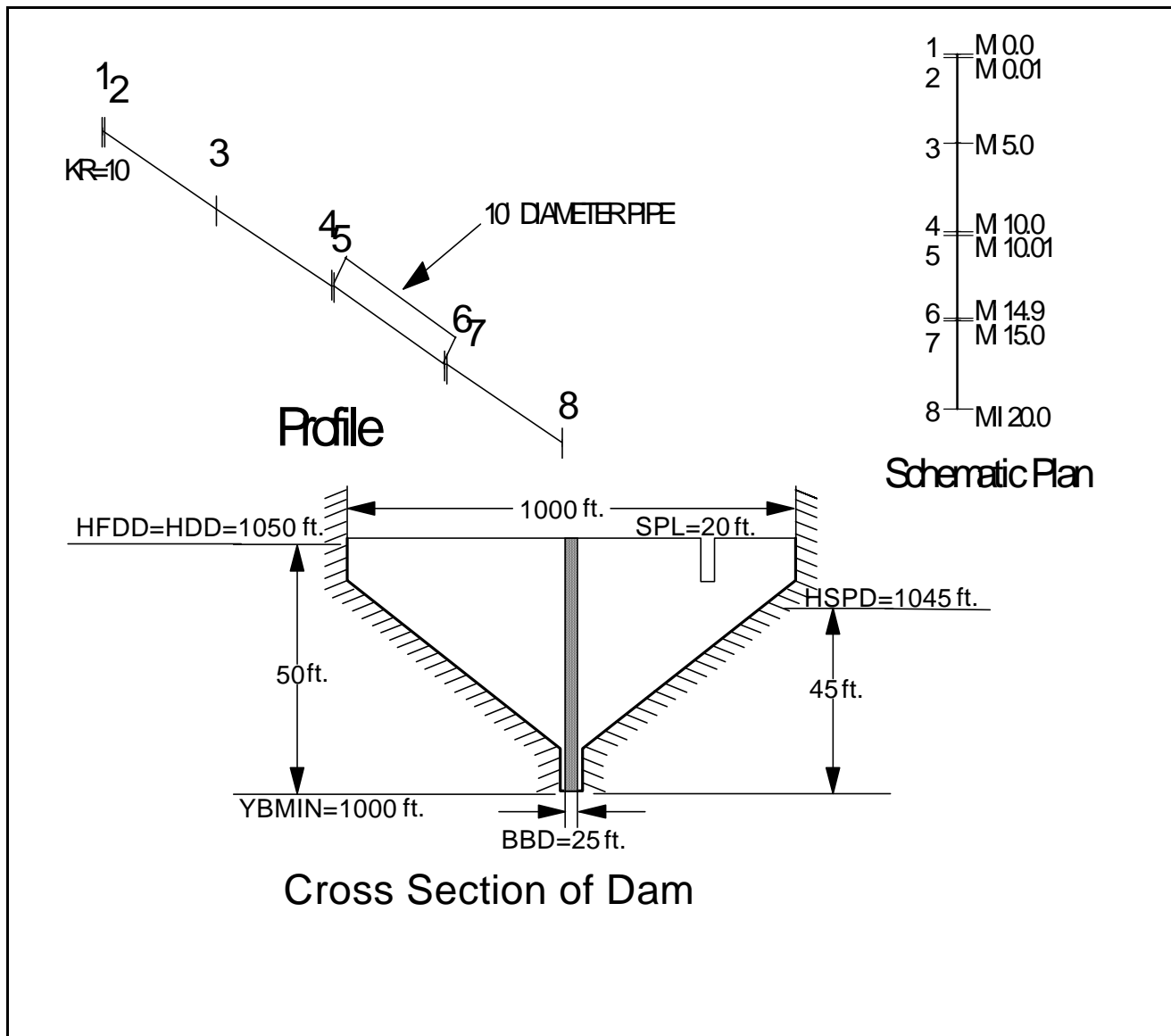


Figure 22.6 - Example 6.0 – Free Surface/Pressurized Flow.

Table 22.11 Input Data Set for Example 6

PROBLEM E-6
EOM
NO DESC

[illegible]

Table 22.12 Echo Print of Example 6

PROGRAM FLDWAV - BETA VERSION 1.0 2/1/95

HYDROLOGIC RESEACH LABORATORY
W/OH3 OFFICE OF HYDROLOGY
NOAA, NATIONAL WEATHER SERVICE
SILVER SPRING, MARYLAND 20910

*** SUMMARY OF INPUT DATA ***

PROBLEM E-6

EPSY	THETA	F1	XFACT	DTHYD	DTOUT	METRIC	
0.010	1.000	0.600	5280.000	0.000	0.000	0	

JN	NU	ITMAX	KWARM	KFLP	NET	ICOND	FUTURE DATA
1	4	10	2	0	0	0	0 0 0

NYQD	KCG	NCG	KPRES				
0	0	0	1				

NCS	KPL	JNK	KREVR5	NFGRF			
4	2	5	0	0			

IOBS	KTERM	NP	NPST	NPEND			
0	0	0	0	0			

TEH	DTHII	DTHPLT	FRDFR	DTEXP	MDT		
20.000	0.02500	0.20000	0.00	0.00000	0		

NLEV	DHLV	DTHLV					
0	0.00000	0.00000					

RIVER NO.	NBT	NPT1	NPT2	EPQJ	COFW	VWIND	WINAGL
1	8	1	8	100.00	0.00	0.00	0.00

RIVER NO.	KU	KD	NQL	NGAGE	NRCM1	NQCM	NSTR	FUTURE DATA
1	2	4	0	6	4	0	0	0 0 0

RIVER NO.	MIXF	MUD	KFTR	KLOS	FUTURE DATA		
1	0	0	0	0	0 0 0 0 0 0		

XT(I, 1)	I=1,NB(1)						
0.000	0.010	5.000	10.000	10.100	14.900	15.000	20.000

DXM(I, 1)	I=1,NB(1)						
2.000	0.100	0.100	0.050	0.100	0.050	0.120	

KRCH(I, 1)	I=1,NRCH						
10	0	0	0	0	0	0	

RIVER NO.	1,	DAM NO.	1				
-----------	----	---------	---	--	--	--	--

SAR(L, 1, 1)	L=1,8						
1500.00	0.00	0.00	0.00	0.00	0.00	0.00	0.00

HSAR(L, 1, 1)	L=1,8						
1050.00	1000.00	0.00	0.00	0.00	0.00	0.00	0.00

LAD	HDD	CLL	CDOD	QTD	ICHAN		
1	1050.00	1000.00	3.00	0.00	0		

ICG	HSPD	SPL	CSD	HGTD	CGD		
0	1045.00	20.00	3.00	0.00	0.00		
TFH	DTHDB	HFDD	BBD	ZBCH	YBMIN	BREXP	CPIP
0.500	0.00000	1050.00	25.00	0.00	1000.00	1.00	0.00

PLOTTING/OBSERVED TIME SERIES FOR RIVER J= 1

I	NGS	ID
1	1	MI 000.
2	2	MI .010
3	3	MI 5.0
4	4	MI 10.0
5	5	MI 10.1
6	6	MI 14.9

ST1(K,1), K = 1, NU
3000.00 13000.00 3000.00 3000.00

T1(K,1), K = 1, NU
0.00 1.00 20.00 50.00

RIVER NO. 1

I=	1	FLDSTG=	0.00	YDI=	1049.90	QDI=	0.	AS1=	0.
		HS=	1000.00		1010.00		1060.00		
		BS=	50.0		50.0		1000.0		1000.0
		BSS=	0.0		0.0		0.0		0.0
I=	2	FLDSTG=	0.00	YDI=	0.00	QDI=	0.	AS1=	0.
		HS=	1000.00		1010.00		1025.00		1050.00
		BS=	50.0		50.0		150.0		150.0
		BSS=	0.0		0.0		0.0		0.0
I=	3	FLDSTG=	0.00	YDI=	0.00	QDI=	0.	AS1=	0.
		HS=	975.00		985.00		1000.00		1025.00
		BS=	50.0		50.0		150.0		150.0
		BSS=	0.0		0.0		0.0		0.0
I=	4	FLDSTG=	0.00	YDI=	0.00	QDI=	0.	AS1=	0.
		HS=	950.01		960.01		975.00		1000.00
		BS=	50.0		50.0		150.0		150.0
		BSS=	0.0		0.0		0.0		0.0
I=	5	FLDSTG=	0.00	YDI=	0.00	QDI=	0.	AS1=	0.
		HS=	950.00		960.00		962.10		990.00
		BS=	50.0		50.0		0.0		0.0
		BSS=	0.0		0.0		0.0		0.0
I=	6	FLDSTG=	0.00	YDI=	0.00	QDI=	0.	AS1=	0.
		HS=	925.00		935.00		937.10		965.00
		BS=	50.0		50.0		0.0		0.0
		BSS=	0.0		0.0		0.0		0.0
I=	7	FLDSTG=	0.00	YDI=	0.00	QDI=	0.	AS1=	0.
		HS=	925.00		935.00		950.00		975.00
		BS=	50.0		50.0		150.0		150.0
		BSS=	0.0		0.0		0.0		0.0
I=	8	FLDSTG=	0.00	YDI=	0.00	QDI=	0.	AS1=	0.
		HS=	900.00		910.00		925.00		950.00
		BS=	50.0		50.0		150.0		150.0
		BSS=	0.0		0.0		0.0		0.0

REACH INFO RIVER NO. 1

FKEC(I,1), I = 1, NM(1)
0.00 0.00 0.00 0.00 0.00 0.00 0.00

NCM(K, 1), K=1,NRCM1(1)
1 2 4 5

CM(K, 1, 1)=	0.0400	0.0400	0.0400	0.0400
CM(K, 2, 1)=	0.0400	0.0500	0.0400	0.0400
CM(K, 3, 1)=	0.0400	0.0350	0.0400	0.0400
CM(K, 4, 1)=	0.0400	0.0400	0.0400	0.0400

0.0

22.7 FLDWAV Example 7.0 -- Multiple Rivers, Levees

This example illustrates the use of FLDWAV to model two rivers simultaneously. The main stem which is 40 miles long has a 20-mile tributary coming into it below mile 20 at a 90° angle. There are levees on both sides of the main stem and on the tributary. Each cross section reach within the length of each levee is a levee reach resulting in 7 levee reaches in the system. There are also 3 floodplain/ponds in the system that interact with the levees. The upstream boundary condition for each river is a discharge hydrograph. The downstream boundary condition for the main river is a generated looped rating curve. The downstream boundary for the tributary is the computed water-surface elevation at the confluence.

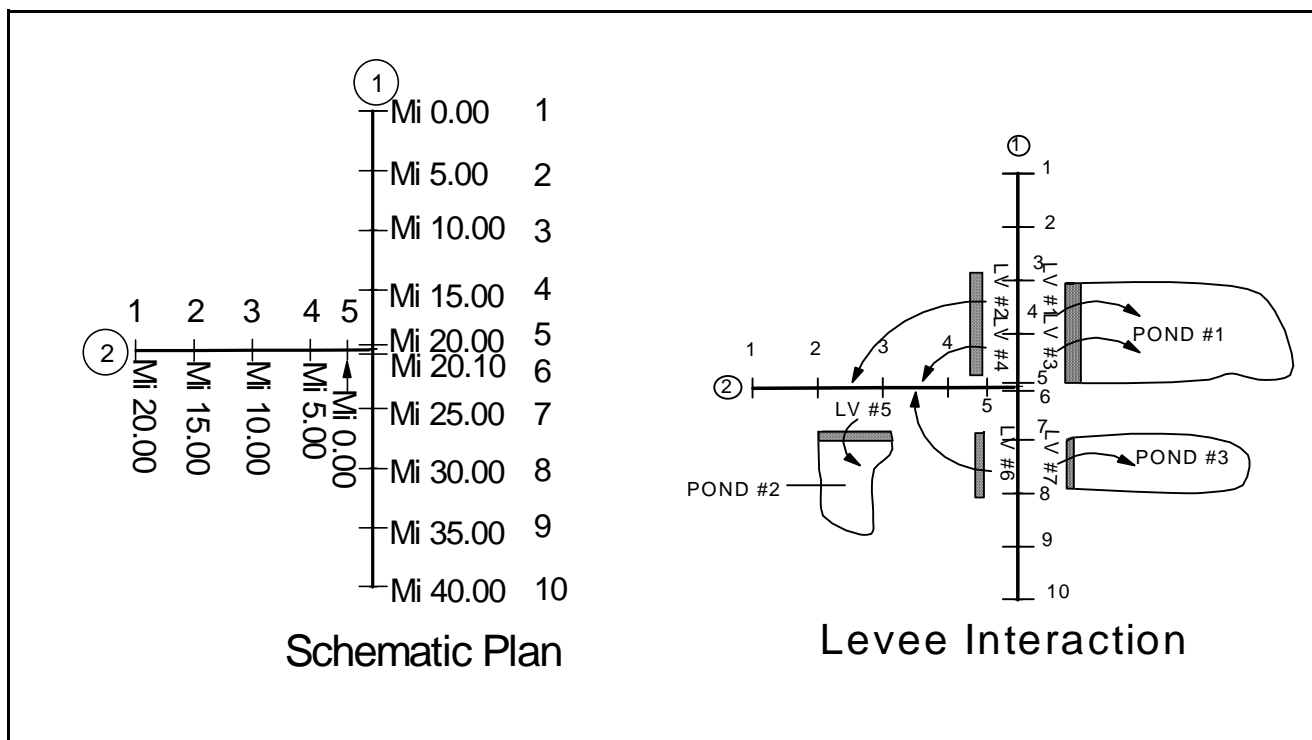


Figure 22.7 - Example 7.0 – Multiple Rivers, Levees.

Table 22.13 Input Data Set for Example 7

PROBLEM	LV																
EOM																	
NO	DESC																
.01		0.7	0.6	5280.	24.	0											
	2	4	10	0	0	0	0	0	0	0	0						
0	0	0	0														
	3	2	109	1	0												
	0	0	0	0	0												
60.	2.0	2.0	0	0	0												
	7	0.0	0.50														
1	3	1	0														
1	3	2	2														
1	4	1	0														
1	4	2	3														
2	2	2	0														
1	7	2	3														
1	7	3	0														
	10	1	100	10.	0.	0.	0.										
	5	1	100	1	5	90.	10.	0.	0.	0.							
2	4	0	6	9	0	0	0	0	0								
2	0	0	5	4	0	0	0	0	0								
0	0	0	0	0	0	0	0	0	0	0							
0	0	0	0	0	0	0	0	0	0	0							
0.	5.	10.	15.	20.	20.1	25.	30.										
35.	40.																

0.	0.	1.25	2.5	0.	0.	1.0	0
0.							
0	0	0	0	0	0	0	0
0.	5.	10.	15.	20.			
0.	2.50	1.25	0.				
	0	0	0	0			
107.00	3.0000	2.5	500.0	1000.0	105.0	0.0001	
107.00	3.0000	2.5	500.0	1000.0	105.0	0.0001	
100.50	-3.000	2.5	500.0	1000.0	98.50	0.0001	
90.0	5.0						
102.50	3.0000	2.5	500.0	1000.0	100.5	0.0001	
104.50	3.0000	2.5	500.0	1000.0	102.5	0.0001	
100.00	3.000	2.5	500.0	1000.0	98.0	0.0001	
91.000	3.0000	2.5	5000.0	91.000	89.0	0.0001	
94.0							
1000.0	1000.0	0	0	0	0	0	0
60.0	1000.0	0	0	0	0	0	0
85.0							
1000.0	1000.0	0	0	0	0	0	0
60.0	1000.0	0	0	0	0	0	0
70.0							
1000.0	1000.0	0	0	0	0	0	0
60.0	1000.0	0	0	0	0	0	0
	1	3	5	6	7	9	
	1	2	3	4	5		

MI 0

MI 10

MI 20

MI 20.1

MI 30

MI 40

MI 0

MI 5

MI 10

MI 15

MI 20

3000.	20000.	3000.	3000.
-------	--------	-------	-------

3000.	6000.0	3000.	3000.
-------	--------	-------	-------

0.	0.	3000.	0.
----	----	-------	----

100.	110.	125.	
------	------	------	--

0.	500.	1000.	
----	------	-------	--

0.	0	0	
----	---	---	--

0.	0.	0.	0.
----	----	----	----

95.	105.	120.	
-----	------	------	--

0.	500.	1000.	
----	------	-------	--

0.	0	0	
----	---	---	--

0.	0.	0.	0.
----	----	----	----

90.	100.	115.	
-----	------	------	--

0.	500.	1000.	
----	------	-------	--

0.	0	0	
----	---	---	--

0.	0.	0.	0.
85.	95.	110.	
0.	500.	1000.	
0.	0	0	
0.	0.	0.	0.
80.	90.	105.	
0.	500.	1000.	
0.	0	0	
0.	0.	0.	0.
80.	90.	105.	
0.	500.	1000.	
0.	0	0	
0.	0.	0.	0.
75.	85.0	100.0	
0.	500.	1000.	
0.	0	0	
0.	0.	0.	0.
70.	80.0	95.0	
0.	500.	1000.	
0.	0	0	
0.	0.	0.	0.
65.	75.	90.0	
0.	500.	1000.	
0.	0	0	
0.	0.	0.	0.

60.	70.	85.0		
0.	500.	1000.		
0.	0	0		
0.	0.	3000.	0.	
100.	110.	125.		
0.	500.	1000.		
0.	0	0		
0.	0.	0.	0.	
95.	105.	120.		
0.	500.	1000.		
0.	0	0		
0.	0.	0.	0.	
90.	100.	115.		
0.	500.	1000.		
0.	0	0		
0.	0.	0.	0.	
85.	95.	110.		
0.	500.	1000.		
0.	0	0		
0.	0.	0.	0.	
80.	90.	105.		
0.	500.	1000.		
0.	0	0		
0 0 0 0 0 0 0 0 0				
2	3	4	5	6
			7	8
				9
				10

.04	.04	.04	
.04	.04	.04	
.04	.04	.04	
.04	.04	.04	
.04	.04	.04	
.04	.04	.04	
.04	.04	.04	
.04	.04	.04	
.04	.04	.04	
0	0	0	0
2	3	4	5
.04	.04	.04	
.04	.04	.04	
.04	.04	.04	
.04	.04	.04	

0 0

4/2 THEN 4 MAIN REACH TO 2/4 THEN 4 TRIB REACH AND 3 POND

LV RIVER

LV RIVER

END

EXIT

Table 22.14 Echo Print of Example 7

PROGRAM FLDWAV - BETA VERSION 1.0 2/1/95

HYDROLOGIC RESEACH LABORATORY
W/OH3 OFFICE OF HYDROLOGY
NOAA, NATIONAL WEATHER SERVICE
SILVER SPRING, MARYLAND 20910

*** SUMMARY OF INPUT DATA ***

PROBLEM LV

EPSY	THETA	F1	XFACT	DTHYD	DTOUT	METRIC		
0.010	0.700	0.600	5280.000	24.000	0.000	0		
JN	NU	ITMAX	KWARM	KFLP	NET	ICOND	FUTURE DATA	
2	4	10	0	0	0	0	0 0 0	
NYQD	KCG	NCG	KPRES					
0	0	0	0					
NCS	KPL	JNK	KREVRS	NFGRF				
3	2	109	1	0				
IOBS	KTERM	NP	NPST	NPEND				
0	0	0	0	0				
TEH	DTHII	DTHPLT	FRDFR	DTEXP	MDT			
60.000	2.00000	2.00000	0.00	0.00000	0			
NLEV	DHLV	DTHLV						
7	0.00000	0.50000						
LEVEE NO	NJFM(L)	NIFM(L)	NJTO(L)	NITO(L)				
1	1	3	1	0				
2	1	3	2	2				
3	1	4	1	0				
4	1	4	2	3				
5	2	2	2	0				

6	1	7	2	3
7	1	7	3	0

RIVER NO.	NBT	NPT1	NPT2	MRV	NJUN	ATF	EPQJ	COFW	VWIND	WINAGL
1	10	1	100				10.00	0.00	0.00	0.00
2	5	1	100	1	5	90.00	10.00	0.00	0.00	0.00

RIVER NO.	KU	KD	NQL	NGAGE	NRCM1	NQCM	NSTR	FUTURE DATA
1	2	4	0	6	9	0	0	0 0 0
2	2	0	0	5	4	0	0	0 0 0

RIVER NO.	MIXF	MUD	KFTR	KLOS	FUTURE DATA
1	0	0	0	0	0 0 0 0 0 0
2	0	0	0	0	0 0 0 0 0 0

XT(I, 1) I=1,NB(1)								
0.000	5.000	10.000	15.000	20.000	20.100	25.000	30.000	
35.000	40.000							

DXM(I, 1) I=1,NB(1)								
0.000	0.000	1.250	2.500	0.000	0.000	1.000	0.000	
0.000								

KRCH(I, 1) I=1,NRCH								
0	0	0	0	0	0	0	0	
0								

XT(I, 2) I=1,NB(2)					
0.000	5.000	10.000	15.000	20.000	

DXM(I, 2) I=1,NB(2)				
0.000	2.500	1.250	0.000	

KRCH(I, 2) I=1,NRCH				
0	0	0	0	

L	NJFM	NIFM	NJTO	NITO	X	HWLV	TFLV	WCLV	BLVMX	HFLV	HLVMN	SLV
HPLV			DPLV									
1	1	3	1	0	10.00	107.00	3.00	2.50	500.00	1000.00	105.00	
0.00010	100000.00			0.00								
2	1	3	2	2	10.00	107.00	3.00	2.50	500.00	1000.00	105.00	
0.00010	100000.00			0.00								
3	1	4	1	0	15.00	100.50	-3.00	2.50	500.00	1000.00	98.50	
0.00010	90.00			5.00								
4	1	4	2	3	15.00	102.50	3.00	2.50	500.00	1000.00	100.50	
0.00010	100000.00			0.00								
5	2	2	2	0	5.00	104.50	3.00	2.50	500.00	1000.00	102.50	
0.00010	100000.00			0.00								

6	1	7	2	3	25.00	100.00	3.00	2.50	500.00	1000.00	98.00
0.00010	100000.00			0.00							
7	1	7	3	0	25.00	91.00	3.00	2.50	5000.00	91.00	89.00
0.00010	100000.00			0.00							

POND=	1	HPOND=	94.00								
SAPOND:	1000.	1000.	0.	0.	0.	0.	0.	0.	0.		
HSAP:	60.00	1000.00	0.00	0.00	0.00	0.00	0.00	0.00	0.00	0.00	

POND=	2	HPOND=	85.00								
SAPOND:	1000.	1000.	0.	0.	0.	0.	0.	0.	0.	0.	
HSAP:	60.00	1000.00	0.00	0.00	0.00	0.00	0.00	0.00	0.00	0.00	

POND=	3	HPOND=	70.00								
SAPOND:	1000.	1000.	0.	0.	0.	0.	0.	0.	0.	0.	
HSAP:	60.00	1000.00	0.00	0.00	0.00	0.00	0.00	0.00	0.00	0.00	

PLOTTING/OBSERVED TIME SERIES FOR RIVER J= 1

I	NGS	ID
1	1	MI 0
2	3	MI 10
3	5	MI 20
4	6	MI 20.1
5	7	MI 30
6	9	MI 40

PLOTTING/OBSERVED TIME SERIES FOR RIVER J= 2

I	NGS	ID
1	1	MI 0
2	2	MI 5
3	3	MI 10
4	4	MI 15
5	5	MI 20

ST1(K,1), K = 1, NU

3000.00	20000.00	3000.00	3000.00
---------	----------	---------	---------

T1(K,1), K = 1, NU

0.00	24.00	48.00	72.00
------	-------	-------	-------

ST1(K,2), K = 1, NU

3000.00	6000.00	3000.00	3000.00
---------	---------	---------	---------

T1(K,2), K = 1, NU

0.00	24.00	48.00	72.00
------	-------	-------	-------

RIVER NO. 1

I=	1	FLDSTG=	0.00	YDI=	0.00	QDI=	3000.	AS1=	0.
		HS=	100.00	110.00	125.00				
		BS=	0.0	500.0	1000.0				
		BSS=	0.0	0.0	0.0				
I=	2	FLDSTG=	0.00	YDI=	0.00	QDI=	0.	AS1=	0.
		HS=	95.00	105.00	120.00				
		BS=	0.0	500.0	1000.0				
		BSS=	0.0	0.0	0.0				
I=	3	FLDSTG=	0.00	YDI=	0.00	QDI=	0.	AS1=	0.
		HS=	90.00	100.00	115.00				
		BS=	0.0	500.0	1000.0				
		BSS=	0.0	0.0	0.0				
I=	4	FLDSTG=	0.00	YDI=	0.00	QDI=	0.	AS1=	0.
		HS=	85.00	95.00	110.00				
		BS=	0.0	500.0	1000.0				
		BSS=	0.0	0.0	0.0				
I=	5	FLDSTG=	0.00	YDI=	0.00	QDI=	0.	AS1=	0.
		HS=	80.00	90.00	105.00				
		BS=	0.0	500.0	1000.0				
		BSS=	0.0	0.0	0.0				
I=	6	FLDSTG=	0.00	YDI=	0.00	QDI=	0.	AS1=	0.
		HS=	80.00	90.00	105.00				
		BS=	0.0	500.0	1000.0				
		BSS=	0.0	0.0	0.0				
I=	7	FLDSTG=	0.00	YDI=	0.00	QDI=	0.	AS1=	0.
		HS=	75.00	85.00	100.00				
		BS=	0.0	500.0	1000.0				
		BSS=	0.0	0.0	0.0				
I=	8	FLDSTG=	0.00	YDI=	0.00	QDI=	0.	AS1=	0.
		HS=	70.00	80.00	95.00				
		BS=	0.0	500.0	1000.0				
		BSS=	0.0	0.0	0.0				
I=	9	FLDSTG=	0.00	YDI=	0.00	QDI=	0.	AS1=	0.
		HS=	65.00	75.00	90.00				
		BS=	0.0	500.0	1000.0				
		BSS=	0.0	0.0	0.0				
I=	10	FLDSTG=	0.00	YDI=	0.00	QDI=	0.	AS1=	0.
		HS=	60.00	70.00	85.00				
		BS=	0.0	500.0	1000.0				

BSS=	0.0	0.0	0.0
------	-----	-----	-----

RIVER NO. 2

I=	1	FLDSTG=	0.00	YDI=	0.00	QDI=	3000.	AS1=	0.
		HS=	100.00	110.00	125.00				
		BS=	0.0	500.0	1000.0				
		BSS=	0.0	0.0	0.0				

I=	2	FLDSTG=	0.00	YDI=	0.00	QDI=	0.	AS1=	0.
		HS=	95.00	105.00	120.00				
		BS=	0.0	500.0	1000.0				
		BSS=	0.0	0.0	0.0				

I=	3	FLDSTG=	0.00	YDI=	0.00	QDI=	0.	AS1=	0.
		HS=	90.00	100.00	115.00				
		BS=	0.0	500.0	1000.0				
		BSS=	0.0	0.0	0.0				

I=	4	FLDSTG=	0.00	YDI=	0.00	QDI=	0.	AS1=	0.
		HS=	85.00	95.00	110.00				
		BS=	0.0	500.0	1000.0				
		BSS=	0.0	0.0	0.0				

I=	5	FLDSTG=	0.00	YDI=	0.00	QDI=	0.	AS1=	0.
		HS=	80.00	90.00	105.00				
		BS=	0.0	500.0	1000.0				
		BSS=	0.0	0.0	0.0				

REACH INFO RIVER NO. 1

FKEC(I,1), I = 1, NM(1)								
0.00	0.00	0.00	0.00	0.00	0.00	0.00	0.00	0.00
0.00								

NCM(K, 1), K=1,NRCM1(1)									
2	3	4	5	6	7	8	9	10	
CM(K, 1, 1)=			0.0400		0.0400		0.0400		
CM(K, 2, 1)=			0.0400		0.0400		0.0400		
CM(K, 3, 1)=			0.0400		0.0400		0.0400		
CM(K, 4, 1)=			0.0400		0.0400		0.0400		
CM(K, 5, 1)=			0.0400		0.0400		0.0400		

CM(K, 6, 1)=	0.0400	0.0400	0.0400
CM(K, 7, 1)=	0.0400	0.0400	0.0400
CM(K, 8, 1)=	0.0400	0.0400	0.0400
CM(K, 9, 1)=	0.0400	0.0400	0.0400

REACH INFO RIVER NO. 2

FKEC(I,2), I = 1, NM(2)			
0.00	0.00	0.00	0.00

NCM(K, 2), K=1,NRCM1(2)				
2	3	4	5	

CM(K, 1, 2)=	0.0400	0.0400	0.0400
CM(K, 2, 2)=	0.0400	0.0400	0.0400
CM(K, 3, 2)=	0.0400	0.0400	0.0400
CM(K, 4, 2)=	0.0400	0.0400	0.0400

0 0

22.8 FLDWAV Example 8.0 -- Same as Example 2.0 Except with Metric Option

This example illustrates the use of the metric option which is activated by specifying the input parameter (METRIC) equal to 1. The equivalent metric (SI) units for input used in FLDWAV are shown in Table 20.1. Example #8 is identical to Example #2. In the metric option, both the input and output are in metric units rather than English units.

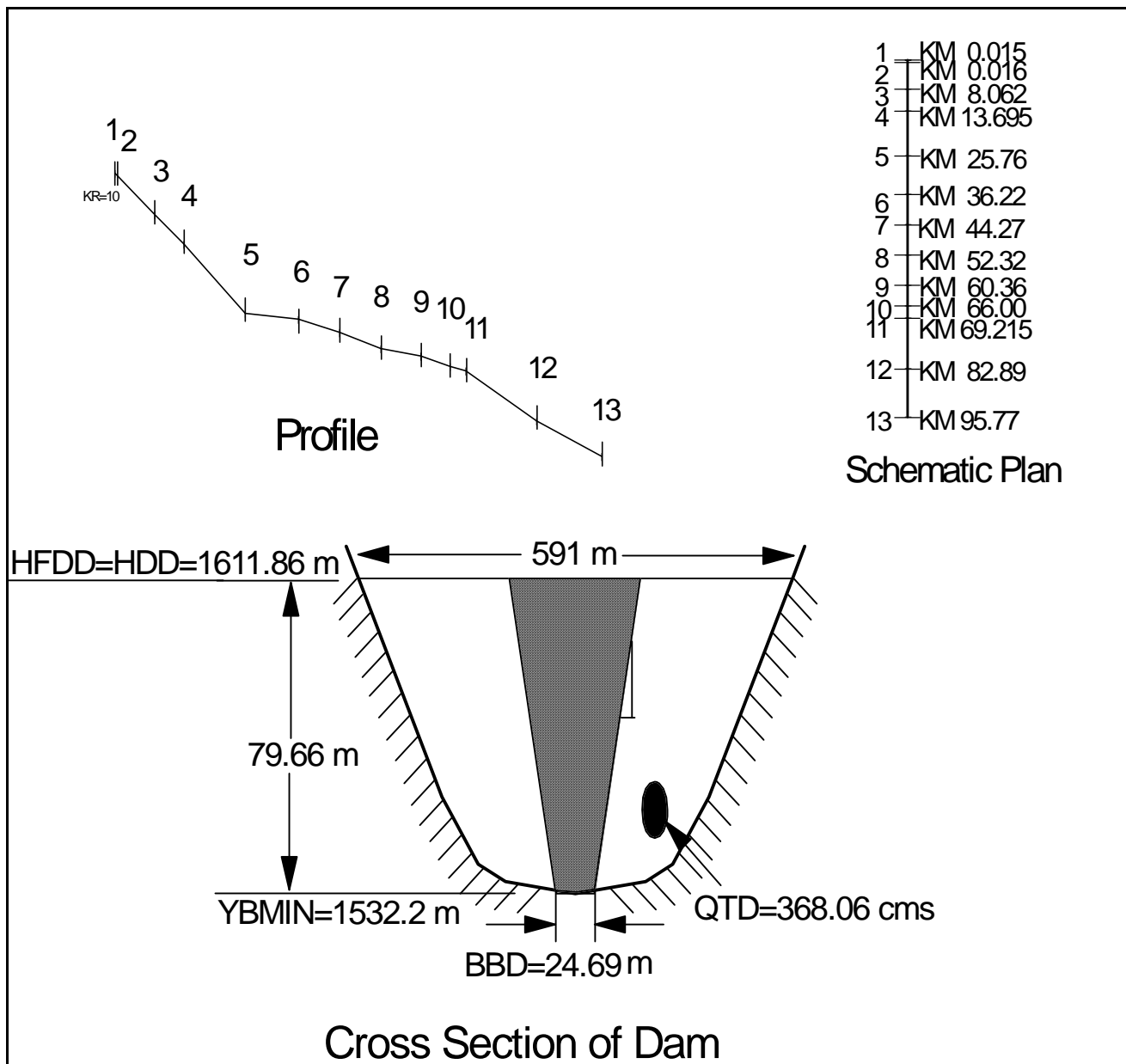


Figure 22.8 - Example 8.0 – Same as Example 2.0 Except with Metric Option.

PROBLEM E-8
EOM
NO DESC

22.55

0.	0.	0.	0.	0.
1538.25	0	0	0	
1532.15	1535.20	1539.47	1556.53	1562.02
0.	179.82	249.92	344.41	365.74
0.	0.	0.	0.	0.
1519.35	0	0	0	
1513.26	1517.83	1528.50	1530.02	1533.07
0.	259.07	335.26	365.74	396.22
0.	0.	1066.75	1310.58	1615.36
1507.47	0	0	0	
1499.54	1502.59	1506.25	1509.60	1511.12
0.	243.83	1219.14	3352.64	4571.78
0.	0.	0.	2133.50	3047.85
1472.11	0	0	0	
1468.15	1471.20	1476.68	1477.69	1478.82
0.	269.43	1219.14	3352.64	6705.27
0.	0.	9143.55	8229.20	7619.63
1469.06	0	0	0	
1464.99	1466.62	1467.24	1470.59	1472.11
0.	304.79	365.74	3352.64	4876.56
0.	0.	0.	1828.71	2438.28
1462.97	0	0	0	
1459.31	1460.53	1463.58	1465.41	1466.02
0.	87.17	2133.50	3047.85	3352.64
0.	0.	0.	1066.75	1523.93
1455.96	0	0	0	
1451.39	1455.04	1455.96	1456.87	1458.40
0.	107.28	1523.93	3047.85	5486.13
0.	0.	2743.07	4876.56	7314.84
1452.91	0	0	0	
1448.34	1451.69	1453.22	1454.74	1456.26
0.	137.15	1066.75	1828.71	2743.07
0.	0.	1219.14	2590.67	3657.42
1449.56	0	0	0	
1443.46	1449.56	1451.08	1451.69	1453.22
0.	164.58	609.57	1219.14	1828.71
0.	0.	1127.70	1127.70	1676.32
1447.42	0	0	0	

1441.33	1443.77	1447.42	1449.86	1450.47				
0.	76.20	178.91	533.37	609.57				
0.	0.	0.	457.18	609.57				
1424.56	0	0	0					
1418.47	1419.99	1422.74	1425.78	1427.31				
0.	21.33	107.28	121.91	128.01				
0.	0.	0.	0.	0.				
1405.67	0	0	0					
1402.32	1403.23	1403.84	1406.58	1408.11				
0.	74.67	137.15	152.39	158.48				
0.	0.	0.	0.	0.				
.0	.0	-.90	.0	.0	.100	-.5	.0	
.0	.0	.0	.0	.0	.0			
1	3	4	5	6	7	8	11	
.080	.080	0.080		.080	.080			
.06	.06	.06		.06	.06			
.031	.031	.031		.031	.031			
.034	.034	.034		.034	.034			
.038	.038	.038		.038	.038			
.037	.037	.037		.037	.037			
.034	.034	.034		.034	.034			
.036	.036	.036		.036	.036			
0.0000								

END OF MY DATA -- E-8

E-8 RIVER

Table 22.16 Echo Print of Example 8

PROGRAM FLDWAV - BETA VERSION 1.0 2/1/95

HYDROLOGIC RESEACH LABORATORY
W/OH3 OFFICE OF HYDROLOGY
NOAA, NATIONAL WEATHER SERVICE
SILVER SPRING, MARYLAND 20910

*** SUMMARY OF INPUT DATA ***

PROBLEM E-8

EPSY	THETA	F1	XFACT	DTHYD	DTOUT	METRIC	
0.010	1.000	0.600	1000.000	0.000	0.000	1	
JN	NU	ITMAX	KWARM	KFLP	NET	ICOND	FUTURE DATA
1	3	10	2	0	0	0	0 0 0
NYQD	KCG	NCG	KPRES				
0	0	0	0				
NCS	KPL	JNK	KREVR5	NFGRF			
5	2	5	0	0			
IOBS	KTERM	NP	NPST	NPEND			
0	0	0	0	0			
TEH	DTHII	DTHPLT	FRDFR	DTEXP	MDT		
55.000	0.07150	0.07150	0.00	0.00000	0		
NLEV	DHLV	DTHLV					
0	0.00000	0.00000					
RIVER NO.	NBT	NPT1	NPT2	EPQJ	COFW	VWIND	WINAGL
1	13	1	13	100.00	0.00	0.00	0.00
RIVER NO.	KU	KD	NQL	NGAGE	NRCM1	NQCM	NSTR
1	2	4	0	7	8	0	0
							0 0 0
RIVER NO.	MIXF	MUD	KFTR	KLOS	FUTURE DATA		
1	0	0	0	0	0 0 0 0 0 0		
XT(I, 1)	I=1,NB(1)						
0.015	0.016	8.062	13.695	25.760	36.220	44.270	52.320
60.360	66.000	69.215	82.890	95.770			
DXM(I, 1)	I=1,NB(1)						
10.000	0.810	0.810	1.207	1.609	1.609	1.609	1.609
1.609	1.609	1.770	2.253				
KRCH(I, 1)	I=1,NRCH						
10	0	0	0	0	0	0	
0	0	0	0				
RIVER NO.	1,	DAM NO.	1				
SAR(L, 1, 1)	L=1,8						
7.84	4.68	2.34	0.87	0.00	0.00	0.00	0.00
HSAR(L, 1, 1)	L=1,8						
1611.86	1593.57	1553.95	1535.66	1532.15	0.00	0.00	0.00

LAD	HDD	CLL	CDOD	QTD	ICHAN		
1	1611.86	16.83	50.49	368.06	0		
ICG	HSPD	SPL	CSD	HGTD	CGD		
0	0.00	0.00	0.00	0.00	0.00		
TFH	DTHDB	HFDD	BBD	ZBCH	YBMIN	BREXP	CPIP
1.430	0.00000	1611.86	24.69	1.04	1532.15	1.00	0.00

PLOTTING/OBSERVED TIME SERIES FOR RIVER J= 1

I	NGS	ID
1	1	KM 00.01
2	2	KM 00.016
3	3	KM 8.062
4	4	KM 13.695
5	5	KM 25.76
6	11	KM 69.215
7	13	KM 95.77

ST1(K,1), K = 1, NU
368.06 368.06 368.06

T1(K,1), K = 1, NU
0.00 1.00 55.00

RIVER NO. 1

I=	1	FLDSTG=	1538.25	YDI=	1611.86	QDI=	0.	AS1=	0.
		HS=	1532.15	1535.20	1539.47	1556.53	1620.00		
		BS=	0.0	179.8	249.9	344.4	591.0		
		BSS=	0.0	0.0	0.0	0.0	0.0		
I=	2	FLDSTG=	1538.25	YDI=	0.00	QDI=	0.	AS1=	0.
		HS=	1532.15	1535.20	1539.47	1556.53	1562.02		
		BS=	0.0	179.8	249.9	344.4	365.7		
		BSS=	0.0	0.0	0.0	0.0	0.0		
I=	3	FLDSTG=	1519.35	YDI=	0.00	QDI=	0.	AS1=	0.
		HS=	1513.26	1517.83	1528.50	1530.02	1533.07		
		BS=	0.0	259.1	335.3	365.7	396.2		
		BSS=	0.0	0.0	1066.8	1310.6	1615.4		
I=	4	FLDSTG=	1507.47	YDI=	0.00	QDI=	0.	AS1=	0.
		HS=	1499.54	1502.59	1506.25	1509.60	1511.12		
		BS=	0.0	243.8	1219.1	3352.6	4571.8		
		BSS=	0.0	0.0	0.0	2133.5	3047.9		
I=	5	FLDSTG=	1472.11	YDI=	0.00	QDI=	0.	AS1=	0.
		HS=	1468.15	1471.20	1476.68	1477.69	1478.82		
		BS=	0.0	269.4	1219.1	3352.6	6705.3		
		BSS=	0.0	0.0	9143.5	8229.2	7619.6		
I=	6	FLDSTG=	1469.06	YDI=	0.00	QDI=	0.	AS1=	0.
		HS=	1464.99	1466.62	1467.24	1470.59	1472.11		
		BS=	0.0	304.8	365.7	3352.6	4876.6		
		BSS=	0.0	0.0	0.0	1828.7	2438.3		
I=	7	FLDSTG=	1462.97	YDI=	0.00	QDI=	0.	AS1=	0.
		HS=	1459.31	1460.53	1463.58	1465.41	1466.02		
		BS=	0.0	87.2	2133.5	3047.9	3352.6		
		BSS=	0.0	0.0	0.0	1066.8	1523.9		
I=	8	FLDSTG=	1455.96	YDI=	0.00	QDI=	0.	AS1=	0.
		HS=	1451.39	1455.04	1455.96	1456.87	1458.40		
		BS=	0.0	107.3	1523.9	3047.9	5486.1		
		BSS=	0.0	0.0	2743.1	4876.6	7314.8		
I=	9	FLDSTG=	1452.91	YDI=	0.00	QDI=	0.	AS1=	0.
		HS=	1448.34	1451.69	1453.22	1454.74	1456.26		
		BS=	0.0	137.1	1066.8	1828.7	2743.1		
		BSS=	0.0	0.0	1219.1	2590.7	3657.4		

I=	10	FLDSTG=	1449.56	YDI=	0.00	QDI=	0.	AS1=	0.
		HS=	1443.46	1449.56	1451.08	1451.69	1453.22		
		BS=	0.0	164.6	609.6	1219.1	1828.7		
		BSS=	0.0	0.0	1127.7	1127.7	1676.3		
I=	11	FLDSTG=	1447.42	YDI=	0.00	QDI=	0.	AS1=	0.
		HS=	1441.33	1443.77	1447.42	1449.86	1450.47		
		BS=	0.0	76.2	178.9	533.4	609.6		
		BSS=	0.0	0.0	0.0	457.2	609.6		
I=	12	FLDSTG=	1424.56	YDI=	0.00	QDI=	0.	AS1=	0.
		HS=	1418.47	1419.99	1422.74	1425.78	1427.31		
		BS=	0.0	21.3	107.3	121.9	128.0		
		BSS=	0.0	0.0	0.0	0.0	0.0		
I=	13	FLDSTG=	1405.67	YDI=	0.00	QDI=	0.	AS1=	0.
		HS=	1402.32	1403.23	1403.84	1406.58	1408.11		
		BS=	0.0	74.7	137.1	152.4	158.5		
		BSS=	0.0	0.0	0.0	0.0	0.0		

REACH INFO RIVER NO. 1

FKEC(I,1), I = 1, NM(1)							
0.00	0.00	-0.90	0.00	0.00	0.10	-0.50	0.00
0.00	0.00	0.00	0.00				

NCM(K, 1), K=1,NRCM1(1)

	1	3	4	5	6	7	8	11
CM(K, 1, 1)=								
		0.0800		0.0800		0.0800	0.0800	0.0800
CM(K, 2, 1)=		0.0600		0.0600		0.0600	0.0600	0.0600
CM(K, 3, 1)=		0.0310		0.0310		0.0310	0.0310	0.0310
CM(K, 4, 1)=		0.0340		0.0340		0.0340	0.0340	0.0340
CM(K, 5, 1)=		0.0380		0.0380		0.0380	0.0380	0.0380
CM(K, 6, 1)=		0.0370		0.0370		0.0370	0.0370	0.0370
CM(K, 7, 1)=		0.0340		0.0340		0.0340	0.0340	0.0340
CM(K, 8, 1)=		0.0360		0.0360		0.0360	0.0360	0.0360

0.0000

22.9 FLDWAV Example 9.0 -- Supercritical Flow Downstream of Dam

This example illustrates the use of FLDWAV to simulate unsteady flow and the development of a breach hydrograph at a dam via dynamic routing through a 26-mile reach. The 16-mile reach above the dam is subcritical with 12 ft/mi slope, while the 10-mile reach below the dam is supercritical with a slope of 100 ft/mi. The entire reach is routed simultaneously using the LPI algorithm (MIXF(1)=5).

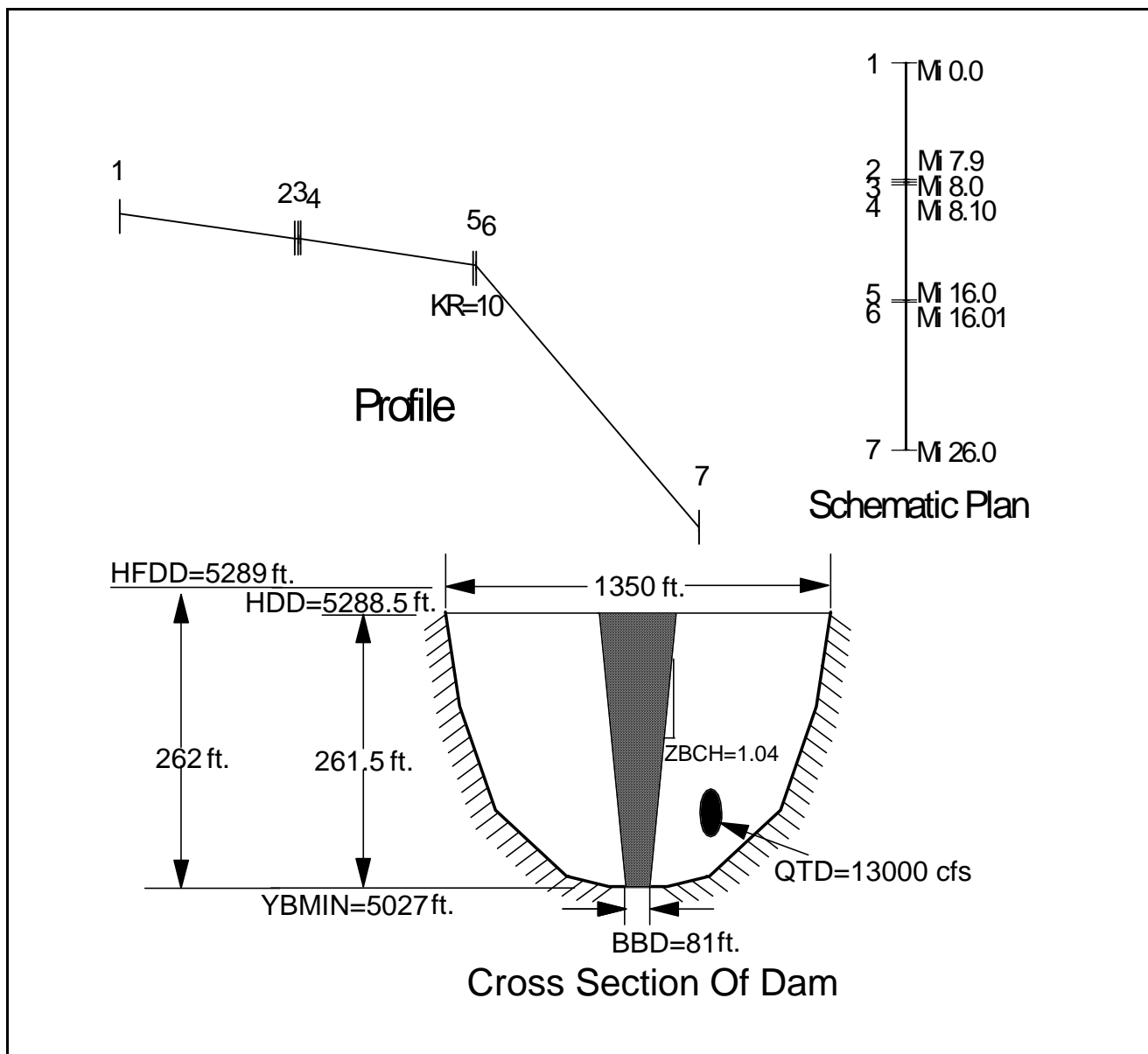


Figure 22.9 - Example 9.0 – Supercritical Flow Downstream of Dam.

PROBLEM E-9
EOM
NO DESC

22.62

200.0	350.0	600.0	725.0	800.0
.0	.0	.0	.0	.0
.00	.0	0.0	0.0	
5123.5	5133.5	5170.0	5225.0	5290.0
200.0	350.0	600.0	725.0	800.0
.0	.0	.0	.0	.0
5037.00	5288.5	0.0	0.0	
5027.0	5037.0	5100.0	5200.0	5290.0
200.0	500.0	1000.0	1250.0	1350.0
.0	.0	.0	.0	.0
.0	.0	.0	.0	.0
5027.0	5037.0	5057.0	5157.0	5257.0
.0	300.0	1000.0	1100.0	1200.0
.0	.0	.0	.0	.0
.0	.0	.0	.0	.0
4027.0	4037.0	4057.0	4067.0	4080.0
.0	300.0	1000.0	1100.0	1225.0
.0	.0	.0	.0	.0
0.0	0.0	0.0	0.0	0.0
0.0	0.0	0.0	0.0	0.0
1	2	4	6	
.060	.060	.050	.040	.040
.060	.060	.030	.030	.030
.030	.030	.030	.030	.030
.030	.030	.040	.040	.040
0.00000				

END OF THE DATA

E-9 RIVER

Table 22.18 Echo Print of Example 9

PROGRAM FLDWAV - BETA VERSION 1.0 2/1/95

HYDROLOGIC RESEACH LABORATORY
W/OH3 OFFICE OF HYDROLOGY
NOAA, NATIONAL WEATHER SERVICE
SILVER SPRING, MARYLAND 20910

*** SUMMARY OF INPUT DATA ***

PROBLEM E-9

EPSY	THETA	F1	XFACT	DTHYD	DTOUT	METRIC	
0.010	1.000	0.600	5280.000	0.000	0.000	0	
JN	NU	ITMAX	KWARM	KFLP	NET	ICOND	FUTURE DATA
1	3	10	2	0	0	0	0 0 0
NYQD	KCG	NCG	KPRES				
0	0	0	0				
NCS	KPL	JNK	KREVR5	NFGRF			
5	2	5	0	0			
IOBS	KTERM	NP	NPST	NPEND			
0	0	0	0	0			
TEH	DTHII	DTHPLT	FRDFR	DTEXP	MDT		
55.000	0.07150	0.71500	0.00	0.00000	0		
NLEV	DHLV	DTHLV					
0	0.00000	0.00000					
RIVER NO.	NBT	NPT1	NPT2	EPQJ	COFW	VWIND	WINAGL
1	7	34	54	100.00	0.00	0.00	0.00
RIVER NO.	KU	KD	NQL	NGAGE	NRCM1	NQCM	NSTR
1	2	4	0	5	4	0	0
							0 0 0
RIVER NO.	MIXF	MUD	KFTR	KLOS	FUTURE DATA		
1	2	0	0	0	0 0 0 0 0 0		
XT(I, 1)	I=1,NB(1)						
0.000	7.900	8.000	8.100	16.000	16.010	26.000	
DXM(I, 1)	I=1,NB(1)						
0.500	0.100	0.100	0.500	100.000	0.500		
KRCH(I, 1)	I=1,NRCH						
0	0	0	0	10	0		
RIVER NO.	1,	DAM NO.	1				
LAD	HDD	CLL	CDOD	QTD	ICHAN		
5	5288.50	100.00	3.00	13000.00	0		
ICG	HSPD	SPL	CSD	HGTD	CGD		
0	0.00	0.00	0.00	0.00	0.00		
TFH	DTHDB	HFDD	BBD	ZBCH	YBMIN	BREXP	CPIP
1.430	0.00000	5289.00	81.00	1.04	5027.00	1.00	0.00

PLOTTING/OBSERVED TIME SERIES FOR RIVER J= 1

I	NGS	ID	
1	1	MI	0.00
2	3	MI	8.00
3	5	MI	16.00
4	6	MI	16.01
5	7	MI	26.00

ST1(K,1), K = 1, NU
13000.00 50000.00 13000.00

T1(K,1), K = 1, NU
0.00 1.00 55.00

RIVER NO. 1

I=	1	FLDSTG=	5230.00	YDI=	0.00	QDI=	0.	AS1=	0.
		HS=	5220.00	5230.00	5240.00	5250.00	5290.00		
		BS=	200.0	200.0	200.0	200.0	200.0		
		BSS=	0.0	0.0	0.0	0.0	0.0		
I=	2	FLDSTG=	0.00	YDI=	0.00	QDI=	0.	AS1=	0.
		HS=	5123.50	5133.50	5170.00	5225.00	5290.00		
		BS=	200.0	350.0	600.0	725.0	800.0		
		BSS=	0.0	0.0	0.0	0.0	0.0		
I=	3	FLDSTG=	0.00	YDI=	0.00	QDI=	0.	AS1=	0.
		HS=	5123.50	5133.50	5170.00	5225.00	5290.00		
		BS=	200.0	350.0	600.0	725.0	800.0		
		BSS=	0.0	0.0	0.0	0.0	0.0		
I=	4	FLDSTG=	0.00	YDI=	0.00	QDI=	0.	AS1=	0.
		HS=	5123.50	5133.50	5170.00	5225.00	5290.00		
		BS=	200.0	350.0	600.0	725.0	800.0		
		BSS=	0.0	0.0	0.0	0.0	0.0		
I=	5	FLDSTG=	5037.00	YDI=	5288.50	QDI=	0.	AS1=	0.
		HS=	5027.00	5037.00	5100.00	5200.00	5290.00		
		BS=	200.0	500.0	1000.0	1250.0	1350.0		
		BSS=	0.0	0.0	0.0	0.0	0.0		
I=	6	FLDSTG=	0.00	YDI=	0.00	QDI=	0.	AS1=	0.
		HS=	5027.00	5037.00	5057.00	5157.00	5257.00		
		BS=	0.0	300.0	1000.0	1100.0	1200.0		
		BSS=	0.0	0.0	0.0	0.0	0.0		
I=	7	FLDSTG=	0.00	YDI=	0.00	QDI=	0.	AS1=	0.
		HS=	4027.00	4037.00	4057.00	4067.00	4080.00		
		BS=	0.0	300.0	1000.0	1100.0	1225.0		
		BSS=	0.0	0.0	0.0	0.0	0.0		

REACH INFO RIVER NO. 1

FKEC(I,1), I = 1, NM(1)
0.00 0.00 0.00 0.00 0.00 0.00

NCM(K, 1), K=1,NRCM1(1)
1 2 4 6

CM(K, 1, 1)=	0.0600	0.0600	0.0500	0.0400	0.0400
CM(K, 2, 1)=	0.0600	0.0600	0.0300	0.0300	0.0300
CM(K, 3, 1)=	0.0300	0.0300	0.0300	0.0300	0.0300
CM(K, 4, 1)=	0.0300	0.0300	0.0400	0.0400	0.0400

0.00000

22.10 FLDWAV Example 10.0 – Two Dams

This example illustrates the use of FLDWAV to simulate the breach of an upstream dam immediately at $t=0$ since the initial water surface elevation (5288.5 ft) is the same as the elevation required for breaching. Another dam is located 58.5 miles downstream. This dam fails when it is overtopped by at least 0.5 ft. The entire reach is routed simultaneously with level-pool routing in the upstream reservoir and dynamic routing throughout the entire reach downstream of the upstream dam.

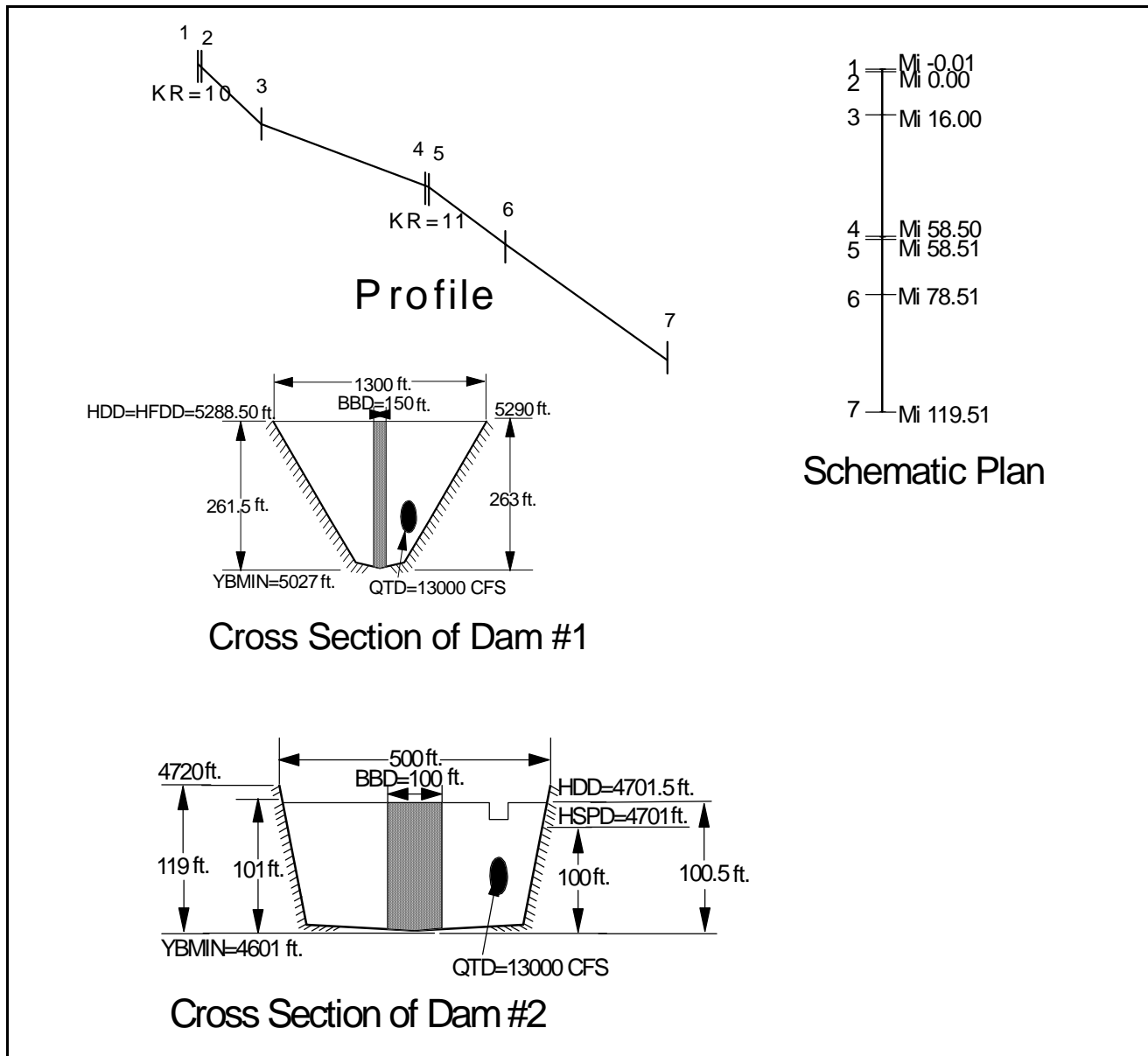


Figure 22.10 - Example 10.0 – Two Dams.

Table 22.19 Input Data Set for Example 10

```

PROBLEM E-10
EOM
NO DESC

.01          1.          .6          5280.          0.00          0

      1  2  10  2  0  0  0  0  0  0

0  0  0  0

      3  2 005  0  0

      0  0  0  0  0

50.  .0625  0.  0.  0.  0

0  0  0

7    1  7  100.  0.  0.  0.

2  4    0    6    1  0  0  0  0  0

0    0  0  0  0  0  0  0  0  0

-.01  0.  16.  59.5  59.51  79.51  119.51

100.  .5  .9  100.  .5  .9

      10  0  0  11  0  0

1936. 0.  0.  0.  0.  0.  0.  0.

5287. 5027.  0.  0.  0.  0.  0.  0.

1    5288.5  1.  3.  13000. 0

0    0.  0.  0.  0.  0.

1.25  0.  5288.5  150.  0.  5027.  0.  0.

4    4701.5  33.3333  3.  13000  0

0    4701.0  0.  0.  0.  0.

4701. 4702. 4703. 4706. 4711. 0 0 0

0.    100.  283.  1118. 3162. 0 0 0

1.    0  4702.  100.  0.  4601.  0.  0.

1  2  3  4  5  7

MI -0.01

MI 0.

MI 16.

MI 59.5

MI 59.51

MI 119.5

13000.  13000.

0.    100.

      0.  5288.50  0.  0.

5027.1  5037.  5112.

```

0.	590.	1200.
0.	0.	0.
0.	0	0. 0.
5027.	5037.	5112.
0.	590.	1200.
0.	0.	0.
0.	0.	0. 0.
4817.	4827.	4852.
0.	1000.	10000.
0.	0.	20000.
0.	4701.0	0. 0.
4601.	4606.	4720.
0.	400.	500.
0.	0.	0.
0.	0	0. 0.
4601.00	4606.	4660.
0.	400.	500.
0.	0.	0.
0.	0.	0. 0.
4401.	4406.	4460.
0.	400.	500.
0.	0.	0.
0.	0.	0. 0.
4000.	4006.	4060.
0.	400.	500.
0.	0.	0.
0.	0.	0. 0 0 0 0
1		
.045	.045	.045
0.		
END OF DATA -- E-10		
E-10 RIVER		

Table 22.20 Echo Print of Example 10

PROGRAM FLDWAV - BETA VERSION 1.0 2/1/95

HYDROLOGIC RESEACH LABORATORY
W/OH3 OFFICE OF HYDROLOGY
NOAA, NATIONAL WEATHER SERVICE
SILVER SPRING, MARYLAND 20910

*** SUMMARY OF INPUT DATA ***

PROBLEM E-10

EPSY	THETA	F1	XFACT	DTHYD	DTOUT	METRIC		
0.010	1.000	0.600	5280.000	0.000	0.000	0		
JN	NU	ITMAX	KWARM	KFLP	NET	ICOND	FUTURE DATA	
1	2	10	2	0	0	0	0 0 0	
NYQD	KCG	NCG	KPRES					
0	0	0	0					
NCS	KPL	JNK	KREVR5	NFGRF				
3	2	5	0	0				
IOBS	KTERM	NP	NPST	NPEND				
0	0	0	0	0				
TEH	DTHII	DTHPLT	FRDFR	DTEXP	MDT			
50.000	0.06250	0.06250	0.00	0.00000	0			
NLEV	DHLV	DTHLV						
0	0.00000	0.00000						
RIVER NO.	NBT	NPT1	NPT2	EPQJ	COFW	VWIND	WINAGL	
1	7	1	7	100.00	0.00	0.00	0.00	
RIVER NO.	KU	KD	NQL	NGAGE	NRCM1	NQCM	NSTR	FUTURE DATA
1	2	4	0	6	1	0	0	0 0 0
RIVER NO.	MIXF	MUD	KFTR	KLOS	FUTURE DATA			
1	0	0	0	0	0 0 0 0 0 0			
XT(I, 1)	I=1,NB(1)							
-0.010	0.000	16.000	59.500	59.510	79.510	119.510		
DXM(I, 1)	I=1,NB(1)							
100.000	0.500	0.900	100.000	0.500	0.900			
KRCH(I, 1)	I=1,NRCH							
10	0	0	11	0	0			
RIVER NO.	1,	DAM NO.	1					
SAR(L, 1, 1)	L=1,8							
1936.00	0.00	0.00	0.00	0.00	0.00	0.00	0.00	
HSAR(L, 1, 1)	L=1,8							
5287.00	5027.00	0.00	0.00	0.00	0.00	0.00	0.00	
LAD	HDD	CLL	CDOD	QTD	ICHAN			
1	5288.50	1.00	3.00	13000.00	0			

ICG	HSPD	SPL	CSD	HGTD	CGD		
0	0.00	0.00	0.00	0.00	0.00		
TFH	DTHDB	HFDD	BBD	ZBCH	YBMIN	BREXP	CPIP
1.250	0.00000	5288.50	150.00	0.00	5027.00	0.00	0.00

RIVER NO. 1, DAM NO. 2

LAD	HDD	CLL	CDOD	QTD	ICHAN		
4	4701.50	33.33	3.00	13000.00	0		
ICG	HSPD	SPL	CSD	HGTD	CGD		
0	4701.00	0.00	0.00	0.00	0.00		
RHI(L, 2, 1), L=1,8							
4701.00	4702.00	4703.00	4706.00	4711.00	0.00	0.00	0.00
RQI(L, 2, 1), L=1,8							
0.00	100.00	283.00	1118.00	3162.00	0.00	0.00	0.00
TFH	DTHDB	HFDD	BBD	ZBCH	YBMIN	BREXP	CPIP
1.000	0.00000	4702.00	100.00	0.00	4601.00	0.00	0.00

PLOTTING/OBSERVED TIME SERIES FOR RIVER J= 1

I	NGS	ID
1	1	MI -0.01
2	2	MI 0.
3	3	MI 16.
4	4	MI 59.5
5	5	MI 59.51
6	7	MI 119.5

ST1(K,1), K = 1, NU
13000.00 13000.00

T1(K,1), K = 1, NU
0.00 100.00

RIVER NO. 1

I=	1	FLDSTG=	0.00	YDI=	5288.50	QDI=	0.	AS1=	0.
		HS=	5027.10		5037.00				
		BS=	0.0		590.0				
		BSS=	0.0		0.0				
I=	2	FLDSTG=	0.00	YDI=	0.00	QDI=	0.	AS1=	0.
		HS=	5027.00		5037.00				
		BS=	0.0		590.0				
		BSS=	0.0		0.0				
I=	3	FLDSTG=	0.00	YDI=	0.00	QDI=	0.	AS1=	0.
		HS=	4817.00		4827.00				
		BS=	0.0		1000.0				
		BSS=	0.0		0.0				
I=	4	FLDSTG=	0.00	YDI=	4701.00	QDI=	0.	AS1=	0.
		HS=	4601.00		4606.00				
		BS=	0.0		400.0				
		BSS=	0.0		0.0				
I=	5	FLDSTG=	0.00	YDI=	0.00	QDI=	0.	AS1=	0.
		HS=	4601.00		4606.00				
		BS=	0.0		400.0				
		BSS=	0.0		0.0				
I=	6	FLDSTG=	0.00	YDI=	0.00	QDI=	0.	AS1=	0.
		HS=	4401.00		4406.00				
		BS=	0.0		400.0				
		BSS=	0.0		0.0				
I=	7	FLDSTG=	0.00	YDI=	0.00	QDI=	0.	AS1=	0.
		HS=	4000.00		4006.00				
		BS=	0.0		400.0				

```

BSS=          0.0      0.0      0.0

REACH INFO RIVER NO.  1

FKEC(I,1), I = 1, NM(1)
      0.00      0.00      0.00      0.00      0.00      0.00

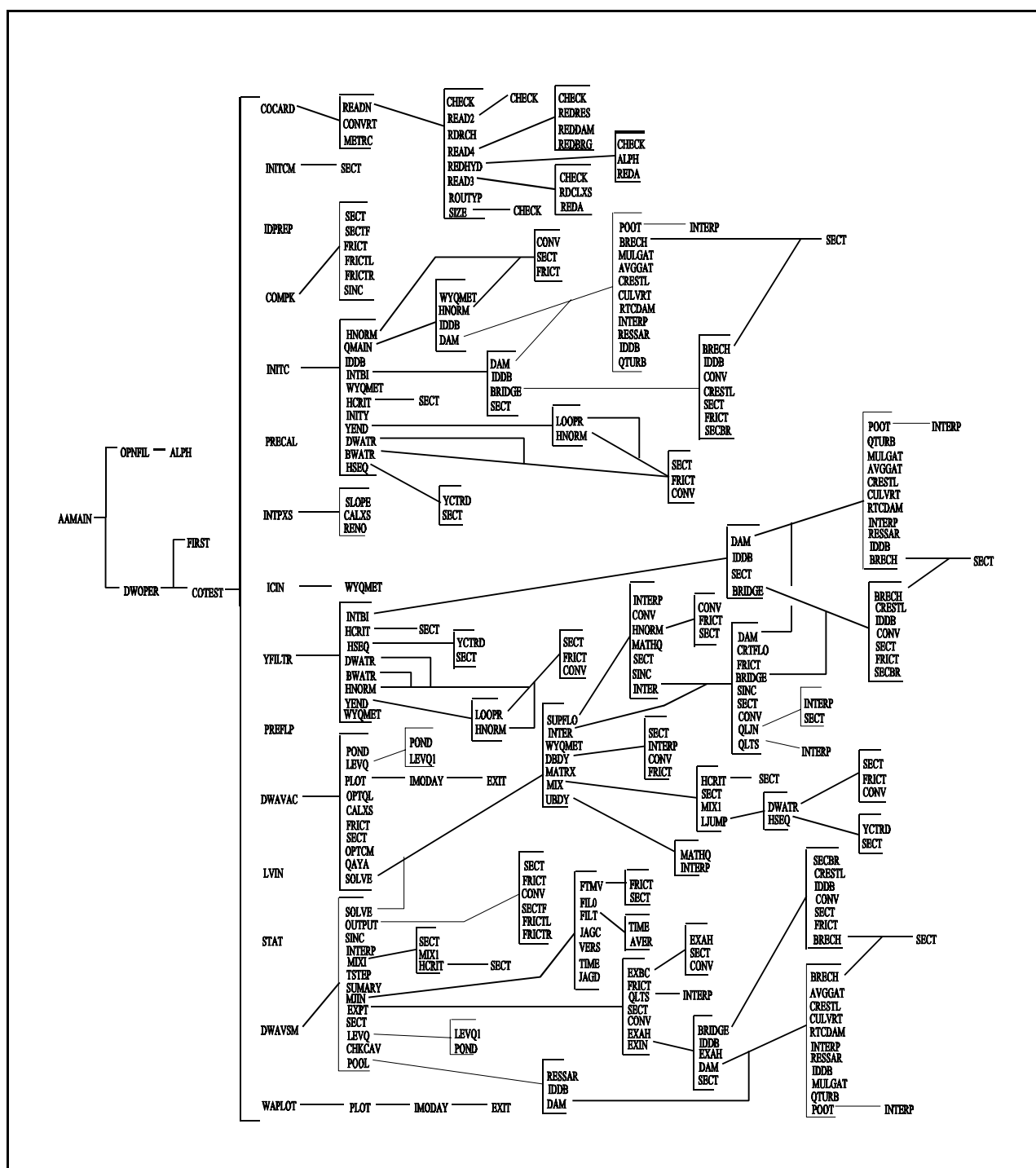
NCM(K, 1), K=1,NRCM1( 1)
      1

CM(K, 1, 1)=      0.0450      0.0450      0.0450

0.

```

23.FLDWAV Model Program Structure



24. REFERENCES

- Amein, M. and Fang, C.S. (1970). 'Implicit Flood Routing in Natural Channels,' Journal of Hydraulics Division, ASCE, Vol. 96, No. HY12, pp. 2481-2500.
- Arcement, G.J., Jr. and Schneider, V.R. (1984). Guide for Selecting Manning's Roughness Coefficients for Natural Channels and Flood Plains, Report No. RHWA-TS-84-204, U.S. Geological Survey for Federal Highway Administration, National Tech. Information Service, PB84-242585, 61 pp.
- Baltzer, R.A. and Lai, C. (1968). 'Computer Simulation of Unsteady Flow in Waterways,' Journal of Hydraulics Division, ASCE, Vol. 94, No. HY4, pp. 1083-1117.
- Barkow, R.L. (1990). UNET One-Dimensional Unsteady Flow Through a Full Network of Open Channels, Users Manual, Hydrologic Engineering Ctr., U.S. Army Corps of Engineers, Davis, California
- Barnes, H.H., Jr. (1967). Roughness Characteristics of Natural Channels, Geological Survey Water-Supply Paper 1849, United States Government Printing Office, Washington, D.C., 223 pp.
- Basco, D.R. (1987). 'Improved Robustness of the NWS DAMBRK Algorithm,' Hydraulic Engineering, (Proc. of the 1987 National Conference on Hydraulic Engineering), ASCE, New York, Aug., pp. 776-781.
- Brater, E. (1959). 'Hydraulics,' Civil Engineering Handbook, edited by L. C. Urquhart, Sect. 4, McGraw-Hill Book Co., New York, pp.4.44-4.60.
- Chaudhry, Y. M. and Contractor, D.N. (1973). 'Application of the Implicit Method to Surges in Open Channel' . Water Resources Research, 9, No. 6, Dec., pp. 1605-1612.
- Chow, V.T. (1959). Open-Channel Hydraulics, McGraw-Hill, New York.
- Chow, V.T.; Maidment, D.R. and Mays, L.W. (1988). Applied Hydrology, McGraw-Hill, New York.
- Cristofano, E.A. (1965). Method of Computing Rate for Failure of Earth Fill Dams. Bureau of Reclamation, Denver, Colorado, April.
- Cunge, J.A. and Wegner, M. (1964). 'Numerical Intergration of Barre de Saint-Venant's Flow Equations by Means of an Implicit Scheme of Finite Difference. Applications in the Case of Alternately Free and Pressurized Flow in a Tunnel,' La Houille Blanche, No. 1, pp. 33-39.
- Davies, W.E., Bailey, J.F. and Kelly, D.B. (1972). 'West Virginia's Buffalo Creek Flood: A Study of the Hydrology and Engineering Geology,' Geological Survey Circular 667, U.S. Geological Survey, 32 pp.

- DeLong, L.L. (1986). 'Extension of the Unsteady One-Dimensional Open-Channel Flow Equations for Flow Simulation in Meandering Channels with Flood Plains,' Selected Papers in Hydrologic Science, U.S. Geological Survey Water Supply Paper 2220, pp. 101-105.
- DeLong, L.L. (1989). 'Mass Conservation: 1-D Open Channel Flow Equations,' Journal of Hydraulics Division, Vol. 115, No. 2, pp. 263-268.
- Dressler, R.F. (1954). 'Comparision of Theories and Experiments for the Hydraulic Dam-Break Wave,' Internet. Assoc. Sci. Pubs., 3, No. 38, pp. 319-328.
- Fread, D.L. (1971). 'Discussion of Implicit Flood Routing in Natural Channels,' by M. Amein and C. S. Fang, Journal of Hydraulics Division, ASCE, Vol. 97, No. HY7, pp. 1156-1159.
- Fread, D.L. (1973a). 'Technique for Implicit Dynamic Routing in Rivers with Tributaries,' Water Resources Research, Vol. 9, No. 4, pp. 918-926.
- Fread, D.L. (1973b). 'A Dynamic Model for Stage-Discharge Relations Affected by Changing Discharge,' NOAA Technical Memorandum NWS HYDRO-16, U.S. Department of Commerce, NWS, NOAA, November, 45 pp.
- Fread, D.L. (1974a). 'Implicit Dynamic Routing of Floods and Surges in the Lower Mississippi,' Presented at American Geophysical Union Spring Meeting in Washington, D.C., April, pp. 26
- Fread, D.L. (1974b). Numerical Properties of Implicit Four-Point Finite Difference Equations of Unsteady Flow, HRL-45, NOAA Tech. Memo NWS HYDRO-18, Hydrologic Research Laboratory, National Weather Service, Silver Spring, Md.
- Fread, D.L. (1975). 'Computation of Stage-Discharge Relationships Affected by Unsteady Flow,' Water Resources Bulletin, American Water Resources Association, Vol. 11, No. 2, April, pp.213-228.
- Fread, D.L. (1977). 'The Development and Testing of a Dam-Break Flood Forecasting Model,' Proc. of Dam-Break Flood Modeling Workshop, U.S. Water Resources Council, Washington, D.C., pp. 164-197.
- Fread, D.L. (1978a). Theoretical Development of Implicit Dynamic Routing Model, HRL-113,Hydrologic Research Laboratory, National Weather Service, Silver Spring, Md.
- Fread, D.L. (1978b). 'Nws Operational Dynamic Wave Model,' Verification of Mathematical and Physical Models, Proceedings of 26th Annual Hydr. Division Specialty Conf., ASCE,College Park, Md., pp. 455-464.
- Fread, D.L. (1981a). 'Flood Routing: a Synopsis of Past, Present, and Future Capability,' Proceedings: International Symposium on Rainfall-Runoff Modeling, Mississippi State, Mississippi, May 18-22, pp. 521-541.

- Fread, D.L. (1981b). 'Some Limitations of Contemporary Dam-Breach Flood Routing Models,' Preprint 81-525: Annual Meeting of American Society of Civil Engineers, St.Louis, Missouri, October 27, 1981B, 15 pp.
- Fread, D.L. (1983a). Applicability Criteria for Kinematic and Diffusion Routing Models, HRL-176, Hydrologic Research Laboratory, National Weather Service, Silver Spring, Md., 16 pp.
- Fread, D.L. (1983b). 'Computational Extensions to Implicit Routing Models,' Proceedings of the Conference on Frontiers in Hydraulic Engineering, ASCE, MIT, Cambridge, Mass., pp. 343-348.
- Fread, D.L. (1984a). 'A Breach Erosion Model for Earthen Dams,' Proceedings of Specialty Conference on Delineation of Landslides, Flash Flood, and Debris Flow Hazards in Utah, Utah State University, June 15, 30 pp.
- Fread, D.L. (1984b). 'An Implicit Dynamic Wave Model for Mixed Flows in Storm Sewer Networks,' Proceedings, 1984 International Symposium on Urban Hydrology, Hydraulics, and Sediment Control, University of Kentucky, Lexington, Kentucky, July 23-25, pp. 215-222.
- Fread, D.L. (1985a). 'Breach: An Erosion Model for Earthen Dam Failures,' Hydrologic Research Lab, January, 34 pp.
- Fread, D.L. (1985b). 'Channel Routing,' Chapt. 14, Hydrological Forecasting, (Eds: M.G. Anderson and T.P. Burt), John Wiley and Sons, New York, Chapter 14, pp. 437-503.
- Fread, D.L. (1988). The NWS DAMBRK Model: Theoretical Background/User Documentation, HRL-256, Hydrologic Research Laboratory, National Weather Service, Silver Spring, Md., 315 pp.
- Fread, D.L. (1989a). 'Flood Routing and the Manning n,' Proc. Of the International Conference for Centennial of Manning's Formula and Kuichling's Rational Formula, (Ed: B.C.Yen), Charlottesville, Va., pp. 699-708.
- Fread, D.L. (1989b). 'National Weather Service Models to Forecast Dam-Breach Floods,' Hydrology of Disasters (Eds: O. Starosolszky and O.M. Melder), Proc. of the World Meteorological Organization Technical Conference, November 1988, Geneva, Switzerland, pp. 192-211.
- Fread, D.L. (1992). 'Flow Routing,' Chapter 10, Handbook of Hydrology, editor E.R. Maidment, McGraw-Hill Book Company, New York, pp. 10.1-10.36.
- Fread, D.L. (1998). 'Dam-Break Modeling and Flood Routing: A Perspective on Present Capability and Future Directions,' Presented at International Workshop on Dam Break Processes, Stillwater, OK, March 10-11.
- Fread, D.L. and Harbaugh, T.E. (1971). 'Open Channel Profiles by Newton's Iteration Technique,' Journal of Hydrology, Vol. 13, pp. 70-80.

- Fread, D.L. and Harbaugh, T.E.(1973). 'Transient Hydraulic Simulation of Breached Earth Dams,' Journal of the Hydraulics Division, American Society of Civil Engineers, Vol. 99, No. HY1, January, pp. 139-154.
- Fread, D. L. and Jin, M. (1993). 'Real-time Dynamic Flood Routing with NWS FLDWAV Model Using Kalman Filter Updating,' Proceedings: ASCE International Symposium on Engineering Hydrology, San Francisco, California, July 25-30, pp. 946-951.
- Fread, D.L.; Jin, M. and Lewis, J. M., (1996). 'An LPI Numerical Implicit Solution for Unsteady Mixed-Flow Simulation,' North American Water and Environment Congress '96, ASCE, Anaheim, California, June 22-28.
- Fread, D.L. and Lewis, J.M. (1986). 'Parameter Optimization for Dynamic Flood-Routing Applications with Minimal Cross-Sectional Data,' Proceedings: ASCE Water Forum '86, World Water Issues in Evolution, Long Beach, California, August 4-6, pp. 443-450.
- Fread, D.L. and Lewis, J.M. (1988). 'FLDWAV: A Generalized Flood Routing Model,' Proc.of National Conference on Hydraulic Engineering, ASCE, Colorado Springs, Co., pp.668-673.
- Fread, D.L. and Lewis, J.M. (1993). 'Selection of Δx and Δt Computational Steps for Four-Point Implicit Nonlinear Dynamic Routing Models,' Proceedings:ASCE National Hydraulic Engineering Conference, San Francisco, California, July 26-30, pp.1569-1573.
- Fread, D.L.; McMahon, G.F. and Lewis, J.M. (1988). 'Limitations of Level-Pool Routing in Reservoirs,' Proceedings, Third Water Resources Operations and Management Workshop, ASCE, Computational Decisions Support Systems for Water Managers, Fort Collins, Co.
- Fread, D.L. and Smith, G.F. (1978). 'Calibration Technique for 1-D Unsteady Flow Models,' Journal of Hydraulics Division, ASCE, Vol. 104, No. HY7, pp. 1027-1044.
- Froehlich, D.C. (1987). 'Embankment-Dam Breach Parameters,' Proc. of the 1987 National Conf. on Hydraulic Engr., ASCE, New York, August, pp. 570-575.
- Froehlich, D.C. (1995). 'Embankment-Dam Breach Parameters Revisited,' Proc. of the First International Conf. on Water Resources Engr., ASCE, San Antonio, August, pp. 887-891.
- Hagen, V.K. (1982). 'Re-Evaluation of Design Floods and Dam Safety,' Presented at Fourteenth ICOLD Congress, Rio de Janeiro.
- Harris, G.W. and Wagner, D. A. (1967). Outflow from Breached Dams, Univ. of Utah.
- Havnø, K. and Brorsen, M. (1986). 'A General Mathematical Modeling System for Flood Forecasting and Control', Proc. Internat'l Conf. on Hydraulics of Floods and Flood Control, Cambridge, UK; BHRA, Stevenage.

- Jarrett, R.D. (1984). 'Hydraulics of High-Gradient Streams,' Journal of Hydraulics Division, ASCE, Vol. 110, No. HY11, Nov., pp. 1519-1539.
- Jarrett, R.D. (1985). 'Determination of Roughness Coefficients for Streams in Colorado,' U.S. Geological Survey Water-Resources Investigations Report 85-4004, Lakewood, Colorado, pp.54.
- Jelesnianski, C.P. (1972). 'SPLASH (Special Programs to List Amplitudes of Surges and Hurricanes) 1. Landsfall Storms,' NOAA Technical Memorandum NWS TDL-46.
- Jelesnianski, C.P. (1976). 'A Sheared Coordinate System for Storm Surge Equations of Motion with a Mildly Curved Coast,' NOAA Technical Memorandum NWS TDL-61, July.
- Jin, M. and Fread, D. L. (1996). 'Channel Routing with Flow Losses,' Journal of Hydraulic Engineering, ASCE, Vol. 122, No. 10, October, pp. 580-582.
- Jin, M. and Fread, D.L. (1997). 'Dynamic Flood Routing with Explicit and Implicit Numerical Solution Schemes,' Journal of Hydraulic Engineering, ASCE, Vol. 123, No. 3, March.
- Johnson, F.A. and Illes, P. (1976). 'A Classification of Dam Failures,' Water Power and Dam Construction, Dec., pp. 43-45.
- Lewis, J.M.; Fread, D.L. and Jin, M. (1996). 'An Extended Relaxation Technique for Modeling Unsteady Flows in Channel Networks Using the NWS FLDWAV Model,' North American Water and Environment Congress '96, ASCE, Anaheim, California, June 22-28.
- Liggett, J.A. and Cunge, J.A. (1975). 'Numerical Methods of Solution of the Unsteady Flow Equations,' Unsteady Flow in Open Channels, Vol. I, (Eds: K. Mahmood and V. Yevjevich), Chapter 4, pp. 89-182, Water Resources Pub., Fort Collins, Co.
- Linsley, R.K.; Kohler, M.A. and Paulhus, J.L.(1958). Hydrology for Engineers, McGraw- Hill Book Co., New York, pp. 216-244.
- MacDonald, T.C. and Langridge-Monopolis, J. (1984). 'Breaching Characteristics of Dam Failures,' Journal of Hydraulics Division, ASCE, 110, No. 5, May, pp. 567-586.
- McQuivey, R.S. and Keefer, T.N. (1975). 'Application of Simple Dam Break Routing Model,' Proceedings, 16th Congress, IAHR, Sao Paulo, Brazil, July 27-August 1, Vol. 2, pp. 315-324.
- Molinas A. and Yang, C.T. (1985). 'Generalized Water Surface Profile Computations,' Journal of Hydraulics Division, ASCE, 111, HY3, March, pp. 381-397.
- Morris, H.M. and Wiggert, J.M. (1972). Applied Hydraulics in Engineering, The Ronald Press Co., New York, pp. 570-573.

- O'Brien, J.S. and Julien, P. (1984). 'Physical Properties and Mechanics of Hyper-Concentrated Sediment Flows,' Delineation of Landslide, Flash Flood, and Debris Flow Hazards in Utah, Utah State Univ., Utah Water Research Laboratory, Logan, Utah, (Ed: D.S.Bowles), General Series UWRL/G-85/03, pp. 260-279.
- Ponce, V.M. and Tsivoglou, A.J. (1981). 'Modeling of Gradual Dam Breaches,' Journal of Hydraulics Division, ASCE, 107, HY6, June, pp. 829-838.
- Preissmann, A. (1961). 'Propagation of transitory waves in channels and rivers,' in Proc., First Congress of French Assoc. for Computation, Grenoble, France, pp. 433-442.
- Ray, H. A.; Kjelstrom L. C.; Crosthwaite, E. G. and Low, W. H. (1976). 'The Flood in Southeastern Idaho from the Teton Dam Failure of June 5,' Unpublished open file report, U.S. Geological Survey, Boise, Idaho.
- Ré, R. (1946). 'A Study of Sudden Water Release from a Body of Water to Canal by the Graphical Method,' La Houille Blanche (France), No. 3, pp. 181-187.
- Ritter, A. (1892). 'The Propagation of Water Waves,' Ver. Deutsch Ingenieure Zeitschr. (Berlin), 36, Pt. 2, No. 33, pp. 947-954.
- Saint-Venant, Barré de (1871). 'Theory of Unsteady Water Flow, with Application to River Floods and to Propagation of Tides in River Channels,' Comptes Rendus, Vol. 73, Acad.Sci., Paris, France, pp. 148-154, 237-240. (Translated into English by U.S. Corps of Engrs., No. 49-g, Waterways Experiment Station, Vicksburg, Miss., 1949.)
- Sakkas, J.G. and T. Strelkoff. (1973). 'Dam-Break Flood in a Prismatic Dry Channel,' Journal of Hydraulics Division, ASCE, 99, HY12, Dec., pp. 2195-2216.
- Samuels, P.G. (1985). Models of Open Channel Flow Using Preissmann's Scheme, Cambridge University, Cambridge, England, pp. 91-102.
- Schocklitsch, A. (1917). 'On Waves Created by Dam Breaches,' Akad. Wiss. (Vienna) Prox., 126, Pt. 2A, pp. 1489-1514.
- Singh, K.P. and Snorrason, A. (1982). 'Sensitivity of Outflow Peaks and Flood Stages to the Selection of Dam Breach Parameters and Simulation Models,' University of Illinois State Water Survey Division, Surface Water Section, Champaign, Illinois, June, pp. 179.
- Strelkoff, T. (1969). 'The One-Dimensional Equations of Open-Channel Flow,' Journal of Hydraulics Division, ASCE, Vol. 95, No. HY3, pp. 861-874.
- Strelkoff, T. (1970). 'Numerical Solution of Saint-Venant Equations,' Journal of Hydraulics Division, ASCE, Vol. 96, No. HY1, pp. 223-252.

- Stoker, J.J. (1957). Water Waves, Interscience, New York, pp. 452-455.
- Traver, R.G. (1988). 'Transition Modeling of Unsteady One Dimensional Open Channel Flow Through the Subcritical-Supercritical Interface,' unpublished Ph.D. Dissertation, Pennsylvania State University, College Park, Pennsylvania.
- U.S. Army Corps of Engineers (1960). 'Floods Resulting from Suddenly Breached Dams--Conditions of Minimum Resistance, Hydraulic Model Investigation,' Misc. Paper 2-374, Report 1, WES, Feb., 176 pp.
- U.S. Dept. Transportation/Federal Highway Administration (1978). 'Hydraulics of Bridge Waterways,' Hydraulic Design Series No.1, Washington D.C., pp.45-46.
- Venard, J.K. (1954). Elementary Fluid Mechanics, John Wiley and Sons, New York, pp.312-325.
- Walton, R. and Christenson, B.A.. (1980). 'Friction Factors in Storm-Surges over Inland Areas,' Journal of Waterway, Port, Coastal and Ocean Division, ASCE, 106, WW2, pp. 261-271.
- Wetmore, J.N. and Fread, D.L. (1984). 'The NWS Simplified Dam Break Flood Forecasting Model,' Printed and Distributed by the Federal Emergency Management Agency (FEMA), 1984, pp.122
- Wortman, R.T. (1983). 'Dominoes on the Columbia: Chief Joseph Dambreak Model,' North Pacific Division, U.S. Army Corps of Engineers, Portland, OR, Presented at NWS Dam-Break Symposium, Tulsa, Oklahoma, June.

25 INDEX

backwater	i, 4.2, 5.6, 7.4-7.6, 8.4, 8.5, 9.3, 14.3, 17.17
backwater condition	3.15, 19.1, 19.2
backwater effect	1.1, 1.2, 1.5, 2.2, 2.3, 3.5, 3.14, 5.16, 7.1, 8.5, 11.4, 12.1, 14.9, 15.1
box scheme	2.11
breach	v, 1.4, 1.6, 1.7, 2.2, 3.7, 6.1-6.9, 11.4, 11.6-11.8, 12.5, 13.1, 16.4, 17.1-17.3, 17.7, 17.10, 17.11, 18.1
breach outflow	3.11, 6.1, 6.7, 8.5, 8.6, 15.3, 17.3, 17.9, 18.2
breach parameter	ii, 1.4, 6.1, 6.2, 6.8, 6.9, 16.4, 17.2, 17.5, 17.8, 17.11, 18.1, 18.2
bridge	i, v, 1.2, 1.4, 1.6, 2.3, 3.5-3.7, 3.12-3.14, 5.6, 5.7, 5.14, 5.16, 6.1, 7.1, 8.7, 9.3, 11.4, 14.11, 14.12, 16.4, 18.1-18.3, 19.1
bridge embankment	6.1, 21.7, 26.7
broad-crested weir	1.4, 6.1, 6.2, 8.5, 8.6, 12.2-12.5, 15.3
Buffalo Creek	iii, 17.1, 17.7-17.11
calibration	ii, iii, v, 1.7, 9.1, 9.3, 14.1, 14.7, 14.10, 14.13, 16.2, 17.13, 17.18, 19.2-19.4
celerity	2.1, 8.5, 12.7,
channel conveyance	9.1
characteristic	i, 1.9, 2.2, 2.7, 3.3, 5.10-5.12, 6.7, 8.1, 8.3, 16.2, 18.1
coefficient matrix	2.14, 2.15
composite	ii, 2.5, 2.7, 10.1, 10.2, 18.3, 20.3, 21.13
computational difficulties	11.1, 13.1
computational robustness	13.1, 13.2
Computational Time Step	1.7, 1.9, 2.9, 2.11, 4.3, 5.14, 8.5, 11.6-11.8, 13.2
conservation	2.3, 2.4, 3.6, 5.10, 6.6, 6.7, 7.1, 8.3, 10.3, 15.3, 26.3, 26.10
conveyance	ii, iii, 1.8, 2.5, 8.5, 9.1, 10.2, 10.3, 13.1, 16.2
Courant condition	5.14, 8.1, 19.3, 21.3
crevasse	ii, v, 6.5, 12.1, 12.2, 12.5
critical flow	1.4, 2.15, 3.4, 3.6, 3.14, 5.1, 5.2, 5.4, 5.6-5.9, 5.15
critical slope	5.1, 26.5
cross section	ii, 1.2-1.5, 1.7-1.9, 2.6-2.8, 2.14, 3.2-3.4, 3.6, 3.14, 4.1, 4.2, 5.7-5.10, 5.14, 5.15, 6.1, 7.2, 7.4, 7.5, 8.1-8.5, 8.7, 8.8, 9.1, 10.1-10.3, 11.1, 11.2, 11.4, 11.5, 12.4, 12.6, 14.6, 14.10, 14.13, 14.14, 15.4, 16.1, 16.3, 16.4, 17.1-17.3, 17.7, 18.2, 18.3, 19.1-19.5
dam-breach	v, 1.2, 2.1, 3.9, 5.9, 6.1, 11.4, 24.3, 26.4, 26.11
Darcy f	ii, v, 1.2, 1.3, 1.6, 3.2, 3.6, 7.1, 7.3-7.5, 9.2, 14.10, 14.13, 17.16, 20.3, 26.7
dead storage	i
diffusion wave	v, 2.1, 5.9, 8.7, 8.8, 11.1, 11.2, 11.4-11.8, 13.3, 15.1, 19.6
dispersion	2.1, 11.6, 11.7
distance step	ii, v, 5.9, 8.7, 8.8, 11.1, 11.2, 11.4-11.6, 11.8, 13.3, 19.6
DWOPER	i, v, 1.2-1.7, 1.10, 17.1, 19.1
DXM	8.7, 8.8, 11.1, 11.2, 11.4, 11.5, 11.8, 17.3, 17.8, 18.3,
Dynamic Routing	iii, 1.9, 5.5, 5.15, 14.10, 14.11, 15.2, 15.3, 17.3, 18.2, 19.1
dynamic wave	1.1, 1.2, 2.2, 2.3, 5.11, 8.5, 12.7
expansion/contraction coefficient	18.3

Explicit methods	2.9
F1I	13.1
falls	3.14, 17.3
fixed-gate	3.9
FLDWAV	1, i-v, 1.1, 1.3-1.10, 2.1-2.3, 2.8, 2.13-2.15, 3.1-3.3, 3.6, 3.7, 3.14, 3.15, 4.1, 4.3, 5.1, 5.2, 5.4, 5.9, 5.10, 5.14, 6.1, 6.2, 6.5, 6.8, 6.9, 7.3, 8.6, 8.7, 10.3, 11.1, 11.2, 11.4, 11.5, 11.7, 12.1, 12.2, 12.5-12.8, 13.1, 13.2, 14.1, 14.12, 14.13, 16.1, 17.7, 17.16, 17.18, 18.1, 18.2, 19.4-19.6
floodplain compartments	8.8
flow hydrograph	5.10, 14.1, 17.3, 17.4, 17.9, 18.2
Flow routing	7.1, 8.1
friction slope	2.4, 10.1, 11.1, 13.1
Froude	5.1-5.4, 5.7, 5.9, 5.11
Froude number	5.1-5.4, 5.7, 5.9, 5.11,
Gate	iii, v, 1.1, 1.10, 3.6-3.12, 3.14, 3.15, 5.7, 6.4, 11.3, 11.7, 12.6, 13.1, 15.1, 15.3, 16.4, 17.4,
Gate controlled spillway	15.3
Gaussian elimination	2.14
hydraulic depth	2.7, 2.13, 3.5, 5.1, 8.5, 15.3, 26.2
hydraulic jump	5.8, 5.9
hydraulic radius	1.8, 2.5, 2.13, 9.1, 13.1, 14.6
hydraulic routing	2.1, 2.2
hydrologic routing	1.1, 1.2, 2.2
implicit schemes	2.9, 5.14
inflow	1.1, 1.7, 1.9, 2.4, 3.2, 4.3, 6.7, 8.7, 8.8, 15.2, 15.3, 17.3, 18.1, 19.1, 19.5
initial conditions	i, ii, 1.7, 2.13, 4.1-4.3, 5.9, 7.5, 12.8, 14.2, 14.6, 19.1, 19.5
instability	2.11, 3.5, 4.1
internal boundary	ii, v, 1.2, 1.4, 3.6, 3.7, 3.12, 3.14, 3.15, 5.2, 5.14, 15.4, 19.2
interpolation	1.7, 1.8, 2.8, 8.7, 9.1, 12.2, 19.3
JNK	13.1
KFLP	10.2, 10.3,
kinematic wave velocity	11.3
KPRES	2.13
Lateral Flow	ii, 1.2, 1.8, 2.4, 3.6, 4.1, 7.3, 12.1, 12.5, 12.6, 14.10, 19.4, 19.5
lateral inflow	2.4, 8.8, 12.2, 12.5, 14.2, 14.6, 14.10, 14.13
lateral outflow	2.4
Levee	ii, iii, v, 1.1, 1.2, 1.4, 1.6, 2.4, 6.1, 8.6, 8.8, 9.2, 12.1-12.5, 16.1, 17.4, 17.12, 18.2, 18.3
Level-Pool Routing	ii, iii, 15.2-15.4, 17.3, 18.2
loop-rating	3.3-3.5, 4.2, 17.3
loop-rating curve	17.3
Low-Flow Filter	ii, 13.1
Manning equation	3.3, 4.2, 11.3, 14.6, 16.2
MANNING n	ii, iii, v, 1.7, 1.8, 3.15, 5.10, 6.7, 8.7, 9.1-9.3, 10.1, 10.2, 12.8, 14.1, 14.5, 14.12, 14.13, 15.1, 16.2, 16.3, 17.1, 17.2, 17.6, 17.8, 17.13, 19.3
meandering	2.6, 10.2, 10.3

Metric	iii, 6.3, 8.1, 18.1, 19.5
mixed flow	1.6, 5.1, 5.2, 5.6, 5.9, 5.10, 20.9, 20.30, 21.21, 22.30, 24.3
momentum coefficient	2.4, 2.6
momentum equation	2.4, 5.2-5.4, 10.3
movable-gate	1.4, 3.9, 3.11
mud	v, 1.4, 1.10, 2.4, 2.7, 2.8, 4.1
NCS	2.5
negative flows	1.7
Newton-Raphson method	2.14, 4.2, 7.1
nonconvergence	13.2, 13.1, 21.2, 21.11
numerical convergence	10.2
numerical stability	5.14, 6.7, 26.2
off-channel (dead) storage	1.8, 8.3
Off-Channel Storage	ii, 1.2, 2.4, 2.8, 3.14, 5.14, 8.3-8.6, 16.1, 18.3
one-dimensional	v, 1.2, 1.4, 2.2, 2.3, 8.3, 16.1
open channels	12.7
Outflow	i, 1.2, 1.4, 1.8, 2.4, 3.6, 5.9, 6.1, 6.7, 6.9, 8.8, 11.4, 12.2, 15.3, 17.3, 17.4, 17.9, 17.10, 18.1, 18.2,
pipe	6.2
ponding area	8.5, 12.3
power function	2.7, 14.10, 14.12
Pressurized Flow	ii, iii, v, 12.1, 12.6-12.8
rapidly-varied flow	3.6
Rapids	i, 3.4, 3.6, 3.14
Relaxation	ii, 7.3, 7.5, 7.6
reverse flows	2.7
Saint-Venant Equation	i, v, 1.4, 2.3, 2.9, 2.14, 3.1, 3.2, 3.6, 3.15, 5.2, 5.6, 5.9, 5.10, 6.6, 7.1-7.3, 8.1, 8.3, 8.4, 10.2, 10.3, 11.1, 11.4-11.6, 12.2, 12.3, 12.5-12.8, 13.1, 13.2, 14.1, 16.1, 17.3, 19.6
Single-value	3.3, 3.4, 3.6, 19.2
Sinuosity	ii, 2.3, 2.6, 10.2, 10.3
sinuosity coefficients	2.6
Sinuosity Factor	ii, 2.4-2.6, 10.2, 10.3
SMPDBK	6.8, 11.4
sparse matrix	7.1
spillway	v, 1.2, 1.3, 3.6-3.9, 3.12, 3.14, 18.1
Storage	ii, 1.1, 1.2, 1.8, 1.9, 2.1, 2.4, 2.8, 2.14, 6.1, 8.2-8.7, 12.3, 12.4, 13.1, 17.1, 17.3, 17.4, 17.11, 18.3, 19.3
subcritical flow	2.14, 5.2, 5.10, 17.8
submergence correction	3.8, 3.9, 6.1, 12.3, 12.4
Supercritical Flow	iii, 2.14, 5.1, 5.2, 5.6, 5.9, 18.2, 18.3, 21.10
tailwater	3.6, 3.9, 3.10, 3.15, 6.1, 6.2, 19.2, 21.9
Teton	iii, 6.7, 17.1-17.4, 17.9-17.11
TFI	11.7
time of failure	6.5, 11.6, 17.2

time of formation	6.7
time of rise	2.2, 2.8, 11.2, 11.6, 15.1, 15.3
Time Step . . ii, 1.4, 1.7-1.9, 2.9, 2.14, 4.2, 4.3, 5.7, 5.8, 5.13-5.16, 7.1-7.3, 8.3, 11.1, 11.6, 11.7, 13.1, 13.2, 13.1, 17.7, 17.11, 17.18, 19.6	
topography	16.1, 19.3
topwidth	2.4, 2.8, 3.12, 8.1, 8.7, 10.2, 12.7, 17.2, 19.3
tributary inflow	2.3, 7.1, 7.3, 14.3
Uncertainty	iii, 6.9, 9.3, 16.2, 16.3
unsteady flow . . . v, 1.1, 1.2, 1.4, 1.6, 2.2, 2.3, 3.6, 4.1, 4.3, 5.2, 5.4-5.6, 6.6, 7.1, 7.3, 8.3, 12.1, 12.6, 12.7, 14.2, 14.9, 15.2	
upstream boundary condition	1.7, 5.8, 5.16, 7.3, 14.1, 14.7, 19.2
viscosity	2.7
viscous	2.4
Volume Loss	iii, 12.5, 17.4
weighting factor	2.11, 5.9, 13.2,
XS	10.2
yield strength	2.7
zero inertia	5.2

26. MATHEMATICAL NOTATION AND DEFINITION

A	channel/floodplain cross-sectional area (ft ²) of flow for active flow portion of cross section. Eqs. (2.1, 2.2, 2.4-2.7, 2.9-2.13, 2.19-2.22, 3.4, 3.6-3.9, 4.2, 4.3)
\hat{A}	cross section area (ft ²) at the i^{th} or $(i+1)^{\text{th}}$ locations (contracting or expanding reaches) for determining the maximum allowable computational distance step. Eqs. (11.3-11.5)
A_{br}	computed cross-sectional flow area (ft ²) of the bridge opening at section I+1. Eqs. (3.31, 3.41)
A_g	user-specified fixed gate flow area (ft ²). Eq. (3.18)
A_o	computed inactive (off-channel storage) cross-sectional area (ft ²). Eqs. (2.1, 2.19)
A_{o_k}	off-channel storage area (ft ²) at k^{th} elevation. (Sub-section 8.2)
A_s	surface area (acres) of the reservoir at the top of the dam . Sub-section 6.2.2
B	channel/floodplain topwidth (ft) at elevation h for active flow portion of cross section. Eqs. (2.2, 2.20, 2.25, 8.2)
B_c	topwidth (ft) of channel portion of channel/floodplain cross section. Eq. (14.13)
B_{c_k}	topwidth (ft) of channel portion of channel/floodplain cross section at k^{th} elevation. Eq. (10.1)
B_d	reservoir width (ft) at the dam elevation $H_d/2$. Eq. (6.3)
B_f	topwidth (ft) of floodplain portion of channel/floodplain cross section. Eq. (14.14)
B_i	topwidth (ft) of the i^{th} cross-section . Eq. (2.25)
B_k	user-specified topwidth (ft).
\overline{B}_k	distance weighted average topwidth (ft) for k^{th} depth of flow or k^{th} elevation along a reach having (I) total number of cross sections. Eq. (8.2)
B_{o_k}	off-channel storage topwidth (ft) at k^{th} elevation. Eqs. (8.3, 8.5)
C	user-specified coefficient of bridge flow which accounts for piers, alignment, etc. Eqs. (3.32, 3.42, 3.44)
C'	reduced coefficient of bridge flow due to orifice effects. Eq. (3.44)

C_n	Courant number of the Courant-Friedrich-Lewy condition for numerical stability of explicit solutions of Saint-Venant equations. Eq. (5.31)
C_o	flow coefficient for orifice flow through moveable gate. Eqs. (3.20, 3.21)
C_w	user-specified non-dimensional wind coefficient. Eq. (2.3)
D	hydraulic depth, (ft). Eq. (2.13)
\bar{D}_t	average hydraulic (A/B) depth (ft) along tributary with backwater Eq. (8.4)
DXM_i	user-specified computational distance step (mi). Eqs. (11.2, 11.6, 11.12, 11.13)
$E_{pk}(\%)$	maximum normalized error in the computed discharge peak profiles. (Sub-section 5.1)
$E_{rms}(\%)$	normalized root-mean-square (RMS) error in the computed discharge hydrographs (Sub-section 5.1)
F_r	Froude number. Eqs. (5.4, 5.5, 5.6)
\hat{G}^+	numerical functions for (+) characteristic direction and dependent upon the local Froude number; used in explicit finite-difference Saint-Venant Eqs. (5.19, 5.20). Eqs. (5.19-5.28)
\hat{G}^-	numerical functions for (-) characteristic direction and dependent upon the local Froude number; used in explicit finite-difference Saint-Venant Eqs. (5.19, 5.20). Eqs. (5.19-5.28)
H_g	user-specified movable-gate height (ft). Eqs. (3.19, 3.22, 3.23)
$IG(t)$	user-specified parameter which is a function of time; it is used in lock/dam internal boundary to control type of flow. (Sub-section 3.3.4)
IT	inertial terms of Saint-Venant momentum equation divided by the water-surface slope. Eq. (5.6)
J	sequence number of user-specified tabular values of depth representing the maximum depth. Eqs. (2.9, 2.10)
K	flow conveyance factor, (ft ³ /sec). Eqs. (2.4-2.8, 9.1)
K_c	user-specified channel conveyance (ft ³ /sec). Eqs. (2.4-2.8, 2.10, 2.11, 3.8, 9.1)
K_w	computed kinematic wave factor. Eqs. (11.7, 11.8)
L	the momentum effect of lateral flow (ft ³ /sec ²). Eqs. (2.2, 2.20)

L_1	represents the last (downstream) i^{th} Δx_i river reach associated with the ii^{th} floodplain. Eq. (12.6)
L_2	represents the last (downstream) i^{th} Δx_i river reach associated with the ii^{th} floodplain. Eq. (12.6)
L_d	user-specified length (ft) of the dam crest less L_s (spillway) and the length of the gates located along the dam crest. Eq. (3.31)
L_{sp}	user-specified spillway length (ft). Eq. (3.17)
L_u	user-specified length (ft) of the upper bridge-embankment crest perpendicular to the flow direction including the length of bridge at elevation h_{cu} . Eq. (3.32)
L_l	user-specified length (ft) of the lower bridge-embankment crest perpendicular to the flow direction at elevation h_{cl} . Eq. (3.32)
M	new number of computational distance steps within the original user-specified distance step. Eqs. (11.2, 11.3)
M'	represents the number of computational time steps within the time interval (T_r). Eqs. (11.15-11.17)
M_j	number of stage-discharge observations within the j^{th} stratum (range) of discharge values. Eq. (14.12)
N	denotes the sequence number of the last most downstream cross section or total number of cross sections along the river. Sub-sections (2.2, 3.2)
P	wetted perimeter (ft). Eq. (2.27)
P_1	cross-sectional area function in conservation form of the Saint-Venant equations. Eqs. (5.11, 5.12, 5.13, 5.14, 5.15, 5.19, 5.20)
P_2	cross-sectional area function in conservation form of the Saint-Venant equations. Eqs. (5.11, 5.12, 5.13, 5.14, 5.19, 5.20)
P_i	computed wetted perimeter (ft). Eqs. (2.27-2.29)
Q	discharge (cfs) or flow (- if directed upstream). Eqs. (2.1, 2.2, 2.4, 2.12, 2.13)
\bar{Q}	average discharge (cfs) between locations x_A and x_B . Eq. (14.12)
$Q(h)$	discharge (cfs) as a function of water-surface elevation. Eq. (3.5)

$Q(t)$	user- specified flow (cfs) as a function of time. Eqs. (3.1, 3.3)
Q_1	flow (cfs) at cross-section 1 (the most upstream cross section).Eq. (3.1)
Q_b	the dam-breach flow (cfs).Eqs. (3.15, 6.1, 6.3, 6.4)
Q_B	computed flow (cfs) at cross section B. Sub-section (14.2)
Q_{dam}	dam overtopping flow (cfs). Eqs. (3.16, 3.31)
Q_{gate}	time-dependent gate and fixed gate orifice flow (cfs). Eqs. (3.16, 3.19, 3.20, 3.24, 3.29)
Q_i	flow (cfs) at i^{th} cross section. Eqs. (2.19, 2.20, 2.23, 3.14, 4.1, 4.2)
Q_{i+1}	flow (cfs) at $(i+1)^{th}$ cross section. Eqs. (2.19, 2.20, 2.23, 3.14, 4.1, 4.2)
Q_{ii}	total levee overtopping inflow or outflow (cfs) with respect to the ii^{th} floodplain compartment; summation of all levee overtopping lateral flows into or out of the $(ii)^{th}$ floodplain compartment. Eq. (12.6)
Q_N	flow (cfs) at N^{th} (most downstream) cross section. Eqs. (3.5, 3.6, 3.9, 3.11, 4.3)
Q_o	initial flow (cfs) at $t=0$ for computing loss induced lateral flow (q). Eq. (12.10)
Q_{og}	overtopping gate flow (cfs). Eqs. (3.20, 3.23)
Q_p	estimated peak breach discharge (cfs). Eq. (6.13)
Q_p^*	estimated peak breach discharge (cfs). Eq. (6.12)
Q_s	total non-breach flow at dam or at bridge (cfs). Eqs. (3.15, 3.16, 3.32)
$Q_{spillway}$	spillway or bridge flow (cfs). Eqs. (3.16, 3.17)
Q_t	turbine flow (cfs) which may be a constant flow which is head independent or variable with time. Sub-section (3.3.1.6); Eq. (3.16)
$Q'(t)$	computed flow (cfs) at the last section of the upstream supercritical sub-reach as a function of time (t). Eq. (5.8)
Q'_A	flow (cfs) at upstream boundary cross section A. Eq. (14.1)
$Q'_A(t)$	user-specified flow (cfs) at section A as a function of time series. Eq. (14.1)
R	hydraulic radius, (ft). Eqs. (2.4-2.7, 2.24)

S	instantaneous dynamic energy slope (ft/ft). Eqs. (3.6, 3.7, 3.8, 4.2)
S	storage (ft ³) in level-pool routing. Eq. (15.4)
S_a	user-specified reservoir surface area (acres). Eqs. (15.5, 15.6)
S_{a_k}	surface area (acres) of portion of tributary inundated by backwater. Eq. (8.3)
S_c	computed critical slope (ft/mi). Eqs. (5.1, 5.2, 5.3)
S_f	computed channel/floodplain boundary friction slope (ft/ft). Eqs. (2.2, 2.4, 2.19, 2.22)
S_e	expansion-contraction slope (ft/ft). Eqs. (2.2, 2.12, 2.20)
S_g	flow direction factor (from river into floodplain compartment) or (from floodplain compartment into river or (no flow)). Eqs. (12.1, 12.3, 12.4)
S_i	computed additional friction slope (ft/ft) associated with internal viscous dissipation of non-Newtonian fluids such as mud/debris flows. Eqs. (2.1, 2.13, 2.20)
S_{ii}	storage (acre-ft) of (ii) th floodplain compartment which is a function of h_{ii} (water-surface elevation in the (ii) th floodplain compartment). Eq. (12.5)
Sm_i	the channel/river bottom slope (ft/mi) of i^{th} reach. Eqs. (5.2, 5.3, 11.10, 11.12, 11.13)
S_o	the channel/river bottom slope (ft/ft). Eqs. (3.13, 4.3, 4.4, 5.2, 5.3, 11.9, 11.17)
T_{p_i}	the time (hr) of occurrence of the peak of an observed hydrograph at each i^{th} location. Eq. (11.1)
T_r	the time of rise (hr) of hydrograph. Eqs. (11.6, 11.14, 15.2)
V	the velocity (ft/sec) of flow. Sec. (2.1, 3.3.2, 11.1); Eqs. (3.32, 3.43, 11.7, 11.9)
W^j	Gaussian <u>white noise process</u> with specified statistical features. Eq. (12.12)
V_f	volume (acre-ft) of floodplain below levee crest. Eqs. (8.5, 8.6)
V_r	volume (acre-ft). Eqs. (6.10, 6.11, 6.12)
V_{rw}	computed velocity (ft/sec) of the wind relative to the velocity of the channel flow. (Sub-section 2.1)
V_w	user-specified velocity (mi/hr converted by model to ft/sec) of the wind (- if aiding the river flow velocity). Eq. (2.3)

W_f	computed effect (ft^3/sec^2) of wind resistance on the flow. Eqs. (2.2, 2.20)
W_g	user-specified width (ft) of gate opening (time series). Eqs. (3.19, 3.20, 3.22, 3.27)
Y_c	flow depth (ft) in channel portion of channel/floodplain cross section. Eq. (14.13)
Y_f	flow depth (ft) in floodplain portion of channel/floodplain cross section. Eq. (14.14)
Y^j	a vector representation of the system of state variables. Eq. (12.12)
a	magnitude of acceleration effects of unsteady flow to cause departure (loop) from single-value rating curves. Eqs. (3.12, 3.13)
b	terminal bottom width (ft) of dam breach. Eqs. (6.7, 6.9)
\bar{b}	average dam breach width (ft). Eqs. (6.7, 6.10, 6.13)
b'	exponent in Manning n error equations. Eqs. (16.1-16.3)
b_i	computed instantaneous breach bottom width (ft). Eqs. (6.1, 6.5)
c	represents the channel. Eqs. (2.6, 2.8-2.11)
c	local dynamic wave velocity (ft/sec). Eqs. (5.16, 5.31)
\hat{c}	kinematic or bulk wave velocity (mi/hr). Eqs. (11.6, 11.7, 11.10, 11.11, 16.3)
c_d	user-specified discharge coefficient for overtopping flow over the crest of the dam. Eq. (3.31)
\hat{c}_e	kinematic or bulk wave velocity (mi/hr) associated with an erroneous Manning n_e value. Eq. (16.3)
c_g	user-specified fixed-gated spillway discharge coefficient. Eq. (3.19)
c_ℓ	user-specified weir discharge coefficient for levee overtopping/crevasse flow. Eq. (12.1)
c_o	flow correction factor for orifice flow through bridge. Eqs. (3.44-3.46)
c_{sp}	user-specified uncontrolled spillway discharge coefficient. Eq. (3.16)
c_v	computed velocity of approach correction factor. Eqs. (6.1, 6.3)
d	the flow depth (ft) associated with the correct Manning n value. Eq. (16.1)

\hat{d}	estimated rise in river water-surface elevation (ft) during the filling of floodplain storage below levee crest. Eq. (8.6)
d_B/d_y	derivative of topwidth (B) with respect to depth (y); approximately equal to $\Delta B/\Delta y$ (ft/ft). Eq. (11.8)
d_e	flow depth (ft) associated with an erroneous Manning n_e value. Eq. (16.1)
d_i	computed flow depth (ft) at section I.
e'	user-specified parameter for routing losses which selects the pattern of the change in total active volume. Eq. (12.10)
f	Darcy friction factor. Eq. (9.2)
g	constant for the acceleration due to gravity. Eqs. (2.2, 2.20, 3.4, 3.7, 3.18, 3.32, 3.47, 5.4, 5.7, 5.10)
h	computed water-surface elevation. Eqs. (2.2, 3.16, 3.18, 3.21, 3.22, 3.25, 3.26, 3.30, 6.1, 6.2, 6.3, 6.4, 6.6)
h_b	computed instantaneous elevation (ft) of the breach bottom. Eqs. (6.1, 6.2, 6.3, 6.5, 6.6)
h_{bm}	user-specified final (terminal) elevation (ft) of the breach bottom. Eqs. (6.3, 6.8)
h_{br}	user-specified elevation of the bottom of the bridge deck. Eq. (3.47)
h_{c_i}	user specified levee-crest elevation. Eqs. (12.1, 12.3, 12.4, 12.9)
h_{ct}	user-specified critical tailwater elevation for gate controlled flow at a particular lock/dam. Sub-section (3.3.4)
h_{cu}	user-specified elevation of the upper bridge embankment crest (ft). Eqs. (3.32, 3.37, 3.38, 3.40)
h_d	height (ft) of dam. Eqs. (6.7, 6.8, 6.12, 6.13)
h_d	height (ft) of water over the breach bottom. Eqs. (6.10, 6.11)
h_e	sequent water-surface elevation of the adjacent upstream supercritical section. Sub-section (5.2)
h_f	user-specified elevation which when first attained by the reservoir water-surface elevation initiates the formation of the breach. Sub-section (6.2)

h_{fp}	water-surface elevation of the (ii) th floodplain. Eqs. (12.3, 12.4, 12.9)
h_g	user-specified center-line elevation of the gated spillway, or the computed tailwater elevation if the latter is greater. Eq. (3.19)
h_g	user-specified gate sill elevation. Eqs. (3.22, 3.26, 3.27)
h_i	computed water-surface elevation (ft) at section i (slightly upstream of bridge). Eq. (2.20, 4.2)
\overline{h}_i	computed average water-surface elevation of the river between the i th and (i+1) th cross sections. Eqs. (12.1-12.4)
h_i^{j+1}	computed water-surface elevation (ft) at future time level (j+1). Eqs. (2.20, 3.49)
h_{i+1}	computed water-surface elevation (ft) at section I+1. Eq. (2.20, 4.2)
h_{i_k}	user-specified water-surface elevation (ft) at cross section i and at k th entry of top-width table. Eq. (2.29)
h_k	elevation of top-widths (ft) at k th entry to topwidth-elevation table.
h_N	starting water-surface elevation (ft) at downstream boundary location, I=N. Eq. (4.4)
h_p	user-specified center-line elevation (ft) of the pipe breach of a dam. Eqs. (6.5, 6.6)
h_{pt}	user-specified target-pool elevation (ft) to be maintained just upstream of a lock/dam. Eq. (3.48)
h_r	ratio (ft/ft) for computing k_s (submergence correction factor for levee overtopping broad-crested weir flow). Eqs. (12.7-12.9)
h_{ru}	ratio (ft/ft) for computing k_u (submergence correction factor for upper bridge-embankment overtopping broad-crested weir flow). Eqs. (3.33-3.37)
h_{sp}	user-specified uncontrolled spillway crest elevation (ft). Eqs. (3.16, 3.17)
h_t	downstream tailwater elevation.
h_{tw}	tailwater elevation (ft) just downstream of a dam. Eq. (3.18, 3.30)
$h'_A(t)$	observed water-surface elevation or stage (ft) as a function of time at cross section A
h'_B	water-surface elevation or stage at cross section B. Eq. (14.2)

$h'_B(t)$	observed water-surface elevation or stage (ft) as a function of time at cross section B. Eq. (14.2)
h_1	water-surface elevation (ft) at cross section 1. Eq. (3.2)
i	designates the x-position in x-t solution domain for Saint-Venant equations
ii	the sequential number of the floodplain compartment. Eqs. (12.5, 12.6)
i_s	describes the unsteady flow within the elementary reach.
j	designates the particular time line in x-t solution domain for Saint-Venant equations.
k_{ce}	user-specified expansion-contraction coefficient for each Δx_i between user-specified cross sections. Eq. (2.12)
k_d	computed submergence correction for tailwater effects on dam-overtopping flow. Eq. (3.31)
k_n	value to which the expansion /contraction coefficient is changed for reverse flows. Sub-section (2.1)
k_s	computed broad-crested weir submergence correction factor. Eqs. (6.1, 6.2)
k_{sp}	computed submergence correction for tailwater effects on spillway flow. Eq. (3.17, 3.18)
k_u	computed submergence correction factor for flow over the upper bridge-embankment crest. Eqs. (3.32, 3.34)
l	represents the left floodplain. Eqs. (2.5, 2.8-2.11)
ℓ	represents lower bridge-embankment crest, etc. Eq. (3.2)
m	cross section shape factor. Eq. (16.2)
m_c	cross-section shape factor for channel. Eqs. (14.13, 14.15)
m_f	cross-section shape factor for floodplain. Eqs. (14.14)
n	the Manning n, a coefficient of frictional resistance.
n_c^k	Manning n for channel at k^{th} elevation. Eq. (10.1)
n_1^j	first trial (starting) values for the $n(\bar{Q})$ function. Eqs. (14.12)

n_j^k	Manning n computed for each j^{th} discharge stratum between adjacent gages. Eqs. (14.8, 14.9)
n_k	composite (total cross section) Manning n. Eq. (10.1)
q	lateral inflow (cfs/ft) or outflow per linear length of channel. Eq. (2.1)
q	computed tributary flow (cfs/ft) at the confluence of the tributary with the main-stem river or another tributary. Eq. (7.1)
q^*	new estimate of q (lateral inflow, cfs/ft) of dynamic tributary iterative computation. Eq. (7.1)
q^{**}	previous estimate of q (cfs/ft) for dynamic tributary iterative computation. Eq. (7.1)
q_o	average unit width discharge (average discharge/average channel topwidth), cfs/ft. Eq. (15.2)
r	represents the right floodplain. Eqs. (2.7-2.11)
s_{co}	user-specified sinuosity factor for conservation of mass equation . (Eq.(2.1, 2.19)
s_m	user-specified sinuosity factor for conservation of momentum equation . (Eq.(2.2, 2.20)
t	time (sec or hr).
t_b	time (hr) since beginning of breach formation. Eqs. (6.8, 6.90)
u'	units conversion factor for computing M' which is used in Eq. (11.16) to compute time step (Δt_j). Eq. (11.17)
v	local cross-section average velocity (ft/sec). Eq. (5.29)
v_x	velocity of dynamic tributary inflow into main-stem river (ft/sec). Eq. (7.2)
w_u	user-specified width (ft), parallel to flow direction, of the crest of the upper embankment. Eq. (3.40)
x	the longitudinal distance along the river(channel/floodplain) (ft or mi).
x_1	upstream beginning location (mi) of the flow loss. Eq. (12.10)
x_2	downstream ending location (mi) of the flow loss . Eq. (12.10)
α	weighting factor ($0 < \alpha \leq 1$) in dynamic tributary computation. Eq. (7.1)

α'	ratio of the flow volume loss to the total active flow. Eq. (12.10)
β	the momentum coefficient for velocity distribution. Eqs. (2.2, 2.11, 2.20)
γ	non-Newtonian fluid's unit weight (lb/ft ³). Eq. (2.13)
γ'	the ratio (the time from initial steady flow to the center of gravity of the hydrograph/ T_p). Eq. (3.3)
ϵ	user-specified convergence criterion (cfs) for automatic calibration of Manning $n(Q)$ values. Eq. (14.10)
ϵ_Q	user-specified convergence criterion (cfs/ft) for dynamic tributary iterative computations.
θ	weighting factor in implicit finite-difference scheme for Saint-Venant equation. Eqs. (2.16-2.20)
κ	non-Newtonian fluid's apparent viscosity (lb-sec ² /ft ²) or scale factor of the power function. Eqs. (2.13, 2.14)
λ_i	local characteristic velocity (ft/sec). Eq. (5.16)
$\hat{\lambda}_1^+$	(+) characteristic direction switch function for local characteristic velocities which depends on local Froude number. Eqs. (5.17, 5.18, 5.21-5.28)
$\hat{\lambda}_1^-$	(-) characteristic direction switch function for local characteristic velocities which depends on local Froude number. Eqs. (5.17, 5.18, 5.21-5.28)
μ	constant in Manning's equation ($\mu=1.49$ for English system of units and $\mu=1.0$ for SI units). Eqs. (2.4-2.7, 2.22, 3.6, 9.1, 11.9, 14.12)
ξ	dummy variable used in integral equations for P_1 and P_2 . Eqs. (5.12, 5.13)
ρ	ratio of Q_p to Q_o . Eq. (3.3)
ρ_o	parameter specifying the degree of nonlinearity in dam-breach formation. Eqs. (6.8, 6.9)
Σ	summation of two or more quantities. Eqs. (8.2, 12.5, 12.6)
σ	numerical filter that modifies the extent of contribution of inertial terms in the momentum equation. Eqs. (5.4, 5.5)
τ	dam-breach time of formation or time of failure (hrs). Eqs. (6.8, 6.9, 6.11)
τ_o	non-Newtonian fluid's yield strength (lb/ft ²). Eqs. (2.13, 2.15)

ϕ	reflects the flow's unsteadiness and hydraulic condition. Eqs. (5.6, 5.7)
ϕ_j	average bias (ft) which is a function of the computed and measured stages (h_A and h'_A). Eqs. (14.3-14.10)
Ψ	represents any variable (Q , h , A , A_o , s_{co} , s_m , etc.) in implicit finite-difference approximation. Eqs. (2.16-2.18)
ω	user-specified acute angle (deg.) between the wind direction and channel flow x-direction Sub-section (2.1)
ω_t	user-specified acute angle (deg.) between main-stem river and tributary or between two tributaries. Eq. (7.2)
DXM	minimum computational distance step between cross sections. (Data group: 19)
ITMAX	maximum number of iterations allowed in the Newton-Raphson Iteration scheme for solving the system of nonlinear equations. (Data group: 2)
IWF	parameter denoting dry-bed routing. (Data group: 16)
JNK	parameter indicating if hydraulic information will be printed. (Data group: 4)
KCG	number of data points in spillway gate control curve of gate opening (GHT) vs. time (TGHT). (Data group: 3)
KFLP	parameter indicating the use of the floodplain (conveyance) option. Data group: 2)
KPRES	parameter indicating method of computing hydraulic radius (R). (Data group: 3)
LQ	sequence number of upstream cross section with lateral inflow. (Data group: 48)
METRIC	parameter indicating if input/output is in English (METRIC=0) or Metric (METRIC=1) units. (Data group: 1)
MUD	parameter indicating the use of the mud/debris flow. (Data group: 14)
NCS	number of values in table of topwidth (BS) vs. elevation (HS). (Data group: 4)

27. ACKNOWLEDGEMENTS

The authors would like to acknowledge Dr. Ming Jin and Dr. Kuang-Shen Hsu of the Hydrologic Research Laboratory (HRL) for their contribution to the development and testing of the FLDWAV model; Mrs. Anise Johnson, Ms. Michele Aleibar, Mr. Columbus Brown, Ms. Anica Hobson, Ms. Oyeronke Bamiduro - all students appointees at HRL who assisted in the testing of the FLDWAV model; Mr. Raul Edwards - a student appointee at HRL for his contribution to the development of the FLDGRF utility; and Mr. Michael Richardson, Ms. Jennifer Sampson, and Mr. Michael Logan - student appointees at HRL for their contribution to the completion the FLDWAV documentation.